

HADRON - NUCLEUS SCATTERING AT 70, 125, AND 175 GEV/C

AND

A HIGH STATISTICS STUDY OF HADRON - PROTON

ELASTIC SCATTERING AT 200 GEV/C

A Dissertation

Presented to the Faculty of the Graduate School

of

Yale University

in Candidacy for the Degree of

Doctor of Philosophy

by

Alan Michael Schiz

December, 1979

To Pam and the Babies

FERMILAB LIBRARY

ABSTRACT

HADRON - NUCLEUS SCATTERING AT 70, 125, AND 175 GEV/C

AND

A HIGH STATISTICS STUDY OF HADRON - PROTON

ELASTIC SCATTERING AT 200 GEV/C

Alan Michael Schiz

Yale University

1979

Results of two studies of small angle elastic scattering are presented. The first experiment measured hadron-nucleus elastic scattering at 70, 125, 175 GeV/c incident momentum. The second experiment is a high statistics study of hadron-proton elastic scattering at 200 GeV/c incident momentum.

Hadron-nucleus elastic scattering was measured for π^{\pm} , K^{\pm} , p , and \bar{p} scattering from Be, C, Al, Cu, Sn, and Pb targets at incident beam momenta of 70 and 175 GeV/c and for π^+ , K^+ , and p scattering from Be, Al, and Pb targets at an incident beam momentum of 125 GeV/c. In all cases the minimum $-t$ is 0.001 (GeV/c)^2 ; the maximum $-t$ is 0.07 , 0.16 , 0.30 (GeV/c)^2 for incident beam momenta of 70, 125, 175 GeV/c respectively. Parameterizations of the differential cross section,

$d\sigma/dt$, in the forward direction are presented.

Elastic scattering for π^-p , π^+p , and pp reactions was measured at an incident momentum of 200 GeV/c in the region of $0.021 < -t < 0.665$ (GeV/c)². The data are sufficiently precise to allow an investigation of the t dependence of the logarithmic forward slope, $b = d/dt[\ln(d\sigma/dt)]$. Significant t dependence of b is observed. The data are also used to test bounds on the elastic scattering amplitude and fit to functional forms for $d\sigma/dt$ suggested by the Additive Quark Model.

The apparatus was a high resolution single arm forward spectrometer located in the Meson Laboratory at Fermilab. It measured scattering angles up to 4 mrad and four momentum transferred squared, t , down to -0.001 (GeV/c)² for incident momentum up to 200 GeV/c. The x ($=p_{\text{measured}}/p_{\text{beam}}$) acceptance was from 0.85 to 1.0. The trajectories of the incident projectile and the fast forward secondary were measured using proportional wire chambers. This information was used to reconstruct the event and to check if an elastic scatter occurred; no information was used concerning the recoil target particle. The incident beam momentum was determined to 0.03% ($\Delta p/p; \sigma$); the outgoing momentum of the scattered particle was determined to 0.1% ($\Delta p/p; \sigma$). Four Cerenkov counters simultaneously identified pions, kaons,

protons, and antiprotons in the beam.

CONTENTS

LIST OF TABLES	iv
LIST OF FIGURES	viii
1. INTRODUCTION	1
2. EXPERIMENTAL APPARATUS	5
3. DATA ACQUISITION	41
4. DATA REDUCTION: NUCLEAR TARGET DATA	66
5. DATA REDUCTION: HIGH- t DATA	83
6. RESULTS: NUCLEAR TARGET DATA	90
7. TOTAL CROSS SECTIONS: A CONSISTENCY CHECK	138
8. RESULTS: HIGH- t DATA	165
9. DISCUSSION: HIGH- t DATA	214
APPENDIX I:	
ALIGNMENT PROCEDURE	238
APPENDIX II:	
PWC CHAMBER RESOLUTION AND ROTATIONS	241
APPENDIX III:	
NUCLEAR TARGET DATA	254
APPENDIX IV:	
DERIVATION OF SOME RESULTS USED IN THE DIRECT MEASUREMENT OF TOTAL CROSS SECTIONS	323
APPENDIX V	336

APPENDIX VI:

CORRECTIONS FOR PLURAL NUCLEAR SCATTERING: HIGH- t DATA	339
REFERENCES AND NOTES	341
ACKNOWLEDGMENTS	346

LIST OF TABLES

2.1	Layout of Apparatus	7
2.2	M6 WEST Beam Line Characteristics	9
2.3	Cerenkov Counters	12
2.4	Scintillation Counter Characteristics	17
2.5	V1 Sizes	18
2.6	Nuclear Target Parameters	24
2.7	Proportional Wire Chamber Characteristics	30
2.8	Electron and Muon Detectors	35
3.1	Computer Latch Information	58
3.2	ADC Information	59
3.3	An Example of Trigger Rates: Carbon at 70 GeV/c	62
3.4	Scaler Ratios: Carbon at 70 GeV/c	63
3.5	An Example of Trigger Rates: High-t Data at 200 GeV/c	64
3.6	Scaler Ratios: High-t Data at 200 GeV/c	65
4.1	PWC Plane Definitions in the Offline Analysis	70
4.2	PWC Cluster Types	72
4.3	Valid PWC Cluster Types	72
4.4	Event Quantities Written onto	

Data Summary Tapes for Nuclear Target Data	76
4.5 Event Quantities Written onto Monte Carlo Summary Tapes for Nuclear Target Data	81
5.1 Event Quantities Written onto Data Summary Tapes for High-t Data	86
5.2 Event Quantities Written onto Monte Carlo Summary Tapes for High-t Data	88
6.1 Cuts to Extract Elastic Signal: Be 175 GeV/c	94
6.2 Cuts to Extract Elastic Signal: Pb 175 GeV/c	95
6.3 Hadron-Nucleus Elastic Scattering Event Totals	110
6.4 Incoherent Scattering Term Parameters and Nuclear Charge Radii	114
6.5 Results of Fits to Nuclear Target Data	122
6.6 Value of Forward Slope, b_A , for $0.018 < -t < 0.125$ (GeV/c) ² for Nuclear Target Data	130
7.1 Total Cross Section Results: Be, C	157
7.2 Comparison Between Total Cross Sections as Derived by Direct Measurement and from Fits to Elastic $d\sigma/dt$ Distributions	161

8.1	Major Cuts to Extract Elastic Signal: High-t Data	167
8.2	Correction for Radiative Effects	179
8.3	Tabulation of Differential Cross Sections: High-t Data	188
8.4	Parameters for Coulomb Scattering Contribution to $d\sigma/dt$: High-t Data	198
8.5	Local Slope Values and Correlations: High-t Data	203
8.6	Results from Fits of $d\sigma/dt$ to $\exp(bt+ct^2)$: High-t Data	207
8.7	Local Slopes with t Bins Different from Those of Table 8.5	209
8.8	Total Elastic Cross Sections	213
9.1	Results of Fits of R^\pm to $C\exp(dt)$	217
9.2	Results of fits of the high-t data to Eqns. 9.1 and 9.2a	223
9.3	Results of fits of the high-t data to Eqns. 9.1 and 9.2b	223
9.4	Results of fits of the high-t data to Eqns. 9.1 and 9.2c	224
9.5	Results of fits of $d\sigma/dt$ to the form factor parameterization using all the high-t data simultaneously	227
9.6	Correlation coefficients from	

fits using all the high-t
data simultaneously

228

LIST OF FIGURES

2.1	Experimental Apparatus (not to scale left of dashed vertical line)	6
2.2	Optics of the M6 WEST Beamline	10
2.3	DISC Cerenkov Counter Pressure Curve: 200 GeV/c	13
2.4	DISC Cerenkov Counter Pressure Curve: 125 GeV/c	14
2.5	Beam Composition versus Incident Momentum. Except where indicated 300 GeV/c protons interacted with the Meson Laboratory target	15
2.6	V1 Counter Construction	19
2.7	Jaw Shaped Veto (V2)	20
2.8	Veto Plane Geometry	21
2.9	Liquid Hydrogen Target Assembly	22
2.10	Nuclear Target Assembly	26
2.11	Nuclear Target Holder	27
2.12	Recoil Detector	28
2.13	Proportional Wire Chamber Readout Electronics	33
2.14	Electron and Muon Calorimeters	36
2.15	Pulse Height Histograms for the Electron Calorimeter: π^+ , p (as	

identified by the Cerenkov counters) at 50 GeV/c incident momentum	37
2.16 Pulse Height Histogram for Muon Calorimeter: 50 GeV/c	38
3.1 Beam Instrumentation and Particle Identification Fast Logic	43
3.2 Data Collection Logic	44
3.3 Beam Rationer Fast Logic	46
3.4 Hardware Scatter/Focus Detector Calculations	48
3.5 HSFD Logic	49
3.6 HSFD Control Logic	50
3.7 Hardware Scatter Detector Efficiency as a function of q_x (beam momentum times the x (horizontal) projection of the scattering angle): 200 GeV/c	53
3.8 Hardware Scatter Detector Efficiency as a function of q_x (beam momentum times the x (horizontal) projection of the scattering angle): 50 GeV/c	54
3.9 Effect of Hardware Scatter Detector	55
3.10 Fast Logic to Activate and Deactivate Data Acquisition	60
4.1 Diagram of Nuclear Target Data Offline Analysis Procedure	67
5.1 Diagram of High-t Data Offline	

Analysis Procedure	84
6.1 Pulse Height Histogram of Muon Calorimeter: Be 175 GeV/c incident momentum. Pulse heights greater than that indicated by the arrow pass cut on muon calorimeter pulse height	96
6.2 Pulse Height Histogram of Muon Calorimeter: Pb 70 GeV/c incident momentum. Pulse heights greater than that indicated by the arrow pass cut on muon calorimeter pulse height	97
6.3 Recoil Mass Squared Histogram: Be 175 GeV/c incident momentum. Arrows indicate cuts on recoil mass squared.	99
6.4 Recoil Mass Squared Histogram: Pb 70 GeV/c incident momentum. Arrows indicate cuts on recoil mass squared.	100
6.5 z Distribution: Be 175 GeV/c incident momentum: $q > 0.03$ GeV/c. Arrows indicate cuts on z.	102
6.6 z Distribution: Be 175 GeV/c incident momentum: $q > 0.3$ GeV/c. Arrows indicate cuts on z.	103
6.7 z Distribution: Pb 70 GeV/c incident momentum: $q > 0.03$ GeV/c. Arrows indicate cuts on z.	104

- 6.8 z Distribution: Pb 70 GeV/c
incident momentum: $q > 0.3$ GeV/c.
Arrows indicate cuts on z. 105
- 6.9 Apparatus Acceptance for π^- , K^- ,
and \bar{p} scattering from Pb at 70 GeV/c
incident momentum 108
- 6.10 Apparatus Acceptance for π^+ , K^+ ,
and p scattering from Be at 175 GeV/c
incident momentum 109
- 6.11 $d\sigma/dt$ for elastic scattering at 175 GeV/c
incident momentum for p-Be, p-C, p-Al;
solid lines are fits to the data
using Eq. 6.6 115
- 6.12 $d\sigma/dt$ for elastic scattering at 175 GeV/c
incident momentum for p-Cu, p-Sn, p-Pb;
solid lines are fits to the data
using Eq. 6.6 116
- 6.13 $d\sigma/dt$ for elastic scattering at 175 GeV/c
incident momentum for p-Be, \bar{p} -Be, K^+ -Be,
 K^- -Be, π^+ -Be, π^- -Be; solid lines are
fits to the data using Eq. 6.6 117
- 6.14 $d\sigma/dt$ for elastic scattering at 175 GeV/c
incident momentum for p-Pb, \bar{p} -Pb, K^+ -Pb,
 K^- -Pb, π^+ -Pb, π^- -Pb; solid lines are
fits to the data using Eq. 6.6 118
- 6.15 $d\sigma/dt$ for p-Be elastic scattering at

- 175, 125, 70 GeV/c incident momentum;
solid lines are fits to the data
using Eq. 6.6 119
- 6.16 $d\sigma/dt$ for p-Pb elastic scattering at
175, 125, 70 GeV/c incident momentum;
solid lines are fits to the data
using Eq. 6.6 120
- 6.17 Contributions to $d\sigma/dt$: p-Pb
175 GeV/c incident momentum 127
- 6.18 Contributions to $d\sigma/dt$: p-Be
175 GeV/c incident momentum 128
- 6.19 Forward slope of nuclear coherent scattering,
 b_A , as a function of target atomic weight,
A for π^+ . Errors shown are statistical only
(for presentation purposes some errors not
shown). Fits for b_A were performed in
the region $0.0018 < -t < 0.0100$ (GeV/c)². 132
- 6.20 Forward slope of nuclear coherent scattering,
 b_A , as a function of target atomic weight,
A for π^- . Errors shown are statistical only
(for presentation purposes some errors not
shown). Fits for b_A were performed in
in the region $0.0018 < -t < 0.0100$ (GeV/c)². 133
- 6.21 Forward slope of nuclear coherent scattering,
 b_A , as a function of target atomic weight,
A for K^+ . Errors shown are statistical only.

- (for presentation purposes some errors not shown). Fits for b_A were performed in the region $0.0018 < -t < 0.0100$ (GeV/c)². 134
- 6.22 Forward slope of nuclear coherent scattering, b_A , as a function of target atomic weight, A for K^- . Errors shown are statistical only (for presentation purposes some errors not shown). Fits for b_A were performed in the region $0.0018 < -t < 0.0100$ (GeV/c)². 135
- 6.23 Forward slope of nuclear coherent scattering, b_A , as a function of target atomic weight, A for p. Errors shown are statistical only (for presentation purposes some errors not shown). Fits for b_A were performed in the region $0.0018 < -t < 0.0100$ (GeV/c)². 136
- 6.24 Forward slope of nuclear coherent scattering, b_A , as a function of target atomic weight, A for \bar{p} . Errors shown are statistical only (for presentation purposes some errors not shown). Fits for b_A were performed in the region $0.0018 < -t < 0.0100$ (GeV/c)². 137
- 7.1 Idealized Apparatus for Total Cross Section Measurement 141
- 7.2 Offline Analysis Procedure for Direct Measurement of Hadron-Nucleus Total Cross Section 145

7.3	Apparatus Acceptance for Direct Measurement of Total Cross Sections: (π^+ , K^+ , p)-C 175 GeV/c incident momentum	149
7.4	Partial Cross Sections: (π^+ , K^+ , p)-Be 175 GeV/c incident momentum. Only typical statistical errors shown.	151
7.5	Partial Cross Sections: (π^+ , K^+ , p)-C 70 GeV/c incident momentum. Only typical statistical errors shown.	152
7.6	Comparison Between (π^+ , K^+ , p)-p Total Cross Sections as Measured by this Experiment and by Carroll et.al. (Fermilab E104)	155
7.7	Hadron - Be Total Cross Sections as a function of Beam Momentum	158
7.8	Hadron - C Total Cross Sections as a function of Beam Momentum	159
7.9	Comparison between hadron - nucleus total cross sections as measured by the direct method and as measured from elastic scattering t distributions using different t regions. Γ is defined as [$\sigma(\text{DIRECT}) - \sigma(\text{EL SCAT})$]/[statistical error on numerator] (see text)	163
8.1	z Distribution: High-t Data: π^+ p, pp 200 GeV/c incident momentum. Arrows indicate cuts on z.	169

- 8.2 Recoil Mass Squared Distribution: High-t
Data: π^+p , pp 200 GeV/c incident
momentum. Arrows indicate cuts on
recoil mass squared. 171
- 8.3 Cuts Made at the Veto Plane: High-t Data 173
- 8.4 Apparatus Acceptance: π^+p , pp at 200
GeV/c incident momentum 177
- 8.5 Apparatus Acceptance: π^-p at 200 GeV/c
incident momentum 178
- 8.6 Radiative Correction: High-t Data 180
- 8.7 Recoil Mass Squared Distribution:
High-t Data: π^+p at 200 GeV/c incident
momentum: $0.6 < q < 0.7$ GeV/c; Solid line
is a fit to the recoil mass squared spectrum;
dashed line is the inelastic scattering
background contribution to the spectrum. 182
- 8.8 Inelastic Scattering Background: High-t
Data: 200 GeV/c incident momentum 183
- 8.9 $d\sigma/dt$ for π^-p elastic scattering
as measured by this experiment
(corrected for Coulomb scattering
contributions, radiative effects, in-
elastic contamination, and plural nuclear
scattering in hydrogen target); also
shown are results from selected
experiments (not corrected for

Coulomb scattering)	185
8.10 $d\sigma/dt$ for π^+p elastic scattering as measured by this experiment (corrected for Coulomb scattering contributions, radiative effects, in- elastic contamination, and plural nuclear scattering in hydrogen target); also shown are results from selected experiments (not corrected for Coulomb scattering)	186
8.11 $d\sigma/dt$ for pp elastic scattering as measured by this experiment (corrected for Coulomb scattering contributions, radiative effects, in- elastic contamination, and plural nuclear scattering in hydrogen target); also shown are results from selected experiments (not corrected for Coulomb scattering)	187
8.12 Local Slope as a function of $-t$ for Examples of $d\sigma/dt$	201
8.13 Local Slopes as a function of $-t$ as Measured by this Experiment: pp , π^+p , π^-p at 200 Gev/c incident momentum. Errors include both statistical and systematic	

	errors added in quadrature.	
	Solid lines present local slope as calculated from fits of $d\sigma/dt$ to $\exp(bt+ct^2)$.	202
8.14	Local Slopes as a function of $-t$ Using Different t Bins from Fig. 8.13: pp , π^+p , π^-p at 200 GeV/c incident momentum	208
9.1	$[d\sigma/dt(pp)]/[d\sigma/dt(\pi^\pm p)]$ as a function of $-t$	216
9.2	Comparison of measurements by several experiments of the logarithmic slope for π^-p , π^+p , and pp elastic scattering	219
9.3	Results from fits to all the high- t data simultaneously using Eqns. 9.1 and 9.2b. Arrows indicate the region of t used in the fits.	230
9.4	Comparison of High- t Data with Bound on Elastic Scattering Amplitude as Derived in Ref. 1.13. Solid line is the bound; closed circles are data. The bound rigorously holds only left of the dashed line.	233
9.5	Right Hand Side minus Left Hand Side	

of Eq. 9.4, R-L, (solid line).

Dashed lines give one standard deviation error band; error

band shown only for $-t > 0.075 \text{ (GeV/c)}^2$ 235

- A2.1 β as a function of Scattering Angle:
PWC Station 3Y. The dashed line is
the fit to the data. 243
- A2.2 β as a function of Scattering Angle:
PWC Station 3X. The dashed line is
the fit to the data. 244
- A2.3 β as a function of Scattering Angle:
PWC Station 4X. The dashed line is
the fit to the data. 245
- A2.4 $\sigma_{s,t}^2$ as a function of $\theta_{s,t}$:
Cluster Type 5 250
- A2.5 $\sigma_{s,t}^2$ as a function of $\theta_{s,t}$:
Cluster Type 6 253

CHAPTER 1

INTRODUCTION

Measurements of hadron-nucleus and hadron-proton elastic scattering are fundamental. The distribution in t , four momentum transferred squared, for elastic scattering provides information about the character of the strong interactions. This study presents data taken at Fermilab for both hadron-nucleus and hadron-proton elastic scattering.

The hadron-nucleus elastic scattering data, in addition to testing theoretical approaches^{1.1,1.2} to the scattering process, also provide valuable engineering information that will aid in the design of high energy experiments. While data exist for hadron-nucleus elastic scattering at 20 - 30 GeV^{1.3,1.4} and at 40 GeV^{1.5}, there are no comparable published measurements at higher energies for nuclear targets heavier than helium^{1.6}. These data taken at Fermilab fill that void.

Specifically the reactions studied are π^\pm , K^\pm , p , and p scattering from Be, C, Al, Cu, Sn, and Pb targets at incident beam momenta of 70 and 175 GeV/c and π^+ , K^+ , and p

scattering from Be, Al, and Pb targets at an incident beam momentum of 125 GeV/c. The t range covered varied with the incident momentum. In all cases the minimum $-t$ is 0.001 (GeV/c)²; the maximum $-t$ is 0.05 , 0.15 , and 0.30 (GeV/c)² for incident beam momenta of 70, 125, and 175 GeV/c respectively.

Parameterizations of $d\sigma/dt$ in the very forward t region ($0.001 < -t < 0.030$ (GeV/c)²) will be presented. Hadron-nucleus scattering is concentrated in the forward direction; therefore, this forward t region represents the bulk of the elastic scattering cross section. This is especially true as the atomic number of the nuclear target increases. It is important to note that the experimental elastic scattering data include both interactions which leave the target nucleus in its ground state (coherent elastic scattering) and interactions which excite or break up the target nucleus (quasielastic scattering).

As mentioned above, the $d\sigma/dt$ distribution for hadron-proton elastic scattering provides information about the nature of the strong interactions. In an optical model this distribution is dependent on the interacting particles' sizes and opacities. In a Regge model this distribution is dependent on the structure of the Pomeron and of any other exchanges which contribute to elastic scattering.

Data from early experiments^{1.7} at $-t < 0.8$ (GeV/c)² and at moderate energies (5 to 30 GeV) were fit with a simple exponential function of t :

$$d\sigma/dt = A \exp(bt) \quad (1.1)$$

where b is a constant. However later results at Fermilab^{1.8,1.9}, SLAC^{1.10}, and the ISR^{1.11} show a more complicated t dependence of $d\sigma/dt$. An exponential with a quadratic term (where b and c are constants)

$$d\sigma/dt = A \exp(bt + ct^2) \quad (1.2)$$

gives a good representation of the data taken with beam energies between 50 and 175 GeV^{1.8} in the intermediate t region ($0.05 < -t < 1.0$ (GeV/c)²). Very precise data at 10 and 14 GeV from SLAC^{1.10} show an even more complicated t dependence, while the ISR^{1.11} results suggest a break in the t distribution for proton proton scattering. Finally data from the CERN SPS^{1.12} on the logarithmic forward slope in the small t region ($-t < 0.05$ (GeV/c)²) are inconsistent with

extrapolated values of the slope as derived from data in the intermediate t region.

The present study concerns π^-p , π^+p , and pp elastic scattering at 200 GeV/c incident momentum. The t range is from -0.021 to -0.665 (GeV/c)² (scattering angles from ~ 0.7 to 4.0 mrad). Thus in a single experiment, $d\sigma/dt$ is measured over the small to intermediate t range. The apparatus was configured such that at the maximum t that was accepted, the data had good statistics. Therefore these data are referred to as the "high - t data".

The large number of events involved in this study allow a detailed analysis of the elastic scattering t distributions. The t dependence of logarithmic slope, $b(t)$, will be presented where

$$b(t) = d/dt[\ln(d\sigma/dt)] \quad (1.3)$$

The " $b(t)$ " in Eq. 1.3 is not to be confused with the " b " used in Eqns. 1.1 and 1.2.

The data are also used to test bounds on the elastic scattering amplitude^{1.13,1.14} and fit to functional forms suggested by the Additive Quark Model.

CHAPTER 2

EXPERIMENTAL APPARATUS

A. Introduction

The apparatus used in this experiment was a single arm forward spectrometer. The momentum and trajectory of the incident particle and of a single fast forward secondary were measured. A diagram of the apparatus is shown in Figure 2.1. Table 2.1 gives the distances of some of the major elements along the beam line.

The momentum of the incoming particle was determined to 0.03% ($\Delta p/p; \sigma$) by a proportional wire chamber (PWC) located at a momentum dispersed focus of the beam. Four Cerenkov counters simultaneously identified pions, kaons, and protons.

The angle of the scattered outgoing particle was measured to 30 rad (σ) by four stations of high resolution proportional wire chambers placed on either side of the target. For stability these chambers were mounted on a 20 ton reinforced concrete block.

A magnetic spectrometer, consisting of two dipole magnets and a station of PWCs, was located just downstream of the concrete block. The spectrometer

Figure 2.1

EXPERIMENTAL APPARATUS

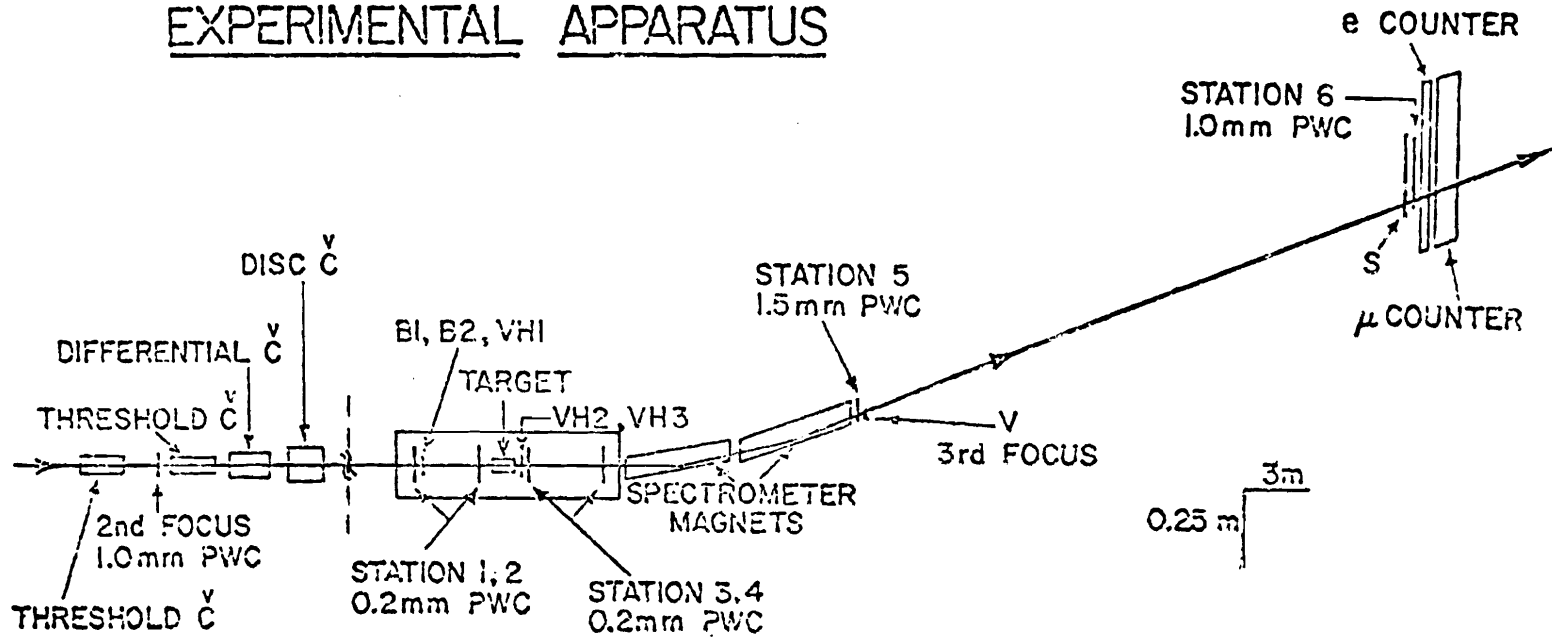
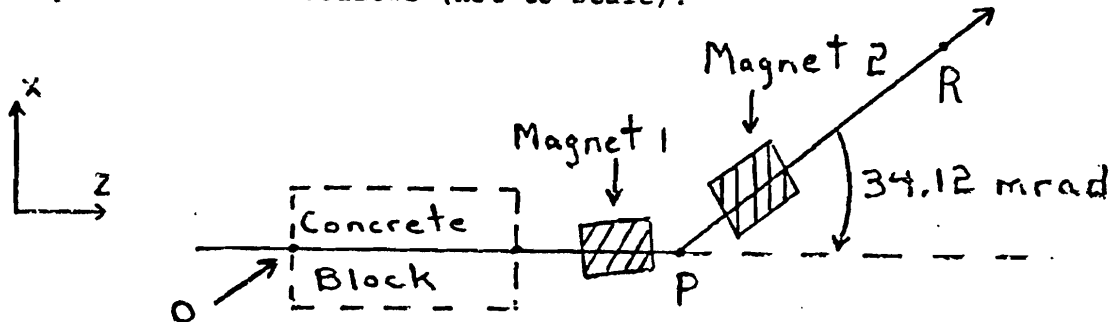


TABLE 2.1
Layout of Apparatus

The trajectory of an on-axis on-momentum unscattered beam particle is as follows (not to scale):



The following elements are measured with respect to upstream end of concrete block (pt.0)

<u>Element</u>	<u>z (cm)</u>
High Resolution PWC1	23.18
High Resolution PWC2	373.38
High Resolution PWC3	625.12
High Resolution PWC4	1075.04
Magnet 1 Entrance ^a	1122.67
Magnet 2 Entrance ^a	1729.68
Bend Point, P	1751.90
Magnet 2 Entrance ^a	1774.12
Magnet 2 Exit ^a	2380.91

The following elements are measured along \overline{PR} with respect to the bend point P:

<u>Element</u>	<u>z (cm)</u>
PWC5 ^b	674.92
Veto Plane	705.47
PWC6	3640.14

^aRefers to z of center of aperture as projected onto unbent beam line

^bThese chambers (an x and y) were tilted 8.477° with respect to line PR

measured the momentum of the outgoing particle to $\pm 0.1\%$ ($\Delta p/p; \sigma$). The current in the magnets was scaled with momentum such that the bend angle of the spectrometer for unscattered particles was 34 mrad. Muons and electrons were identified by an iron-scintillator calorimeter and a lead-scintillator shower calorimeter, respectively.

The various elements are now described in more detail^{2.1}.

B. Beam

The experiment was performed in the M6 west beam line^{2.2} in the Meson Lab at Fermilab. The beam properties are summarized in Table 2.2.

The beam had three stages, each with point to parallel to point optics as shown in Figure 2.2. The momentum spread (maximum $\pm 1\%$) was selected via a horizontal collimator at the first focus. A PWC with 1 mm wire spacing located at the second focus measured the momentum of the incoming particle.

Two scintillation counters, SA and SB, intercepted the entire beam at the second focus. Together with four other remotely controlled counters, E, W, U, D, which

TABLE 2.2
M6W Beam Line Characteristics

Production Target Size for this experiment	width height length	1 mm 1 mm 20.3 cm
Production Angle	θ_p	2.7 mr
Lab Angle	θ_v θ_h	1.0 mr 2.5 mr
Momentum Range	10-200 GeV/c	
Solid Angle	$\Delta\Omega$	1.34 μ sr
Angular Acceptance	$\Delta\theta_h$ $\Delta\theta_v$	± 0.56 mr ± 0.76 mr
Momentum Bite	$\Delta p/p$	$\pm 0.014\%$ to 1.0%
Dispersion 1st focus	$\frac{\Delta x}{\Delta p/p}$	6.30 cm/%
2nd focus	$\frac{\Delta x}{\Delta p/p}$	3.48 cm/%
Properties at 3rd focus		
horizontal magnification		1.5
vertical magnification		1.3
horizontal divergence		± 0.36 mr
vertical divergence		± 0.67 mr

M6-W BEAM

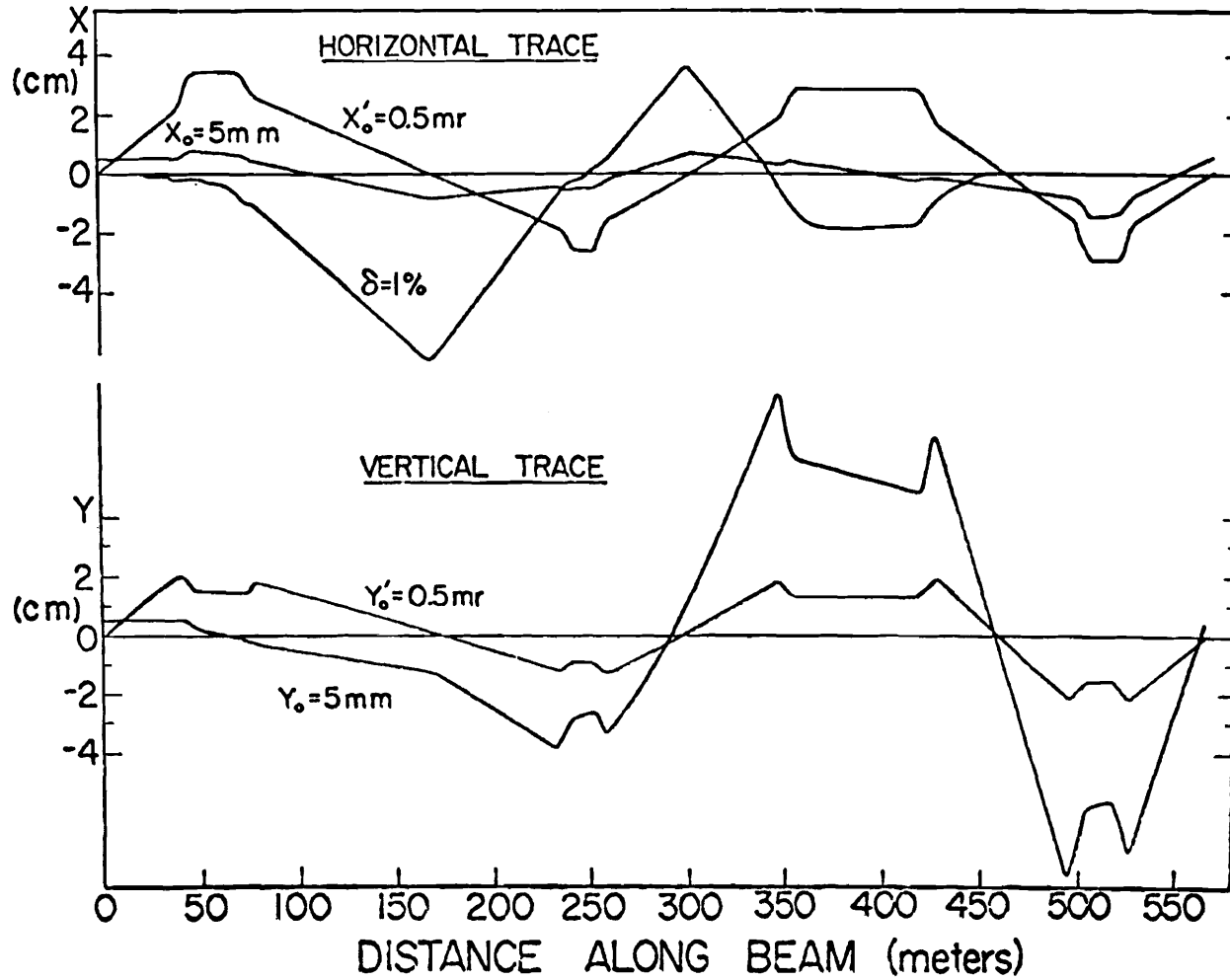


Figure 2.2

formed a variable sized hole veto, these counters defined an upstream aperture. Further downstream, two other scintillation counters, H1 and H2, both with 7.6 diameter holes, rejected particles with improper trajectories.

Four Cerenkov counters simultaneously identified pions, kaons, and protons. The properties of these counters are given in Table 2.3. The upstream counters, M6K1 and M6K2^{2.3}, were used as threshold counters to identify pions. M6K3^{2.4} and M6K4^{2.5} were differential counters used to identify kaons and protons respectively. Figures 2.3 and 2.4 show typical pressure curves for these counters; Figure 2.5 shows the beam composition at the target as a function of beam momentum.

At the third focus the beam was recombined in both space and momentum. Here the beam was focused on a very small scintillation counter, V1. For the high-t data an additional jaw shaped counter, V2, was inserted. These counters are described in more detail below.

C. Detectors and Targets

1. Scintillation Counters

TABLE 2.3

Cerenkov Counters

Name	Type	Length	Number & Type of Phototubes	Annulus Angle	Gas and Pressure, 200 GeV
M6K1	Threshold	29.3 m	2 RCA 31000 M	—	He 0.54 psia
M6K2	Threshold	18.3 m	1 RCA 31000 M	—	He 1.6 psia
M6K3	Differential	13.7 m	3 RCA 31000 M	10 mr	He 28.2 psia
M6K3	Differential	5.8 m	8 Phillips 56 DVP	24.5 mr	He 156 psia

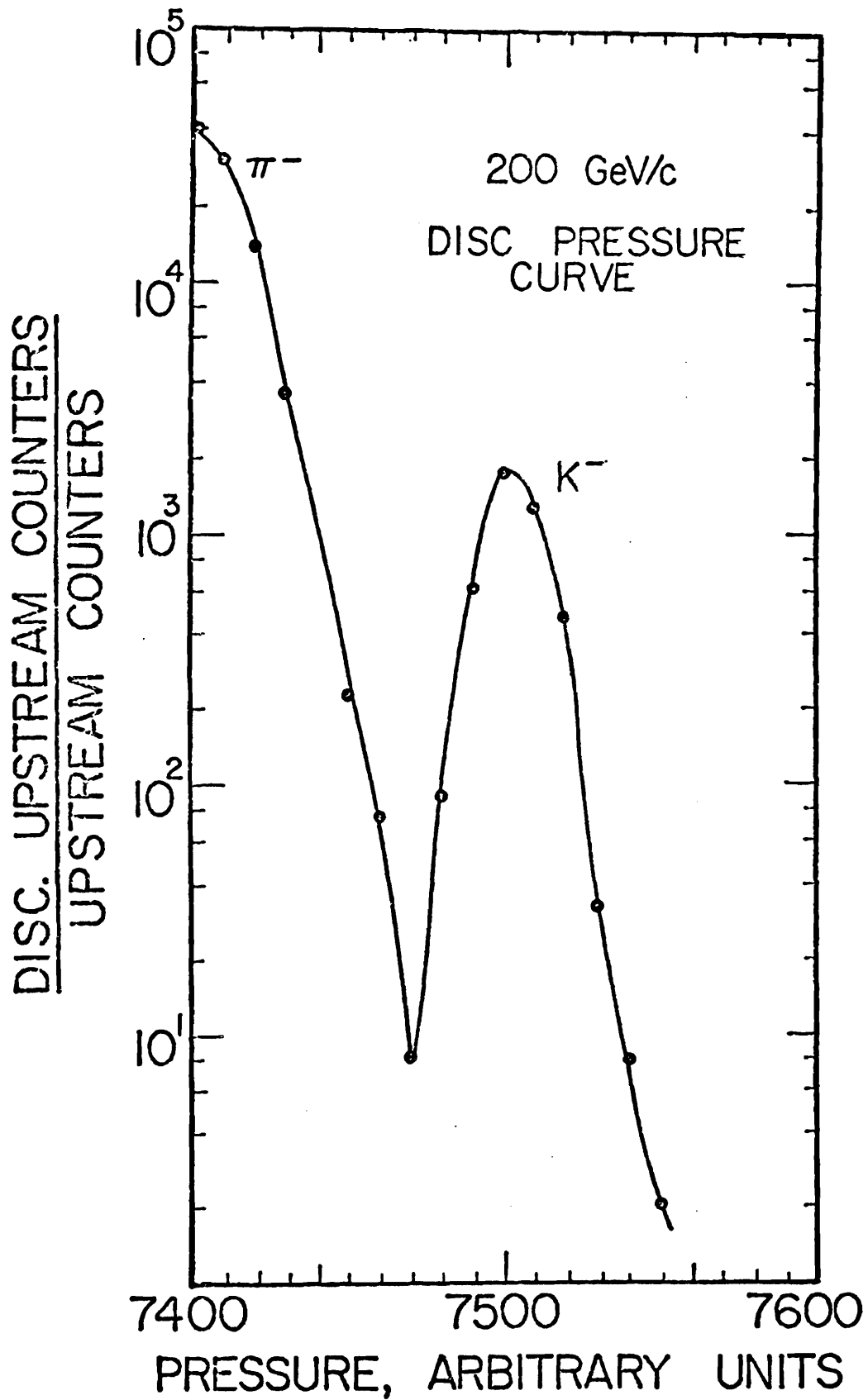


Figure 2.3

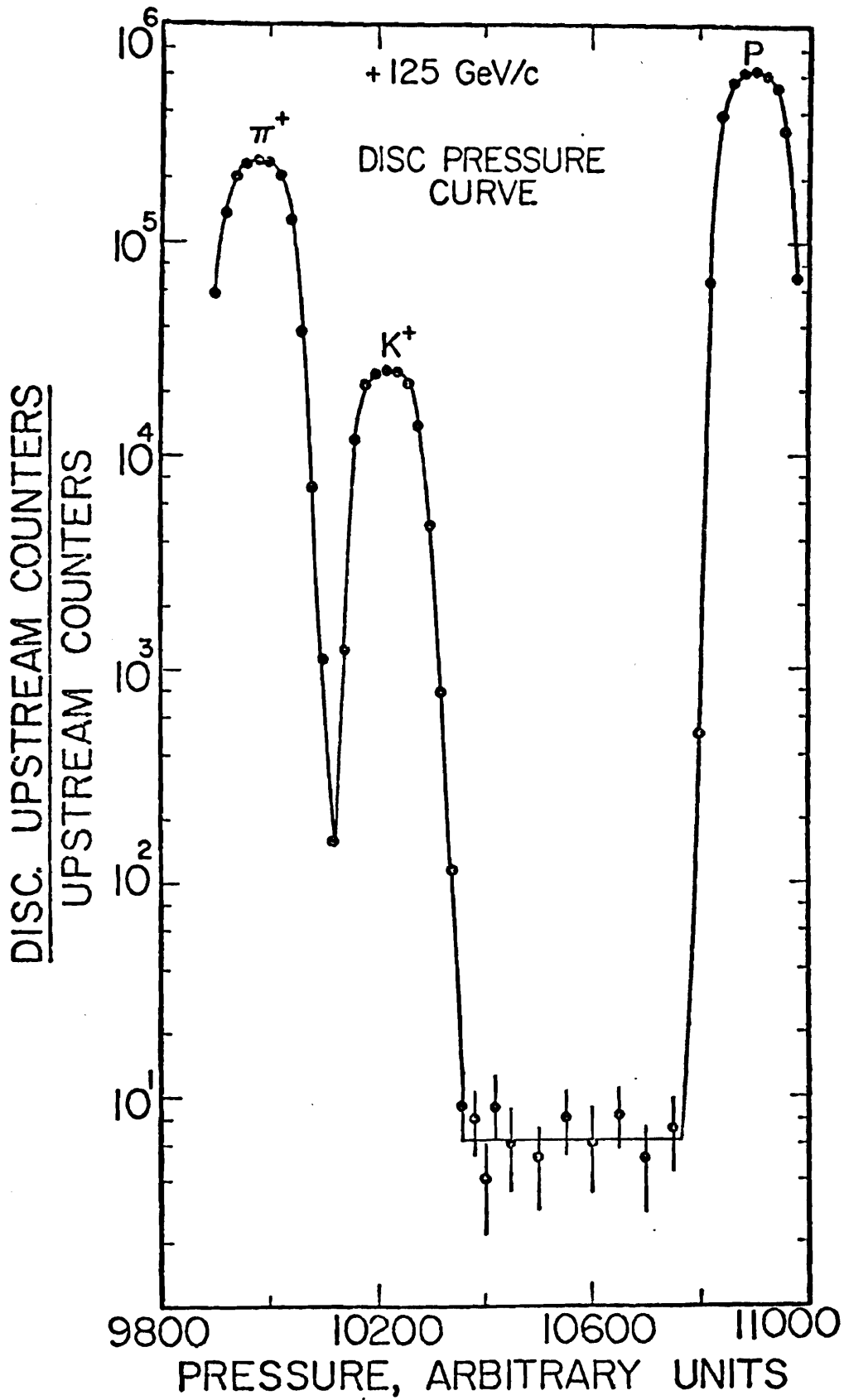


Figure 2.4

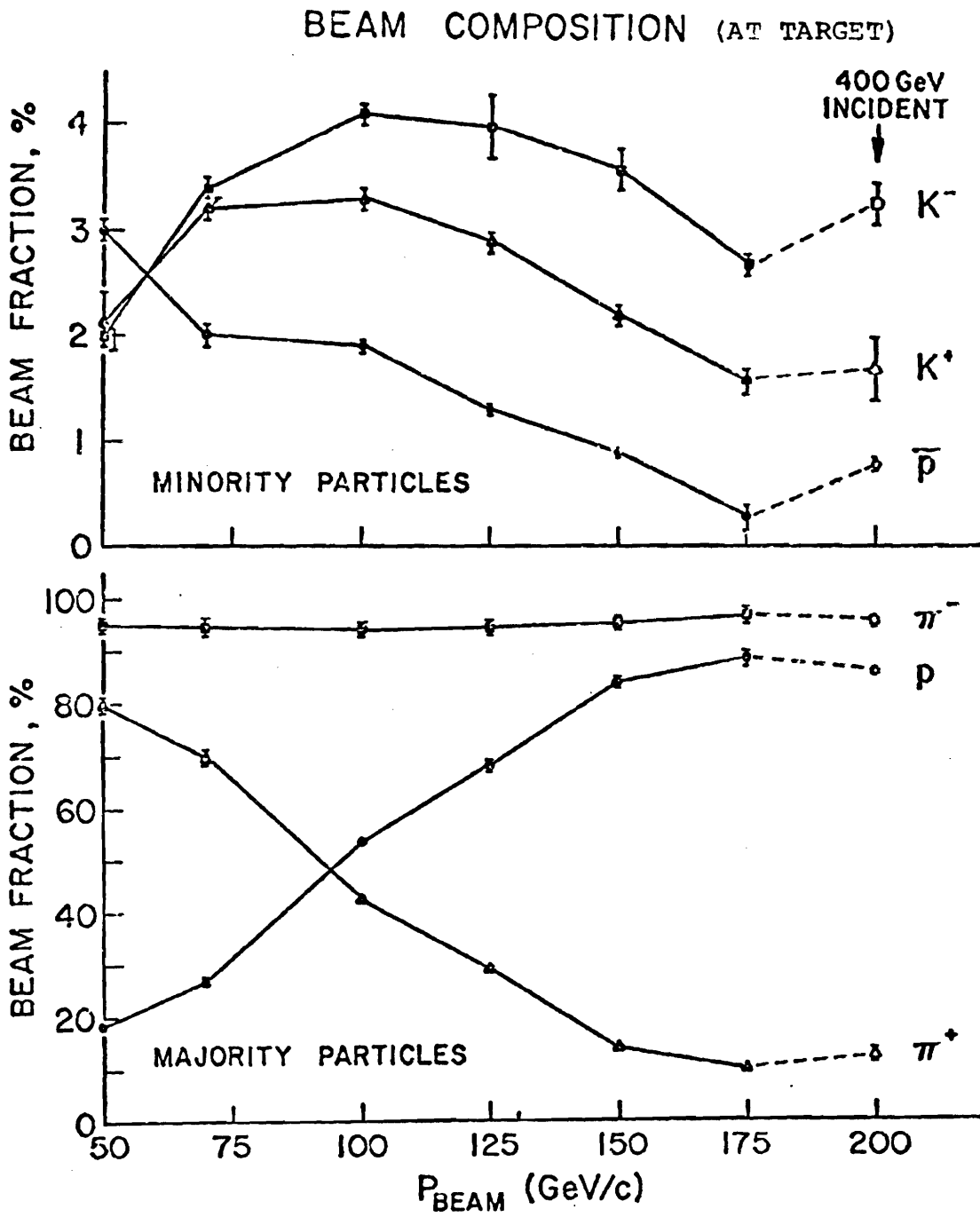


Figure 2.5

B1, B2, VH1, VH2, VH3, and S in Figure 2.1 are scintillation counters. Their dimensions are given in Table 2.4. B1 and B2 defined the beam, while VH1 was a hole veto that removed beam halo. VH2 and VH3 will be described later. S subtended the full aperture at the downstream end of the apparatus.

V1 and V2 were, as mentioned above, placed at the third focus. They were used in the trigger for scattered particles. Several different sizes of V1 were used depending on the incident beam momentum; Table 2.5 gives the various sizes. V1 was viewed via an air light guide and was located in an aluminum foil coated box. The assembly is shown in Figure 2.6. V2 was a jaw shaped counter and is shown in Figure 2.7. Figure 2.8 shows the relative placement of the two vetoes (and also the last magnet aperture projected to the veto plane). A more complete description of the use of V1 and V2 appears in the next chapter.

2. Targets

For the high- t running a liquid hydrogen (LH_2) target, 52.7 cm long, 4.4 cm in diameter, was used. The vacuum windows were extended to just downstream of PWC Station 2 and just upstream of PWC Station 3. Figure 2.9 shows the hydrogen target.

TABLE 2.4

SCINTILLATION COUNTER CHARACTERISTICS

Counter	DIMENSIONS			Hole Dimensions (if applicable)	Phototube
	Horizontal (cm)	Vertical (cm)	Thickness (cm)		
B1	1.91	2.22	.16	--	Amperex 2" 56 DVP
B2	2.54	2.38	.16	--	"
S	30.48	15.24	.64	--	"
VH1	10.16	10.16	.16	3 x 3cm square (4.13cm from lower edge 3.81cm from vertical edge)	"
VH2 ^a	12.7	outer diameter	.95	2.54cm diameter (centered on scintillator center)	"
VH3	35.56	41.91	.64	3.81cm diameter: (19.05cm from lower edge; 17.78cm from vertical edge)	"

^aVH2 was a circular counter

TABLE 2.5

V1 SIZES^a

Momentum (GeV/c)	Horizontal (mm)	Vertical (mm)	Thickness (mm)
±70	20.25	4.90	10.32
±125	20.00	4.00	10.32
±175	20.15	2.52	10.18
±200	20.15	2.52	10.18

^aV1 was coupled to an Amperex 2" 56DVP Phototube.

(14 Stage/K-Cs-Sn Photocathode)

V1 COUNTER CONSTRUCTION

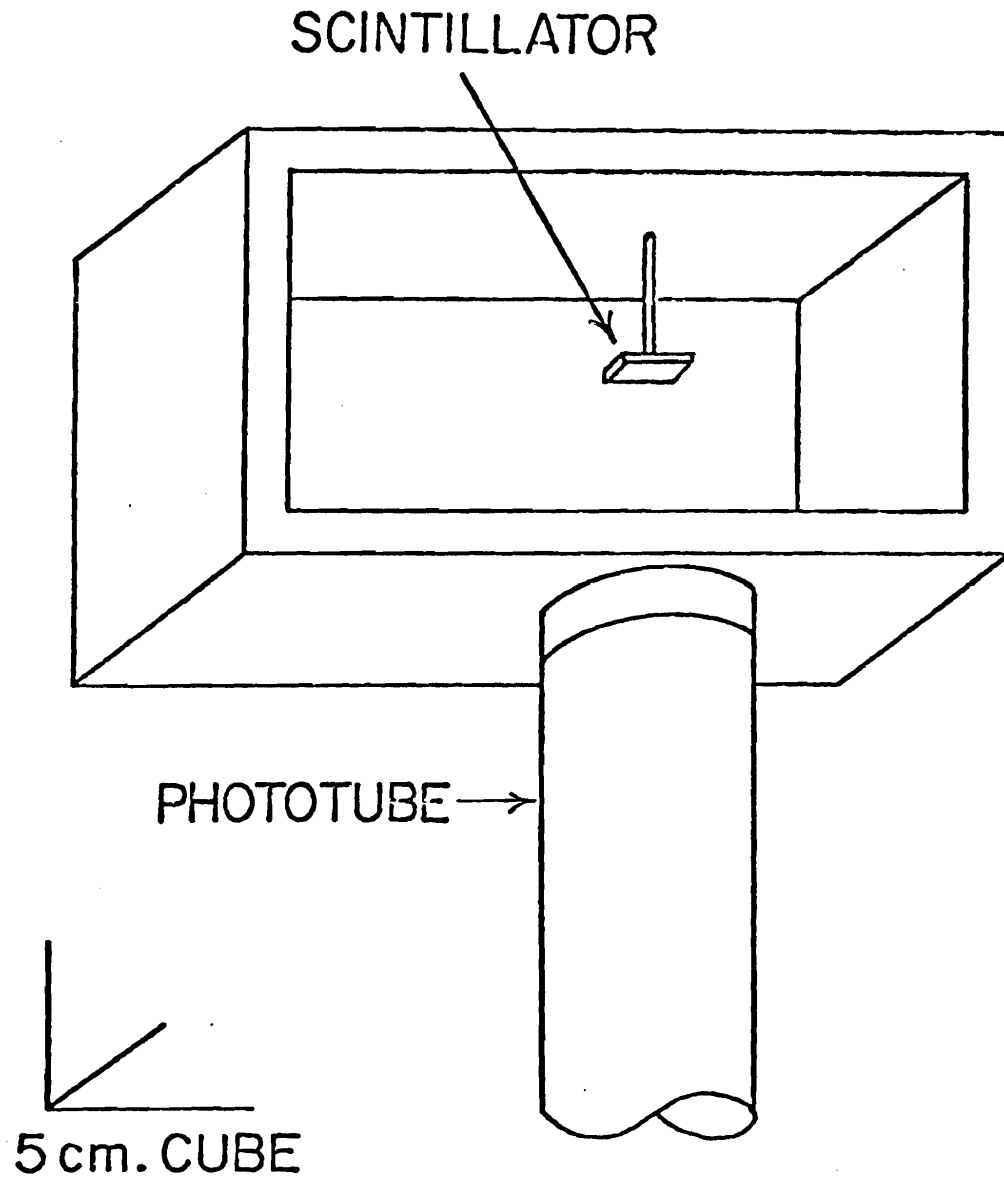
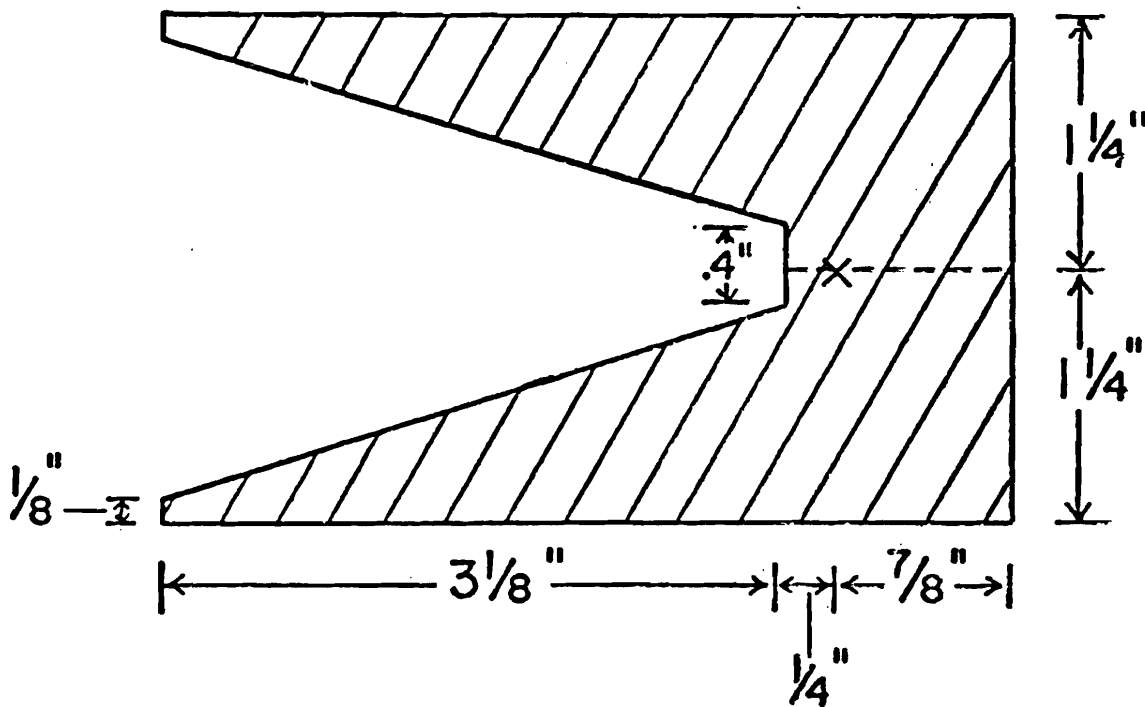


Figure 2.6

JAW SHAPED VETO (V2)^a (ACTUAL SIZE)



X NOMINAL BEAM CENTER

^a V2 WAS COUPLED TO A
AMPEREX 2" 56 DVP
PHOTOTUBE

Figure 2.7

VETO PLANE GEOMETRY

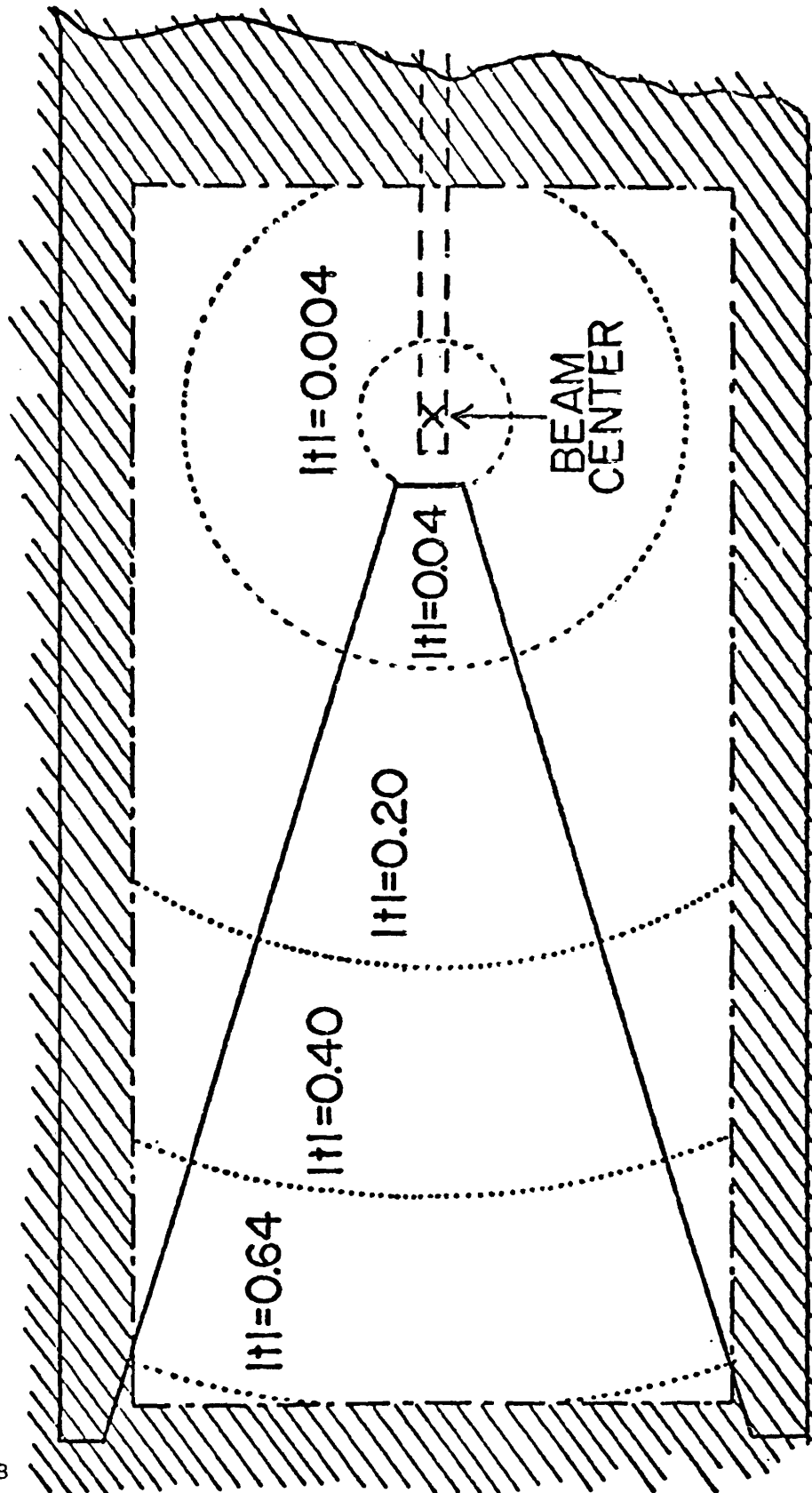


Figure 2.8

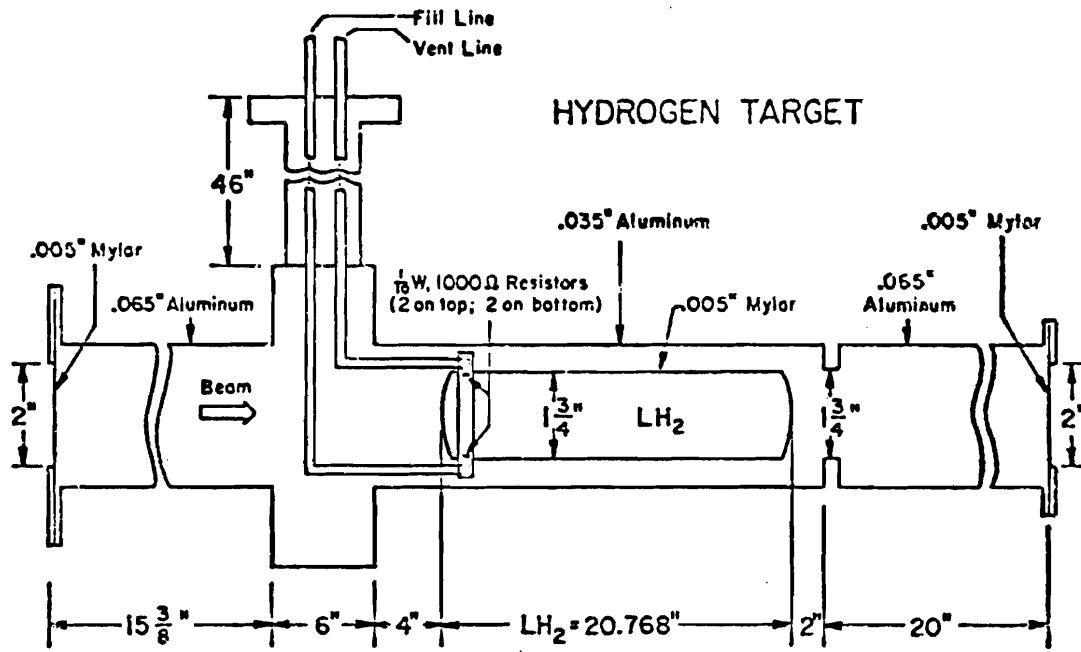


Figure 2.9

The hydrogen pressure was kept at 15.5 ± 0.5 psia; since gas and liquid were in equilibrium, the density of the liquid hydrogen can be computed from its known thermodynamic properties. For the data analysis a value of 0.0705 ± 0.03 gm/cm³ was used. Two sets of carbon resistors in the liquid hydrogen monitored the liquid level. The target was emptied by using a small heat leak into the target to drive the hydrogen into the reservoir. The hydrogen gas density is estimated to vary from 4.4×10^{-4} to 0.9×10^{-4} gm/cm³.

The nuclear targets were sized to give approximately the same multiple scattering as the LH₂ target. This choice had the consequence that the quantity "Length / Interaction Length" decreased with increasing atomic number, giving more background to the scattering. However the angular resolution of the apparatus remained the same for all elements. The target dimensions are given in Table 2.6.

The nuclear targets were placed in a three piece aluminum vacuum can which in turn was mounted to the recoil detector (described in the next section). The pieces were joined by quick disconnect flanges for easy substitution of the targets. Each nuclear target was placed in its own holder and precision positioned by a 31.2 cm long mylar tube to a precision of 1 mm. The

TABLE 2.6

Nuclear Target Parameters

Target	Z	A (amu)	Diameter (cm)	Length (cm)	Density (g/cm ³)	Radiation Length, L _R (g/cm ²)	L/L _R
Be	4	9.01	5.40	1.600	1.85	65.19	0.045
C	6	12.01	5.73	1.259	1.64	42.70	0.048
Al	18	26.98	6.02	0.401	2.73	24.01	0.046
Cu	29	63.55	6.32	0.080	8.96	12.86	0.056
Sn	50	118.69	6.32	0.084	7.31	8.82	0.070
Pb	82	207.19	6.63	0.026	11.35	6.37	0.046

vacuum can and holder are shown in Figures 2.10 and 2.11.

3. Recoil Detector^{2.6}

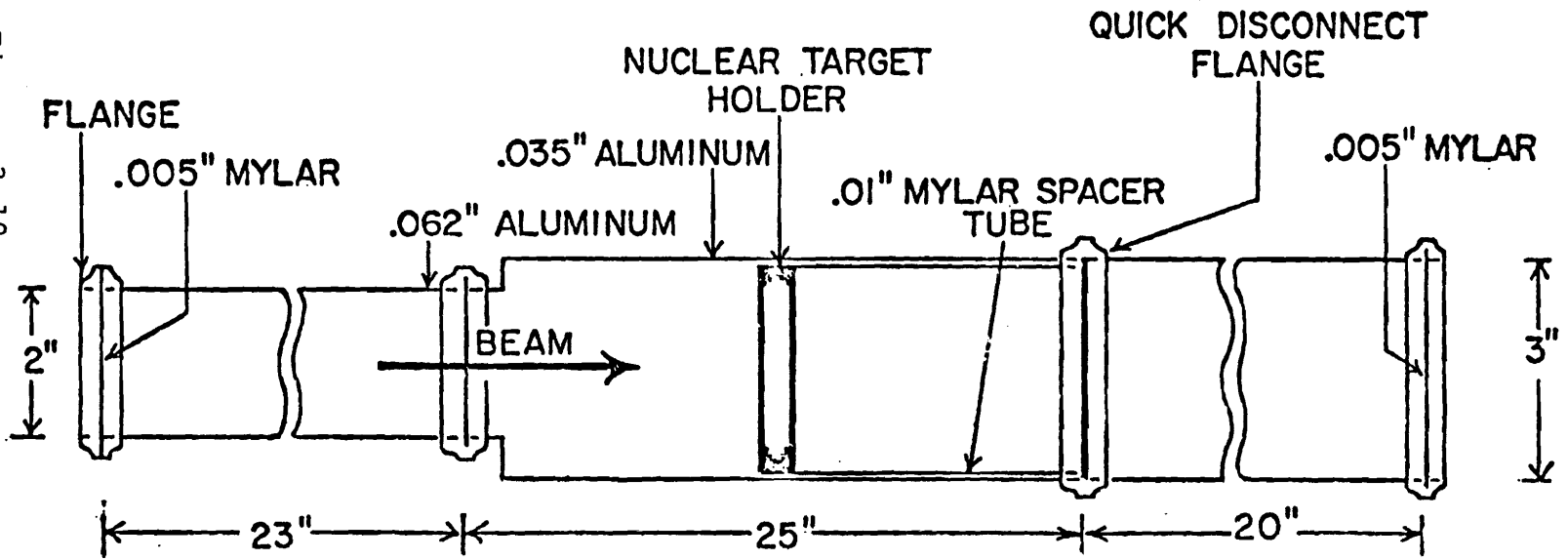
An assembly called the recoil detector, consisting of four U-shaped scintillation counters, was centered around the target. Its function was to help separate elastic from inelastic events. Figure 2.12 shows the assembly. The outer two counters, RV1 and RV2, are 1 cm thick and 40.64 cm along the beam. A 1 cm thick lead plate was sandwiched between them, and this combination was used to detect gamma rays from neutral pions produced in inelastic collisions. A proton needed a kinetic energy of at least 150 Mev (corresponding for elastic scattering to a $-t$, four momentum transferred squared, of $.281 \text{ (GeV/c)}^2$) to reach RV2. The remaining parts of the detector were not used in this experiment.

4. Electron Scattering Rejection

To reject scatters off of electrons in the target, two hole veto scintillation counters, VH2 and VH3, were used. These counters are located immediately upstream of PWC station 3; Table 2.4 gives their dimensions. The upstream counter had a 3.8 cm diameter hole cut 19.05 cm from the lower edge and 17.78 cm from

NUCLEAR TARGET ASSEMBLY

Figure 2.10



SCALE:

1" = 2"

1" = 6"

Handwritten:

$$\begin{array}{r} 23 \\ + 2 \\ \hline 25 \end{array}$$

Handwritten:

$$\begin{array}{r} 122 \\ 20 \\ \hline 322 \end{array}$$

NUCLEAR TARGET HOLDER

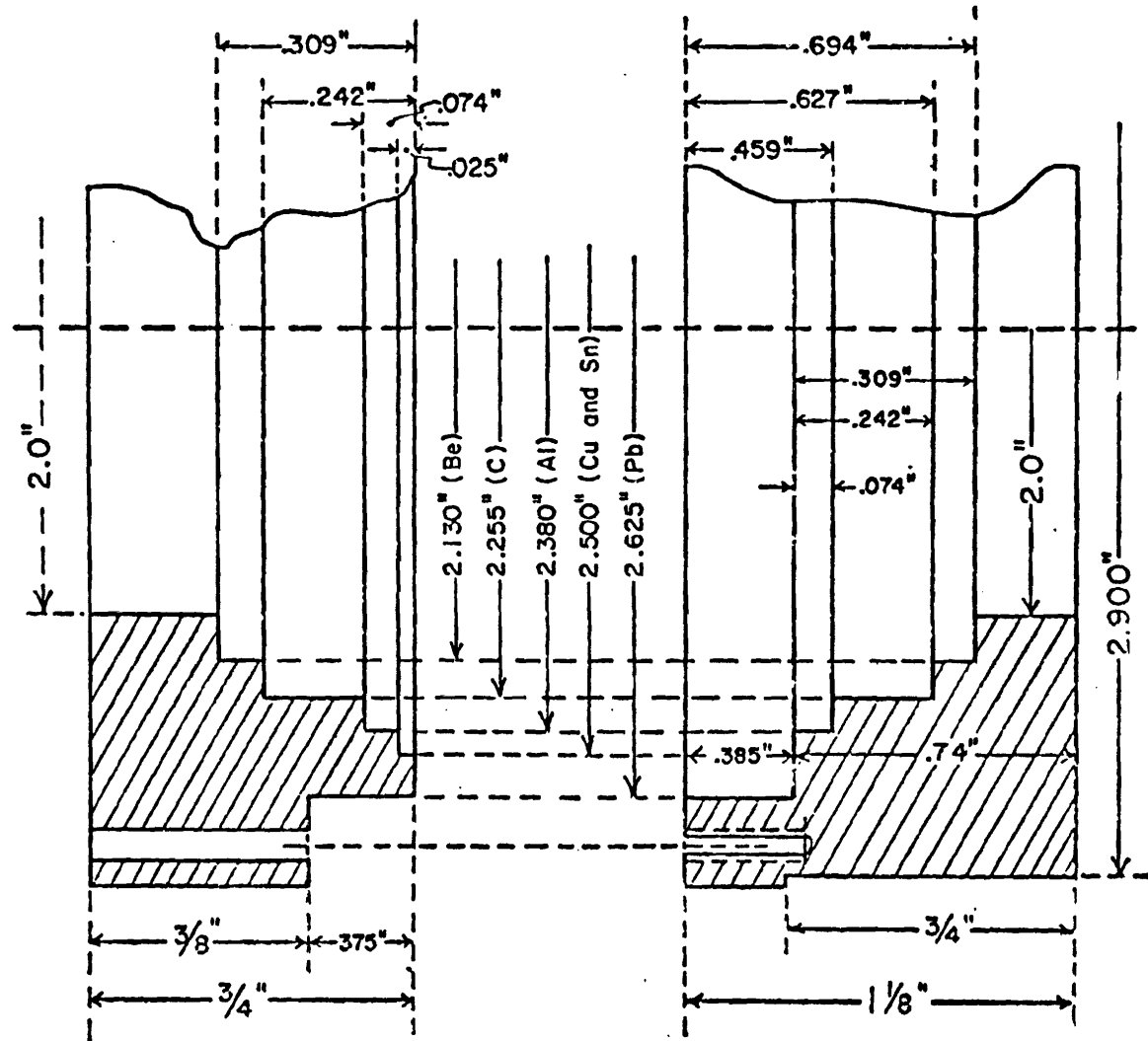


Figure 2.11

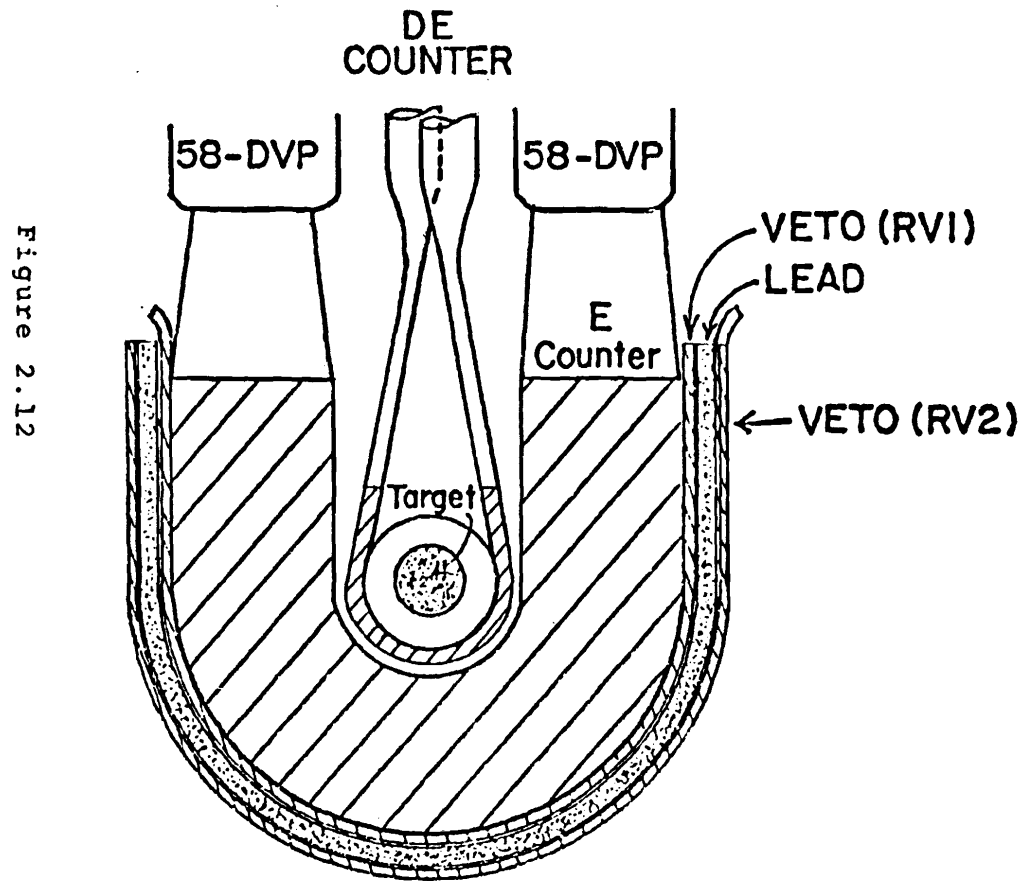


Figure 2.12

CROSS SECTION VIEW OF RECOIL DETECTOR

the vertical edges. Its upstream face was covered by a 1 cm lead sheet to detect gamma rays from neutral pion decay.

The downstream counter of the pair was circular with an outer diameter of 12.7 cm and an inner hole diameter of 2.5 cm.

5. Proportional Wire Chambers (PWCs)

All track measurements were done by PWCs. In addition to the momentum tagging chamber at the second focus, there were six sets or stations of PWCs. Table 2.7 summarizes these chambers' characteristics.

Stations 1 through 4 consisted of high pressure, high resolution chambers^{2.7} (70 μm (σ) spatial resolution) which measured the scattering angle. These stations measured tracks in the x (horizontal) and y (vertical) directions. Station 3 also measured along the u and v directions (rotated from the horizontal 45 and 135 degrees respectively).

Stations 1 to 4 consisted of PWC doublets with an effective wire spacing of 200 μm and an active area 3 cm in diameter. Each PWC singlet had a wire spacing of 400 μm and were assembled into pairs offset by half a wire spacing. This assembled staggered pair is called a

TABLE 2.7
PROPORTIONAL WIRE CHAMBER CHARACTERISTICS

<u>Chamber</u>	<u>High Voltage Plane</u>	<u>Signal Wire</u>	<u>Number of Wires</u>	<u>Wire Spacing (mm)</u>	<u>Gap^a (mm)</u>	<u>Window Size</u>
Momentum Tagging	25 μ m Al Foil	25 μ m W	64	1	8	8.2cm diameter
High Resolution ^b PWC's (Station 1-4)	25 μ m Al Foil	5 μ Tungsten @ 4.6gm Tension	76	0.4	1	3cm diameter active area
Station 5 (x, y)	25 μ m Al Foil	25 μ m W	32	1.5	8	10.2cm diameter
Station 6 ^c	75 μ m Cu Wire	25 μ m W	160	2.0	1.65	17.8 x 35.6cm rectangle

^aDistance between ground plane and signal plane.

^bData given for single plane. Chambers composed of doublet comprised of two singlets offset by 200 μ and separated by 3.8cm.

^cData given for single plane. Chamber had two planes offset by 1mm.

TABLE 2.7 (CONT.)

PROPORTIONAL WIRE CHAMBER CHARACTERISTICS (CONT.)

<u>Gas</u>	<u>Chamber</u>	<u>Operating Voltage (kV)</u>	<u>Output Signal Size</u>	<u>Time Resolution (ns)</u>
ArCO ₂ , Flowed at .1-.2l/min.	Momentum Tagging	3.9		
75% Ar., 24.6% Isobutane, .4% Freon at 50psi (Not Flowed)	High Resolution PWC's (Stations 1-4)	3.0	1mv into 1k Ω	7
ArCO ₂ Flowed at .1-.2l/min.	Station 5 (x, y)	2.9		
ArCO ₂ , Flowed at .2l/min.	Station 6	2.9		

doublet. The signals from the two singlet planes were interleaved by a special connector before being read into the online computer. The gas (75% argon, 25% isobutane, 0.4% freon at 50 psia) was not circulated; indeed the same volume of gas was used for months at a time. Each singlet had an efficiency of $99 \pm 1\%$.

Station 5, consisting of 1.5 mm wire spacing x and y chambers, was located just downstream of the spectrometer magnets. These were used primarily for online monitoring of beam position and size at the third focus. Station 6, located at the end of the experiment, consisted of a pair of 2 mm wire spacing chambers staggered by 1 mm to obtain an effective 1 mm wire spacing. Stations 3, 4, and 6 measured the momentum of the scattered track.

The chamber data was encoded before being read into the online computer. A block diagram of the readout is shown in Figure 2.13. A signal from the fast logic called the COINCIDENCE GATE was needed in order to read the PWC information into the online computer. More details on the fast logic are presented in the next chapter. The details of the readout system are described in references 2.1 and 2.8.

PWC READOUT ELECTRONICS

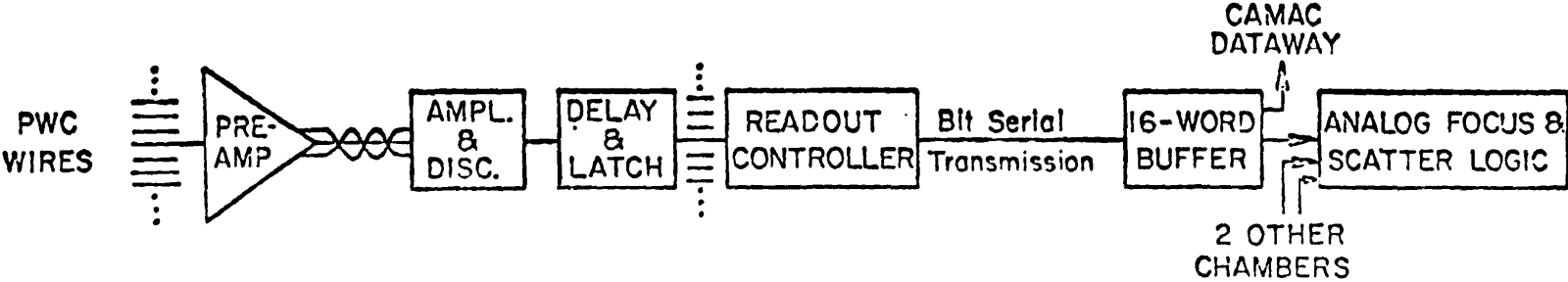


Figure 2.13

6. Muon and Electron Calorimeters

Electrons were identified by a lead-scintillator sandwich counter; muons by a iron-scintillator sandwich counter. Table 2.8 gives these counters' characteristics; Figure 2.14 shows the relative orientation of the counters.

The horizontal spatial dependence of the electron counter response was tested by moving the beam 13 cm left and right from the center of the counter. The response in either phototube changed by over 50% over this range, but the sum of their signals was constant to 2.5%. Plots of the summed pulse heights from the two electron calorimeter phototubes and from the two muon calorimeter phototubes are shown in Figure 2.15 and 2.16, respectively. These plots are for unscattered pions and protons at 50 GeV/c. Clearly a single cut on the summed muon pulse height (pulse height must be greater than that corresponding to the arrow in Fig. 2.16) removes both electrons and muons. This is the case because electrons lost all their energy in the electron calorimeter. Thus for events where the incident projectile was an electron, the pulse height from the muon calorimeter was approximately zero. The electron signal is approximately 2.5% of the incident pions. At 70 GeV/c the percentage of incident electrons

TABLE 2.8

Electron and Muon Detectors

Detector	Construction	Size	Phototubes	Radiation Lengths	Absorption Lengths ^a
Electron	15 - 0.25" Pb sheets interleaved with 14 - 0.25" scintillation sheets	8.0" V 15.75" H	2 - RCA 4522 4" Tubes	17.2	0.64
Muon	13 - 1.5" Fe sheets interleaved with 14 - 0.25" scintillation sheets	22.0" V 39.0" H	2 - Philips 56 DVP 2" Tubes	28.3	3.03

^aIn the absorption length the elastic scattering is subtracted.

ELECTRON AND MUON CALORIMETERS

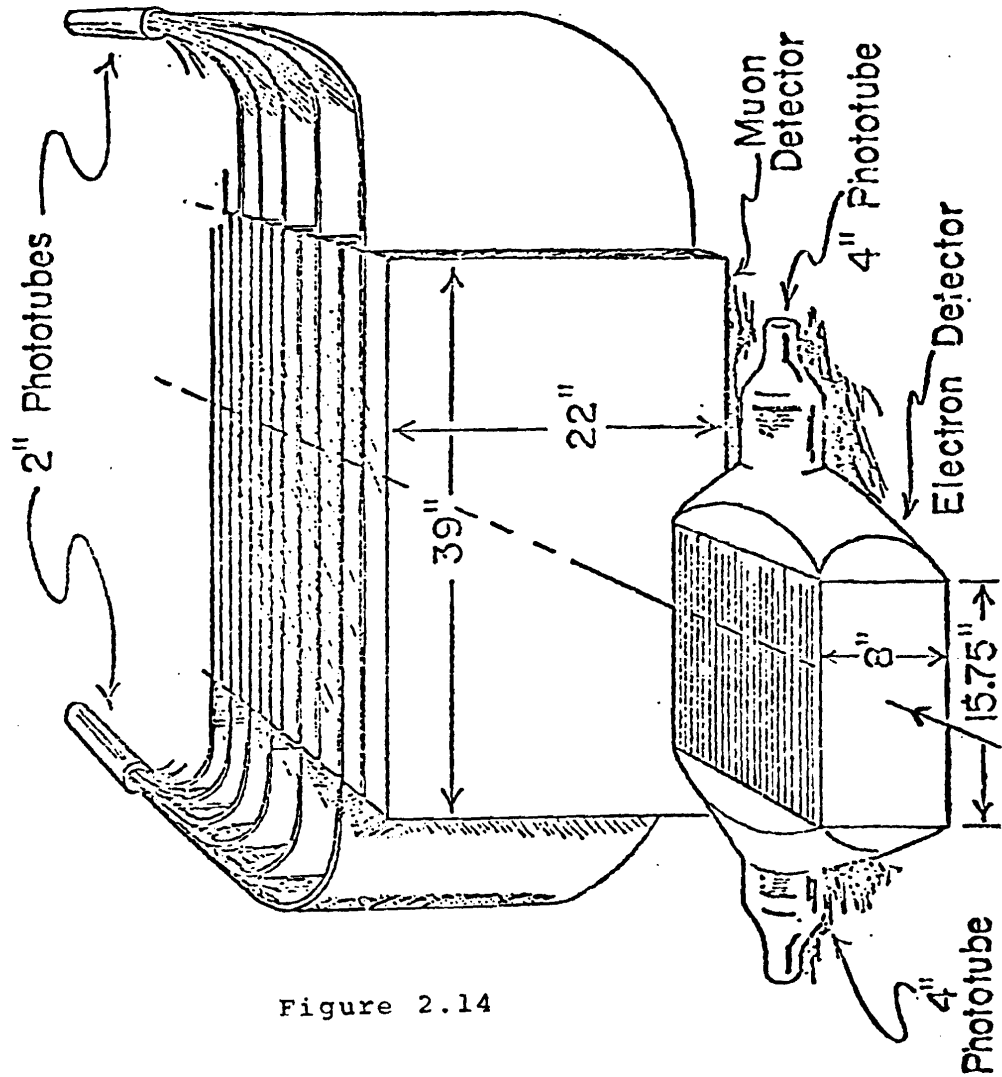


Figure 2.14

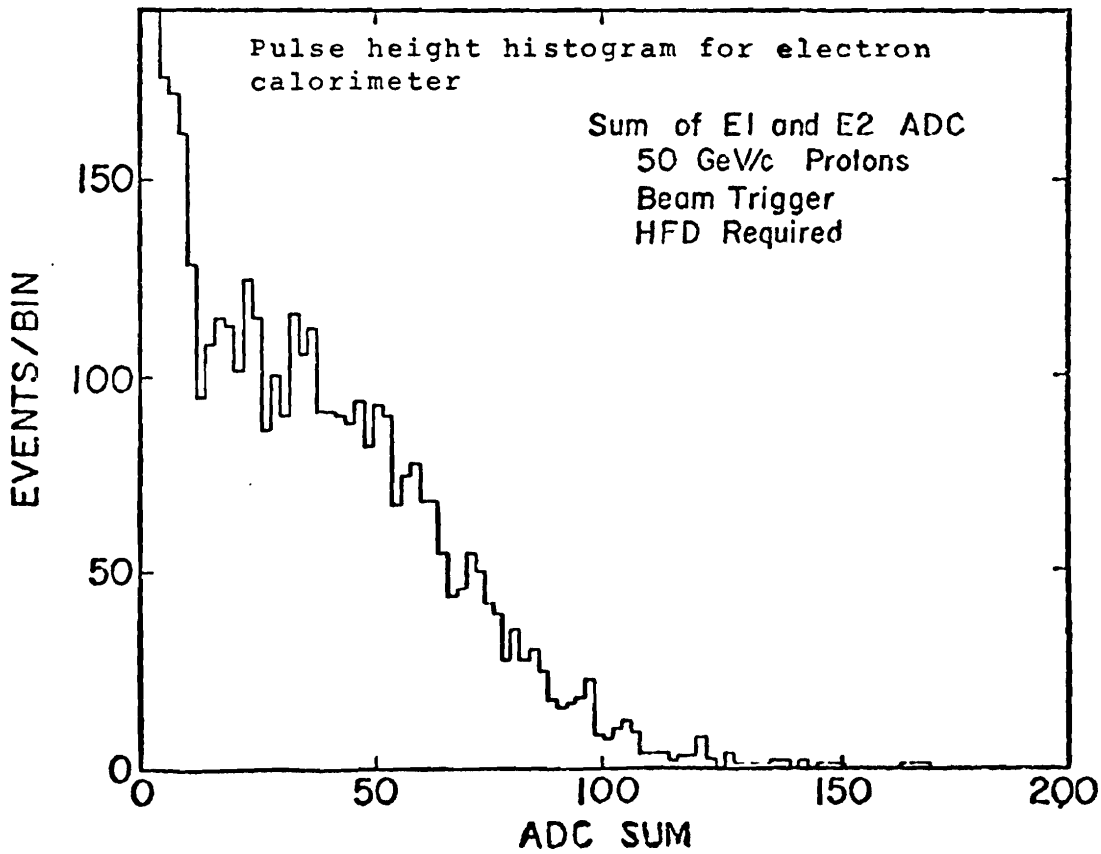
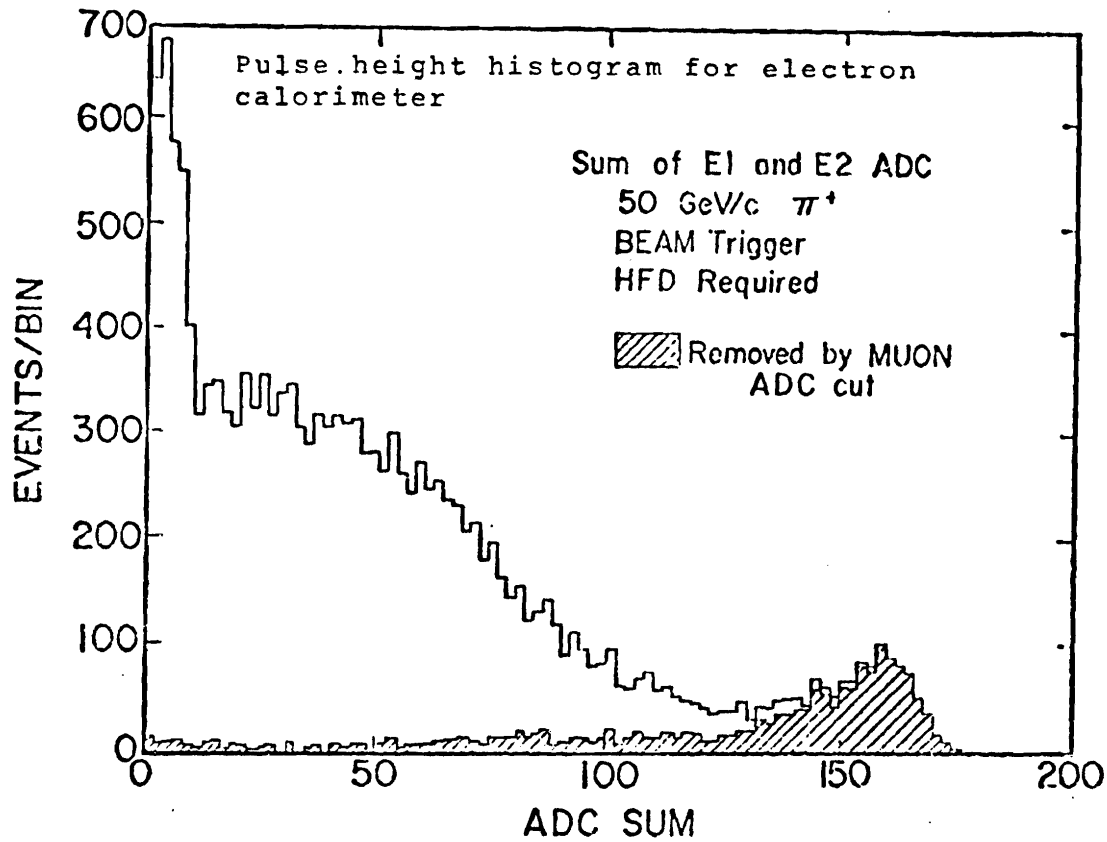


Figure 2.15

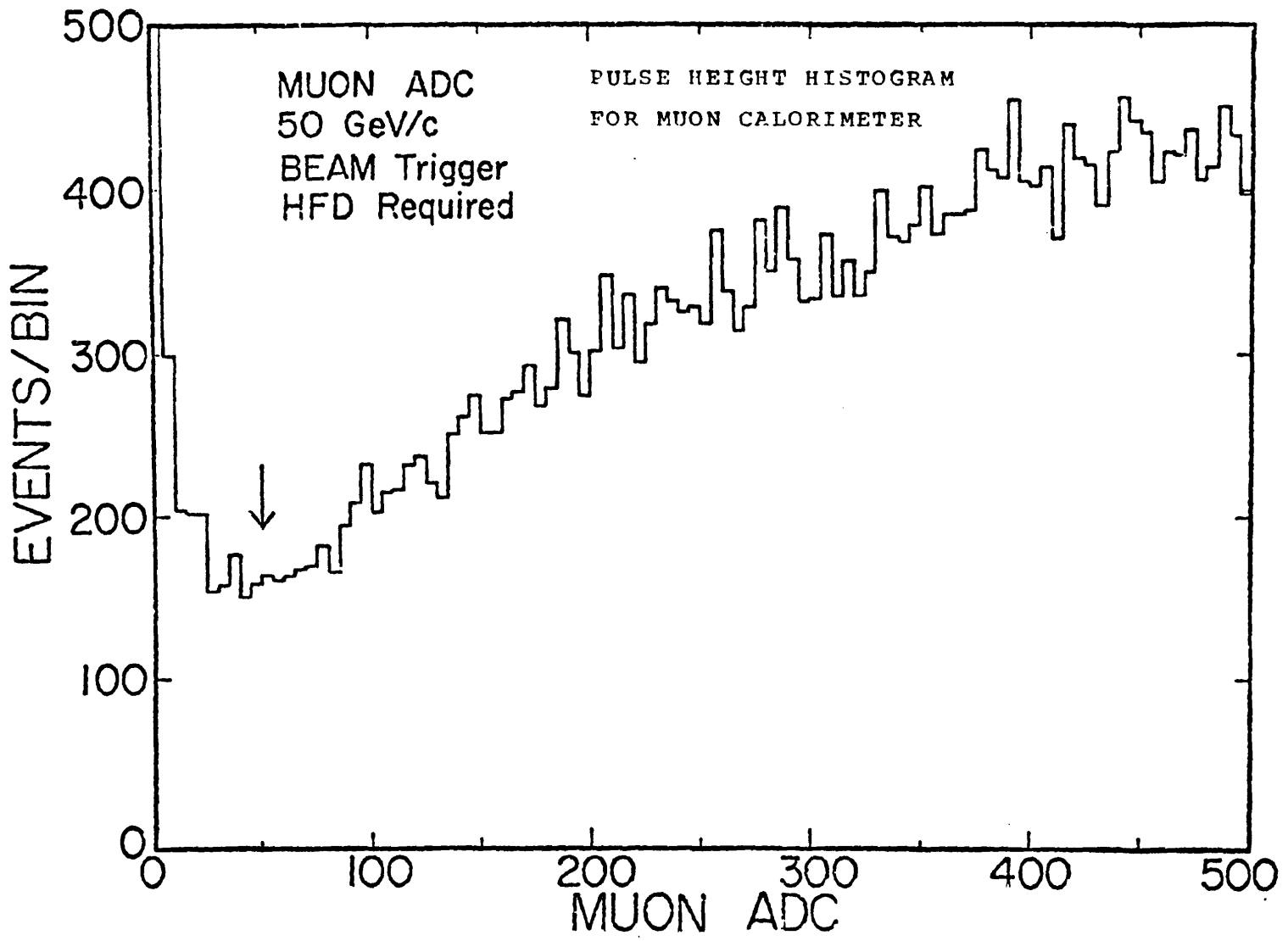


Figure 2.16

to incident pions is less than 2.0%; for 100 GeV/c and above this percentage is less than 0.1%.

D. Spectrometer Magnets

The two spectrometer magnets were identical in design to Fermilab main ring B2 dipoles^{2.9}. They had a 5 cm vertical by 10 cm horizontal aperture and a magnetic length, $\int B \cdot dl / B_{\text{center}}$, of 6.07 meters. In order to maximize the acceptance the upstream magnet was tilted 12.282 mrad with respect to the unbent beamline; the downstream magnet 29.900 mrad. Their net effect was to bend an unscattered beam particle by an angle of 34.12 mrad. A 670.5 cm by 1 cm wide single turn flip coil and a precision charge digitizer were used to map the field as a function of x (horizontal) and y (vertical) to an accuracy of $\pm 0.01\%$. The upstream magnet had a maximum x and y variation over the physical volume of 0.02% and 0.04% respectively. The downstream magnet had no measurable y variation and a x variation of 0.01%.

During the experiment the currents in both the upstream bending magnets and in the spectrometer magnets were monitored by NMR probes located in 0.91 m monitor magnets placed in series with each magnet string. The

NMRs had a 0.1% full scale reading; the magnetic fields were maintained to 0.03% ($\Delta B/B ; \sigma$).

CHAPTER 3

DATA ACQUISITION

A. Introduction

The data collection logic involved a two-level trigger. The first level used the scintillation counters in the experiment to provide a fast trigger. The second level acted on those events that passed the first level and used an analog device called the HARDWARE SCATTER FOCUS DETECTOR (HSFD)^{3.1}.

The three basic trigger types defined by the data acquisition logic were SCATTER, BEAM, and PSACVT. The SCATTER trigger (60% of the data) defined a single incident particle that scattered in the target region at a $-t$ greater than 0.001 (GeV/c)^2 and produced a fast forward secondary that traversed the rest of the apparatus. The BEAM trigger (35% of the data) was a sample of incident beam particles that fulfilled certain criteria upstream of the target. This trigger had no requirements downstream of the target. The third trigger type, PSACVT, was used to study the systematics of the HSFD.

B. Scintillation Triggers

The first part of the various scintillation triggers involved the scintillation and Cerenkov counters upstream of the concrete block. Figure 3.1 shows these elements.

All triggers required a signal from JV and from CTG where

$$JV = SA \cdot SB \cdot \bar{H} \cdot \bar{H1} \cdot \bar{H2}$$

$$H = D + U + W + E$$

$$CTG = \text{Kaon} + \text{Pion} + \text{Proton}$$

The counters D, U, W, E were described in the last chapter. A signal from JV implied the beam particle had a correct trajectory. A signal from CTG implied positive particle identification. The signals from the various Cerenkov counters were scaled (by anywhere from a factor of 1 to 2^{-16}).

Figure 3.2 exhibits the remaining part of the scintillation trigger system. A TAGBM trigger is defined as

$$TAGBM = B1 \cdot B2 \cdot Vh1 \cdot \text{Beam Rationer} \cdot JV \cdot CTG$$

The beam rationer was formed from signals from B1 and

BEAM INSTRUMENTATION AND PARTICLE IDENTIFICATION

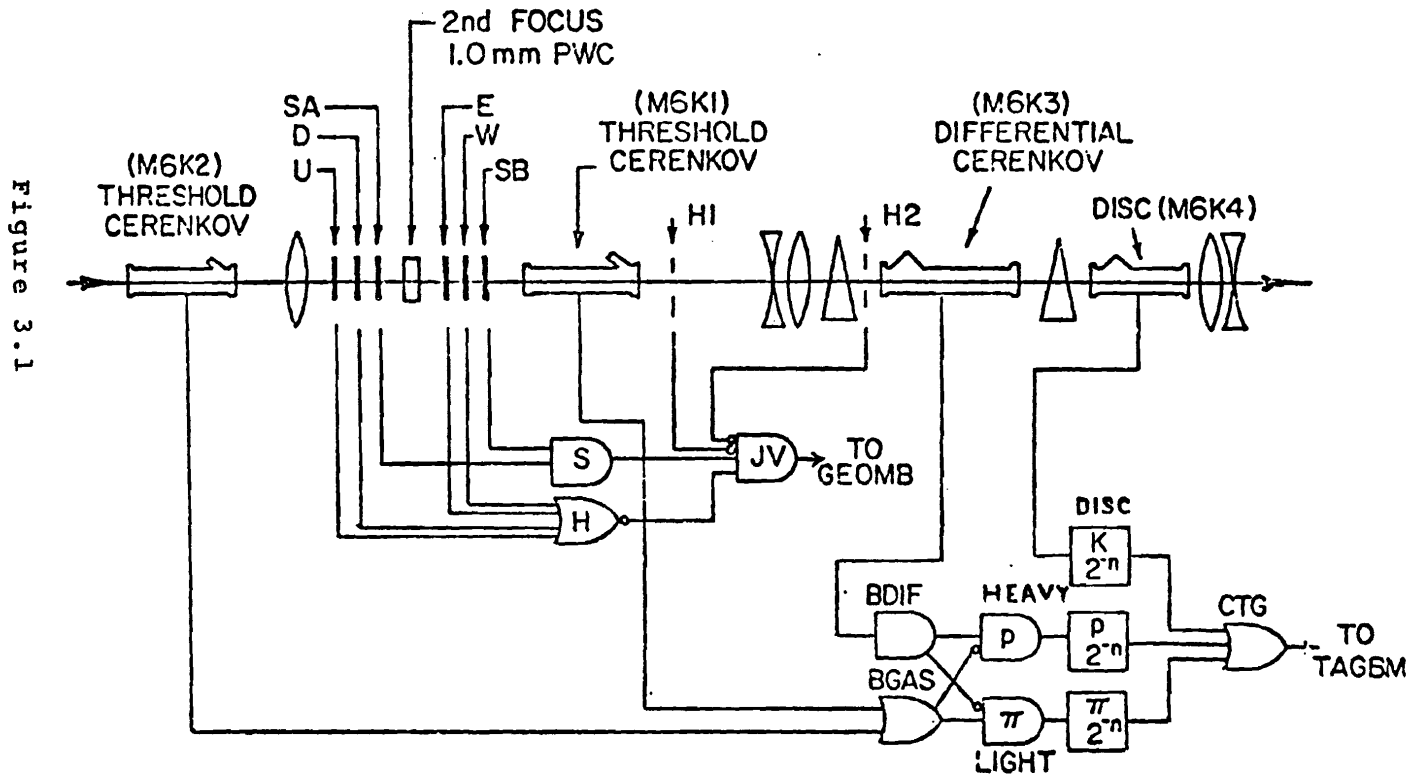
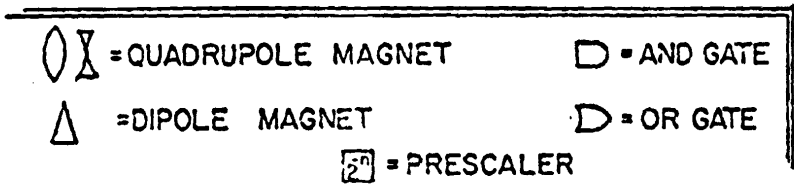
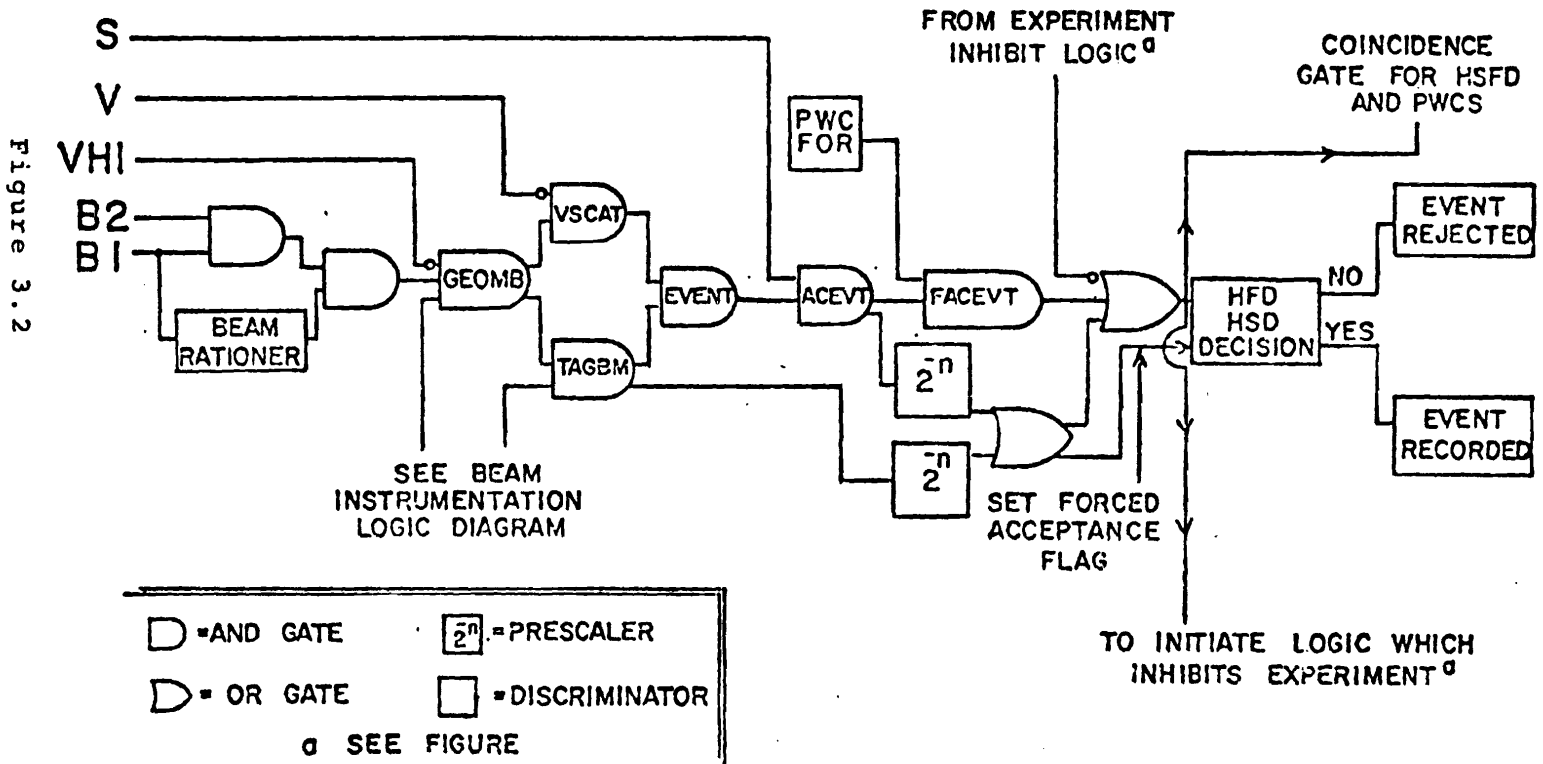


Figure 3.1



DATA COLLECTION LOGIC



rejected incident particles within 400 nsec of another particle. Figure 3.3 shows the ratiomer logic in detail. A certain number of TAGBM triggers were recorded by the online computer (regardless of the particle's subsequent history) for normalization, alignment, and studies of possible systematic errors. These recorded TAGBM triggers are known as BEAM.

The following is the scintillation trigger for a scatter:

$$\text{FACEVT} = \text{TAGBM} \cdot \text{S} \cdot \text{PWCFOR} \cdot \bar{\text{V}}$$

S was the large scintillator that covered the most downstream aperture. A signal from S implies the fast forward particle had traversed the entire spectrometer.

V meant that the particle missed the vetoes at the third focus. For the nuclear target running only V1 was used; for the high-t running V1 was in conjunction with the jaw shaped veto V2.

PWCFOR used the information from the PWCs on the block. It required the x and y chambers of Stations 1 and 2 to have one and only one coordinate; in addition the x and y chambers of Station 4 had to give a signal.

BEAM RATIONER FAST LOGIC (ALSO SEE FIGURE 3.2)

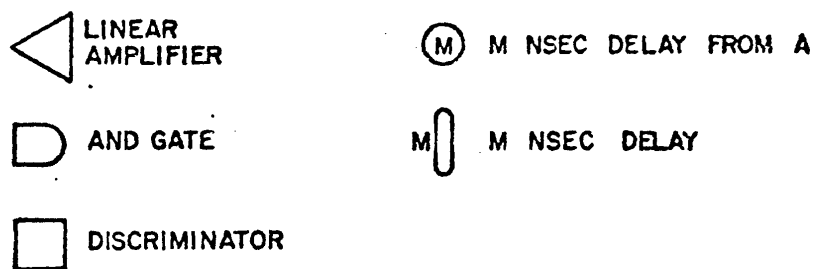
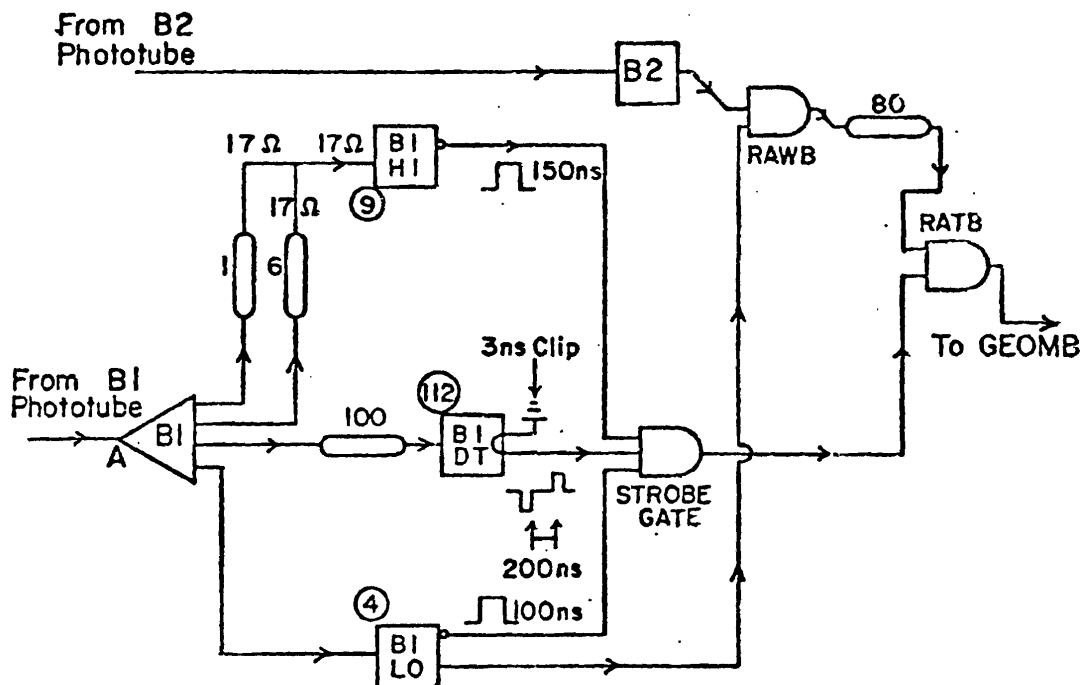


Figure 3.3

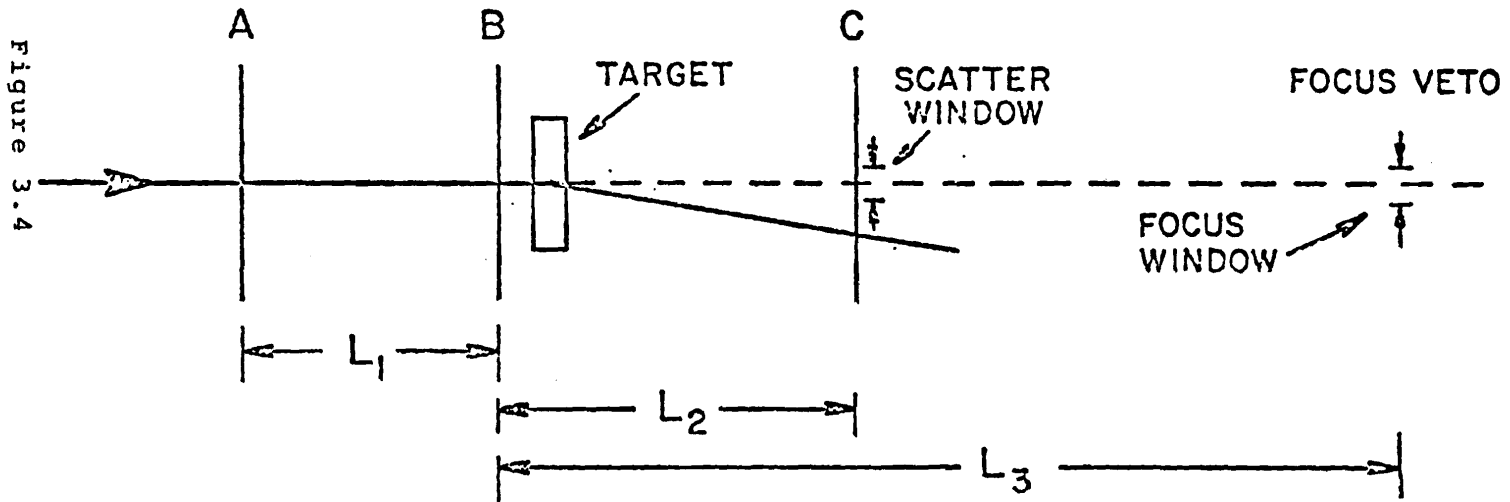
It took approximately 400 nsec for this first level of the trigger to make its decision.

C. Second Level Trigger: Hardware Scatter/Focus Detector

For this experiment a purely scintillation trigger for scattered particles was inadequate. Because of multiple scattering upstream of the target at best only 90% of the unscattered beam could be focused onto V1 (the small veto scintillation counter at the third focus). Since the signal was less than 0.5% of the beam rate, this 10% beam halo would have saturated the online computer data handling capability unless additional steps were taken. The solution was a second level slow trigger called the HARDWARE SCATTER FOCUS DETECTOR (HSFD) which made use of information from the PwCs on the concrete block. A FACEV1 trigger had to pass the HSFD test before being written on magnetic tape.

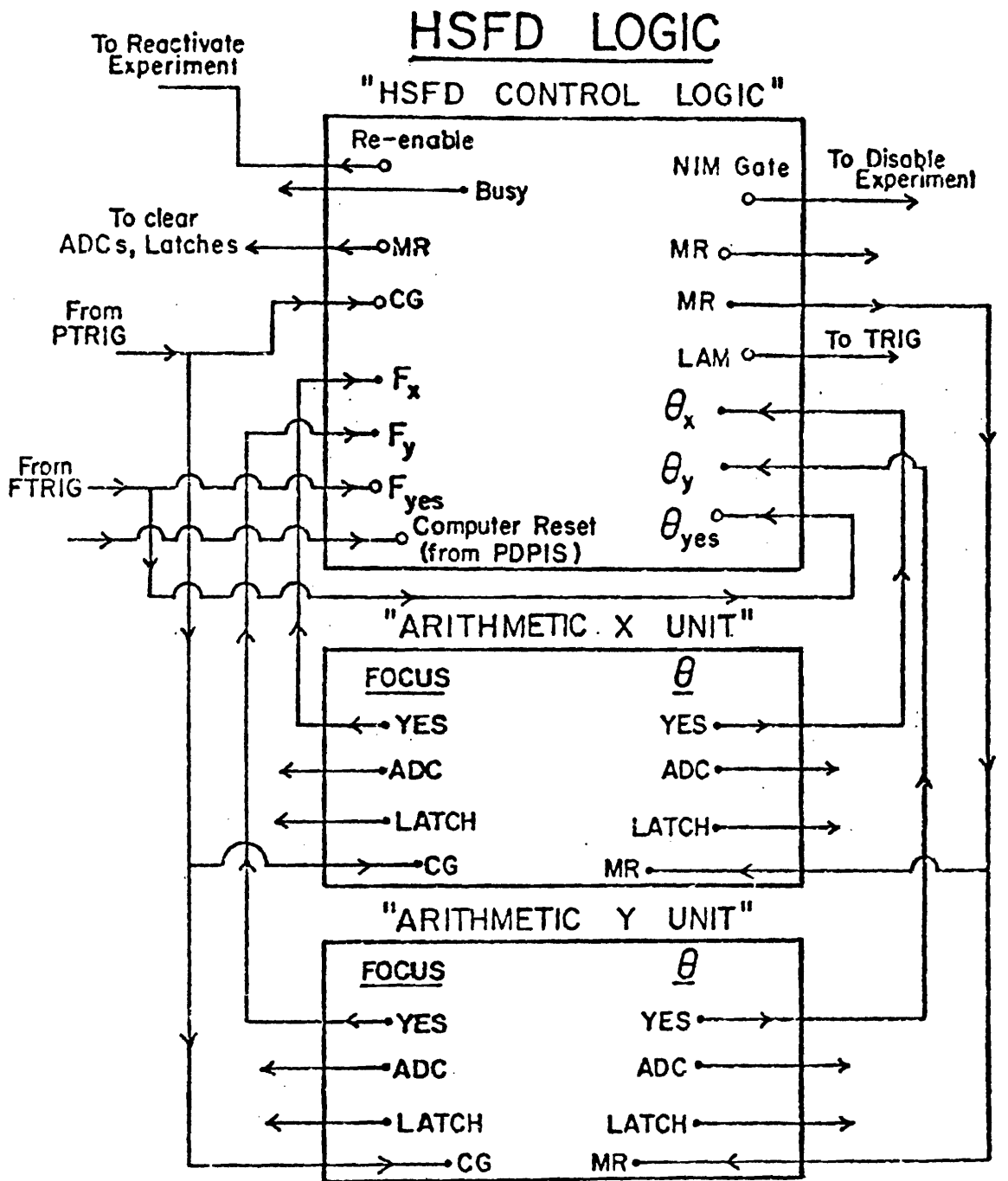
This second level trigger was an analog system which used the information from the high resolution PwCs to perform two calculations in parallel. Figures 3.4 to 3.6 schematically present these calculations which were made in both the x (horizontal) and y (vertical) planes.

HFD and HSD Geometry



SCATTER: $\frac{L_2}{L_1} A + C - \left(\frac{L_1 + L_2}{L_1} \right) B > \text{Scatter Window}$

FOCUS: $\frac{L_3}{L_1} A - \left(1 + \frac{L_3}{L_1} \right) B < \text{Focus Window}$



MR = Master, Reset

CG = Coincidence Gate

LAM = Look-At-Me

• = TTL Pulse

○ = NIM Pulse

 θ = Refers to Hardware Scatter Detector

F = Refers to Hardware Focus Detector

Figure 3.5

HSFD CONTROL LOGIC (ALSO SEE FIGURE 3.5)

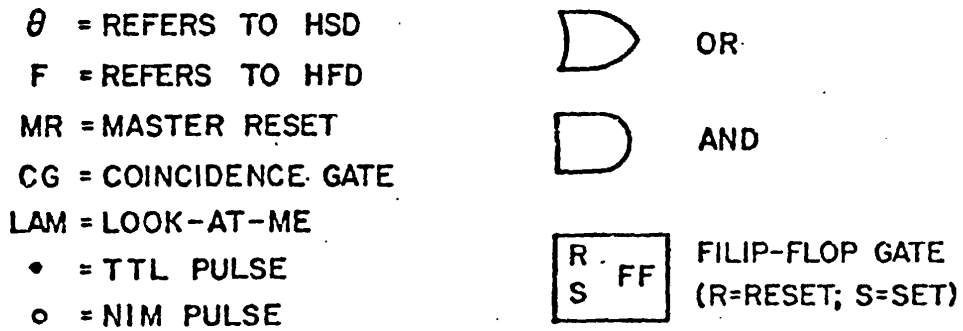
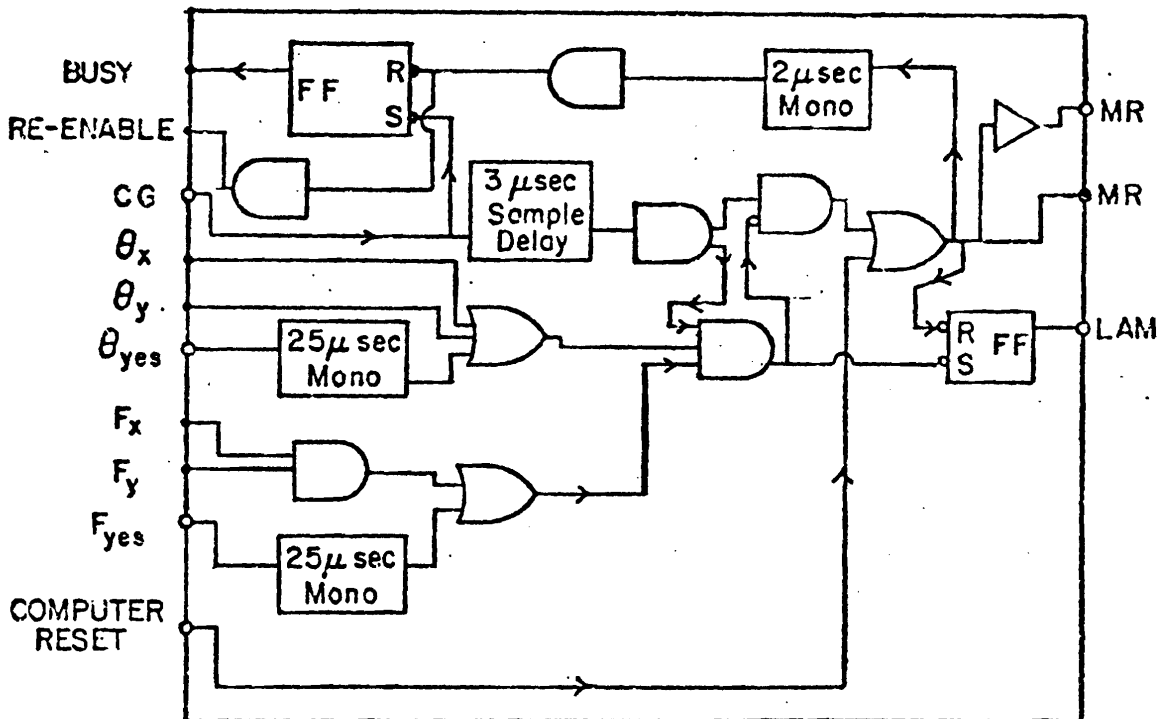


Figure 3.6

In the first calculation the incident trajectory was projected to the veto plane. If the horizontal (vertical) projection was inside a preset window, HFDX (HFDY) was set true. This process selected those particles in the incident beam phase space that would have struck the veto if they were not scattered. In this mode the analog system is called the Hardware Focus Detector (HFD).

In the second calculation the incident trajectory was projected to PwC Station 4 (most downstream PwC on the concrete block). If the projected coordinate and the actual coordinate differed by more than a fixed amount in the x (y) planes, then HSDX (HSDY) was set true. The preset amount corresponded to a t of approximately -0.001 (GeV/c)^2 . In this mode the analog system is called the Hardware Scatter Detector (HSD).

The scatter trigger is then

$$\text{SCATTER} = \text{FACEVT} \cdot (\text{HFDX} \cdot \text{HFDY}) \cdot (\text{HSDX} + \text{HSDY})$$

The results of the HFD and HSD calculations were recorded in analog to digital converters (ADCs). In order to study the effect of the HSD, a prescaled

number of FACEVT triggers were accepted without the processor requirement. These events are called PRESCALED ACCEPTED EVENTS (PSACVT).

Figures 3.7 and 3.8 show the results of the HSF \bar{D} operation. Figure 3.9 presents a sample of PSACVT; the shaded area are those PSACVT rejected by the HSF \bar{D} .

The HSF \bar{D} took approximately 5 μ sec to make its decision.

D. Online Computer

A PDP15/40^{3.2} recorded the data and monitored the apparatus performance. The online program was designed primarily for speed in data acquisition and could read up to 800 events per one second spill. Two factors were instrumental in achieving this high rate.

First an economical event format was implemented. An event generated about 30 18-bit words: about 20 words for the partially encoded PWC hit locations (2000 wires in 16 chambers), 2 words of latch information, and 6 words with 2 ADCs per word. Secondly a double buffering scheme was used. During the spill as one buffer filled with events, the other was written onto the disk within the PDP15. Between spills these records were

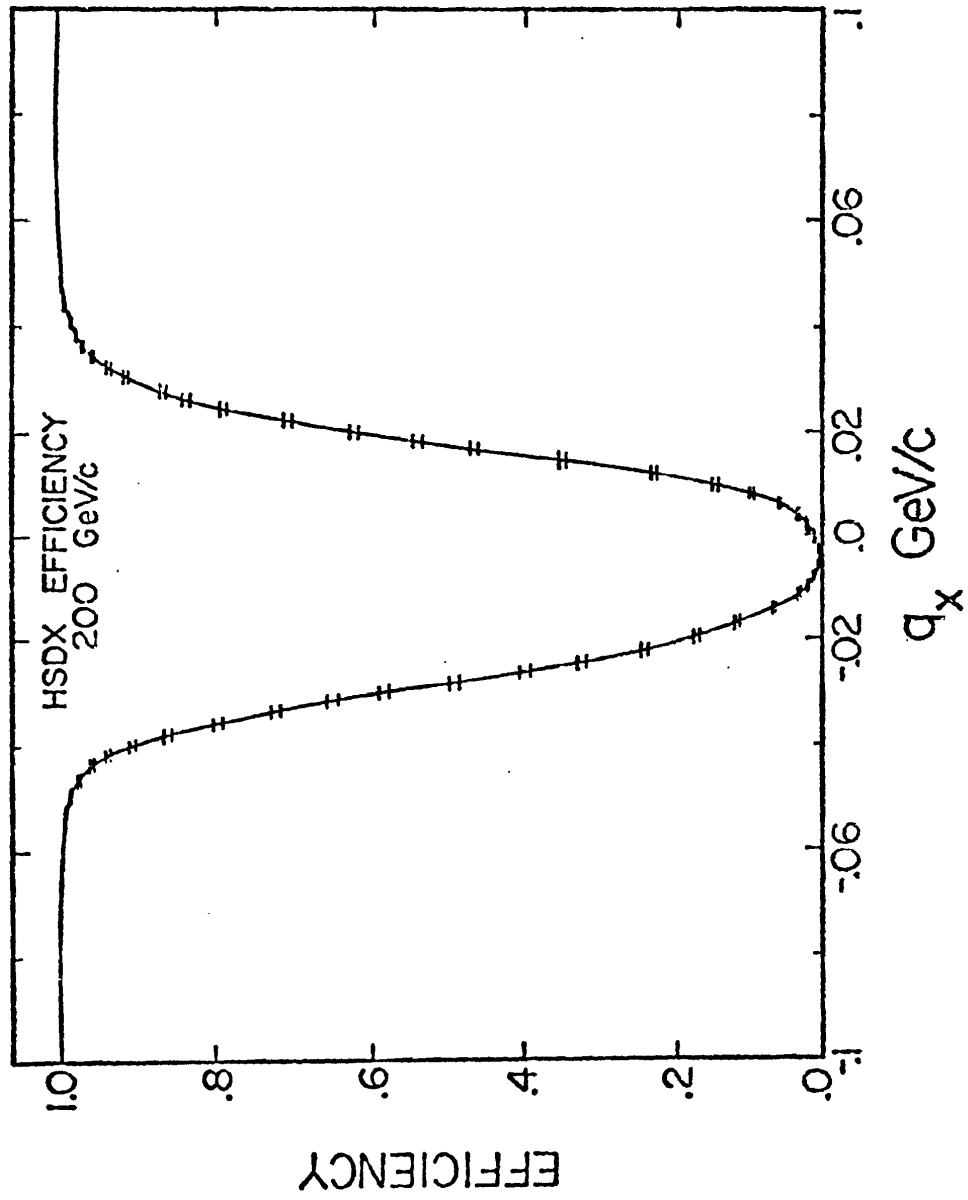


Figure 3.7

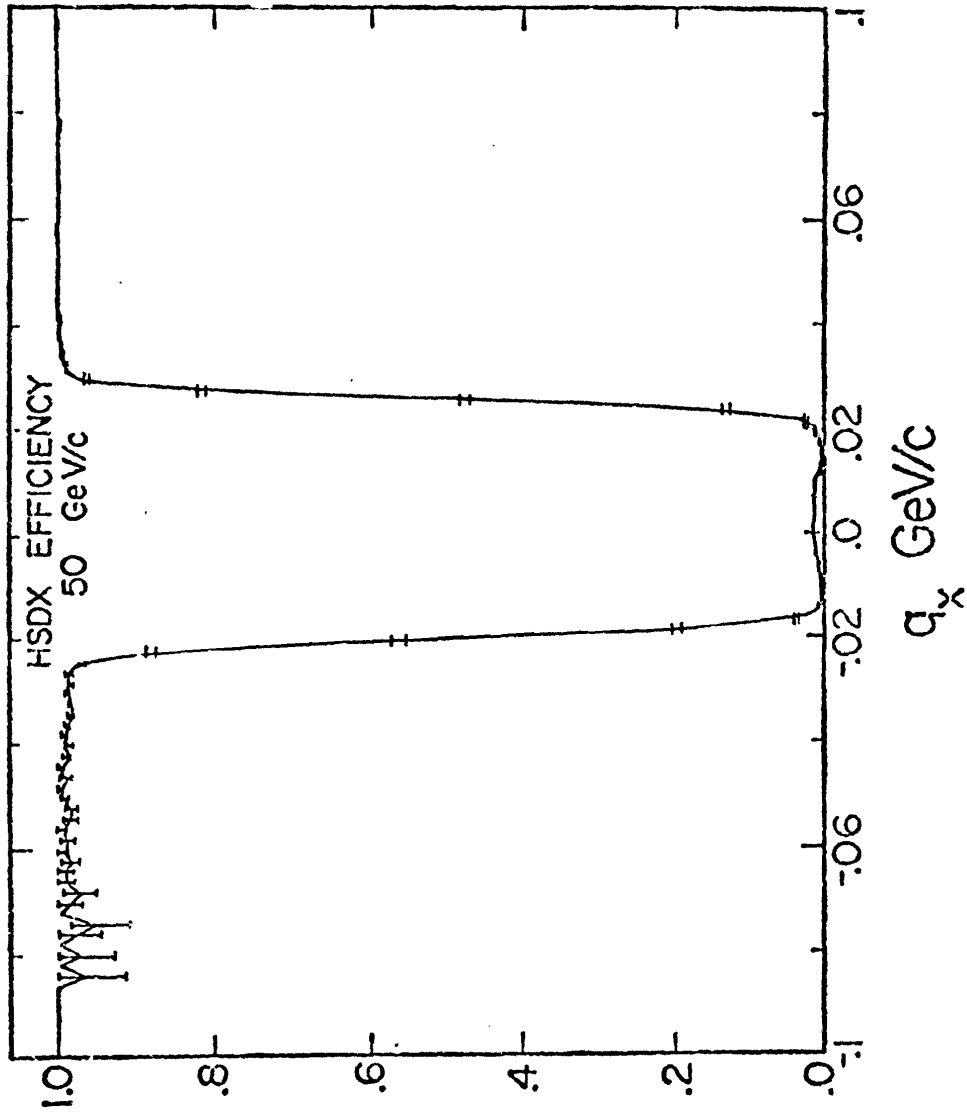


Figure 3.8

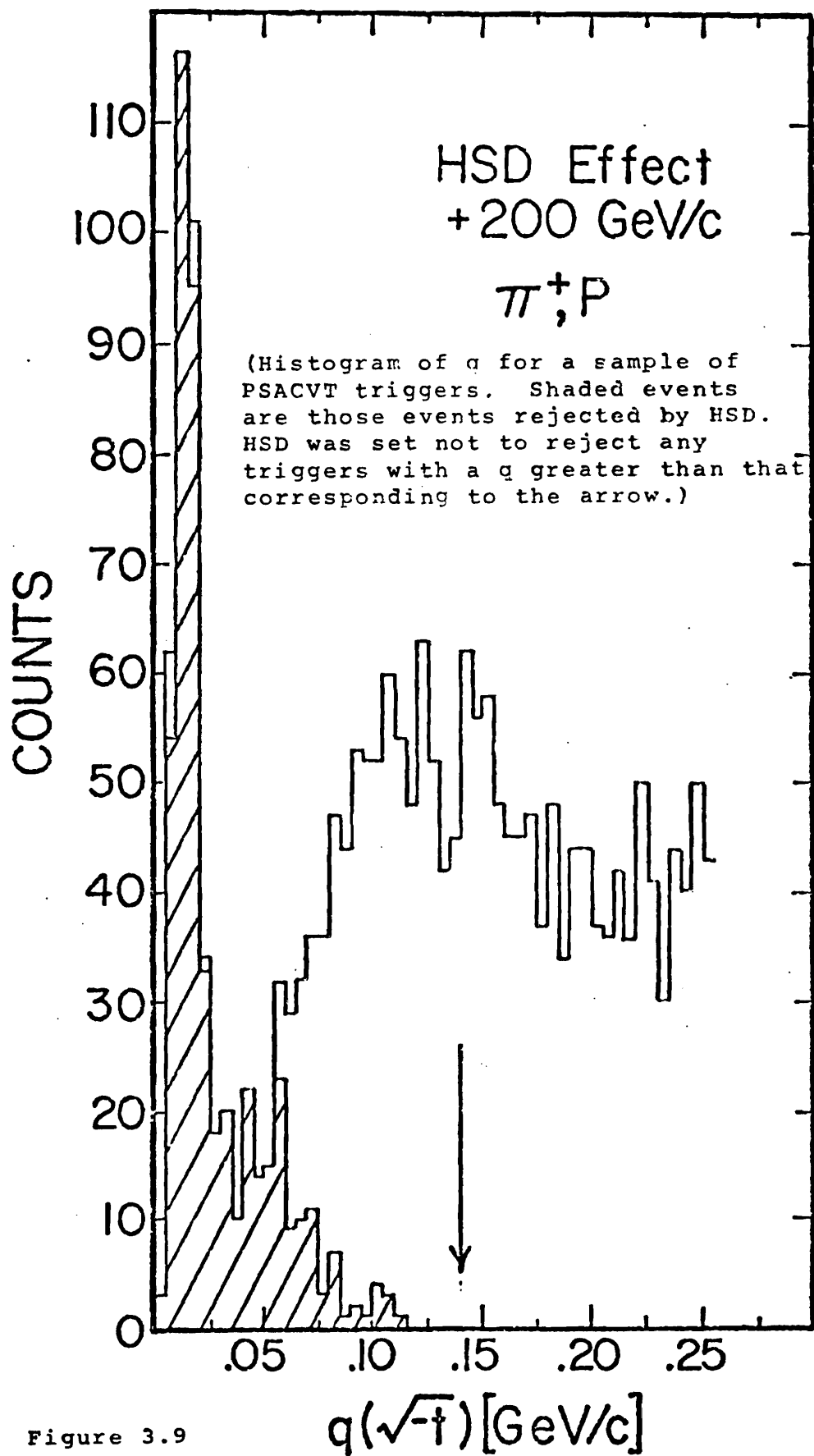


Figure 3.9

transferred from the disk to magnetic tape via the same buffers. The online monitoring was performed while the events were in these buffers.

All information was transferred to and from the computer via CAMAC modules. The PWC encoded information (giving the chamber and wire activated) was stored in special word buffers before being accepted by the computer. These word buffers had a special output in order to input the necessary information to the HFSD. Standard CAMAC modules were used for scaler, 512 channel ADC, and latch information. In addition the computer read in periodically from a scanning digital voltmeter (DVM) values of various phototube voltages and of the LH₂ resistors. Finally there existed a system of "stand-alone" scalers which were independent of the PDP15. These scalers served as diagnostics to insure the apparatus was functioning correctly.

Besides recording the data, the PDP15 monitored the status of the apparatus. Histograms and scattergrams of a variety of quantities could be produced. Some of the more relevant ones were

1. PWC wire map distributions to give information concerning chamber efficiency and the beam tune.

2. ADC pulse height distributions.
3. Scintillation counter latch information to detect failures in the fast logic.

These histograms were made on an event by event basis.

Tables 3.1 and 3.2 give a list of latch and ADC information written for each event onto magnetic tape.

The online computer could write a trigger onto magnetic tape in approximately 1 msec.

E. Trigger Rates

During the time a decision was being made to read in a trigger (e.g. by the HSPD), the logic would not accept new events. The logic to accomplish this and to reactivate the apparatus is shown in Figure 3.10. PTRIG initiated the process that deactivated the equipment; note that a FACEVT, PSACVT, or BEAM activated PTRIG. BEAM and PSACVT also activated FTRIG which started the process such that an event could be read in regardless of the result of the HFSD test. After a trigger was rejected, an event read into the PDP15, or a new spill occurred, the PWC word buffers, ADCs, latches,

TABLE 3.1

Computer Latch Information

<u>Latch</u>	<u>Latch</u>
B1	HFDX (HFD in x plane)
STROBE (from beam rationer)	M6K2 (most upstream Cerenkov counter)
B2	HSDX (HSD in x plane)
JV	HSDY (HSD in y plane)
V1	BEAM
VH2	PSACVT
VH3	FACEVT
DISC ^a	HFDY (HFD in y plane)
RV1	VH1
RV2	FO1 ^b (for x of PWC station 1)
S	FO2 ^b (for y of PWC station 1)
LIGHT ^a	FO3 ^b (for x of PWC station 2)
HEAVY ^a	FO4 ^b (for y of PWC station 2)
BDIF ^a	FO9 ^b (for x of PWC station 4)
BGAS ^a	FO10 ^b (for y of PWC station 4)
V2	FOP ^c

^aSee Figure 3.1

^bFOn on if PWC plane had a wire activated

^cFOP on if any plane in PWC stations 1 and 2 had > i coordinate

TABLE 3.2

ADC Information (512 channels/ADC)

ADC

Muon Counter (sum of both phototubes)

TR	}	Recoil Detector Scintillators (see Fig. 2.12)
R1		
R2		
R3		
R4		

Electron Counter A

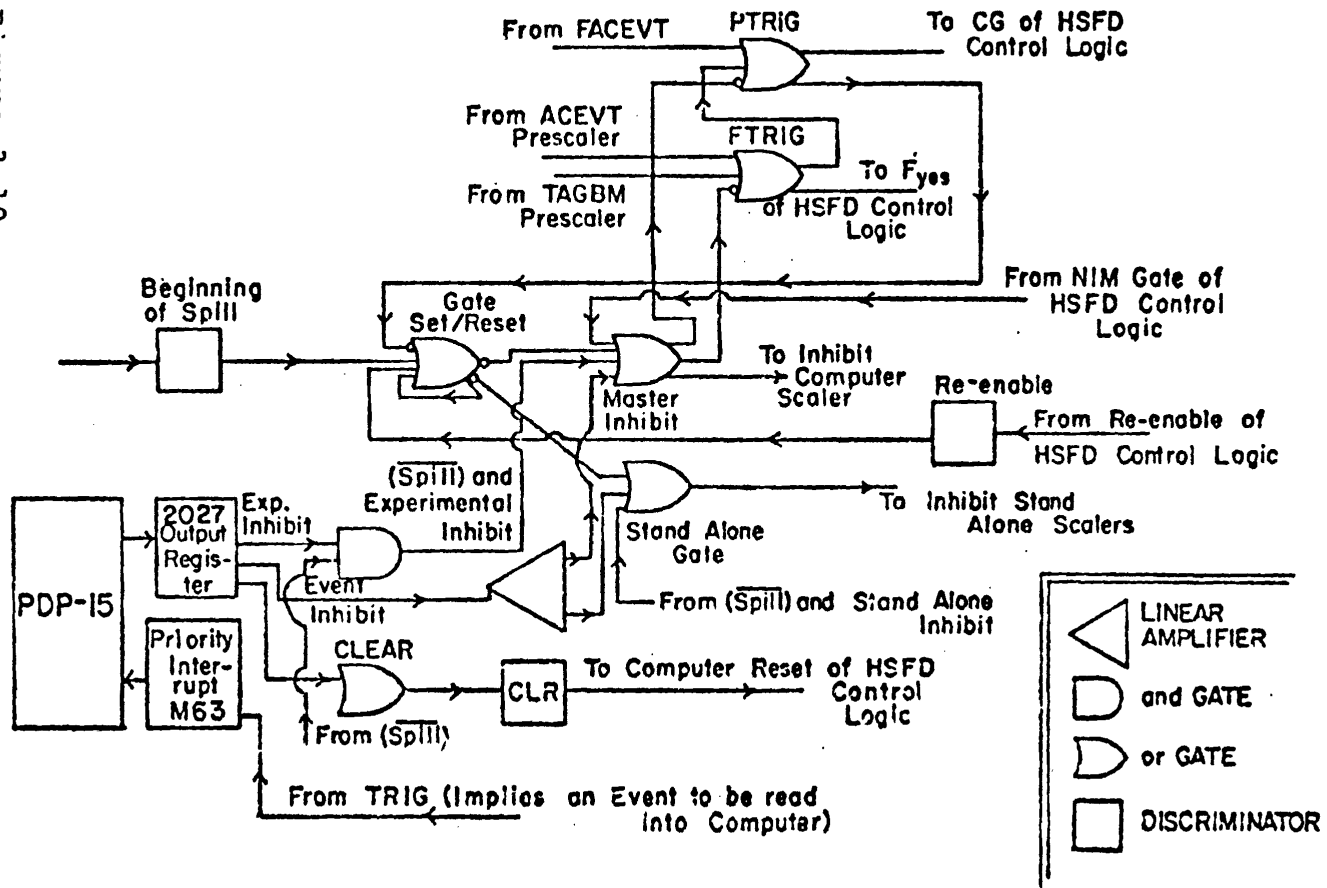
Electron Counter B

HSDX
HSDY
HFDX
HFDY

FAST LOGIC TO ACTIVATE AND DEACTIVATE APPARATUS

(Also see Figs. 3.1, 3.2, 3.5, 3.6*) *other fast logic figures

Figure 3.10



and all scalers were cleared; the logic could now accept a new event.

Tables 3.3 through 3.6 give examples of actual rates. The first two tables apply to the nuclear target running; the latter two to the high-t running. The differences between the scaler totals for the two types of running reflect the effect of the jaw shaped veto V2.

Under typical running conditions 500,000 particles per one second spill were incident upon the apparatus. Approximately 250 triggers were read into the computer. These triggers were of the type FACEVT, PSACVI, and BEAM. The number of the latter two read in depended of course on the factor by which they were scaled. For prescale factors of 2^{-10} for both, about 10 PSACVT and 40 BEAM were accepted by the computer in a one second spill.

In order to record as many of the rarer particles as possible (\bar{p} , K^{\pm}) the predominant particles (π^{\pm} , p) trigger rate was scaled. Typically the predominant particles were scaled to result in a 60% live time for the apparatus and an effective rationed beam of 10,000 per one second spill.

TABLE 3.3

An Example of Trigger Rates:

Carbon at -70 GeV/c

For this example the prescalers were set to the following: ① TAGBM = 2^{-10} ② ACEVT = 2^{-10} ③ Pion = 2^{-4}
 ④ Kaon = 2^0 ⑤ Proton = 2^0

The rates are for a one second spill.

<u>SCALAR</u> ^a	<u>Number of Counts (1K = 10³)</u>
RAWB	419.5k
RATB	328.8k
GLOMB	307.0k
TAGBM	35.5k
VSCAT	127.4k
EVENT	14.6k
ACEVT	12.5k
FACEVT	8.4k
PTRIG	8.4k
TRIG ^b	322
BEAM	36
PSACVT ^b	12

Apparatus Live Time 65%

^aScalers count only during live time

^bTRIG is number of events read in by PDP15.

It includes BEAM, PSACVT, and SCATTERS which passed HSF D requirements.

TABLE 3.4

Scaler Ratios: Carbon at -70 GeV/c

These ratios are derived from Table 3.3

<u>RATIO</u>		<u>COMMENT</u>
RATB/RAWB	.78	Effect of Beam Rationer
GEOMB/RATB	.93	Effect of VH1 and JV
TAGBM/GEOMB	.12	Effect of Cerenkov Tagging
VSCAT/GEOMB	.41	Effect of 3rd Focus Veto ^a
EVENT/SCAT	.11	Effect of Cerenkov Tagging
ACEVT/EVENT	.86	Effect of 5 counter
FACEVT/ACEVT	.67	Effect of High Resolution PWC requirements (PWCFOR)
$\frac{\text{TRIG} - (\text{BEAM} + \text{PSACVT})}{\text{PTRIG} - (\text{BEAM} + \text{PSACVT})}$.03	Effect of HSPD

^aOnly V1 was at the 3rd focus

TABLE 3.5

An Example of Trigger Rates:
High-t Data at +200 GeV/c

The prescalers were set to the following: 1. TAGBM=2⁻¹²
2. ACEVT=2⁻³ 3. Pion=2⁰ 4. Kaon=2⁰ 5. Proton=2⁻¹. The rates are for a one second spill.

SCALER ^a	Number of Counts (1K=10 ³)
RAWB	392K
RATB	293K
GEOMB	280K
TAGBM	156K
VSCAT	24.7K
EVENT	13.2K
ACEVT	1.8K
FACEVT	1.0K
PTRIG	1.1K
TRIG ^b	384
BEAM	37
PSACVT ^b	7

Apparatus Live-Time - 60%

^aScalers count only during live-time

^bTRIG is number of events read in by PDP15. It includes BEAM, PSACVT; and SCATTERS which passed HSF requirements.

TABLE 3.6

Scaler Ratios: High-t at +200 GeV/c. These ratios are derived from Table 3.5.

Ratio		Comment
RATB/RAWB	.75	Effect of Beam Ratios
GEOMB/RATB	.96	Effect of VH1 and JV
TAGBM/GEOMB	.56	Effect of Cerenkov Tagging
VSCAT/GEOMB	.09	Effect of 3 rd Focus Veto
EVENT/SCAT	.53	Effect of Cerenkov Tagging
ACEVT/EVENT	.14	Effect of S counter
FACEVT/ACEVT	.56	Effect of High Resolution PWC Requirement (PWCFOR)
$\frac{\text{TRIG} - (\text{BEAM} + \text{PSACVT})}{\text{PTRIG} - (\text{BEAM} + \text{PSACVT})}$.33	Effect of HSFD

^aBoth V1 and V2 were at the 3rd focus.

CHAPTER 4

DATA REDUCTION: NUCLEAR TARGET DATA

A. Introduction

Data reduction proceeded in several steps as shown in Figure 4.1. There existed 70 data tapes which were written by the PDP15. These tapes contained in encoded form PWC, ADC, latch, DVM, and computer scaler information (see Chapter 3 ,Section D).

The first step was to produce a set of library tapes which were in a format the Fermilab CDC6600 could conveniently read. Alignment parameters of the apparatus were then calculated. Next data summary tapes were produced which contained relevant kinematical quantities (such as $q[=(-t)^{1/2}]$ and the recoil mass of the scatter). Then cuts were applied to the data, and q distributions were produced for the target full and empty data.

In parallel Monte Carlo summary tapes were produced. These tapes contained the same kinematical quantities as the data summary tapes. The same cuts as applied to the data were applied to the Monte Carlo events, and from the passed events the following two

NUCLEAR TARGET OFF-LINE ANALYSIS DIAGRAM

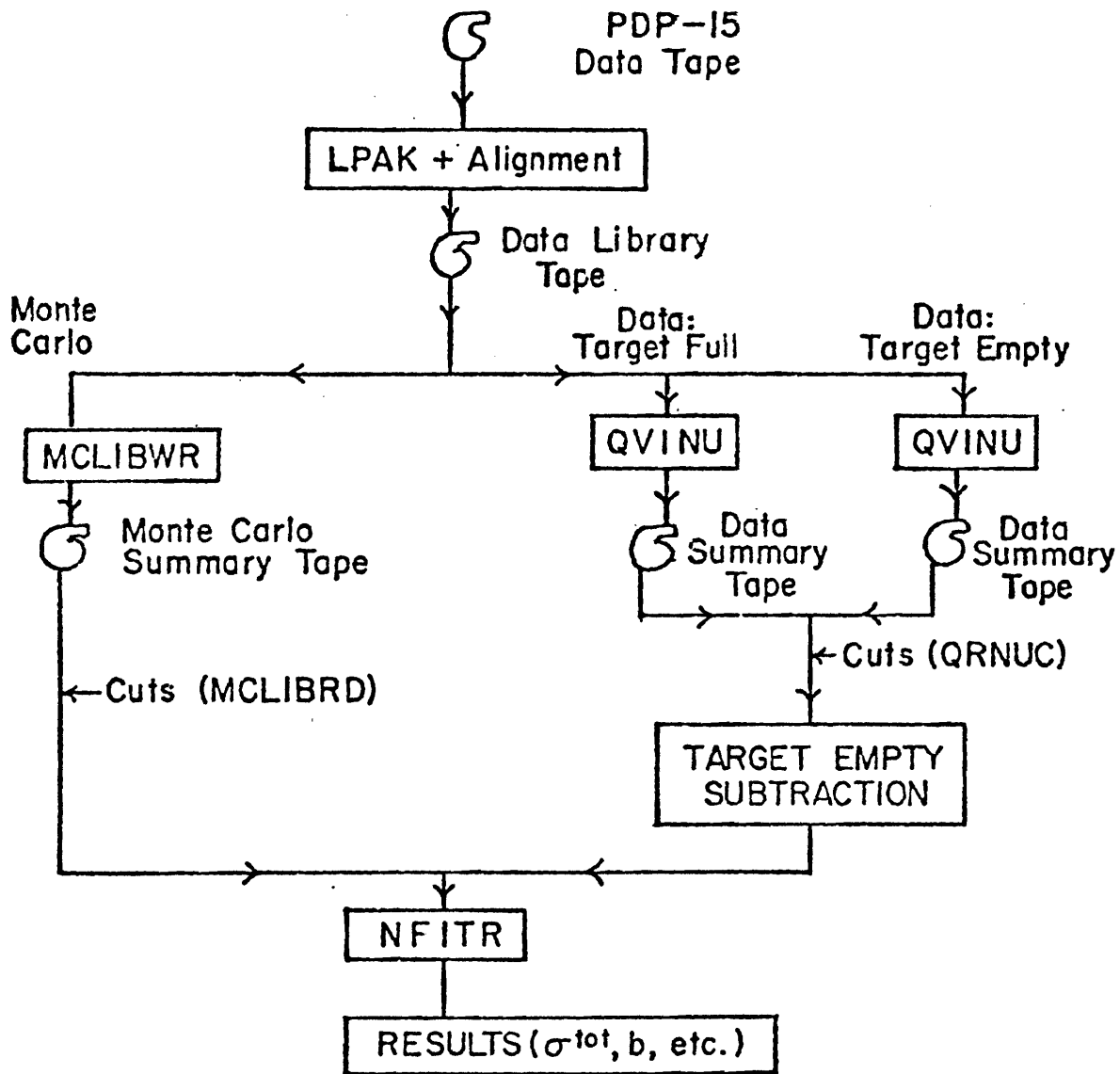


Figure 4.1

effects could be calculated:

1. the apparatus acceptance as a function of q
2. the migration of a generated q to a measured q due to the finite measurement resolution of the apparatus

Finally the data was normalized, and a target empty subtraction was performed. The theoretical form of the cross section was modified via the Monte Carlo results and compared to the normalized data. From this comparison the values of the parameters of interest (total cross section, the forward slope, etc.) were extracted.

B. Data Library Tapes

The data library tapes were produced from the PDP15 data tapes by the program LPAK. The information from the data tapes was decoded and then written onto the library tape in a form the CDC6600 computer could easily handle (note that the PDP15 uses 18 bit words while the CDC6600 uses 60 bit words).

For the purpose of the offline analysis the PWC stations were classified as given in Table 4.1. Thus the momentum tagging PWC was plane 15; the x of PWC station 1 was plane 1, etc. For the case of the high pressure, high resolution PWCs, a plane referred to a doublet (160 wires with an effective wire spacing of 200 μm ; see Chapter 2, Section C). Reference to the wires for these PWCs refer to those of the staggered pair, not of each singlet (thus adjacent wires come from different singlets).

In order for an event to have been written onto the library tape, the following criteria had to be satisfied:

1. One and only one valid coordinate in PWC planes 1,2,3,4,9,10,15
2. At least two of PWC planes 5,6,7,8 had one and only one valid coordinate
3. At least one of PWC planes 11,13,14 had one and only one valid coordinate

What constituted a valid coordinate depended on such factors as whether a chamber contained multiple coordinates, or whether a chamber plane consisted of a staggered pair doublet. The wire pattern of each

TABLE 4.1^a

PWC Plane Definitions in Off-Line Analysis

PWC Element	Plane Number
x = Station 1 ^b	1
y = Station 1 ^b	2
x = Station 2 ^b	3
y = Station 2 ^b	4
x = Station 3 ^b	5
y = Station 3 ^b	6
u = Station 3 ^b	7
v = Station 3 ^b	8
x = Station 4 ^b	9
y = Station 4 ^b	10
x = Station 5	11
y = Station 5	12
x = Station 6	13
x = Station 6	14
Momentum Tagging	15

^aSee Chapter 2, Sec. 5 for PWC station descriptions.

^bA plane refers to a staggered pair doublet.

coordinate was classified via cluster type. Some of the more relevant cluster types are given in Table 4.2. Table 4.3 gives the definition of valid coordinates for the PWCs.

If a chamber was not a doublet and there existed multiple coordinates in that chamber, then the information from that chamber was considered invalid. This could or could not prevent an event from having been written onto the library tape. If the situation occurred in plane 15 (momentum tagging chamber) then by criterion 1 above, the event would have been rejected. But if the situation occurred in plane 13, then the event still had a chance to have been written onto the library tape because of criterion 3 above.

The situation was different for multiple coordinates in a doublet PWC. Here by use of the following algorithm multiple coordinate events could be salvaged:

1. If there was one and only one coordinate with cluster type 5,6, or 7 and all other coordinates had cluster types 1,2,3, or 4, then the first coordinate was considered valid and kept for the future analysis, while the latter coordinates were deleted

TABLE 4.2
PWC Cluster Types^a

Cluster Type Number	Wire Map ^b
1	1010101
	↑
2	10101
	↑
3	101
	↑
4	1
	↑
5	11
	↑
6	111
	↑
7	1101 or 1011
	↑ ↑

^aListed are the most relevant cluster types. In actuality there existed 32 types.

^bThis map gives the pattern of PWC wires hit. For the siamesed PWCs the wire spacing is that of a doublet (i.e. 200 μm) 1 = wire activated; 0 = wire not activated. The arrow indicates centroid.

TABLE 4.3
Valid PWC Cluster Types

PWC Plane	Cluster Type
1 - 9: Single coordinate	3, 4, 5, 6, 7
1 - 9 = Multiple coordinate	5, 6, 7
11, 12, 13, 14, 15	3, 4, 5, 6

Again refer to Table 4.2 for the definition of the cluster types.

This algorithm was developed in light of results from track matching studies using the four singlets of Station 3. These revealed that events with coordinates in only one singlet of a doublet could be ignored when there was a cluster elsewhere in the doublet with hits in both singlets. The coordinates which have wires activated in only one singlet are attributed to delta rays emitted at such large angles that they appear in only one singlet. The angular resolution of the events with salvaged coordinates was the same as that of normal events.

It was found that for a given doublet 97% of the events has a single unambiguous coordinate such that the track position was known to within a wire spacing. The cluster types for these events were as follows:

1. 70% - Cluster type 5
2. 20% - Cluster type 6
3. 5% - Cluster type 4
4. 2% - Cluster type 3

The remaining 3% consisted of inefficiencies and

multiple coordinates.

If an event passed the above tests, the following associated information was written onto the library tape:

1. latch information
2. ADC information
3. the centroid of each PwC coordinate and its cluster type (one per PwC)
4. a PwC status word

The centroid was in units of half wire spacings (e.g. in 100 μm units for the high resolution PwCs; in 1000 μm units for planes 13 and 14). The PwC status word contained the following for each PwC plane:

1. whether a multiple coordinate occurred in that plane
2. whether that plane contained a valid coordinate

In addition the library tapes contained bookkeeping information (run number, date of run, etc.), DVM information, and computer scaler totals for each spill.

C. Alignment

The next step was to calculate the alignment parameters of the apparatus so that the PwC centroid values (in units of one half wire spacing) could be converted to spatial coordinates. The details of the procedure are given in Appendix I.

The procedure used a subset of the BEAM events written onto the library tape. These events had to have one and only one coordinate in each PwC plane. The final result was a set of values in real space for the physical center of each PwC plane. These alignment parameters were then written onto the data library tape.

D. Data Summary Tapes

Next data summary tapes were made from the library tapes. These summary tapes contained the various quantities given in Table 4.4. The program QVINU performed this step of the analysis.

There was one requirement that involved the latch information which was needed in order for an event to have been written onto the summary tape. The following latches had to be set: B1, STROBE, B2, JV, F01, F02, F03, F04, F09, F010 (where F0n refers to the FAST OR

TABLE 4.4

Event quantities written onto Data
Summary Tapes for Nuclear Target Data

Quantity

- 1). Muon ADC
- 2). q ($\equiv \sqrt{-t}$)
- 3). Distance along beam line where scatter occurred ($\equiv Z$)
- 4). Radius in PWC station 4 of event ($\equiv R4$)
- 5). x of event in veto plane^a
- 6). y of event in veto plane^a
- 7). x of event at Station 6
- 8). Recoil mass squared associated with the event.
- 9). Phi (ϕ) of scatter.
- 10). PWC status word
- 11). Latch Information: Particle Type, BEAM, PSACVT, FACEVT, VH2, VH3, RV1, RV2, HSDX, HSDY, FOP^b

^aSee Table 2.1

^bSee Table 3.1

from PWC plane n).

E. Monte Carlo: Philosophy

The goals of the Monte Carlo programs were twofold:

1. to calculate the apparatus geometric acceptance as a function of q ($\sqrt{-t}$)
2. to simulate the effect, due to finite apparatus resolution and multiple scattering, of the migration of a generated q to a measured q . This effect was realized by a q -generated by q -measured matrix.

There were several steps in the Monte Carlo procedure. In the first part events were generated in q (with an arbitrary distribution distribution to optimize computer efficiency), in ϕ (with a flat distribution from minus π to plus π), and in z (with a uniform distribution corresponding to the physical limits of the target). The range of q depended on the incident momentum; the entire range of q of interest was generated. As explained in the next chapter, the method of normalizing the data automatically took absorption effects into account; these effects did not

need to be explicitly calculated. This fact allowed the flat z distribution used in the Monte Carlo. The generated events were traced through the apparatus to check if they would have traversed the entire apparatus. At each point where it occurred, multiple scattering of the particle was simulated. If an event failed to pass through the entire apparatus, its q -generated was noted. No further action was taken; a new event was generated.

If the event passed through the entire apparatus, the second step simulated the finite measurement ability of the apparatus. Using experimentally derived PWC measurement resolutions, the coordinates of the generated event at each PWC were jittered. Appendix II gives the PWC resolutions and the procedure used to calculate them. By means of the same program that calculated kinematic quantities for the data, using the jittered PWC coordinates, the same kinematic quantities were calculated for the Monte Carlo. These were called reconstructed quantities.

For the first step of the procedure (where generated events passed through the apparatus) the experimental apertures did not correspond to their exact physical dimensions. Most apertures were

oversized (such as spectrometer magnet apertures), and the small veto at the third focus (V1) was ignored. Thus the first step acted as a coarse filter of events; this was done for computer efficiency. If a generated event passed through the entire apparatus, the relevant quantities of its trajectory were saved. In a later step cuts were placed on these quantities to correspond to the actual apparatus.

The next step involved all events that passed the loose apparatus cuts. Cuts were placed on the quantities associated with the trajectory of the generated event to correspond to the actual apparatus. Next the same cuts as imposed on the data were imposed on the respective Monte Carlo kinematic (reconstructed) quantities. For events that failed these cuts, the q-generated was noted, and the next event processed. For those events passing the cuts, the q-generated and q-reconstructed were kept.

The final step involved constructing the q-generated q-reconstructed matrix. This matrix normalized by the number of events in each q-generated bin was then used to correct for the effects of acceptance and resolution.

F. Monte Carlo Summary Tapes

The first step in the Monte Carlo procedure, the making of the Monte Carlo summary tapes, was performed by the program LMCWR. These tapes contained the q-generated information, and for those events which passed the loose aperture cuts, a variety of quantities as given in Table 4.5.

The incident beam phase was derived from BEAM events on the library tapes. Each data run contributed to the incident phase space used to derive the final Monte Carlo results. The BEAM events used had the following latches set: B1, STROBE, B2, JV, S1, HFDX, and HFDY.

These tapes were then processed by the program LMCRD which applied the various cuts. LMCRD produced the q-generated q-reconstructed matrix and kept account of the number of events in each q-generated bin.

G. Final Analysis Steps

The remaining analysis procedures are given in more detail in Chapter 6. Briefly, the data were normalized, and a target empty subtraction was performed. The theoretical cross section, $d\sigma/dq$, was modified via the

TABLE 4.5

Event quantities written onto Monte Carlo
Summary Tapes for Nuclear Target Data

1). Reconstructed Quantities^a

1. q of scatter
2. ϕ of scatter
3. Distance along beam line where scatter occurred.
4. Radius at PWC Station 4.
5. x at veto plane
6. y at veto plane
7. x at PWC Station 6
8. Delta p (Pin-Pout) of scatter.

2). Generated Quantities^b

1. Radius at PWC Station 4
- 2.-9. x and y at spectrometer magnet's entrance
and exit apertures.
10. x at veto plane.
11. y at veto plane.
12. x at PWC Station 6.
13. y at PWC Station 6.
14. q generated

^aFinite apparatus measurement error is taken into account.

^bFinite apparatus measurement error is not taken into account (refers to trajectory of the generated Monte Carlo event).

Monte Carlo results and then compared to the data.

CHAPTER 5

DATA REDUCTION: HIGH- t DATA

A. Introduction

The philosophy of the data reduction for the high- t data was very similar to that for the nuclear target data. The only major difference concerned the application of the Monte Carlo results.

The reduction process is shown schematically in Figure 5.1. Different computer programs than in the nuclear target case were used as a matter of convenience. The analysis was performed on 100 PDP15 tapes having the same type of information as the nuclear target data tapes (see Chap. 4, Sect. D).

B. Data Library Tapes

Data library tapes were produced by LPAK and were exactly the same in structure as those for the nuclear target data. See Chap. 4, Sect. B for details.

C. Alignment

HI-T ANALYSIS DIAGRAM

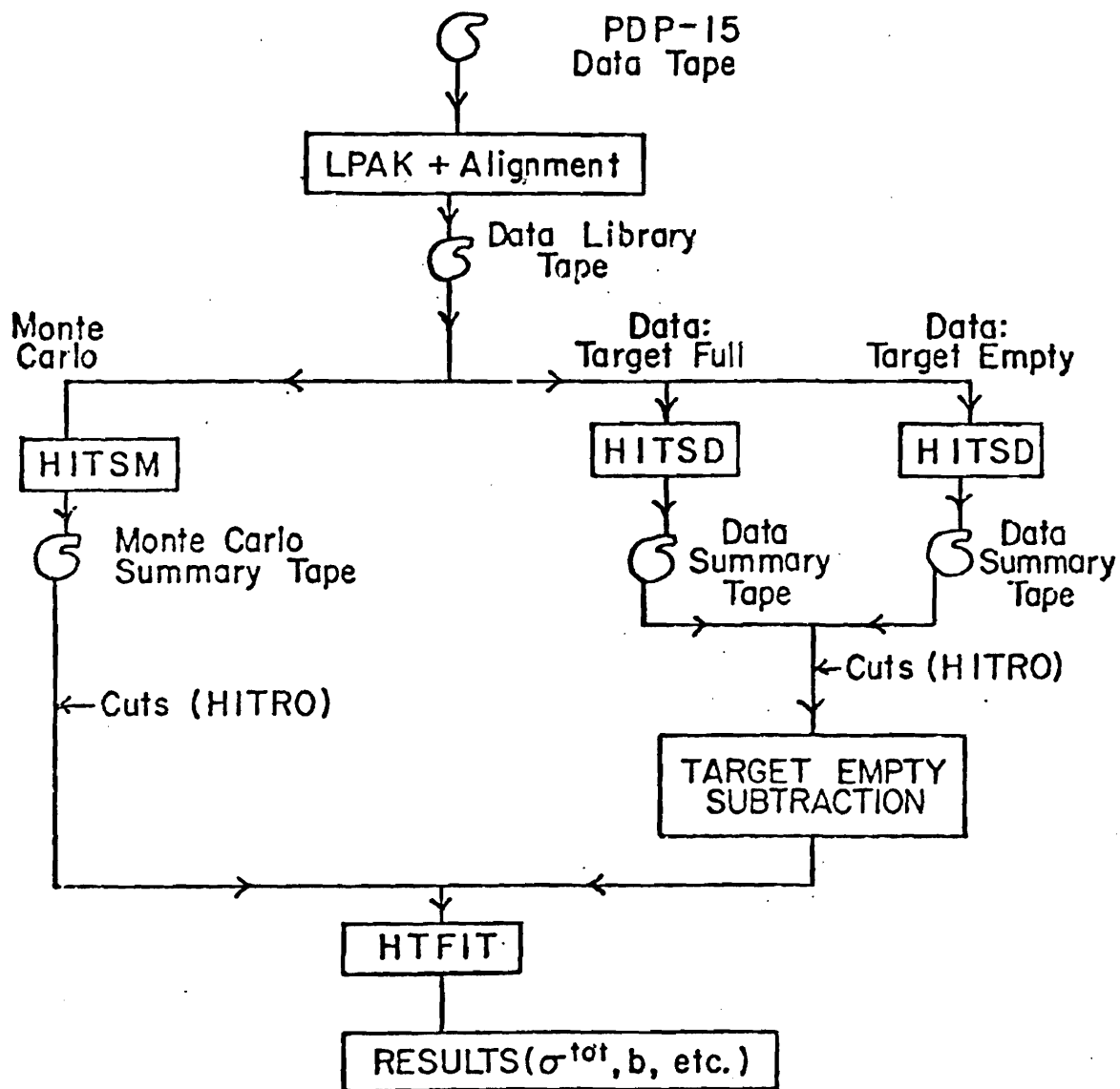


Figure 5.1

The alignment procedure was exactly the same as for the nuclear target data. See Chap. 4, Sect. C for details.

D. Data Summary Tapes

The program HITSO made data summary tapes from the library tapes. The various quantities saved are given in Table 5.1 (a slightly different set from that for the nuclear target data).

Before an event could be written onto the summary tape the following latch conditions had to be satisfied:

1. LATCHES SET: B1, STROBE, B2, S1, HFDX, HFDY, FO1, FO2, FO3, FO4, FO9, FO10
2. LATCHES NOT SET: VH1, FOP

E. Monte Carlo Philosophy

For the high- t analysis there was only one goal for the Monte Carlo programs: to calculate the apparatus geometric acceptance as a function of q . It was shown that the effects due to finite apparatus resolution are negligible for this analysis. The main reason is that the

TABLE 5.1

Event quantities written onto Data

Summary Tape for High -t Data

Quantity

- 1). Muon ADC.
- 2). q ($\equiv\sqrt{-t}$) of scatter.
- 3). Θ_x, Θ_y of scatter.
- 4). Distance along beam line where scatter occurred ($\equiv Z$).
- 5). Phi (ϕ) of scatter.
- 6). x, y at PWC Station 4
- 7). x, y at Veto Plane^a
- 8). x, y at PWC Station 6
- 9). Recoil mass squared associated with the event.
- 10). PWC status word
- 11). Latch Information: Particle Type, PSTGBM, PSACVT, FACEVT, VH2, VH3, RV1, RV2, HSDX, HSDY, V1, V2^b

^aSee Table 2.1^bSee Table 3.1

differential cross section is relatively gentle in the region of q of interest; therefore as many events are as likely to migrate into a given q bin as out.

The Monte Carlo procedure, that of using a two step process, was the same as that for the nuclear target data. The only difference was that the jaw veto counter at the third focus was included. For details see Chap. 4, Sect. E.

F. Monte Carlo Summary Tapes

The first step in the Monte Carlo procedure, the making of Monte Carlo summary tapes, was performed by the program HITSM. These tapes contained q -generated information, and for those events which passed the loose aperture cuts, the quantities given in Table 5.2.

The incident beam phase space was derived from BEAM events on the library tapes. Each data run contributed to the incident phase space. The BEAM events had to pass the following latch requirements:

1. LATCHES SET: B1, STROBE, B2, HFDX, HFDY, FO1, FO2, FO3, FO4
-

TABLE 5.2

Event quantities written onto Monte Carlo Summary Tapes for High -t Data

- 1). Reconstructed Quantities^a
 1. q of scatter.
 2. θ_x , θ_y of scatter.
 3. Distance along beam line where scatter occurred.
 4. x, y at PWC Station 4.
 5. x, y at veto plane.
 6. x, y at PWC Station 6.
- 2). Generated Quantities^b
 1. q
 2. z
 3. x, y at veto plane

^aFinite apparatus measurement error is taken into account.

^bFinite apparatus measurement error is not taken into account.

2. LATCHES NOT SET: VHI, FOP

Next the program HITKO applied the various cuts and stored the results necessary to calculate the geometric acceptance. The final stages of the analysis are given in Chapter 8.

CHAPTER 6

RESULTS: NUCLEAR TARGET DATA

A. Final Analysis Steps

The final analysis steps involving the data were as follows.

The program QRNUC (see Figure 4.1) applied various cuts to the events on the data library tapes. A histogram in q for those events passing the cuts for full and empty data was produced. Also the number of BEAM events passing a subset of the above cuts (basically certain requirements on the beam phase space) for full and empty was kept. It is important to note that these BEAM events were required to traverse the entire apparatus.

Next a target empty subtraction was performed; the following quantity was calculated:

$$D(q) = [(N_S^f(q)/N_t^f) - (N_S^{mt}(q)/N_t^{mt})]/(\Gamma\Delta) \quad (6.1)$$

where

Δ = q bin size

Γ = $N_{\rho x}/A$

N = Avogadro's Number

A = atomic weight of target

ρ = target density

x = target length

$N_S^{f(mt)}(q)$ = number of counts in each q bin for scattered events passing all cuts for full (empty) data

$N_t^{f(mt)}$ = number of BEAM events passing cuts multiplied by Tagbeam Scale Factor for full (empty) data

Note that $N_t^{f(mt)}$ gives the incident beam flux for the full (empty) data respectively; $N_S^{f(mt)}$ gives the number of events scattering into each q bin for the full (empty) data respectively. The units of $D(q)$ were "mb/(GeV/c)".

It is important to realize that the BEAM events used to determine $N_t^{f(mt)}$ traverse the same apparatus as the scattered events. Thus there was no need to correct the number of scattered events for apparatus absorption effects. Both scattered and BEAM events suffered the same amount of absorption.

A theoretical form for the differential cross section, $d\sigma/dq$, contained the parameters of interest (i.e. total cross section, forward slope, etc.). This theoretical form was then modified by the Monte Carlo results to take into account the following:

1. apparatus geometric acceptance
2. apparatus resolution effects

Mathematically this is expressed as follows:

$$T(q_m) = \int d\sigma/dq_{th}(q_g) \cdot A(q_g, q_m) \cdot d(q_g) \quad (6.2)$$

where

$d\sigma/dq_{th}$ = theoretical cross section at $q = q_m$

$A(q_g, q_m)$ = matrix containing Monte Carlo results

q_g = q-generated

q_m = q-measured

The exact form of $d\sigma/dq$ will be given in a later section.

The fitting program used was MINUIT^{6.1} (as a subroutine in NFITR); the parameters were derived by a chi-squared minimization method, comparing $D(q)$ to $T(q)$.

B. Data Cuts

To extract the elastic scattering signal, a set of cuts was applied to both the target full and target empty data. Tables 6.1 and 6.2 present the cuts used for data at an incident momentum of 175 GeV/c for the Pb and Be targets respectively. Also shown are the effects of the cuts.

The track reconstruction requirements refer to requirements on the PWC coordinates such that the event was written on the data summary tapes. Next the Hardware Focus Detector (HFD) latches had to indicate the HFD test was passed in both the x and y projections.

A cut was placed on the pulse height from the muon detector ADC in order to veto any muons in the beam (either muons produced upstream of the apparatus or resulting from pion or kaon decay in flight). This cut varied with the incident beam momentum. Figures 6.1 and 6.2 show the pulse height spectrum from the muon ADC and the cut used.

TABLE 6.1
CUTS TO EXTRACT ELASTIC SIGNAL
Be 175 GeV/c

	Fraction of Events Remaining After Cut		
	π^+	K^+	p
1). Track reconstruction requirements on PWC coordinates	.741	.741	.741
2). HFD test passed.	.734	.736	.736
3). Muon Detector does not signal presence of a muon.	.658	.614	.695
4). No count from VH2 and VH3	.626	.585	.657
5). Outgoing particle trajectory traversed the area inside spectrometer magnet apertures.	.623	.583	.654
6). $[7.9]^2 \leq \text{recoil mass squared} \leq [8.8 \text{ (GeV/c}^2)]^2$.	.596	.554	.624
7). HSD test passed.	.575	.532	.607
8). Scatter vertex in target region.	.292	.258	.363
9). Outgoing particle trajectory $\geq 0.5\text{mm}$ from edges of V1	.282	.249	.354
10). Track ≤ 1.5 cm from center of PWC station 4.	.281	.248	.353
11). Events whose trajectories were in region of $> 90\%$ efficiency in PWC station 4.	.280	.247	.351

TABLE 6.2

CUTS TO EXTRACT ELASTIC SIGNAL

Pb 175 GeV/c

Cut	Fraction of Events Remaining After Cut		
	π^+	K^+	p
1). Track reconstruction requirements on PWC coordinates	.721	.721	.721
2). HFD test passed.	.708	.718	.715
3). Muon Detector does not signal presence of a muon.	.636	.592	.680
4). No count from VH2 and VH3	.631	.587	.673
5). Outgoing particle trajectory traversed the area inside of spectrometer magnet apertures.	.630	.587	.673
6). $[192.6]^2 \leq \text{recoil mass squared} \leq [193.4 (\text{GeV}/c^2)]^2$.	.601	.556	.638
7). HSD test passed.	.571	.527	.608
8). Scatter vertex in target region.	.181	.172	.182
9). Outgoing particle trajectory $\gtrsim 0.5\text{mm}$ from edges of V1	.170	.162	.171
10). Track ≤ 1.5 cm from center of PWC station 4.	.170	.162	.171
11). Events whose trajectories were in region of $> 90\%$ efficiency in PWC station 4.	.170	.162	.171

PULSE HEIGHT HISTOGRAM OF
MUON CALORIMETER

Be: 175 GeV/c

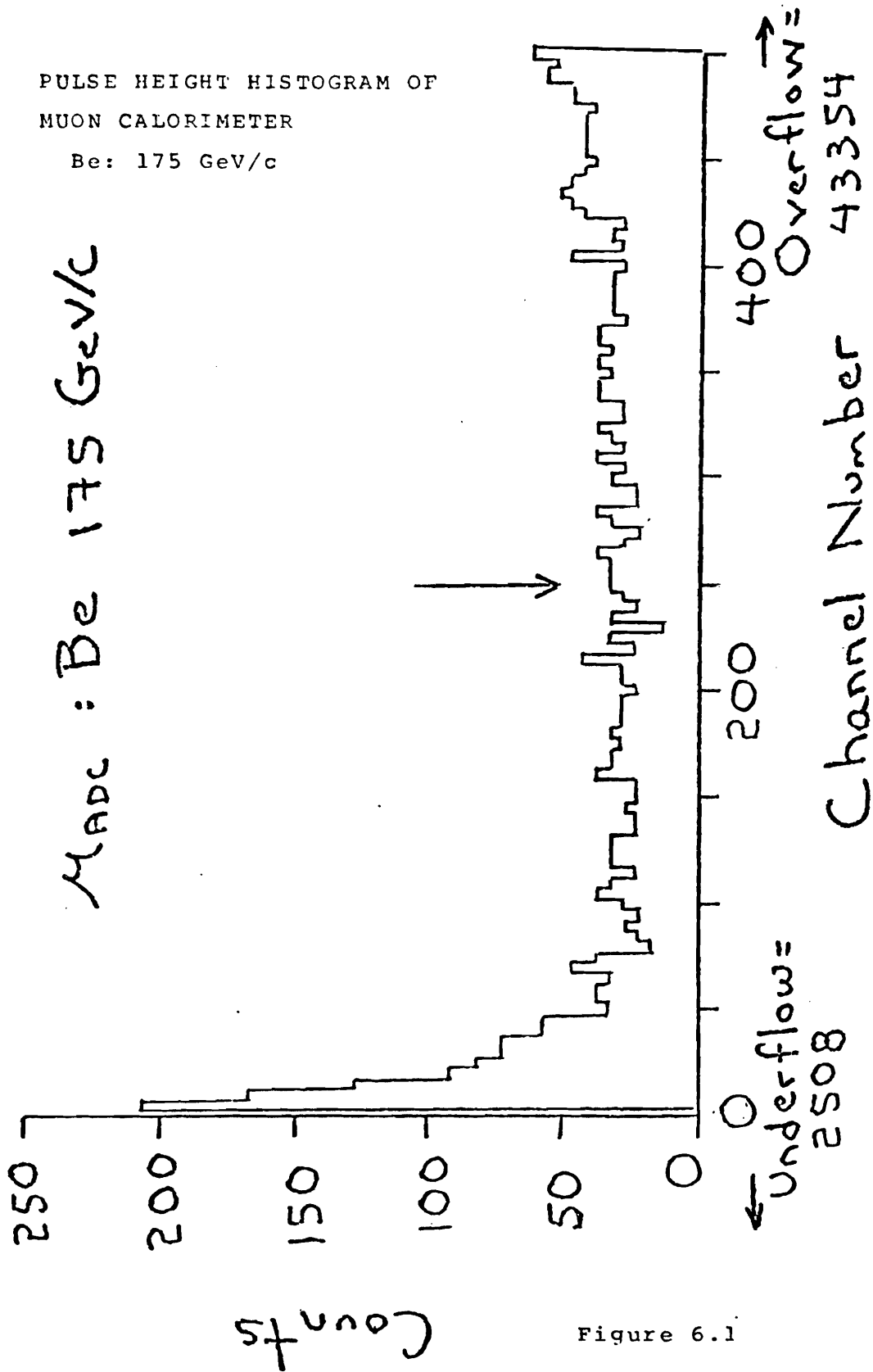


Figure 6.1

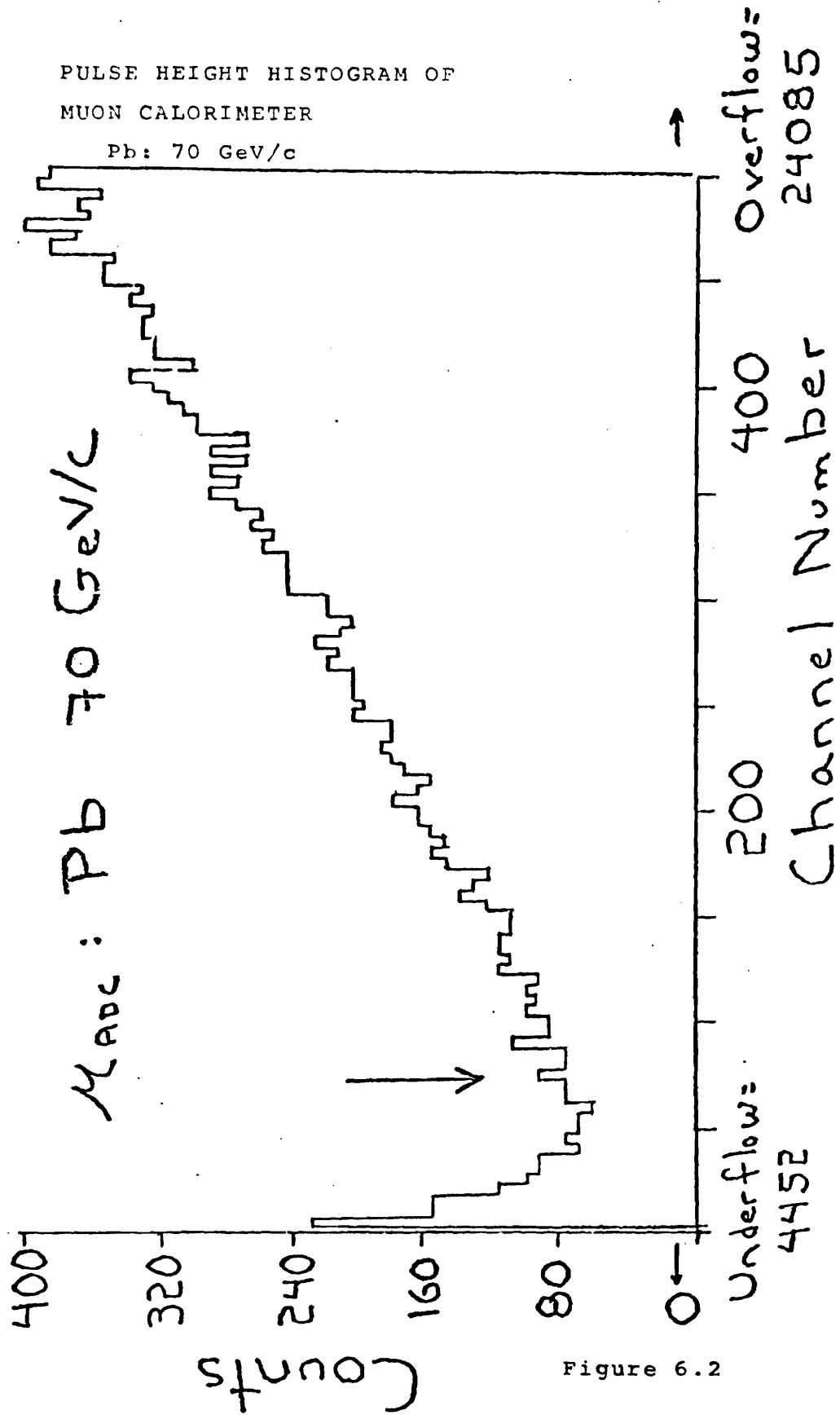


Figure 6.2

The requirement that VH2 and VH3 did not count was to suppress unwanted scatters from target electrons.

The requirement that the outgoing track passed within the spectrometer magnet apertures was fulfilled by the EGG cut where

$$\text{EGG} = (\text{xveto}/\text{a})^m + (\text{yveto}/\text{b})^m \quad (6.3)$$

where

xveto(yveto) = predicted x(y) coordinate at the
veto plane

xveto(yveto) were calculated based on the scattered projectile's outgoing angle and its momentum. The curve given by $\text{EGG} = 1$ represents the actual exit aperture of the most downstream spectrometer magnet as projected to the veto plane. Thus the curve given by $\text{EGG} < 1$ means that the outgoing track had to pass within an area away from the actual magnet edges. For all cases the cut was $\text{EGG} < 0.85$.

The recoil mass cut required that this quantity was consistent with the target mass squared. Figures 6.3 and 6.4 show examples of a recoil mass squared

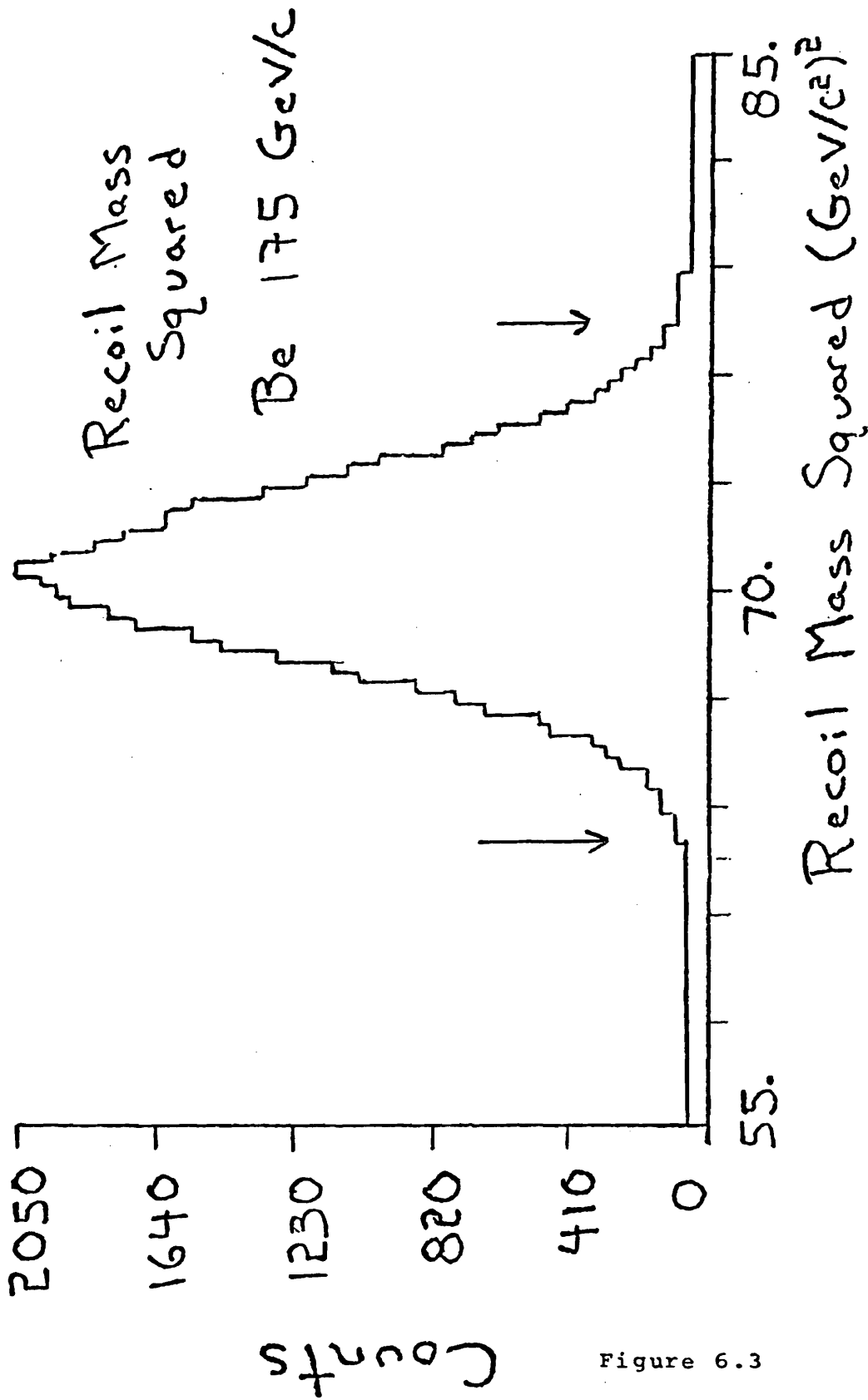


Figure 6.3

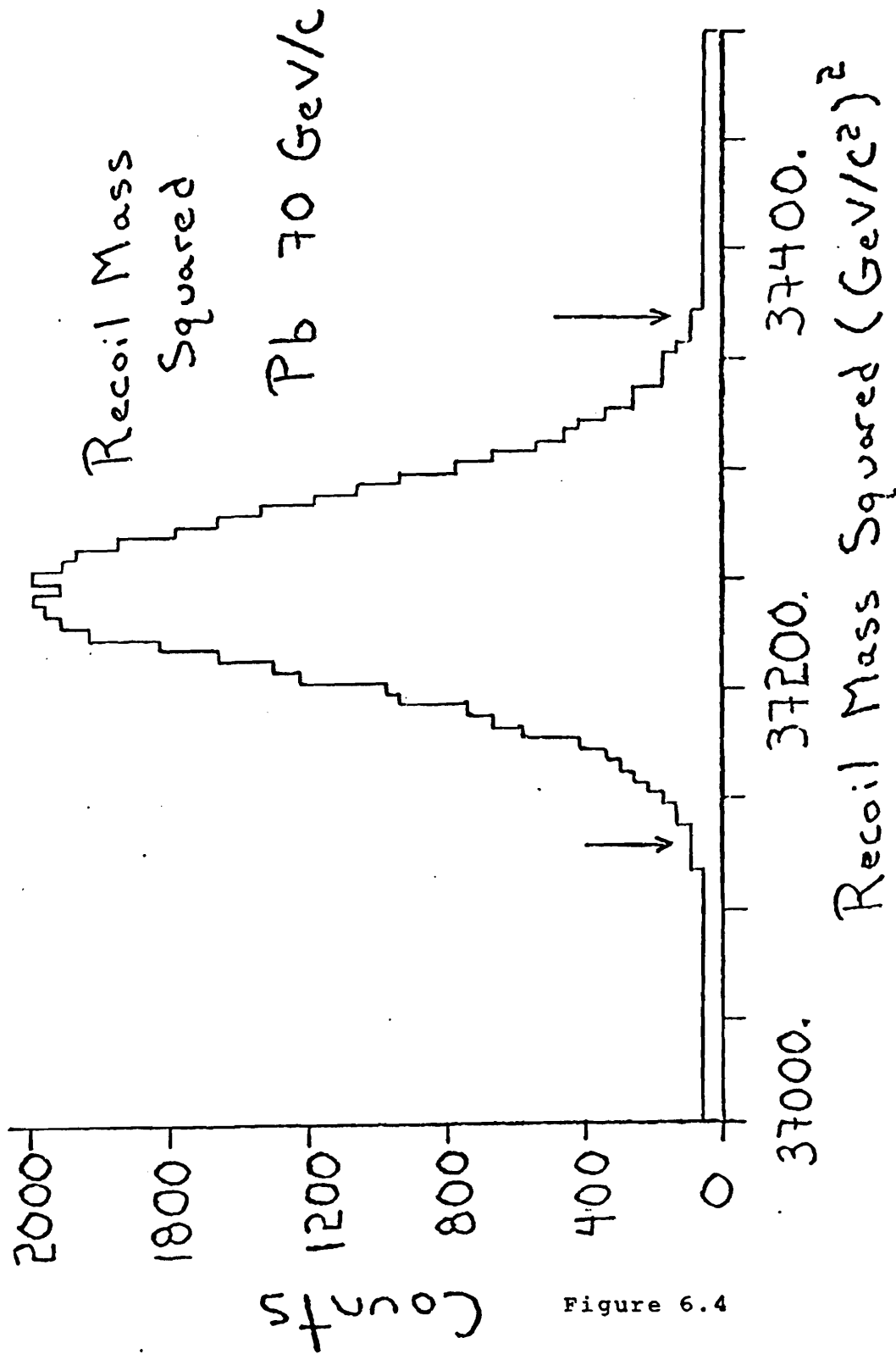


Figure 6.4

distribution along with arrows indicating the cut.

There was a cut made to check that the scatter occurred in the region of the target. A z distribution (where along the beamline the scatter occurred) is shown in Figures 6.5 to 6.8 along with arrows indicating the cuts.

The other cuts, involving PWC Station 4 and the HSD, are self explanatory.

C. Data Normalization and Target Empty Subtraction

To perform the target empty subtraction, the target full and target empty distributions first had to be normalized. The BEAM events provided the normalization information.

Unfortunately due to an error in the hardware trigger logic, the number of incident particles was not merely the number of BEAM events multiplied by a scale factor. The logic error caused a different amount of deadtime for SCATTER and BEAM triggers. The following formula for the number of incident particles corrected for this effect:

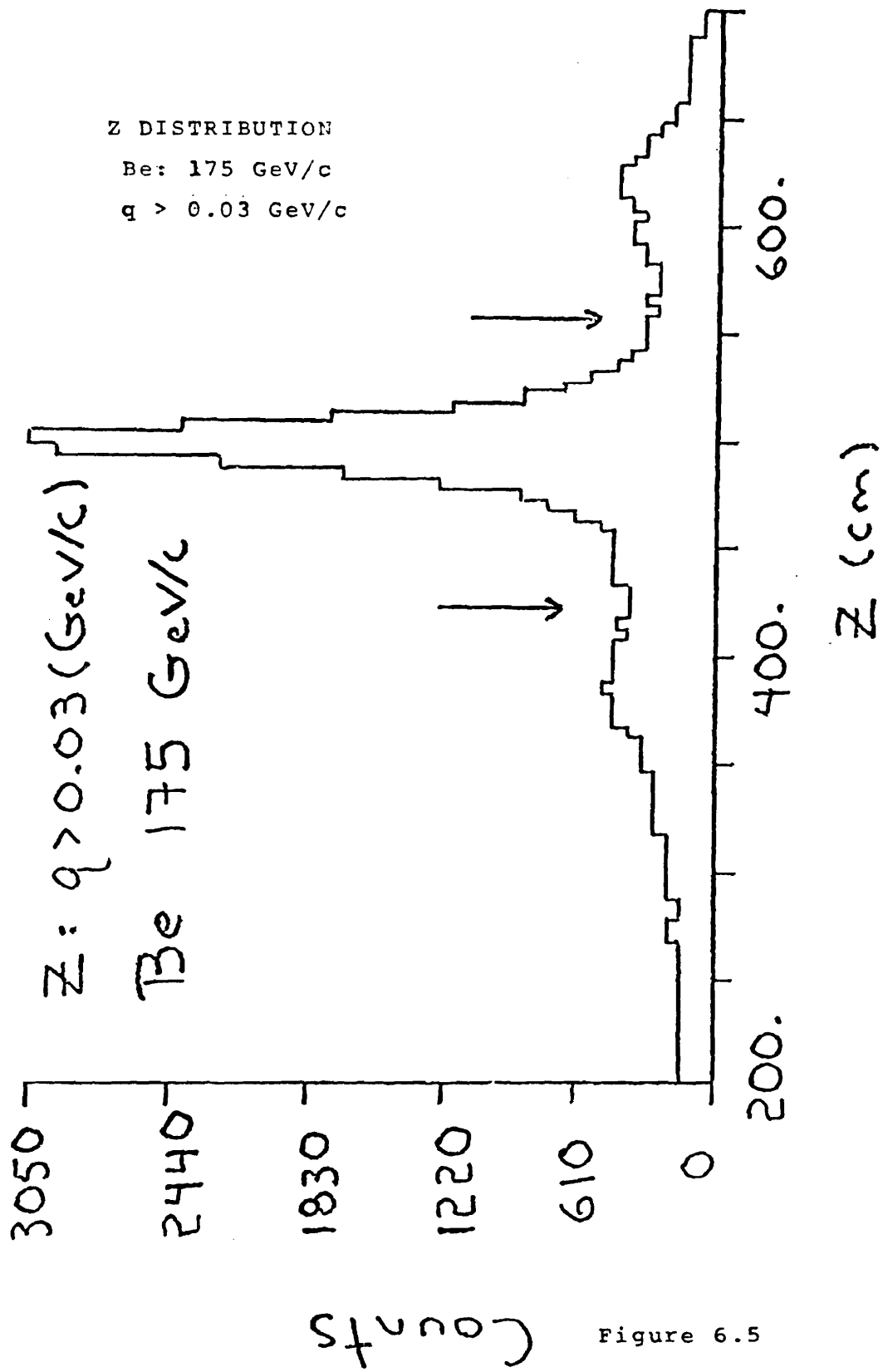


Figure 6.5

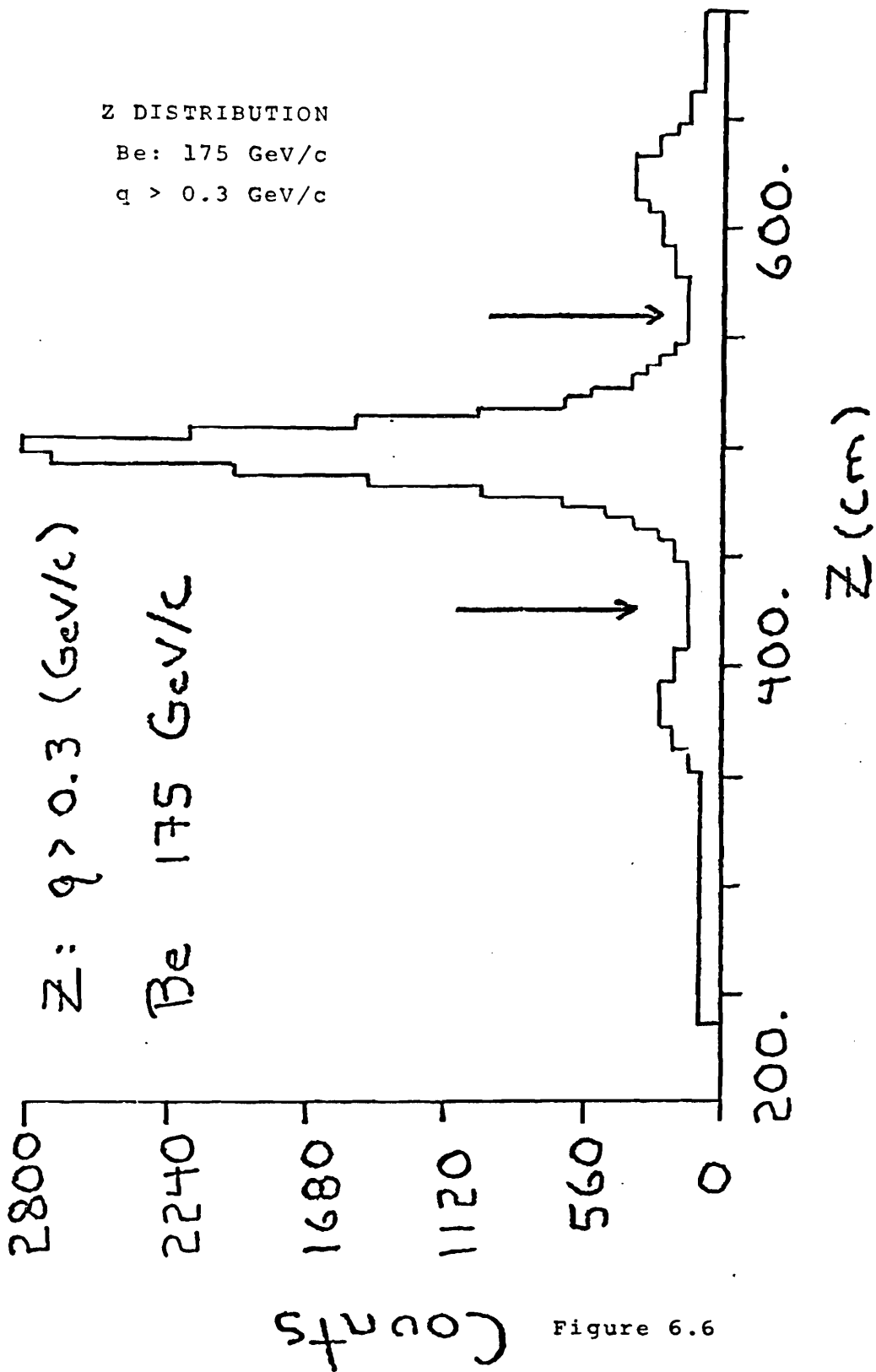


Figure 6.6

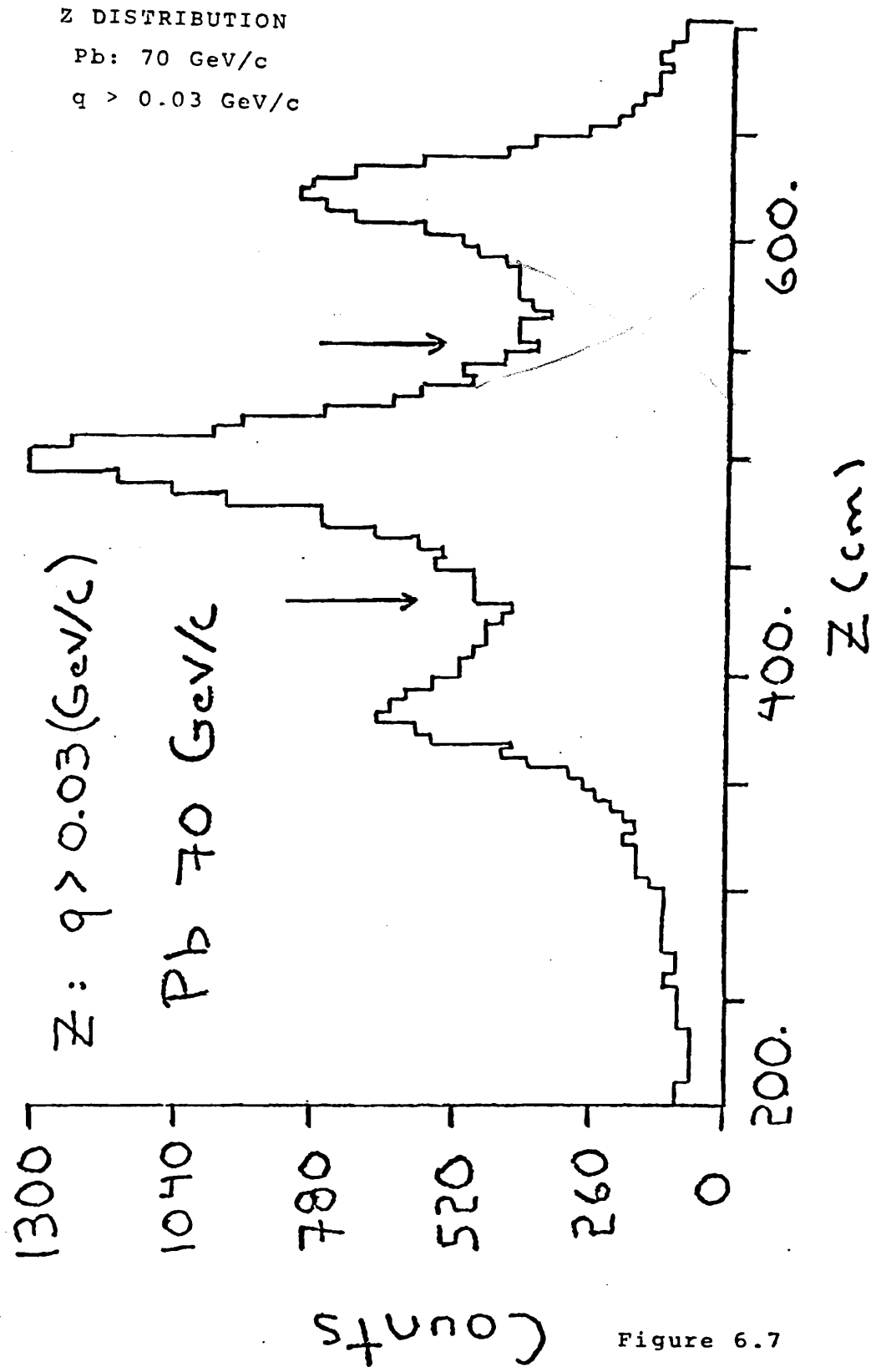


Figure 6.7

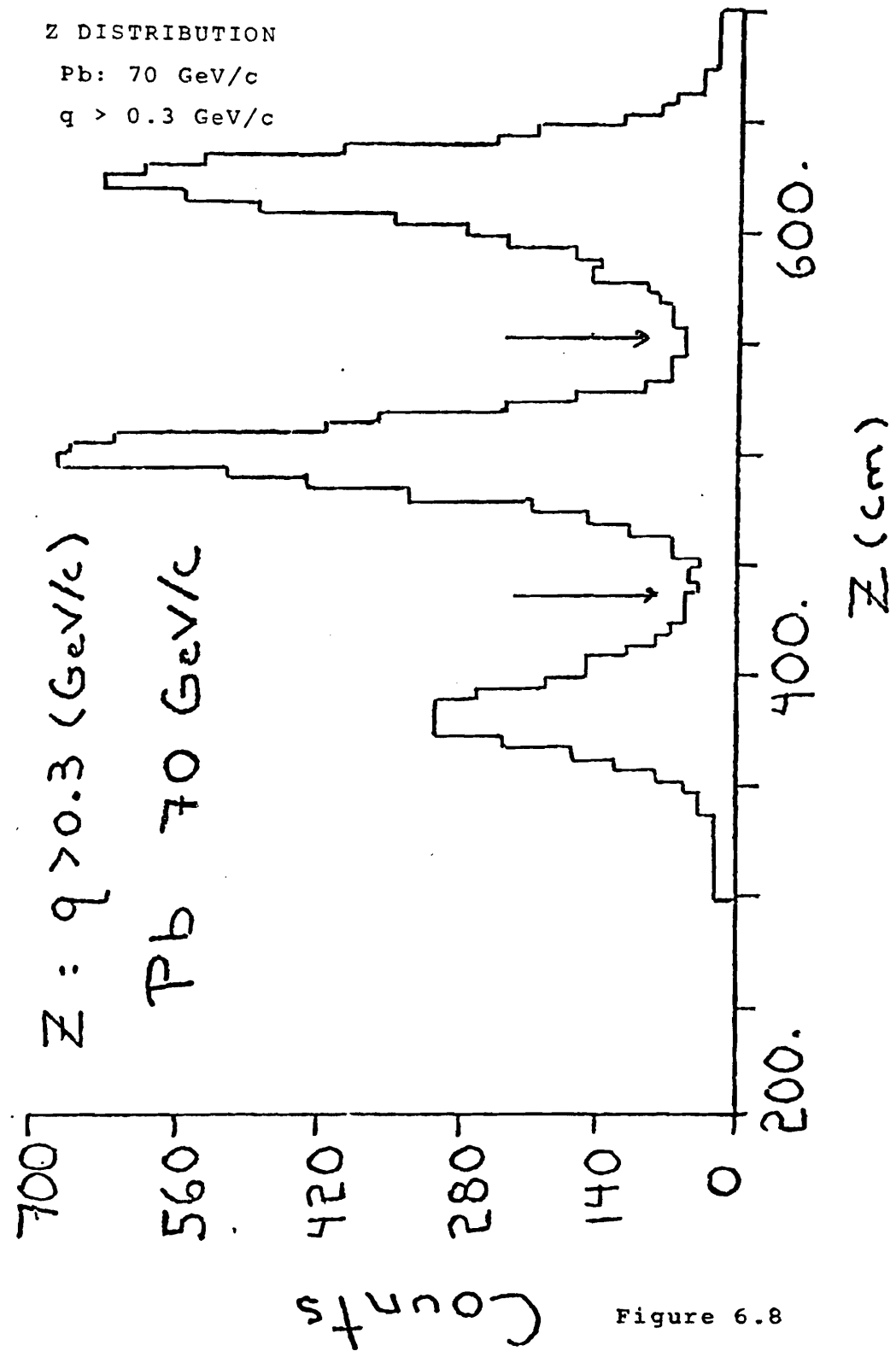


Figure 6.8

$$N_t^f(mt) = N_{\text{beam}}^f(mt) * F / (F * T) \quad (6.4)$$

where

$N_t^f(mt)$ = number of incident particles for full
(empty) target data

$N_{\text{beam}}^f(mt)$ = number of BEAM events (passing cuts)
for full (empty) target data

F = number of SCATTER triggers passing HFD
requirement and $(\overline{VH2} \cdot \overline{VH3})$

(F*T) = number of above SCATTER triggers that had
the BEAM latch set

The BEAM events used had to pass the following cuts:

1. HFD latch set
2. VH2, VH3 did not count

The quantity $D(q)$ was then calculated.

D. Monte Carlo Acceptance

As described in Chap.4, Sect.E there were two types of quantities involved in the Monte Carlo programs, generated and reconstructed.

The cuts applied to the generated quantities simulated the actual experimental apertures. The cuts applied to the reconstructed quantities were exactly the same as applied to the data. By this method, the Monte Carlo simulated the effect of apparatus resolution.

Figures 6.9 and 6.10 present examples of the acceptance.

E. Results

Appendix III presents tables and graphs of the $d\sigma/dt$ distributions for the reactions measured. To calculate $d\sigma/dt$ for the data, the following formula is used:

$$d\sigma/dt_{\text{data}} = D(q)/[2 \cdot q \cdot e(q)] \quad (6.5)$$

where

$e(q)$ = acceptance as a function of q

Table 6.3 presents the event totals for the various reactions.

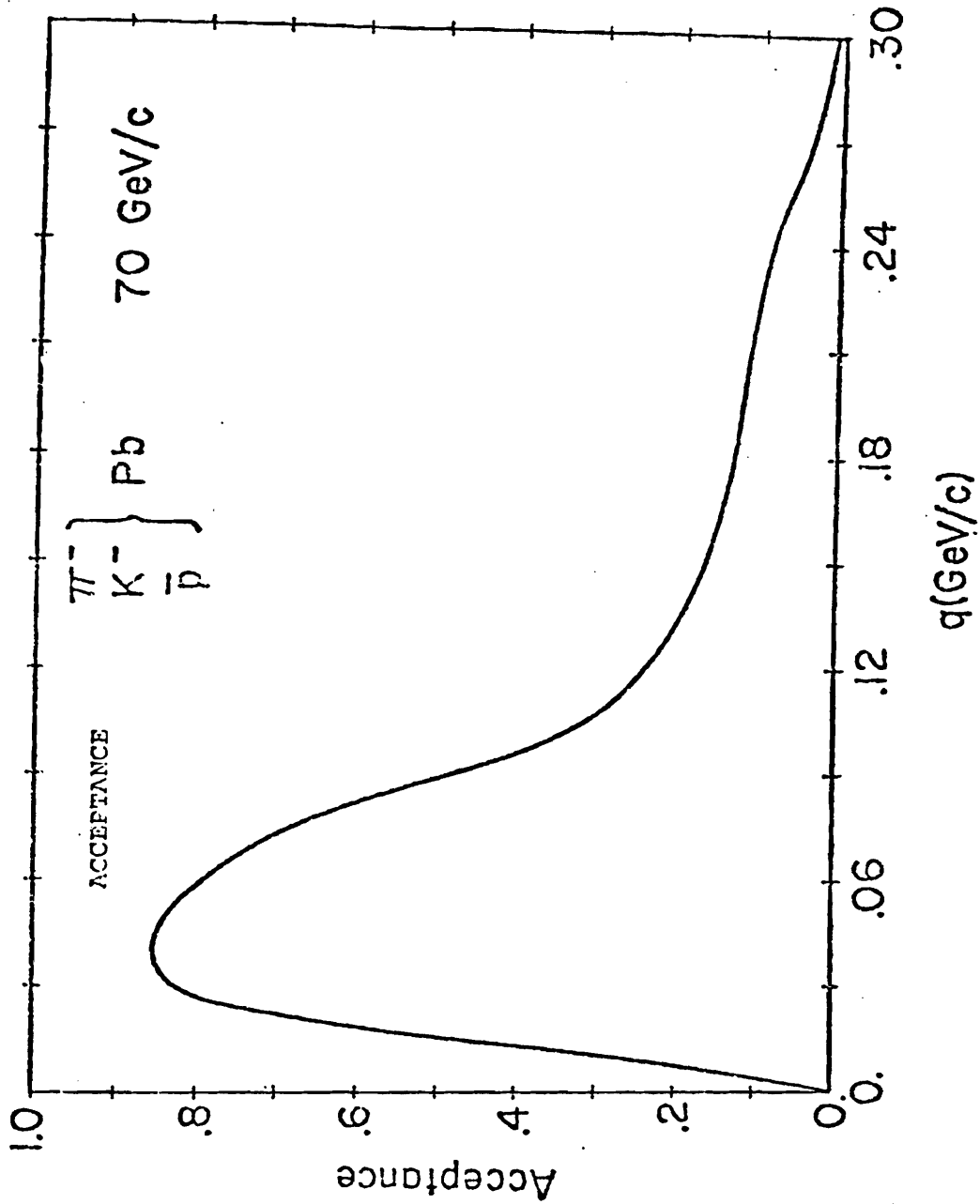


Figure 6.9

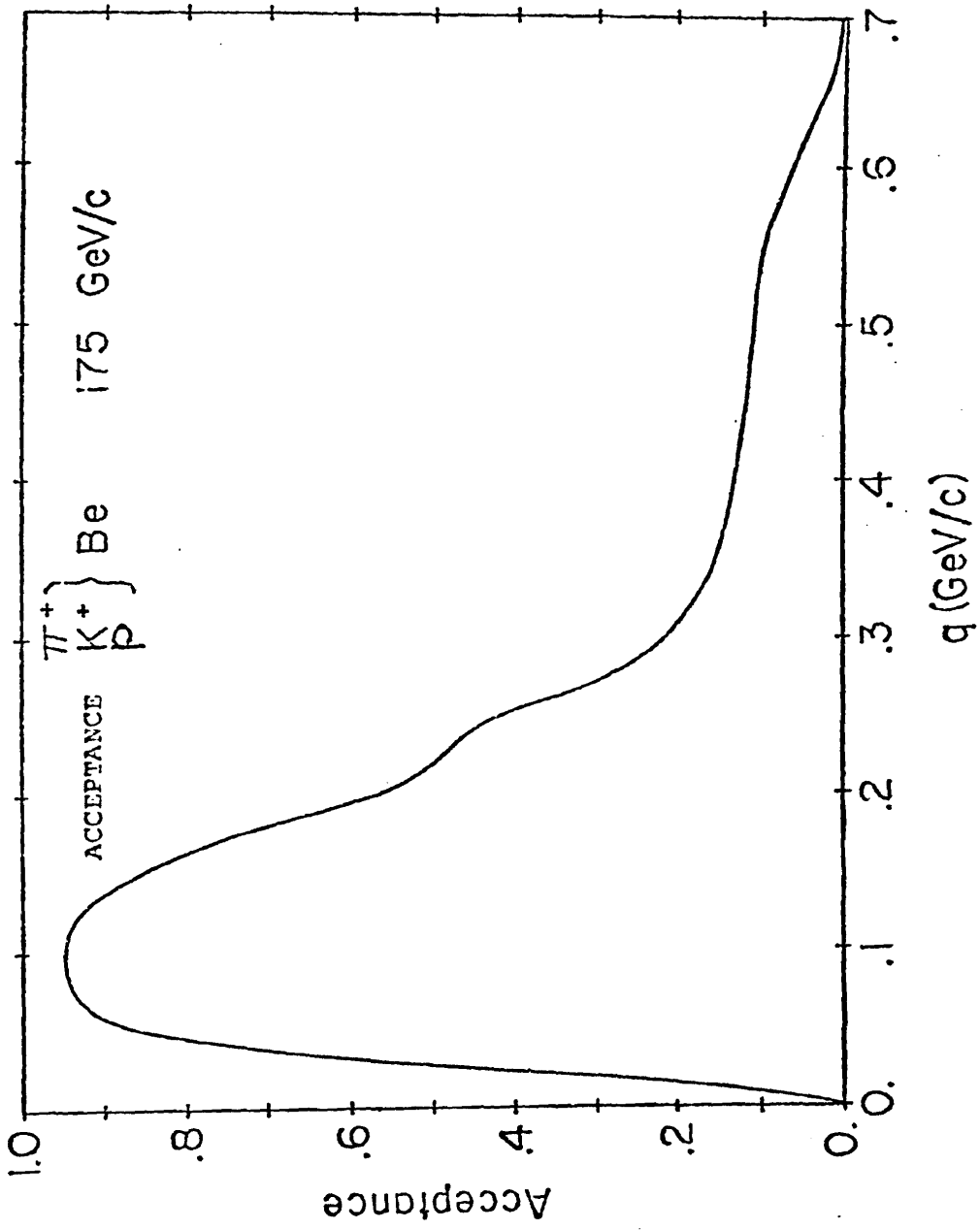


Figure 6.10

TABLE 6.3

HADRON-NUCLEUS ELASTIC SCATTERING EVENT TOTALS

for $-t > -t_{\min} \text{ (GeV/c)}^2$ (in thousands)

Momentum (GeV/c)	Target	π^+	k^+	p^+	π^-	k^-	\bar{p}
175 ($t_{\min} =$ -.0018 (GeV/c) ²)	Be	16.4	7.6	38.0	11.8	4.5	1.5
	C	18.5	9.0	41.2	9.2	3.4	1.1
	Al	12.0	6.0	23.8	5.1	1.9	0.5
	Cu	8.9	4.5	14.9	6.8	2.7	0.6
	Sn	12.6	6.9	18.9	8.8	3.6	0.7
	Pb	12.3	7.0	17.1	8.8	3.9	0.7
125 ($t_{\min} =$ -.0016 (GeV/c) ²)	Be	9.4	3.7	23.3	-	-	-
	Al	11.5	6.6	23.3	-	-	-
	Pb	9.6	6.9	14.0	-	-	-
70 ($t_{\min} =$ -.0013 (GeV/c) ²)	Be	8.2	4.1	13.7	10.0	4.4	8.1
	C	7.3	3.8	11.7	8.8	4.3	6.7
	Al	11.5	6.1	15.0	13.8	13.7	19.1
	Cu	11.0	6.4	11.0	8.2	8.4	9.2
	Sn	15.8	9.5	16.2	15.5	16.6	15.6
	Pb	9.8	6.1	8.9	7.1	7.6	6.4

The theoretical cross section was parameterized as follows:

$$\frac{d\sigma}{dq} \text{ th} = N_0 \left\{ \frac{2q}{\Gamma w^2} \exp(-q^2/w^2) + \frac{8\pi e^4 Z^2}{q^3} \cdot G_p^2 \cdot G_t^2 \right. \\ \cdot \left[1 - \frac{4w^2}{q^2} \left(1 + \frac{2}{\beta} \ln \left[\frac{2q}{5w} \right] \right) \right]^{-1} + \frac{q\sigma_A^2}{8\pi\hbar^2} \exp(-b_A q^2) \\ \left. + \frac{N_A q\sigma_{hp}^2}{8\pi\hbar^2} \exp(-b_p q^2) \right\} \quad (6.6)$$

where Coulomb-nuclear interference was neglected and

N_0 = Normalization factor

Γ = as defined in Eq. 6.1

x = target length

w, β = multiple coulomb scattering parameters

Z = atomic number

G_p = electromagnetic form factor of
projectile^{6.2}

G_t = electromagnetic form factor of nuclear
target^{6.2}

σ_A = total cross section for projectile -
nucleus scattering

b_A = forward slope for coherent projectile -
nucleus elastic scattering

N_A = number of individual nucleons involved in
incoherent projectile - nucleus
scattering

σ_{hp} = projectile - proton total cross section

b_p = forward slope of proton - projectile
elastic scattering

The terms in Eq. 6.6 represent the following processes. The first two terms represent single, plural, and multiple Coulomb scattering^{6.3}. The values of w , in units of $(\text{GeV}/c)^{-2}$, for the targets are 0.0031 (Be), 0.0034 (C), 0.0035 (Al), 0.0040 (Cu), 0.0047 (Sn), and 0.0038 (Pb). The values of β (unitless) for the targets are 12.03 (Be), 11.91 (C), 11.43 (Al), 11.08 (Cu), 10.77 (Sn), and 9.60 (Pb).

The third term represents coherent elastic scattering (from the nucleus as a whole); the fourth represents incoherent scattering (from individual nucleons). The incoherent scattering term represents interactions which excite or break up the nucleus (true elastic scattering leaves the nucleus in its ground state) but which are included in the elastic signal due to the experiment's finite momentum resolution. The parameterization of the incoherent scattering follows the

approach of Ref. 1.3 . The parameters for the incoherent scattering term were taken from Ref. 1.3 and are given in Table 6.4. The fitting program fits for N_0 , b_A , and σ_A only.

Figures 6.11 to 6.16^{6.4} present $d\sigma/dt$ distributions for some of the reactions measured. Figures 6.11 and 6.12 show $d\sigma/dt$ distributions for proton scattering from the various targets (Be, C, Al, Cu, Sn, and Pb) at an incident momentum of 175 GeV/c. Figures 6.13 and 6.14 present the scattering from Be and Pb targets respectively for the various incident projectiles (π^\pm , K^\pm , p, and \bar{p}) at an incident momentum of 175 GeV/c. Finally Figures 6.15 and 6.16 present the momentum dependence (incident momenta of 70, 125, and 175 GeV/c) of $d\sigma/dt$ for proton scattering from Be and Pb targets respectively.

Figures 6.11 to 6.16 show the following. As the atomic number of the target increases, the $d\sigma/dt$ distributions become more sharply peaked. For the Cu, Sn, and Pb target data, a secondary maximum is observed. The t of the second maximum decreases for increasing atomic number of the target. The shape of the t distributions do not depend in a significant manner on the incident beam momentum.

TABLE 6.4

INCOHERENT SCATTERING TERM PARAMETERS AND NUCLEAR CHARGE RADIUS, R

Reaction	Momentum (GeV/c)	N_A	σ_{hp}^a (mb)	b_A (GeV/c) ⁻²	R (fm)
π^\pm, k^\pm -Be	$\pm 175, +125, \pm 70$	3.5	25., 20.	10.	2.20
p, \bar{p} -Be	"	3.5	40.	12.	2.20
π^\pm, k^\pm -C	$\pm 175, \pm 70$	3.4	25., 20.	10.	2.42
p, \bar{p} -C	"	3.4	40.	12.	2.42
π^\pm, k^\pm -Al	$\pm 175, +125, \pm 70$	4.5	25., 20.	10.	3.02
p, \bar{p} -Al	"	4.5	40.	12.	3.02
π^\pm, k^\pm -Cu	$\pm 175, \pm 70$	6.7	25., 20.	10.	3.66
p, \bar{p} -Cu	"	6.7	40.	12.	3.66
π^\pm, k^\pm -Sn	$\pm 175, \pm 70$	8.2	25., 20.	10.	4.55
p, \bar{p} -Sn	"	8.2	40.	12.	4.55
π^\pm, k^\pm -Pb	$\pm 175, +125, \pm 70$	9.5	25., 20.	10.	5.42
p, \bar{p} -Pb	"	9.5	40.	12.	5.42

^aSecond entry refers to Kaon case

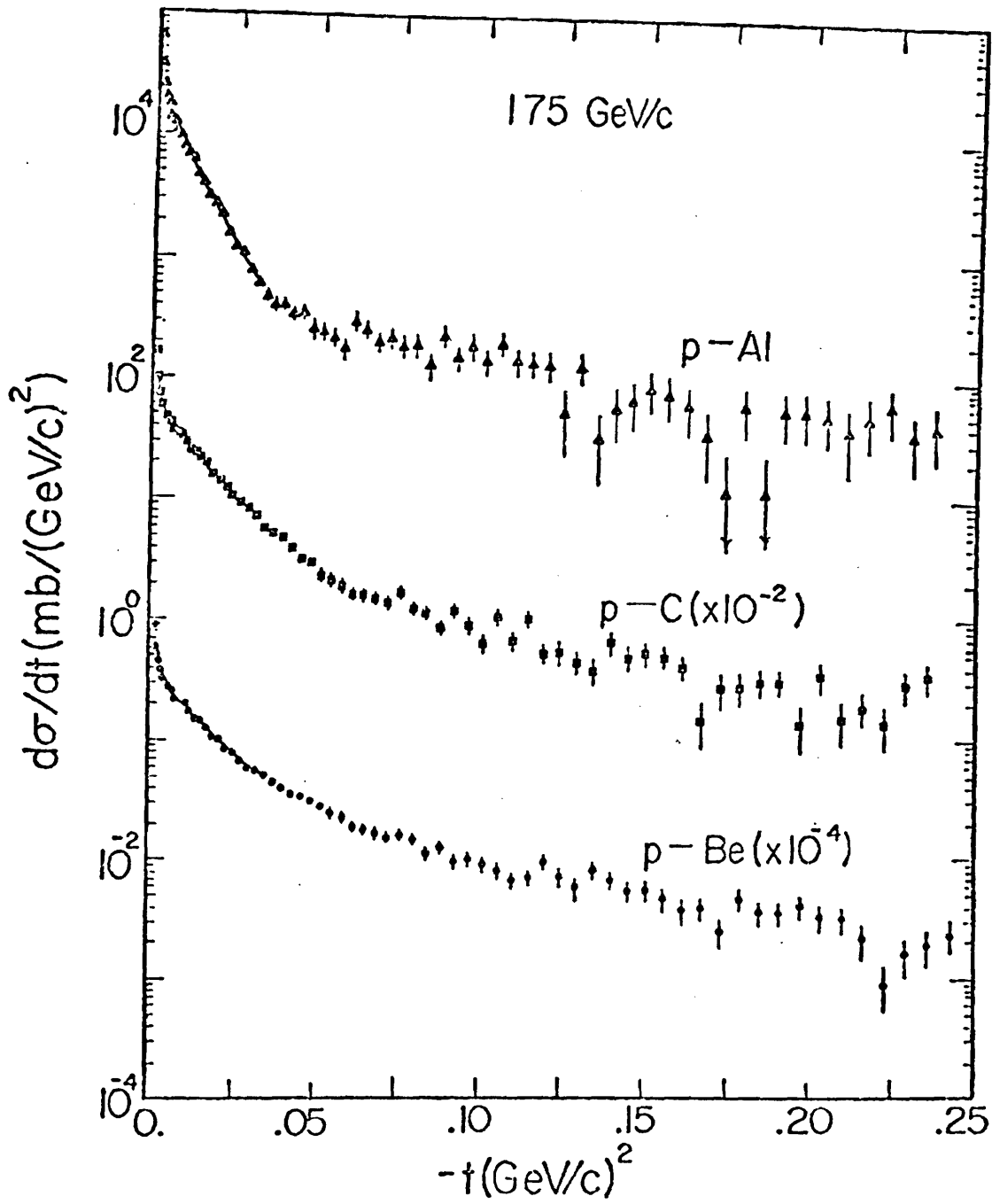


Figure 6.11

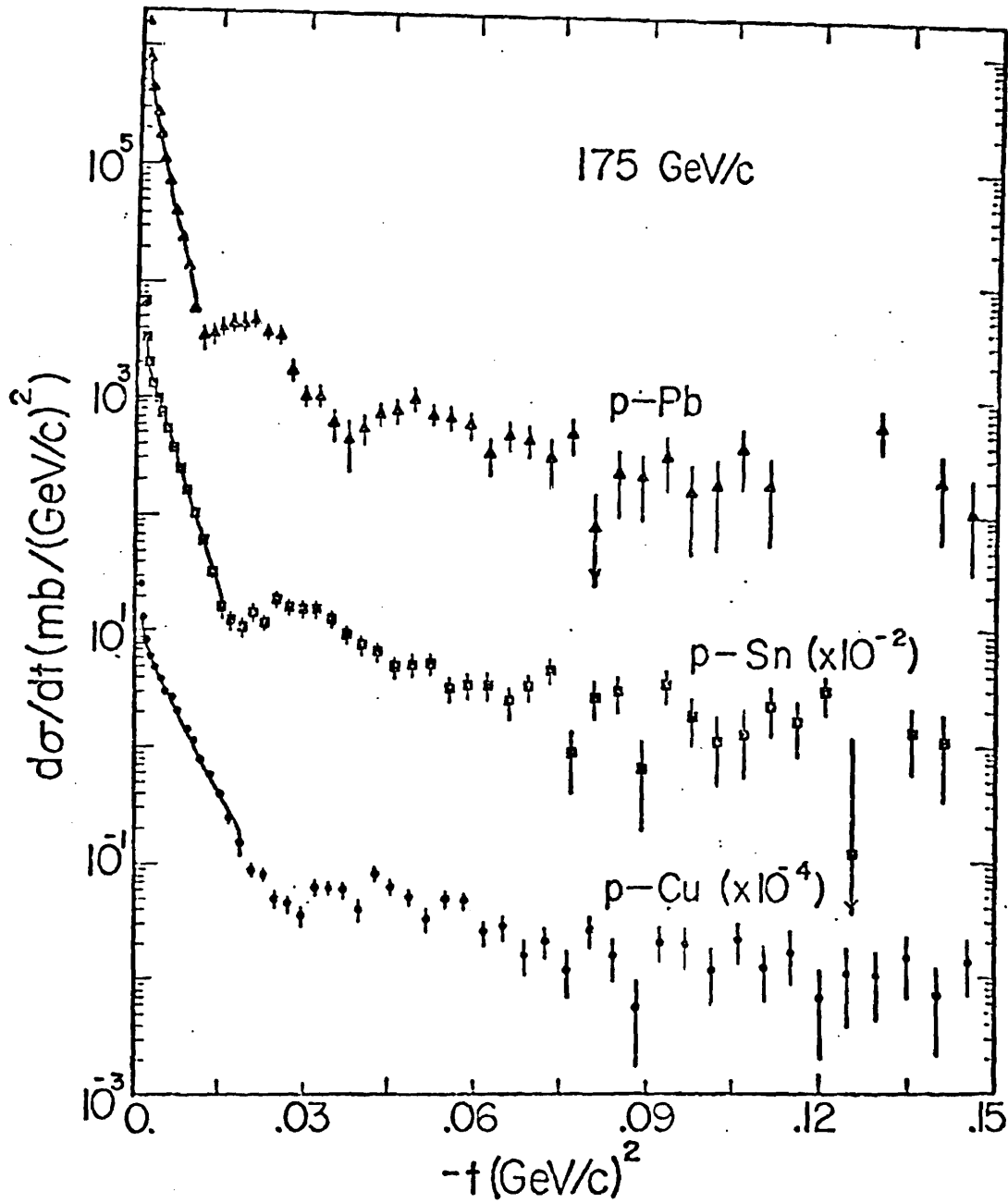


Figure 6.12

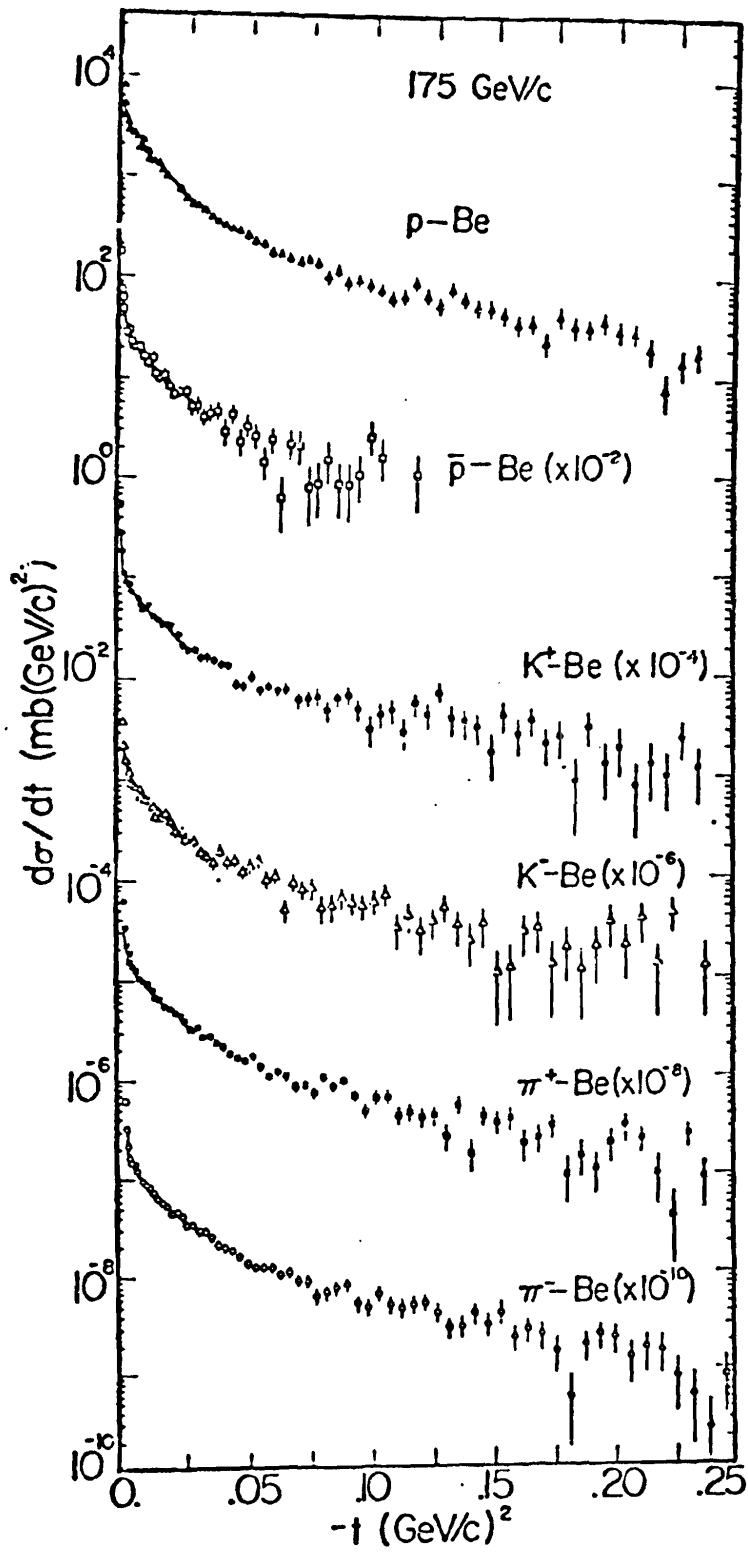


Figure 6.13

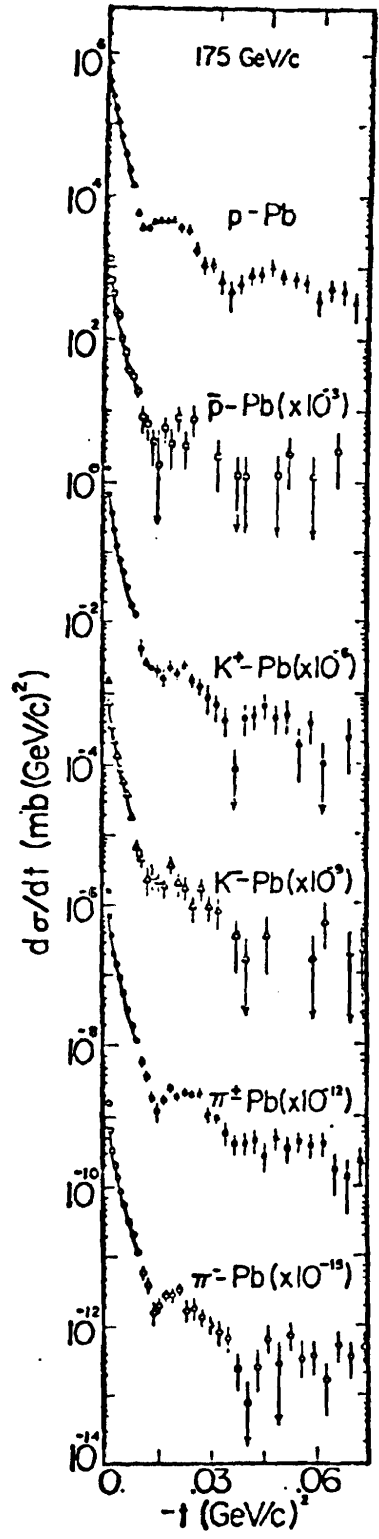


Figure 6.14

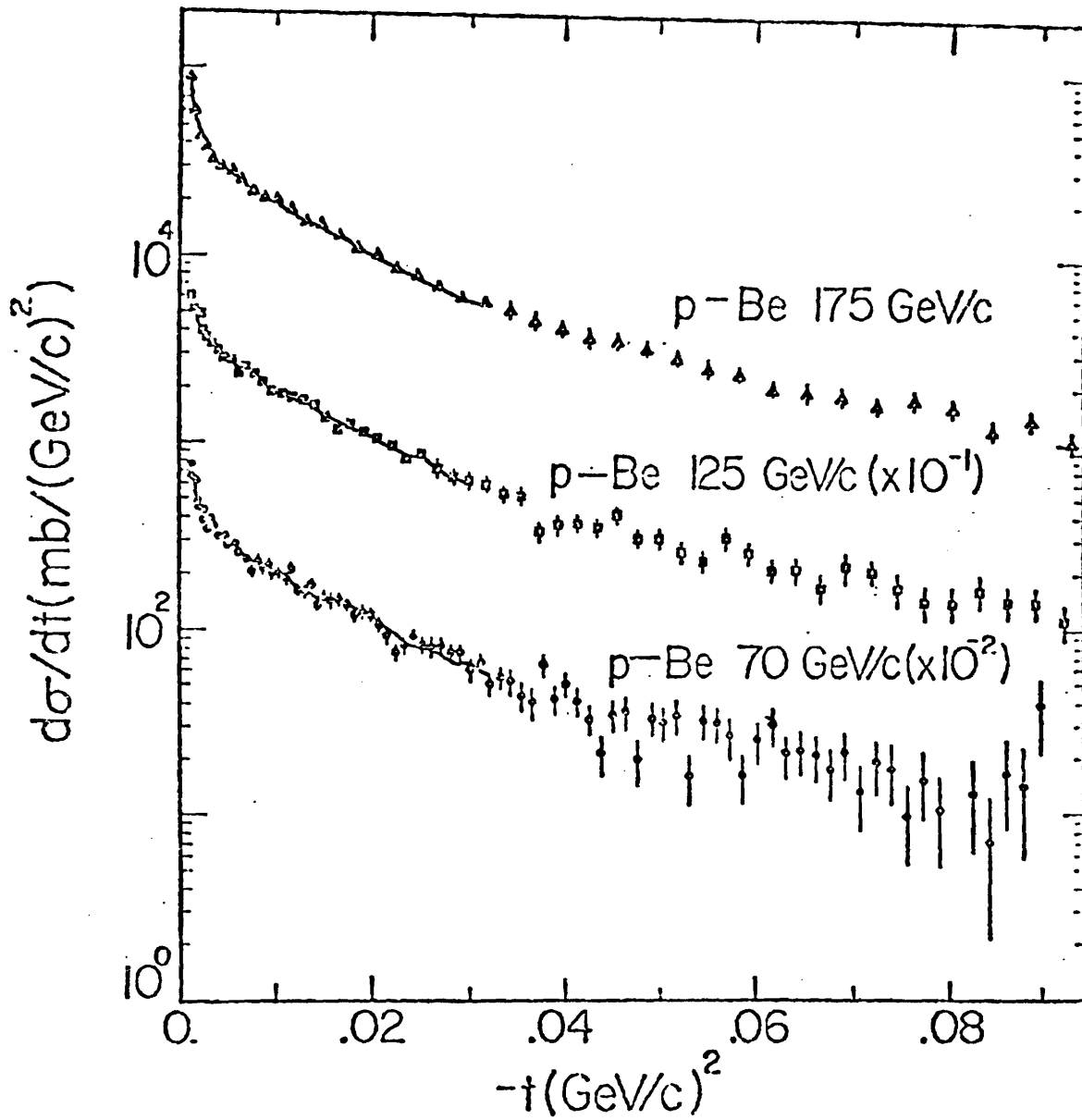


Figure 6.15

Figure 6.16

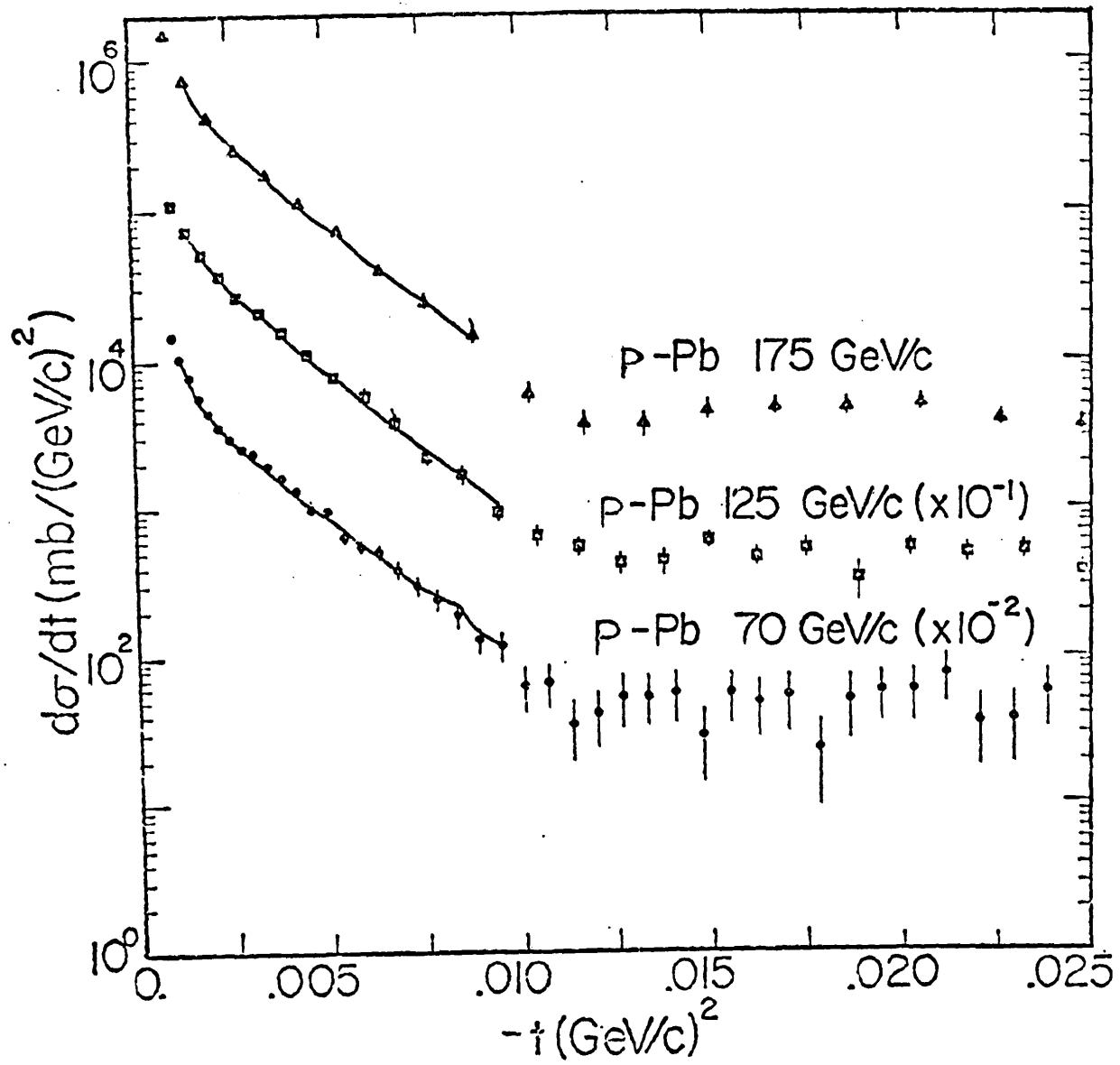


Table 6.5 presents values of N_0 , b_A , and σ_A as derived from the fits. The solid lines in Figures 6.11 to 6.16 present the results of these fits (using the parameterization of Eq. 6.6). Figures 6.17 and 6.18 present the contribution of each term of Eq. 6.6 for some cases.

The systematic errors in Table 6.5 were calculated in the following manner. A series of fits were performed where a cut on a particular kinematic variable (for example recoil mass squared) was varied while keeping all other cuts constant. The range the parameters of interest (i.e. N_0 , b_A , and σ_A) varied for the fits was taken to be the systematic error. In addition the dependence of the results on the values of N_A and b_p in the incoherent scattering term (see Table 6.4) was investigated. A variation of 30% in N_A leads to negligible change in N_0 and σ_A ; however there is some effect on b_A . This effect on b_A is 4% for Be, 3% for C, 2% for Al, 1% for Cu, 0.5% for Sn, and 0.25% for Pb. A variation of one unit in b_p has negligible effect on N_0 and σ_A and, as compared to the effect due to the variation of N_A , a negligible effect on b_A .

It is to be noted that for most reactions N_0 , the overall normalization, is not close to 1.0 as would be expected. Since σ_A , the total cross section for hadron

TABLE 6.5

Results of fits to data using Eq. 6.6
 175 GeV/c: π^+ , k^+ , p

	$ t $ Range (GeV/c) ²	N_0	σ_A (mb)	b_A (GeV/c) ⁻²	χ^2/DOF
π^+ -Be	.0018-.0330	.86±.05(.04)	182.2± 7.2(10.0)	64.9± 1.5(3.0)	18.0/18
k^+ -Be	.0018-.0330	.86±.05(.06)	149.3± 7.4(8.0)	58.0± 2.2(2.0)	20.1/18
p -Be	.0018-.0330	1.08±.06(.05)	249.2± 8.3(10.0)	74.7± 1.0(1.5)	20.3/18
π^+ -C	.0018-.0330	.82±.04(.04)	244.9± 7.5(12.0)	67.6± 1.3(3.0)	21.0/18
k^+ -C	.0018-.0330	.87±.04(.03)	195.4± 7.5(5.0)	60.4± 2.0(2.0)	18.3/18
p -C	.0018-.0330	.91±.04(.03)	345.2± 9.9(15.0)	74.0± 1.0(3.0)	21.6/18
π^+ -Al	.0018-.0330	.76±.04(.05)	507.8± 16.9(15.0)	106.9± 2.0(2.0)	22.1/18
k^+ -Al	.0018-.0330	.80±.04(.02)	442.1± 19.4(10.0)	108.6± 3.0(2.0)	22.5/18
p -Al	.0018-.0330	.72±.04(.03)	764.3± 23.5(15.0)	120.3± 1.5(2.0)	21.9/18
π^+ -Cu	.0018-.0195	.73±.03(.04)	1117.4± 47.9(40.0)	190.3± 4.8(3.0)	13.4/12
k^+ -Cu	.0018-.0195	.73±.04(.06)	926.1± 54.0(45.0)	185.3± 7.4(3.0)	9.5/12
p -Cu	.0018-.0195	.54±.03(.05)	1835.0± 79.9(60.0)	217.8± 3.2(2.0)	14.2/12
π^+ -Sn	.0018-.0160	.62±.03(.04)	2320.3±102.0(80.0)	312.9± 5.2(3.0)	11.7/10
k^+ -Sn	.0018-.0160	.69±.03(.03)	1933.9±106.4(50.0)	309.8± 8.7(3.0)	12.8/10
p -Sn	.0018-.0160	.47±.03(.05)	3465.6±157.6(130.0)	338.3± 4.6(3.0)	13.1/10
π^+ -Pb	.0018-.0096	.61±.04(.03)	3818.4±279.3(150.0)	436.7±15.5(8.0)	7.8/ 6
k^+ -Pb	.0018-.0096	.67±.04(.05)	3210.1±286.7(130.0)	410.5±20.9(7.0)	6.1/ 6
p -Pb	.0018-.0096	.55±.03(.05)	4803.3±219.6(80.0)	455.3±10.1(5.0)	6.5/ 6

TABLE 6.5(cont.)

125 GeV/c: π^+ , k^+ , p

	$ t $ Range (GeV/c) ²	N_0	σ_A (mb)	b_A (GeV/c) ⁻²	χ^2/DOF
π^+ -Be	.0016-.0306	.80±.06(.05)	190.3± 9.7(6.0)	65.6± 2.1(1.0)	24.2/25
k^+ -Be	.0016-.0306	.88±.06(.03)	145.9± 8.1(3.0)	60.1± 2.4(1.0)	23.1/25
p -Be	.0016-.0306	.93±.07(.04)	269.0± 12.4(8.0)	70.7± 1.3(0.7)	27.4/25
π^+ -Al	.0016-.0306	.77±.04(.02)	521.4± 17.4(11.0)	108.1± 2.2(1.7)	27.2/25
k^+ -Al	.0016-.0306	.76±.04(.03)	442.0± 19.2(15.0)	102.5± 3.2(2.9)	26.0/25
p -Al	.0016-.0306	.70±.04(.02)	780.8± 25.9(14.0)	119.1± 1.5(1.8)	26.5/25
π^+ -Pb	.0016-.0100	.50±.04(.03)	4599.0 349.3(150.0)	448.1±13.6(4.0)	4.8/10
k^+ -Pb	.0016-.0100	.59±.04(.03)	3864.7±319.5(175.0)	436.2±16.6(6.0)	9.7/10
p -Pb	.0016-.0100	.41±.04(.04)	6219.2±461.0(180.0)	475.3±10.5(4.0)	11.0/10

70 GeV/c: π^+ , k^+ , p

π^+ -Be	.0013-.0324	1.00±.05(.04)	170.9± 6.7(4.0)	65.1± 2.8(2.0)	32.2/45
k^+ -Be	.0013-.0324	1.02±.06(.03)	135.8± 6.9(5.0)	61.8± 4.4(6.0)	52.1/45
p -Be	.0013-.0324	1.06±.07(.02)	251.6± 10.8(7.0)	70.7± 4.8(3.0)	47.2/45
π^+ -C	.0013-.0324	.86±.04(.02)	237.8± 9.0(6.0)	63.5± 2.8(2.0)	44.1/45
k^+ -C	.0013-.0324	1.06±.05(.02)	167.6± 7.7(7.0)	58.7± 4.3(5.0)	46.6/45
p -C	.0013-.0324	1.00±.04(.03)	325.3± 7.5(7.0)	70.5± 2.4(2.0)	46.4/45

TABLE 6.5 (cont.)

70 GeV/c: π^+ , k^+ , p

	$ t $ Range (GeV/c) ²	N_0	σ_A (mb)	b_A (GeV/c) ⁻²	χ^2/DOF
π^+ -Al	.0013-.0324	.85±.03(.04)	487.6± 13.8(10.0)	107.0± 3.0(2.0)	33.8/45
k^+ -Al	.0013-.0324	.87±.03(.02)	408.9± 15.5(8.0)	105.7± 4.4(2.0)	45.6/45
p -Al	.0013-.0324	.82±.04(.03)	720.3± 22.6(7.0)	118.8± 2.4(3.0)	50.7/45
π^+ -Cu	.0013-.0144	.77±.03(.02)	1090.6± 42.9(15.0)	187.4± 6.9(2.0)	26.8/27
k^+ -Cu	.0013-.0144	.79±.03(.02)	901.1± 47.6(15.0)	173.6±10.1(2.0)	25.9/27
p -Cu	.0013-.0144	.70±.03(.02)	1477.5± 59.1(12.0)	184.0± 5.6(2.0)	28.2/27
π^+ -Sn	.0013-.0110	.73±.02(.02)	1905.2± 76.3(55.0)	259.4± 9.5(3.0)	14.1/22
k^+ -Sn	.0013-.0110	.79±.03(.02)	1512.2± 83.2(36.0)	229.8±13.9(4.0)	14.3/22
p -Sn	.0013-.0110	.65±.03(.02)	2544.3±107.1(30.0)	283.5± 8.3(2.0)	26.8/22
π^+ -Pb	.0013-.0110	.65±.03(.01)	3795.5±220.1(20.0)	421.3±13.0(5.0)	21.6/22
k^+ -Pb	.0013-.0110	.75±.04(.02)	3028.9±231.9(50.0)	401.3±19.7(8.0)	24.4/22
p -Pb	.0013-.0110	.62±.04(.01)	4348.2±273.0(45.0)	431.8±13.2(5.0)	23.8/22

70 GeV/c: π^- , k^- , \bar{p}

π^- -Be	.0013-.0324	.95±.04(.02)	165.9± 5.8(2.0)	61.0± 2.5(1.5)	45.9/46
k^- -Be	.0013-.0324	.92±.05(.05)	150.7± 7.6(10.0)	69.7± 4.0(7.0)	47.2/46
\bar{p} -Be	.0013-.0324	.90±.09(.06)	289.5± 17.6(10.0)	68.5± 3.6(4.0)	46.4/46

TABLE 6.5(cont.)

70 GeV/c: π^- , k^- , \bar{p}

	$ t $ Range (GeV/c) ²	N_0	σ_A (mb)	b_A (GeV/c) ⁻²	χ^2/DOF
π^- -C	.0013-.0324	.88±.03(.02)	222.3± 7.4(4.0)	58.6± 2.6(3.0)	45.8/45
k^- -C	.0013-.0324	.93±.05(.03)	207.6± 9.5(5.0)	68.2± 4.1(3.0)	51.7/45
\bar{p} -C	.0013-.0324	.82±.08(.04)	391.7± 23.1(8.0)	72.3± 2.6(4.0)	50.6/45
π^- -Al	.0013-.0324	.79±.02(.02)	483.9± 12.4(5.0)	103.8± 2.7(1.5)	37.8/45
k^- -Al	.0013-.0324	.84±.02(.03)	428.8± 11.4(6.0)	103.3± 3.1(3.0)	49.2/45
\bar{p} -Al	.0013-.0324	.63±.03(.04)	868.8± 28.7(11.0)	121.7± 2.0(2.0)	53.8/45
π^- -Cu	.0013-.0144	.69±.03(.03)	1077.5± 48.8(55.0)	172.4± 7.7(3.0)	29.2/27
k^- -Cu	.0013-.0144	.77±.03(.03)	900.4± 40.6(55.0)	162.1± 8.5(4.0)	16.4/27
\bar{p} -Cu	.0013-.0144	.56±.04(.03)	1755.5± 90.9(75.0)	199.3± 6.4(3.0)	26.3/27
π^- -Sn	.0013-.0110	.67±.02(.02)	1825.6± 73.5(40.0)	253.9± 9.4(3.0)	21.7/22
k^- -Sn	.0013-.0110	.78±.02(.02)	1524.8± 62.2(25.0)	237.8± 9.9(3.0)	24.3/22
\bar{p} -Sn	.0013-.0110	.61±.03(.02)	2649.1±113.1(90.0)	282.0± 8.0(3.0)	24.1/22
π^- -Pb	.0013-.0110	.65±.03(.03)	3186.6±213.8(40.0)	386.6±16.4(4.0)	17.1/22
k^- -Pb	.0013-.0110	.67±.03(.05)	3088.6±194.3(60.0)	386.4±15.5(5.0)	23.7/22
\bar{p} -Pb	.0013-.0110	.44±.04(.03)	5616.4±408.7(150.0)	461.6±13.7(10.0)	25.2/22

TABLE 6.5(cont.)
175 GeV/c: π^- , k^- , \bar{p}

	$ t $ Range (GeV/c) ²	N_0	σ_A (mb)	b_A (GeV/c) ⁻²	χ^2/DOF
π^- -Be	.0018-.0333	.96±.06(.06)	168.4± 7.4(7.0)	65.8± 1.8(4.0)	20.9/18
k^- -Be	.0018-.0333	1.21±.09(.05)	128.0± 7.5(5.0)	61.6± 3.1(2.0)	11.1/18
\bar{p} -Be	.0018-.0333	1.64±.31(.20)	191.0± 25.1(16.0)	79.0± 6.4(4.0)	7.6/18
π^- -C	.0018-.0333	.86±.05(.06)	237.1± 10.3(7.0)	67.5± 1.9(2.0)	20.3/18
k^- -C	.0018-.0333	1.05±.08(.06)	184.8± 11.3(7.0)	68.0± 3.6(2.5)	20.1/18
\bar{p} -C	.0018-.0333	1.12±.26(.08)	317.6± 48.2(15.0)	79.6± 5.6(2.0)	21.2/18
π^- -Al	.0018-.0333	.83±.05(.06)	477.7± 23.4(18.0)	106.2± 3.2(4.0)	19.5/18
k^- -Al	.0018-.0333	.96±.08(.05)	378.7± 26.8(10.0)	94.3± 5.2(3.0)	9.4/18
\bar{p} -Al	.0018-.0333	.15±.04(.10)	1820.9± 39.6(50.0)	137.8± 4.3(4.0)	24.8/18
π^- -Cu	.0018-.0200	.63±.04(.05)	1208.9± 61.8(45.0)	193.4± 5.3(2.0)	10.6/12
k^- -Cu	.0018-.0200	.75±.05(.06)	978.7± 72.3(40.0)	193.8± 9.9(3.0)	12.0/12
\bar{p} -Cu	.0018-.0200	.47±.19(.06)	2035.5± 507.4(100.0)	225.9±15.3(5.0)	13.0/12
π^- -Sn	.0018-.0160	.55±.03(.02)	2310.8± 123.6(70.0)	299.1± 7.6(3.0)	10.6/10
k^- -Sn	.0018-.0160	.60±.05(.04)	2057.4± 163.9(120.0)	294.4±12.5(3.0)	9.7/10
\bar{p} -Sn	.0018-.0160	.31±.11(.08)	4469.9± 939.9(100.0)	348.9±20.8(8.0)	12.3/10
π^- -Pb	.0018-.0100	.59±.04(.06)	3594.9± 284.8(175.0)	406.5±17.1(9.0)	5.6/ 6
k^- -Pb	.0018-.0100	.70±.06(.06)	3246.5± 365.6(280.0)	418.6±25.9(18.0)	11.2/ 6
\bar{p} -Pb	.0018-.0100	.46±.17(.13)	5271.5±1772.6(400.0)	434.9±54.1(20.0)	6.8/ 5

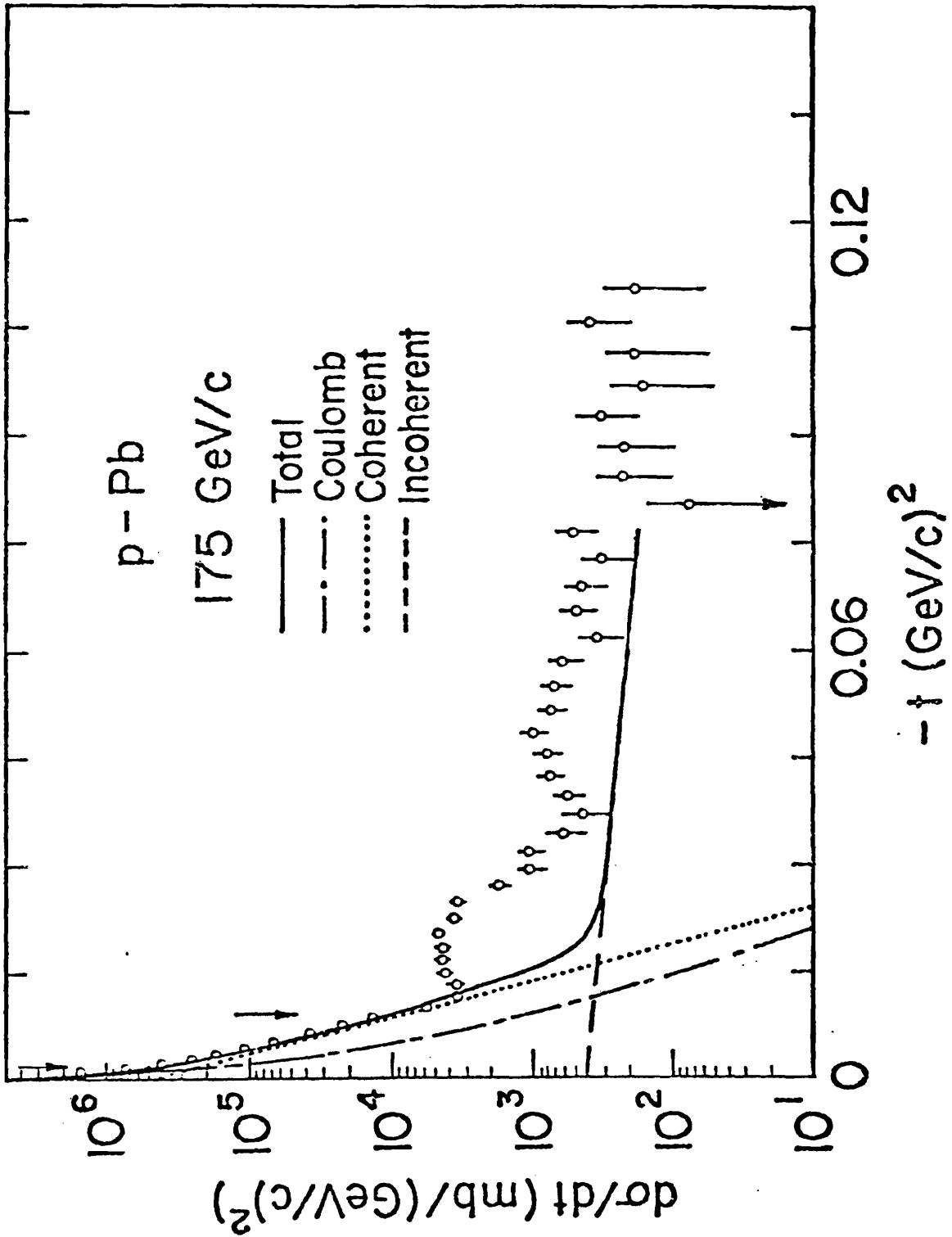
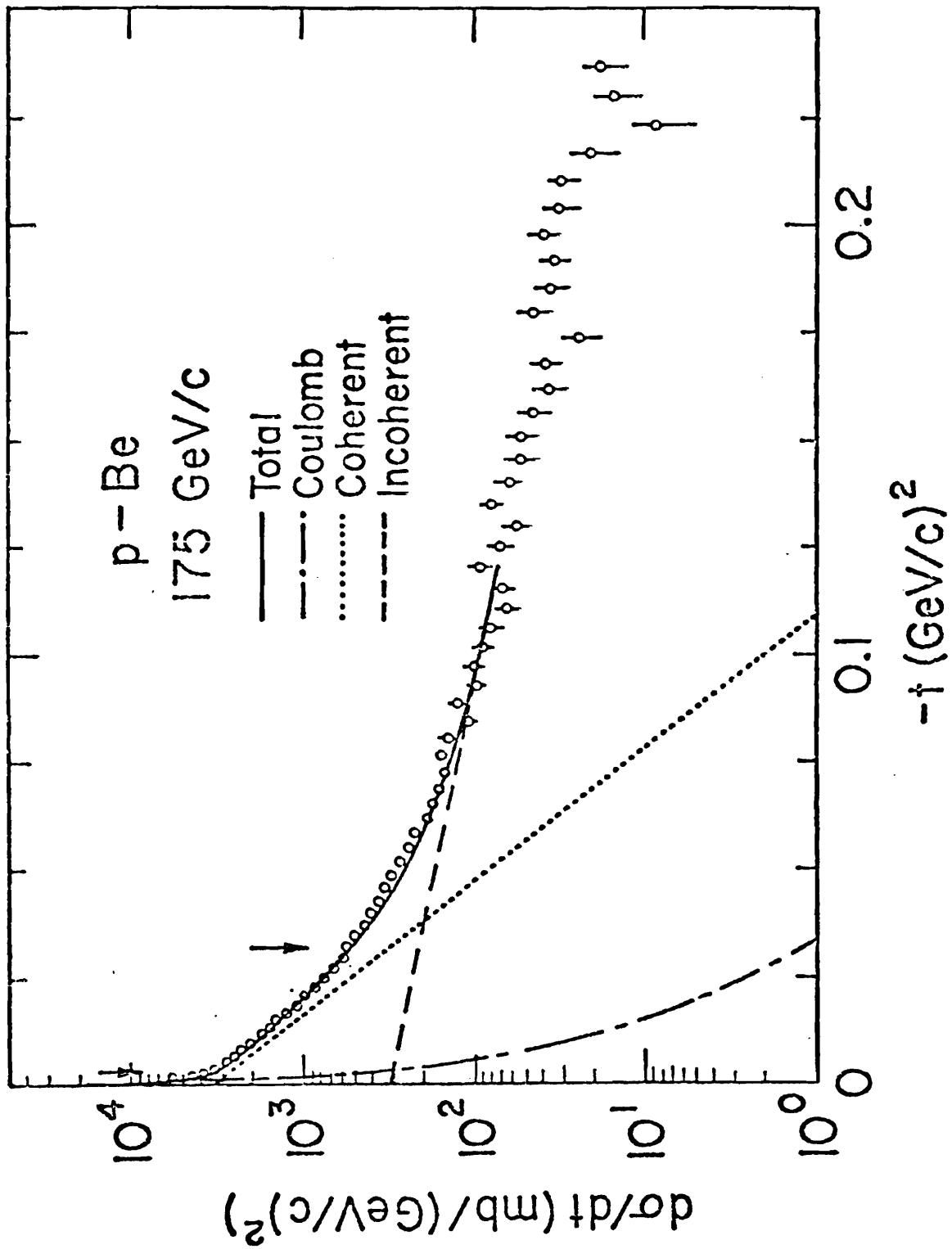
Contributions to $d\sigma/dt$: p-Pb 175 GeV/c

Figure 6.17

Contributions to $d\sigma/dt$: p-Be 175 GeV/c

- nucleus scattering, was found to be strongly correlated with the overall normalization, the values for σ_A are not reliable in themselves. Over the t region fit the parameterization that is presented is reasonably good; however the values of σ_A derived must be used in conjunction with the values N_0 found. Chapter 7 addresses the problem of the overall normalization of the data.

Table 6.6 presents values of b_A derived from fits over approximately the same t region for all reactions. Figures 6.19 to 6.24 present the values of the forward slope for coherent hadron - nucleus scattering (b_A) that were found. In general for a given beam momentum and nuclear target, the forward slope is steepest when the incident projectile is a proton or antiproton and the shallowest when the incident projectile is a kaon.

The data for the Cu, Sn, and Pb targets were fit substituting a Bessel function form for the exponential in the coherent term of Eq. 6.6. This was done in order to attempt to fit beyond the first minimum exhibited by these data. The fits resulted in a poor chi-squared per degree of freedom which implies a more sophisticated theoretical treatment is needed (such as can be found in references 1.1 (Glauber theory) and 1.2).

TABLE 6.6: Value of forward slope, b_A , in the region $0.0018 \leq -t \leq 0.0125$ (GeV/c)²

	Momentum (GeV/c)	b_A (GeV/c) ⁻²	χ^2 /DOF
π^+ -Be	175	64.4± 2.7	2.3/ 8
k^+ -Be	175	57.2± 4.1	11.7/ 8
p^- -Be	175	77.8± 2.5	9.1/ 8
π^- -Be	175	63.3± 3.5	6.8/ 8
\bar{k}^- -Be	175	60.9± 5.6	3.7/ 8
\bar{p}^- -Be	175	75.4± 9.7	3.9/ 8
π^+ -C	175	62.3± 3.3	10.6/ 8
k^+ -C	175	57.5± 5.2	5.1/ 8
p^- -C	175	74.1± 2.7	10.2/ 8
π^- -C	175	65.4± 4.2	6.4/ 8
\bar{k}^- -C	175	59.8± 6.0	6.5/ 8
\bar{p}^- -C	175	85.5± 9.5	10.2/ 8
π^+ -Al	175	106.3± 4.8	12.2/ 8
k^+ -Al	175	111.1± 5.2	10.3/ 8
p^- -Al	175	121.9± 2.6	11.4/ 8
π^- -Al	175	109.2± 7.3	9.6/ 8
\bar{k}^- -Al	175	87.8± 9.4	6.5/ 8
\bar{p}^- -Al	175	131.4±10.7	10.9/ 8
π^+ -Cu	175	186.9± 5.4	8.5/ 8
k^+ -Cu	175	183.6± 7.8	3.6/ 8
p^- -Cu	175	217.4± 4.3	11.5/ 8
π^- -Cu	175	192.8± 8.2	3.8/ 8
\bar{k}^- -Cu	175	192.7±13.1	8.3/ 8
\bar{p}^- -Cu	175	218.2±21.8	7.2/ 8
π^+ -Sn	175	308.1± 7.3	10.1/ 8
k^+ -Sn	175	299.8±11.2	10.5/ 8
p^- -Sn	175	335.1± 5.3	12.1/ 8
π^- -Sn	175	297.6± 7.9	4.1/ 8
\bar{k}^- -Sn	175	293.8±13.2	9.3/ 8
\bar{p}^- -Sn	175	345.5±21.6	10.6/ 8
π^+ -Pb	175	435.2±15.2	8.2/ 8
k^+ -Pb	175	411.6±20.1	6.7/ 8
p^- -Pb	175	455.7± 9.8	7.2/ 8
π^- -Pb	175	407.2±16.8	6.2/ 8
\bar{k}^- -Pb	175	419.3±25.4	10.7/ 8
\bar{p}^- -Pb	175	433.9±53.2	7.4/ 8
π^+ -Be	125	64.1± 3.9	15.7/12
k^+ -Be	125	57.8± 5.2	10.6/12
p^- -Be	125	71.5± 3.3	14.3/12
π^+ -Al	125	110.1± 4.4	9.3/12
k^+ -Al	125	98.2± 5.1	11.9/12
p^- -Al	125	117.7± 2.7	13.7/12

TABLE 6.6 (cont.)

	Momentum (GeV/c)	b_A (GeV/c) ⁻²	χ^2/DOF
π^+ -Pb	125	449.4±13.3	5.5/12
k^+ -Pb	125	435.3±16.4	10.3/12
p -Pb	125	475.9±10.1	12.7/12
π^+ -Be	70	65.0± 3.5	8.7/21
k^+ -Be	70	60.9± 5.3	22.1/21
p -Be	70	71.9± 6.3	23.9/21
π^- -Be	70	60.3± 5.3	20.2/21
k^- -Be	70	64.8± 7.3	24.9/21
\bar{p} -Be	70	68.9± 6.5	19.6/21
π^+ -C	70	61.1± 4.3	13.7/21
k^+ -C	70	58.6± 6.7	16.1/21
p -C	70	70.9± 3.8	24.2/21
π^- -C	70	57.4± 5.6	26.3/21
k^- -C	70	69.3± 6.6	24.0/21
\bar{p} -C	70	69.5± 3.5	25.6/21
π^+ -Al	70	107.6± 7.1	21.1/21
k^+ -Al	70	107.4± 8.2	15.6/21
p -Al	70	117.0± 5.5	25.6/21
π^- -Al	70	105.0± 4.4	14.8/21
k^- -Al	70	102.4± 4.5	19.5/21
\bar{p} -Al	70	120.4± 3.8	21.0/21
π^+ -Cu	70	185.9± 7.9	23.8/21
k^+ -Cu	70	171.8±11.1	23.3/21
p -Cu	70	182.9± 6.3	25.7/21
π^- -Cu	70	167.1± 8.2	18.8/21
k^- -Cu	70	159.9± 9.9	13.4/21
\bar{p} -Cu	70	191.3± 9.5	15.8/21
π^+ -Sn	70	259.4± 7.8	12.4/21
k^+ -Sn	70	229.2±12.1	13.8/21
p -Sn	70	284.0± 7.4	25.1/21
π^- -Sn	70	252.6± 9.7	19.1/21
k^- -Sn	70	237.1±10.3	24.8/21
\bar{p} -Sn	70	281.7± 8.5	26.4/21
π^+ -Pb	70	420.8±12.7	21.3/21
k^+ -Pb	70	403.4±18.8	25.2/21
p -Pb	70	430.2±12.9	23.5/21
π^- -Pb	70	384.4±15.7	15.9/21
k^- -Pb	70	385.1±15.3	22.3/21
\bar{p} -Pb	70	464.2±13.2	24.8/21

FORWARD SLOPE OF COHERENT SCATTERING
VERSUS
ATOMIC WEIGHT: π^+

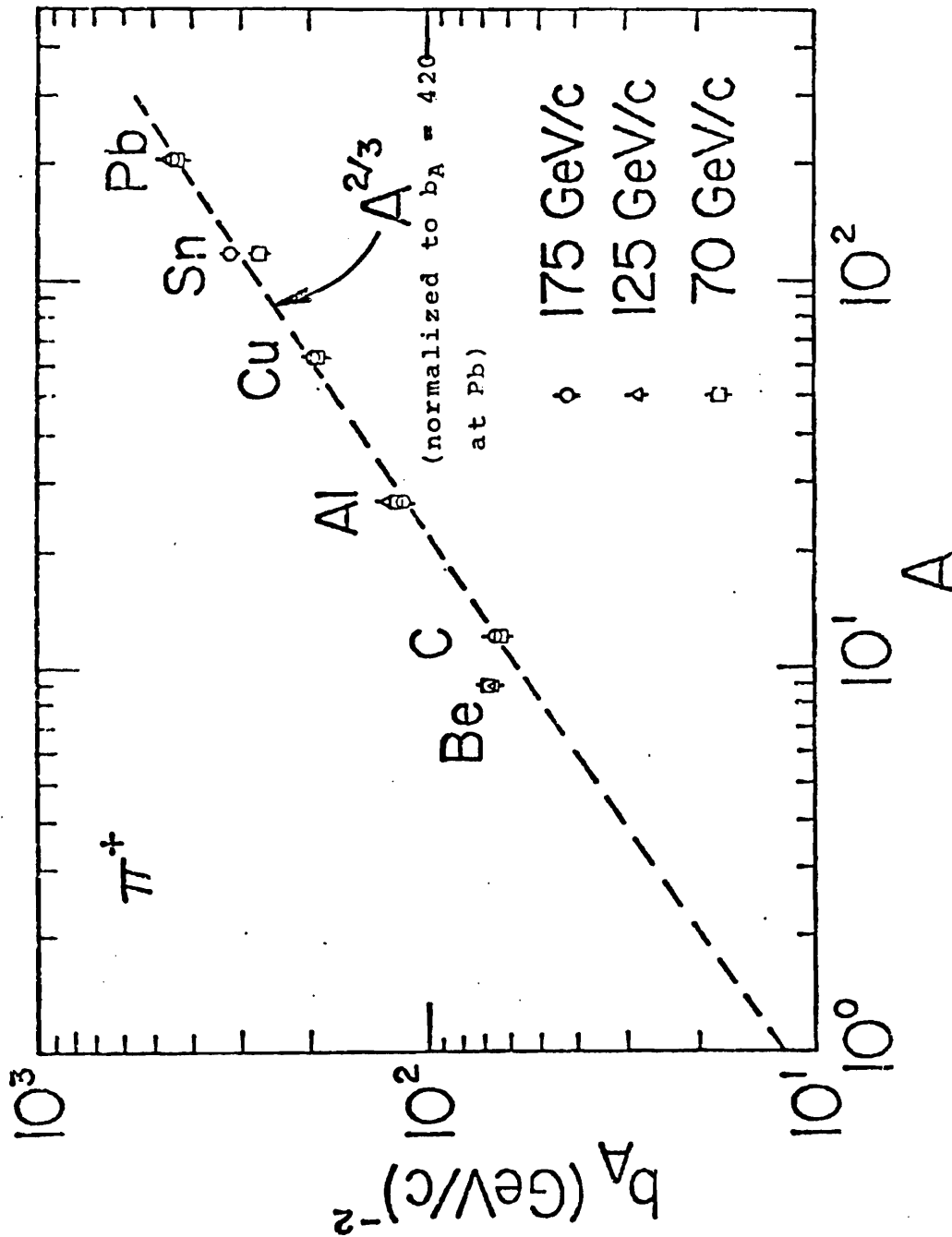


Figure 6.19

FORWARD SLOPE OF COHERENT SCATTERING
 VERSUS
 ATOMIC WEIGHT: π^-

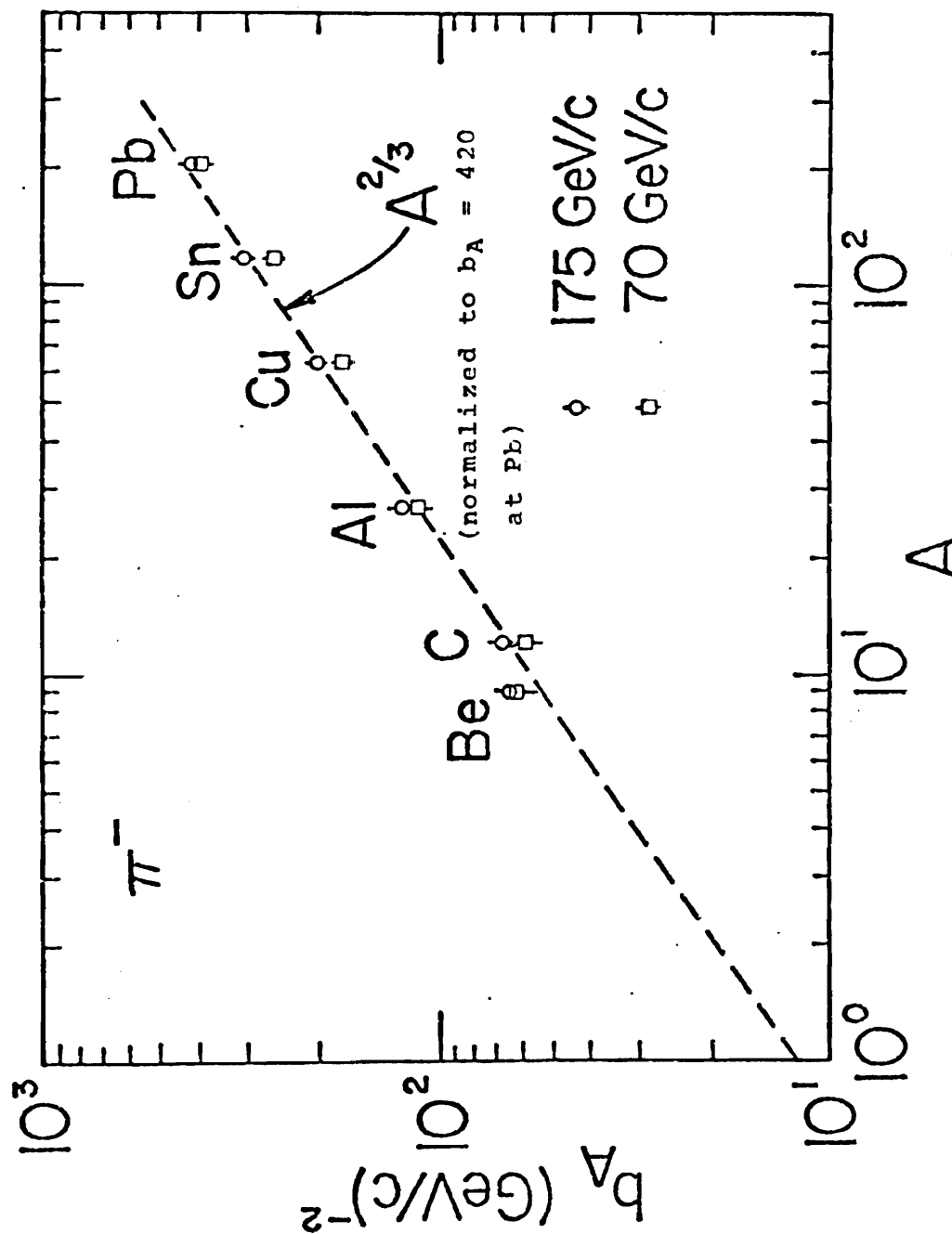


Figure 6.20

FORWARD SLOPE OF COHERENT SCATTERING
 VERSUS
 ATOMIC WEIGHT: K^+

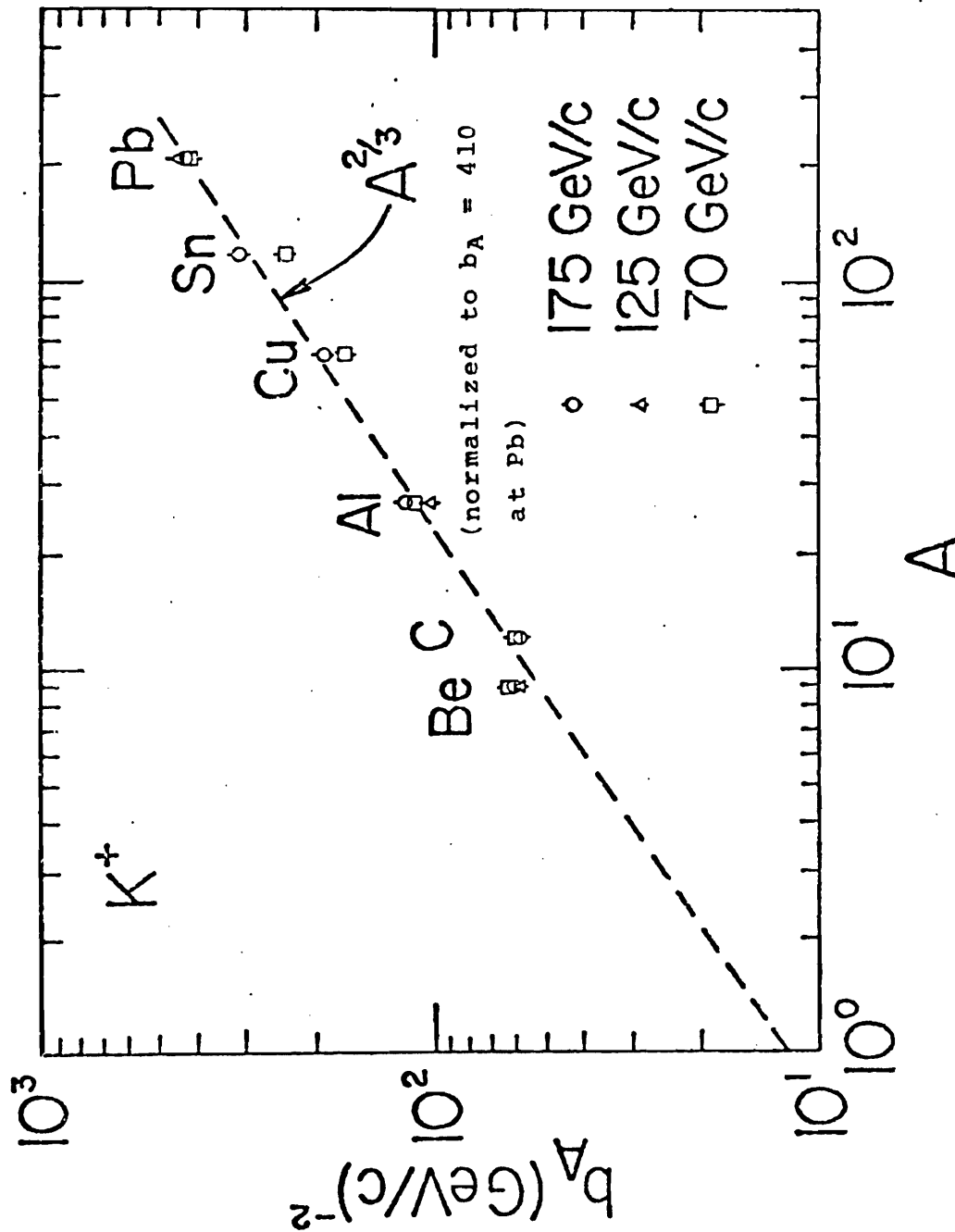


Figure 6.21

FORWARD SLOPE OF COHERENT SCATTERING
 VERSUS
 ATOMIC WEIGHT: K^-

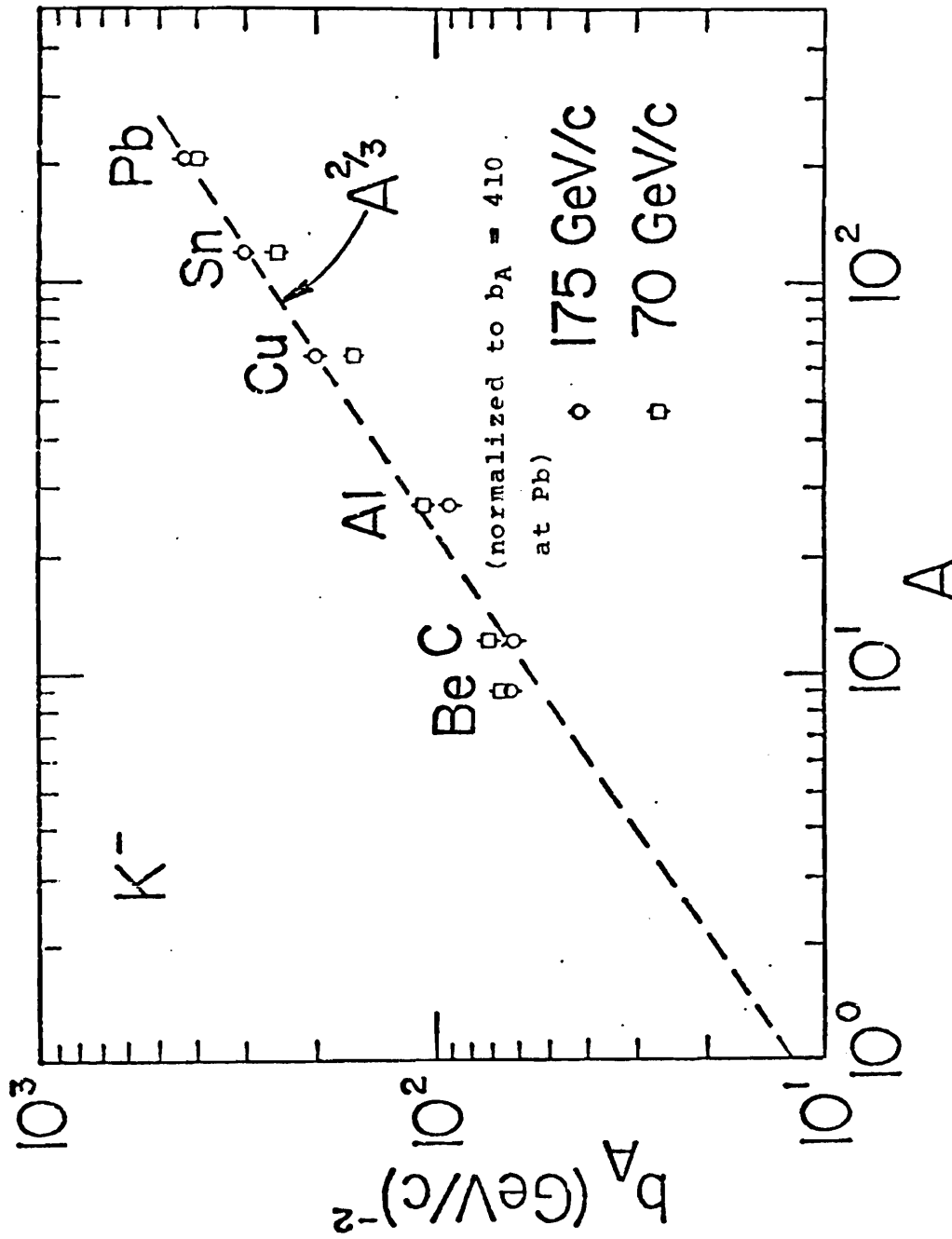


Figure 6.22

FORWARD SLOPE OF COHERENT SCATTERING
 VERSUS
 ATOMIC WEIGHT: p

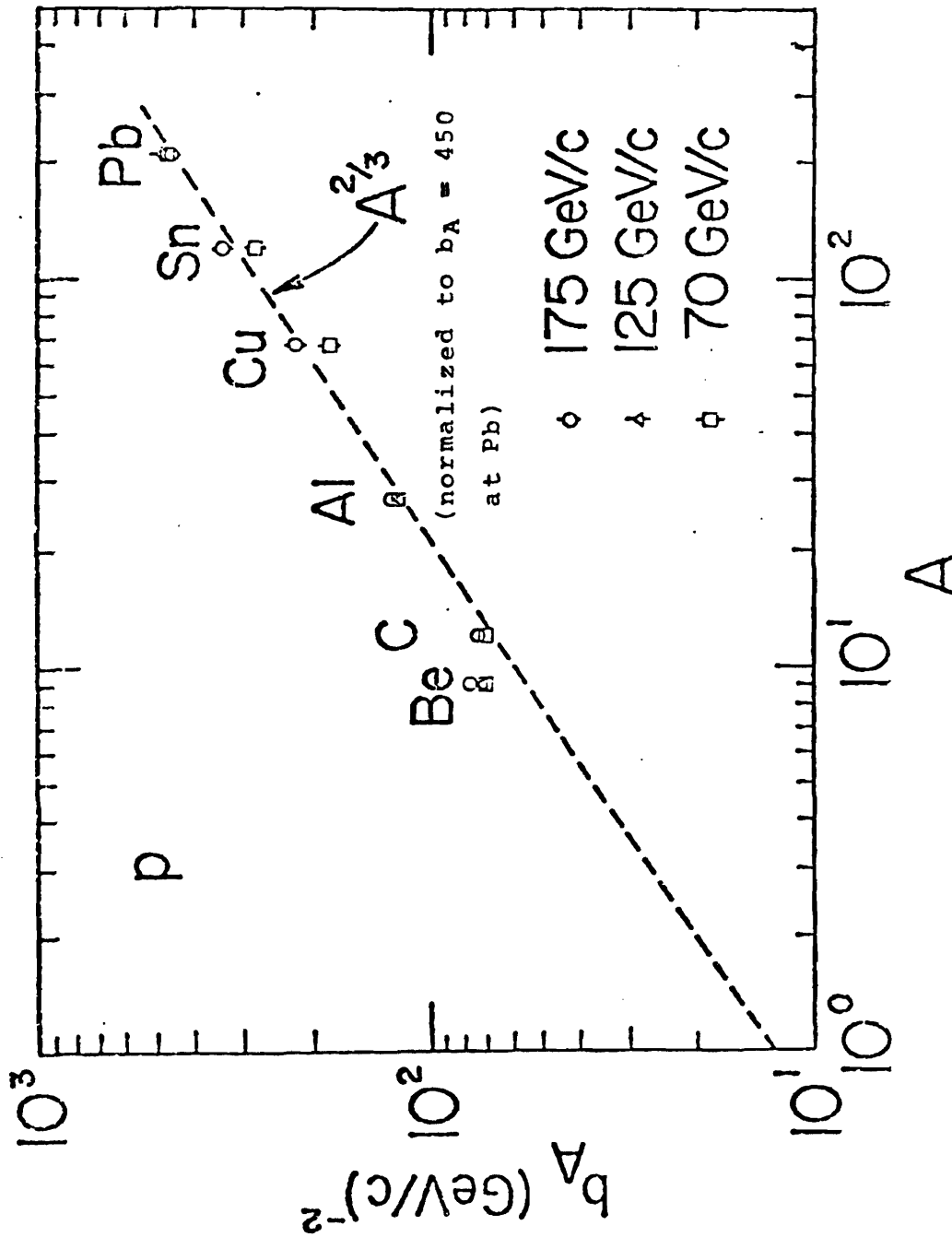


Figure 6.23

FORWARD SLOPE OF COHERENT SCATTERING
 VERSUS
 ATOMIC WEIGHT: \bar{p}

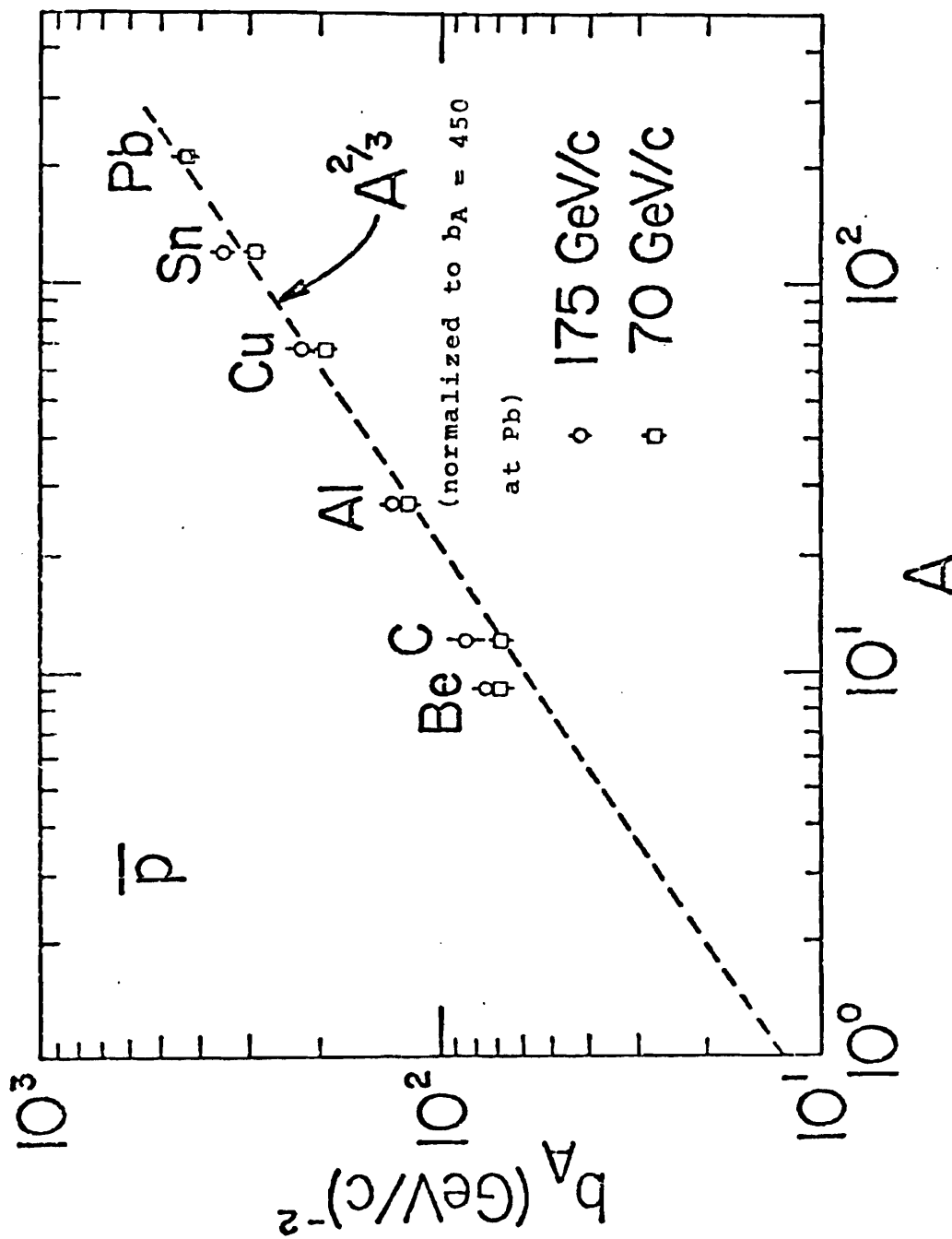


Figure 6.24

CHAPTER 7

TOTAL CROSS SECTIONS: A CONSISTENCY CHECK

A. Introduction

By using the high resolution proportional wire chambers placed on the concrete block, a direct measurement of hadron - nucleus total cross sections was performed by means of the standard good geometry transmission method. Unfortunately since the nuclear target lengths were not optimized for this type of experiment, it was found that a measurement of reasonable accuracy (10 - 15%; σ) could be performed only with the Be and C targets. Thus these results were used as a consistency check between this method of extracting total cross sections and the calculation of total cross sections from the fits to the elastic scattering differential cross sections.

B. General Considerations

In this section the principles behind the measurement of the total cross section via the transmission technique are described.

The total cross section is defined by

$$I_t = I_0 \exp(-n\sigma x) \quad (7.1)$$

where

I_t = number of transmitted particles

I_0 = number of incident particles

σ = total cross section

n = target nuclei/unit volume = $N\rho x/A$

x = target length

ρ = target density

N = Avogadro's Number

A = atomic weight

In a target empty run, the following is measured

$$I_t^{mt}/I_0^{mt} = \exp(-n^{mt}\sigma^{mt}x^{mt})$$

where " n^{mt} , σ^{mt} , x^{mt} " reflect scattering from all objects other than the target itself.

In a target full run, the following is measured

$$I_t^f/I_0^f = \exp(-n\sigma x)\exp(-n^{mt}\sigma^{mt}x^{mt})$$

where "n", "σ", and "x" are as in Eq. 7.1.

Define

$$R^f(mt) = I_t^f(mt) / I_0^f(mt)$$

Then

$$\sigma = (1/nx) \ln(R^{mt} / R^f) \quad (7.2)$$

Experimentally one measures R^f and R^{mt} .

However Eq. 7.2 gives the total cross section, σ , if all that one measures is transmitted beam. But all counters have a finite spatial extent and in addition to transmitted beam measure very small angle scatters. In effect each counter overestimates the number of transmitted particles.

To correct for this effect one can use an apparatus shown in Figure 7.1. Counter M measures the number of incident beams while Counters 1 - 6 measure transmitted particles. Each counter measures a cross section using Eq. 7.2. However these cross sections are partial cross sections defined as follows:

$$\begin{aligned} \sigma_i &= \sigma - \int_0^{\Omega_i} (d\sigma/d\Omega) d\Omega \\ \sigma_i &= (1/nx) \ln(R_i^{mt} / R_i^f) \end{aligned} \quad (7.3)$$

where

IDEALIZED APPARATUS FOR
TOTAL CROSS SECTION
MEASUREMENT

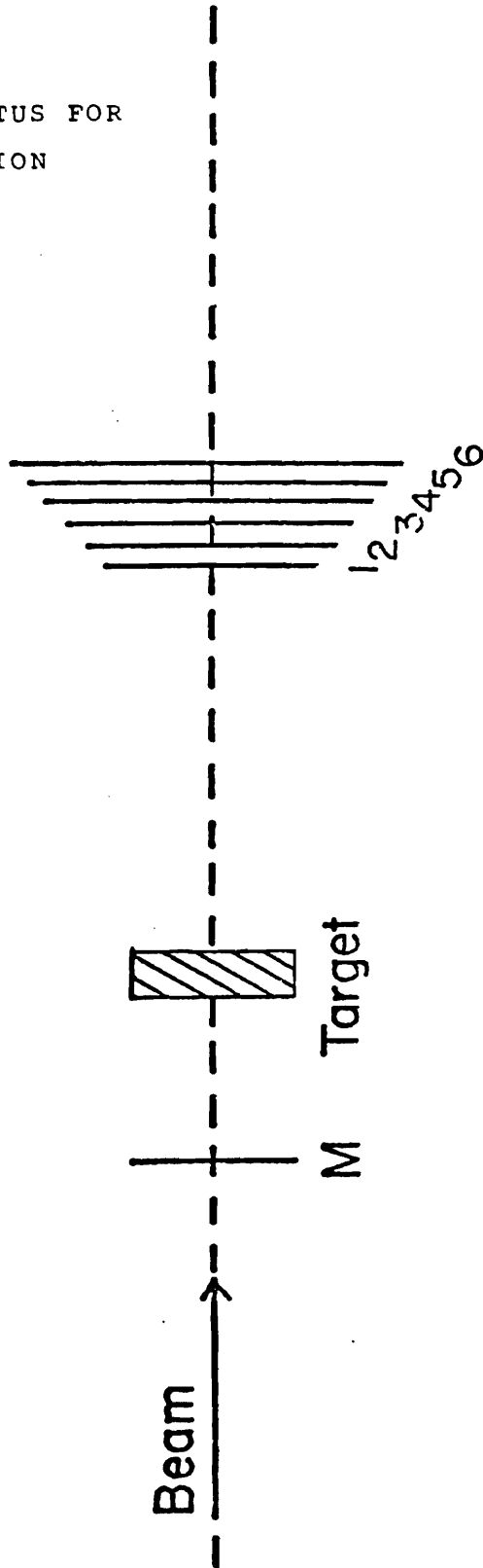


Figure 7.1

$$i = 1, 2, \dots, n$$

Ω_i = the solid angle subtended by the i th counter

The partial cross sections represent the cross section for scattering beyond an angle θ_i (corresponding to Ω_i).

Alternatively we can rewrite Eq. 7.3 as

$$\sigma_i = \sigma - \int_0^{t_i^{\min}} (d\sigma/dt) dt = \int_{-\infty}^{t_i^{\min}} (d\sigma/dt) dt \quad (7.3a)$$

where $d\sigma/dt$ includes all elastic and inelastic processes that can occur.

Therefore to measure the total cross section, σ , one merely extrapolates the partial cross sections, σ_i , to zero solid angle.

The situation is more subtle than the above suggests. We wish to measure the total cross section for strong not electromagnetic processes. However the partial cross sections contain contributions due to electromagnetic processes, i.e.

$$\sigma_i = \int_{-\infty}^{t_i^{\min}} |f_n + f_c|^2 + \sigma_i^{\text{inel}}$$

where

f_n = strong elastic scattering amplitude

f_c = Coulomb scattering amplitude

σ_i^{inel} = contribution to σ_i by strong inelastic scattering processes

Then

$$\sigma_i \approx \int_{-\infty}^{t_i^{\text{min}}} [|f_c|^2 + |f_n|^2 + 2(f_c)\text{Re}(f_n)] dt + \sigma_i^{\text{inel}}$$

where f_c has been assumed to be completely real.

Hence the quantities $(\Delta\sigma_i)_c$ and $(\Delta\sigma_i)_{cn}$ must be subtracted from σ_i before the extrapolation to zero solid angle is performed. Here

$$(\Delta\sigma_i)_c = \int_{-\infty}^{t_i^{\text{min}}} |f_c|^2 dt$$

$$(\Delta\sigma_i)_{cn} = \int_{-\infty}^{t_i^{\text{min}}} [2(f_c)\text{Re}(f_n)] dt$$

Since electromagnetic processes are concentrated in the very forward direction, these corrections will not be too severe because the counters will detect most of the Coulomb scatters. Most electromagnetic scatters, being at small angles, will be considered as transmitted beam, thus not adding to the value of a particular partial cross section.

C. Experimental Procedure and Analysis

For the total cross section measurement, information was needed from only the high resolution PWCs located on the concrete block. Before extrapolating the partial cross sections to zero solid angle, a correction was made for geometric acceptance losses. These were mainly due to the fact that the most downstream high resolution PWC was offset with respect to the beam center.

The PDP15 data tapes used for this measurement were the same as used in the elastic scattering analysis. However after that point the two analyses diverged. The steps of the total cross section are shown in Figure 7.2.

ANALYSIS STEPS:
DIRECT MEASUREMENT OF σ^{TOT}
 (NUCLEAR TARGET DATA)

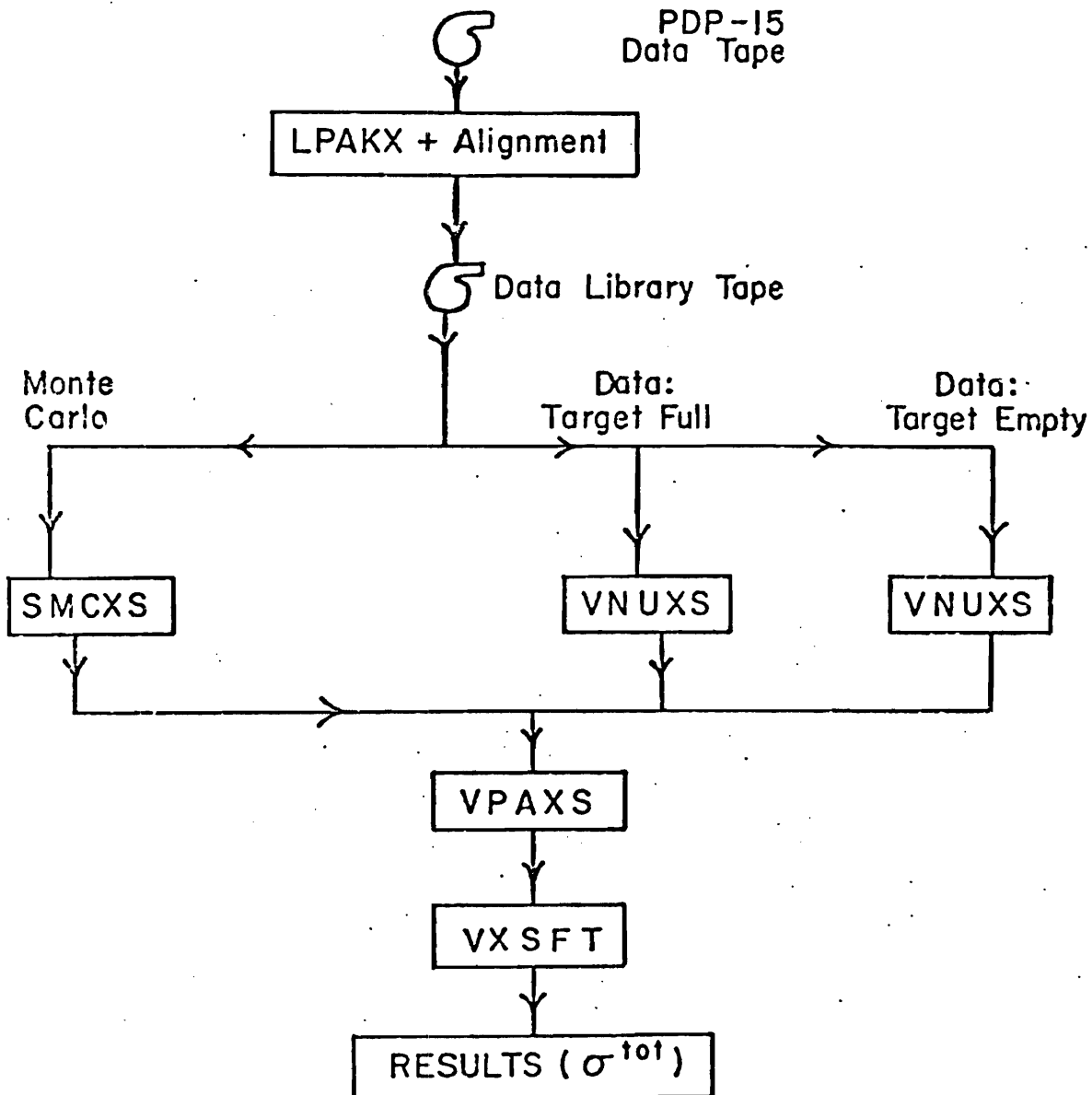


Figure 7.2

First a set of library tapes was written. LPAKX performed this task; basically these new library tapes contained all triggers with the BEAM latch set, in effect a sample of the incident beam particles with no requirements downstream of the target. Specifically the requirements for events written on these library tapes were as follows:

1. BEAM latch set
2. PWC planes 1,2,3,4, and 15 had one and only one good coordinate
3. no requirements on the coordinates in PWC planes 5 - 10

A good coordinate for the PWC planes is the same as defined in Chap. 4, Sect. B. Table 4.1 gives the PWC classification in terms of plane number.

In planes 5 - 10 up to four separate coordinates were kept. Also if these chambers contained errors, this condition was noted.

PWC errors included

1. illegal card address.

2. empty wire map on a valid card.
3. too many PWC coordinates (> 4).

The next step was to accumulate histograms in angular bins of 50° rad for the "transmitted" particles. VNUXS accomplished this job. For an event to be recorded in these histograms, it had to fulfill the following criteria:

1. PWC planes 9 and 10 (X4, Y4) had to contain one and only one good coordinate
2. At least two out the four planes 5, 6, 7, and 8 had to contain one and only one good coordinate

Again good coordinates for the PWC planes are defined in Chap. 4, Sect. B. Also an attempt to salvage events with more than two coordinates in planes 5 - 10 was made, as described in Chap. 4, Sect. B.

For events fulfilling the above criteria the scattering angle was calculated, and a histogram of this quantity was made. This histogram was accumulated for both the target full and target empty runs. In addition the total number of incident beam tracks was recorded in each case.

The program SMCXS was used to calculate the acceptance correction. SMCXS was similar in philosophy to the Monte Carlo programs used in the elastic scattering analysis, especially for the high- t case. As in that case, the migration of data from bin to bin was ignored. Also there was no need to simulate the apparatus downstream of the concrete block. Finally the acceptance was binned in angle, the same bins as for the data scattering angle histogram. A typical acceptance curve is shown in Figure 7.3.

The program VPAXS used the results from VNUXS and SMCXS to calculate the partial cross sections. There were 100 bins in the scattering angle histograms, and hence VPAXS calculated 100 partial cross sections. However only a subset were used in the extrapolation to obtain the total cross section.

The i th partial cross section is given by the following formula:

$$\sigma_i = \ln[(T_i^{mt}/I_0^{mt}) / (T_i^f/I_0^f)] / (n x) \quad (7.4)$$

where

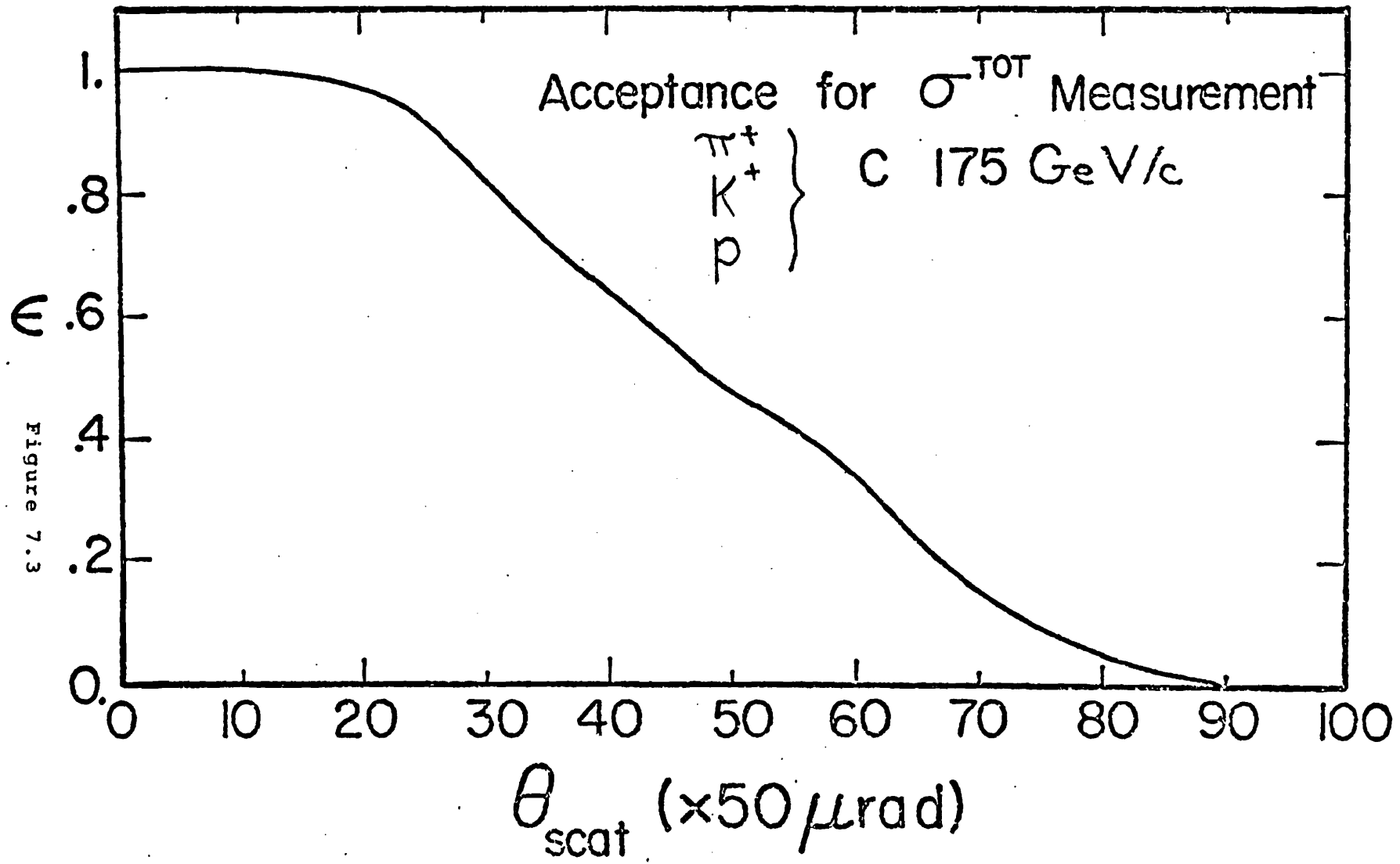


Figure 7.3

$$T_i^{mt} = \sum_{k=1}^i N_k^{mt}$$

$$T_i^f = \sum_{k=1}^i (I_0^f / I_0^{mt}) (1 - \alpha_k) N_k^{mt} + \sum_{k=1}^i N_k^f / \alpha_k$$

k = angle bin number

n = target nuclei/unit volume (see Eq. 7.1)

x = target length

$I_0^{f(mt)}$ = number of incident particles measured
in a full (empty) run

$N_k^{f(mt)}$ = number of transmitted particles
measured in the k th angle bin
for a full (empty) run

α_k = acceptance correction value for the k th
angle bin

A derivation of Eq. 7.4 is given in Appendix IV.

Typical examples of the partial cross sections
calculated are given in Figures 7.4 and 7.5.

The final step to obtain the total cross sections
was the extrapolation to zero solid angle. VSXFT
accomplished this step using the minimization program
MINUIT^{6.1}.

The partial cross sections were fit to the
following function:

$$\sigma_n = \sigma - A(1 - \exp(-B\theta_n^2)) \quad (7.5)$$

PARTIAL CROSS SECTIONS: BE: 175GEV/C

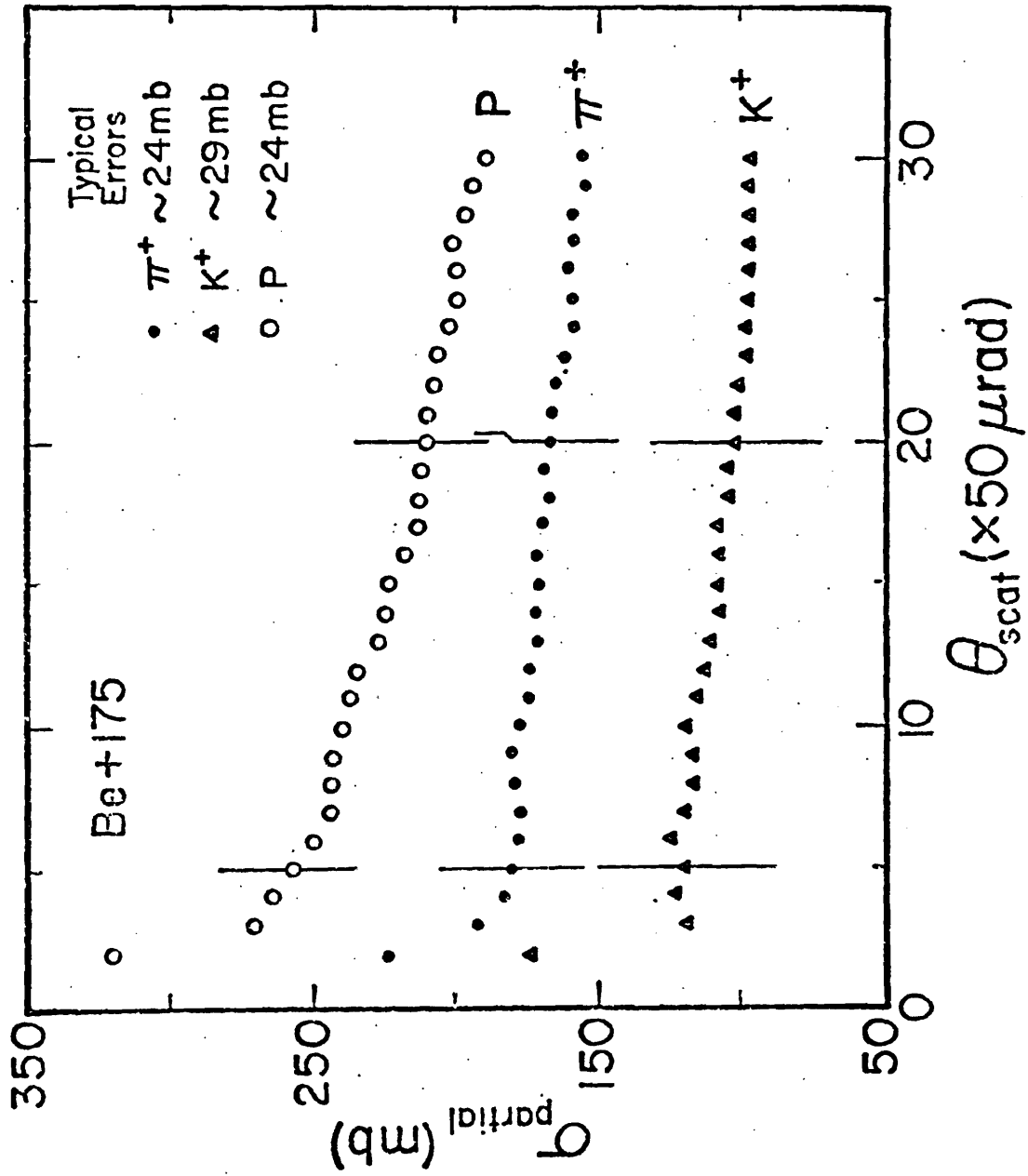


Figure 7.4

PARTIAL CROSS SECTIONS: C: 70GEV/C

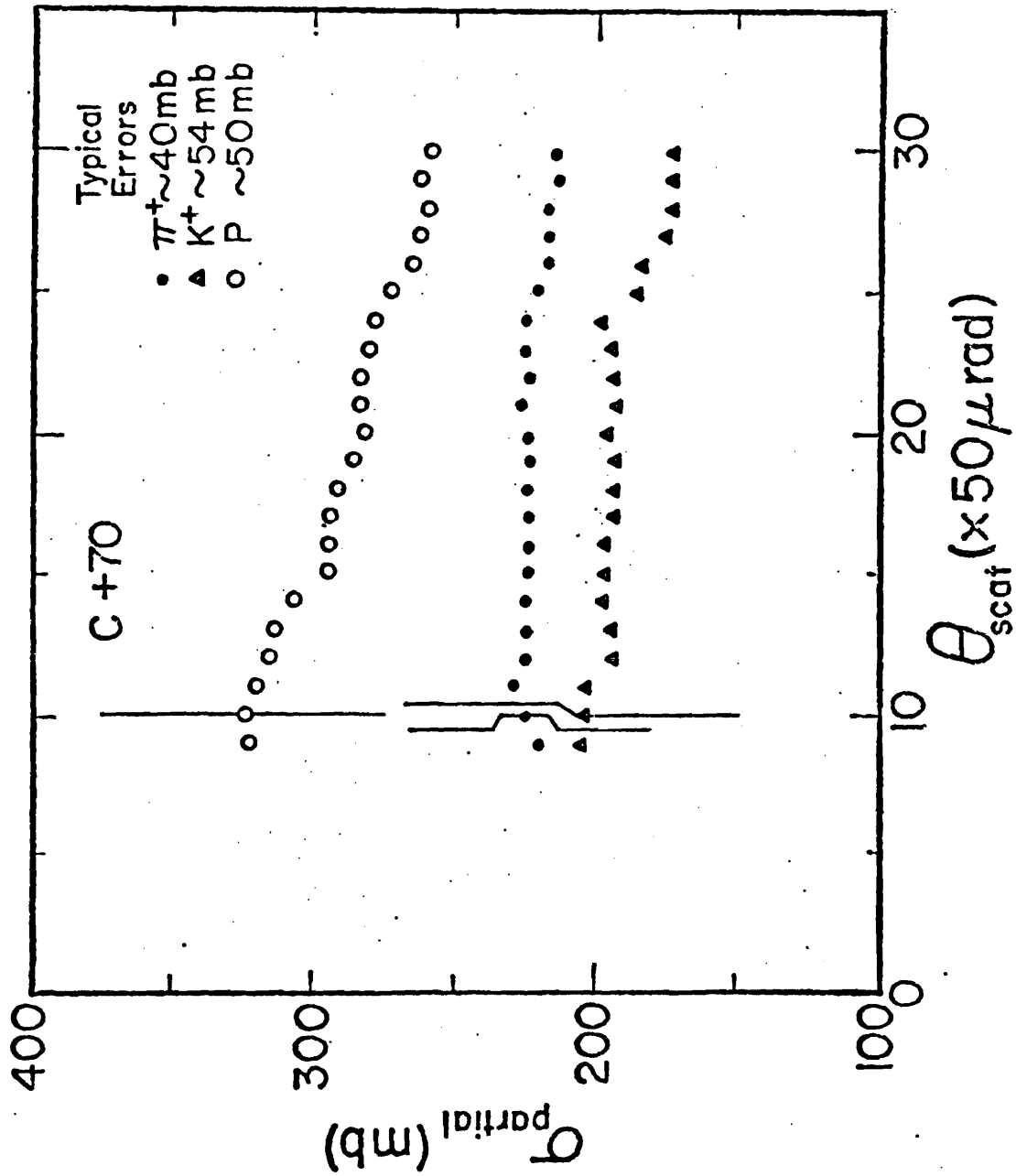


Figure 7.5

where

- σ_n = nth partial cross section representing scattering beyond an angle θ_n
- σ = total cross section

This functional form occurs if one assumes that elastic scattering is the dominate process for small angle scattering. Appendix IV gives a derivation of Eq. 7.5. The quantities σ , A, B were fit for by VXSFT. The fitting program explicitly took into account the correlations between the different partial cross sections. The quantity

$$Q = \sum_j \sum_k (\sigma_k^m - \sigma_k^o) G_{jk} (\sigma_j^m - \sigma_j^o) \quad (7.6)$$

is minimized, where

- σ_i^m = ith measured partial cross section
- σ_i^o = ith theoretical partial cross section
- G_{jk} = inverse of covariance matrix between partial cross sections = $(C)^{-1}_{jk}$

If the off diagonal terms of "G" are zero, then "Q" reduces to the familiar formula for chi-squared. Here

$$C_{jk} = \Delta^2(\sigma_m), \quad m = \min(j,k) \quad (7.7)$$

where $\Delta^2(\sigma_m)$ is the error on the n th partial cross section. A derivation of Eq. 7.7 and the method to calculate the errors on the partial cross sections are given in Appendix IV.

D. Results

To verify that the method used was correct, the total cross sections for π^+ , K^+ , and p scattering from a proton target were measured. The data were taken with the same apparatus but with the liquid hydrogen target substituted for the nuclear targets. These data were part of an experiment to measure the real part of the scattering amplitude in hadron - proton scattering^{6.3}. The results were compared with those of Carroll, et. al.^{7.1}. The incident momenta were 50, 100, and 200 GeV/c (no measurement was made of the total cross section for K^+p reaction at 50 GeV/c).

Figure 7.6 shows the comparison between the two experiments. The errors shown are statistical only. The agreement between the two experiments is satisfactory. For the level of accuracy involved (10 - 15%), the method is adequate.

COMPARISON BETWEEN THIS EXPERIMENT
AND CARROLL ET. AL. (Fermilab E104)

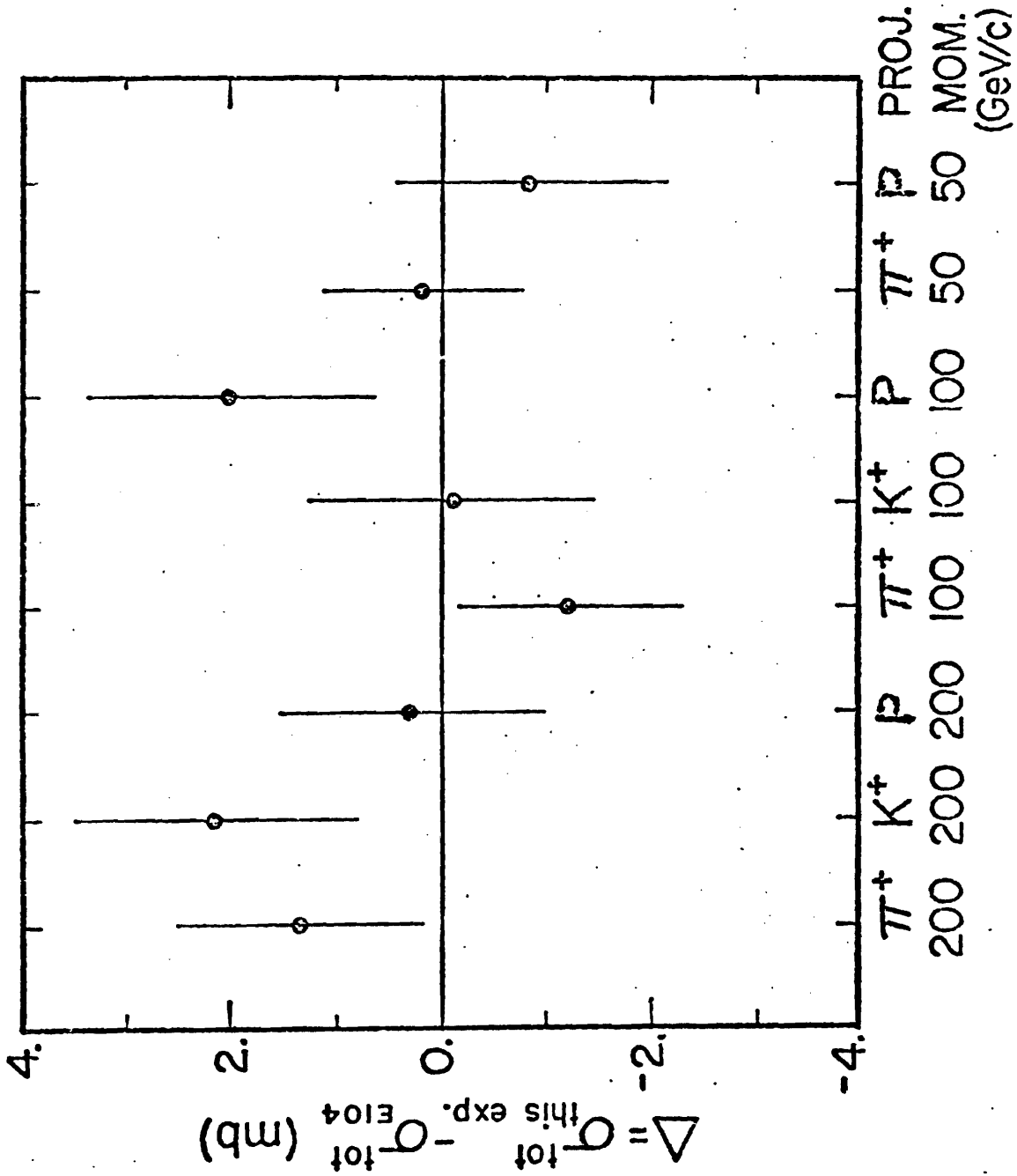


Figure 7.6

The results for the nuclear targets are given in Table 7.1 and in Figures 7.7 and 7.8. Total cross sections for pions, kaons, protons, and antiprotons were obtained at momenta of 175, 70 GeV/c for the Be and C targets and at a momentum of 125 GeV/c for the Be target.

The range of partial cross sections used in the extrapolation was varied; within statistics no variation of the value of the total cross section resulted.

The dimensions and density of the nuclear targets used are given in Table 2.6.

E. Discussion

The above results can be used in a comparison with the values of the total cross sections for hadron - nucleus scattering as derived in the fits to the elastic scattering $d\sigma/dt$ distributions (see Chap. 6, Sect. E). In fact this was the motivation for the above analysis.

Table 7.1
Total Cross Section Results

	Momentum (GeV/c)	$\sigma^{\text{total}}^{\text{a}}$ (mb)		Momentum (GeV/c)	$\sigma^{\text{total}}^{\text{a}}$ (mb)
π^+ Be	175	202.9 \pm 23.1	π^+ C	175	270.6 \pm 36.9
K^+ Be	175	125.2 \pm 28.5	K^+ C	175	169.9 \pm 47.2
p Be	175	288.8 \pm 23.4	p C	175	316.5 \pm 36.5
π^- Be	175	196.3 \pm 13.0	π^- C	175	251.1 \pm 23.9
K^- Be	175	187.2 \pm 20.0	K^- C	175	256.7 \pm 37.2
\bar{p} Be	175	289.1 \pm 55.5	\bar{p} C	175	335.3 \pm 99.6
π^+ Be	125	162.1 \pm 29.5	π^+ C	70	244.7 \pm 39.9
K^+ Be	125	193.9 \pm 37.1	K^+ C	70	211.8 \pm 53.8
p Be	125	272.6 \pm 31.9	p C	70	323.3 \pm 51.5
π^+ Be	70	227.3 \pm 22.3	π^- C	70	217.9 \pm 44.9
K^+ Be	70	117.5 \pm 27.4	K^- C	70	231.3 \pm 54.8
p Be	70	261.1 \pm 27.4	\bar{p} C	70	329.8 \pm 68.6
π^- Be	70	141.3 \pm 24.1			
K^- Be	70	156.2 \pm 29.7			
\bar{p} Be	70	349.1 \pm 40.5			

^aErrors statistical only.

TOTAL CROSS SECTIONS VERSUS MOMENTUM: BE

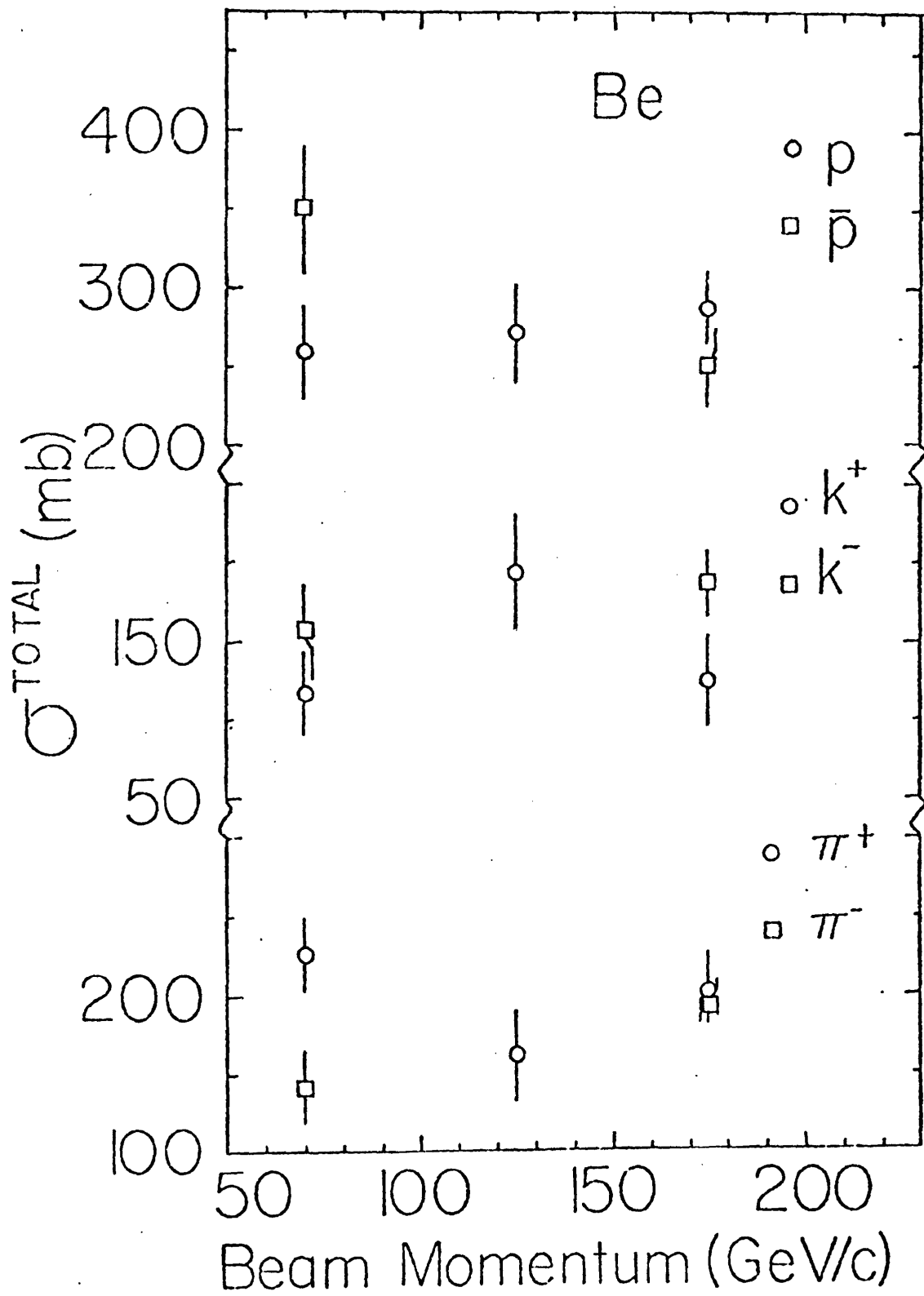


Figure 7.7

TOTAL CROSS SECTIONS VERSUS MOMENTUM: C

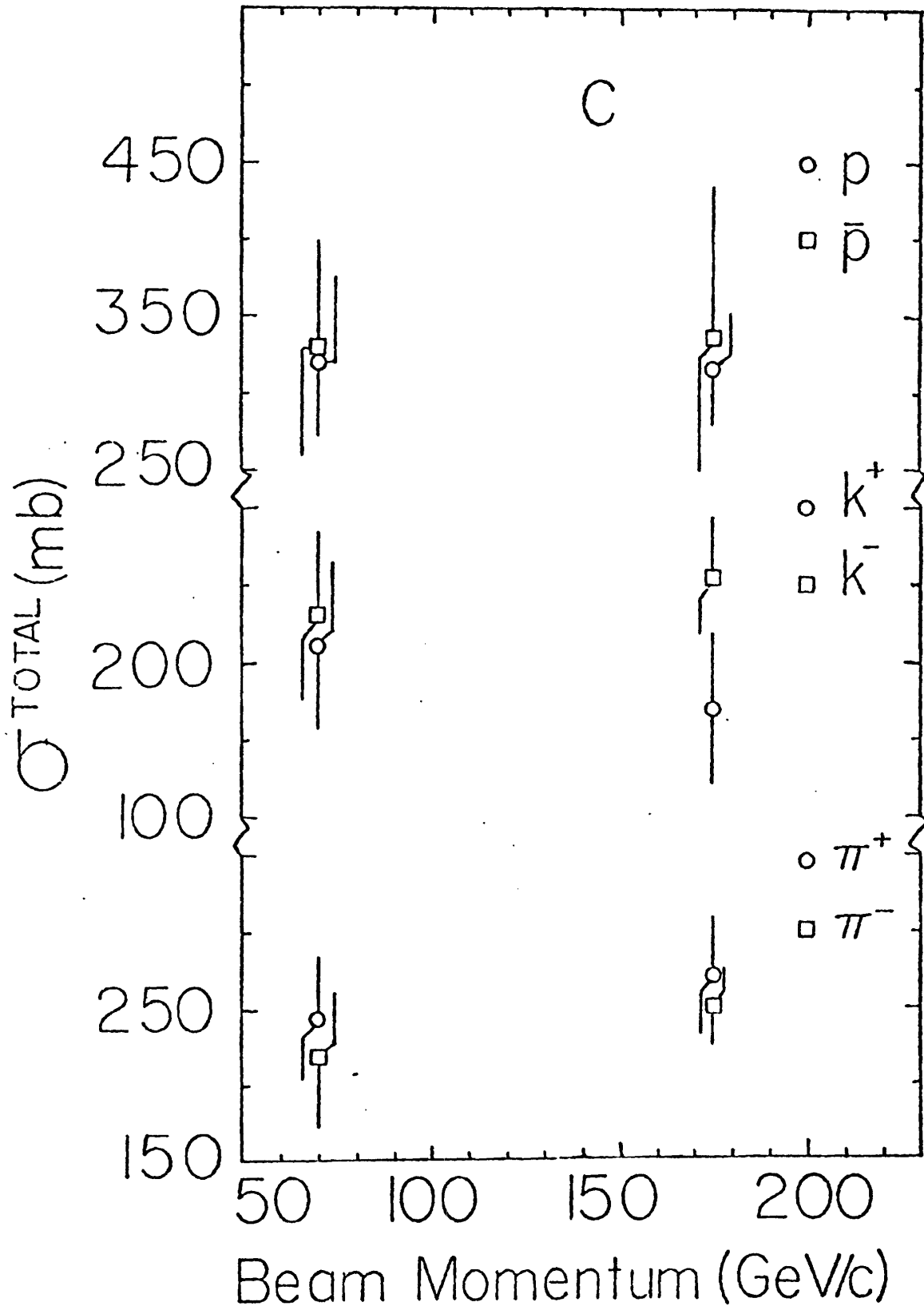


Figure 7.8

Table 7.2 and Figure 7.9 present this comparison. There are three cases involving the measurements using the elastic scattering distributions:

1. Normalization free; fit extends into Coulomb region
2. Normalization fixed to 1; fit extends into Coulomb region
3. Normalization fixed to 1; fit does not extend into Coulomb region

The Coulomb region was loosely defined as that region of t where Coulomb scattering made a significant contribution (typically $.001 < -t < .002 \text{ (GeV/c)}^2$).

Figure 7.9 presents a histogram of the quantity where

$$\Gamma = [\sigma(\text{direct}) - \sigma(\text{el scat})]/E$$

where

$\sigma(\text{direct}) = \sigma$ as measured directly (via transmission method)

$\sigma(\text{el scat}) = \sigma$ as derived from fits to elastic

Table 7.2

Comparison Between Total Cross Sections as Derived by Direct Measurement and from Fits to Elastic $d\sigma/dt$ Distributions

	<u>Momentum</u> (GeV/c)	<u>Direct</u> (mb)	<u>Elastic $d\sigma/dt$ Distribution</u> (mb)		
			<u>Case 1</u>	<u>Case 2</u>	<u>Case 3</u>
π^+ Be	175	202.9 \pm 23.1	182.2 \pm 7.2	164.3 \pm 4.9	167.4 \pm 5.2
K ⁺ Be	175	125.2 \pm 28.5	149.3 \pm 7.4	133.6 \pm 6.2	137.3 \pm 6.4
p Be	175	288.8 \pm 23.4	249.2 \pm 8.3	260.4 \pm 7.1	259.3 \pm 7.3
π^- Be	175	196.3 \pm 13.0	168.4 \pm 7.4	214.3 \pm 6.5	217.4 \pm 6.8
K ⁻ Be	175	187.2 \pm 20.0	128.0 \pm 7.5	191.9 \pm 6.4	194.5 \pm 6.7
\bar{p} Be	175	289.1 \pm 55.5	191.0 \pm 25.1	339.2 \pm 20.8	336.5 \pm 21.3
π^+ Be	125	162.1 \pm 29.5	190.3 \pm 9.7	163.3 \pm 8.1	167.6 \pm 8.4
K ⁺ Be	125	193.9 \pm 37.1	145.9 \pm 8.1	132.9 \pm 7.1	139.9 \pm 7.6
p Be	125	272.6 \pm 31.9	269.0 \pm 12.4	257.1 \pm 9.7	255.8 \pm 10.3
π^+ Be	70	227.3 \pm 22.3	170.9 \pm 6.7	170.5 \pm 4.8	169.7 \pm 5.2
K ⁺ Be	70	117.5 \pm 27.4	135.8 \pm 6.9	137.9 \pm 4.9	133.7 \pm 5.4
p Be	70	261.1 \pm 27.4	251.6 \pm 10.8	261.9 \pm 8.9	257.4 \pm 9.3
π^- Be	70	141.3 \pm 24.3	165.9 \pm 5.8	159.9 \pm 4.4	163.8 \pm 4.6
K ⁻ Be	70	156.2 \pm 29.7	150.7 \pm 7.6	140.4 \pm 5.9	147.0 \pm 6.4
\bar{p} Be	70	349.1 \pm 40.5	289.5 \pm 17.6	271.8 \pm 13.8	270.0 \pm 14.3

Table 7.2 (cont.)

	<u>Momentum</u> (GeV/c)	<u>Direct</u> (mb)	<u>Elastic dσ/dt Distribution</u> (mb)		
			<u>Case 1</u>	<u>Case 2</u>	<u>Case 3</u>
π^+C	175	270.6 ± 36.9	244.9 ± 7.5	214.6 ± 6.9	218.7 ± 7.2
K^+C	175	169.9 ± 47.2	195.4 ± 7.5	176.6 ± 7.3	179.4 ± 7.6
pC	175	316.5 ± 36.5	345.2 ± 9.9	326.8 ± 8.7	327.3 ± 9.1
π^-C	175	251.1 ± 23.9	237.1 ± 10.3	214.3 ± 8.3	217.4 ± 8.7
K^-C	175	256.7 ± 37.2	184.8 ± 11.3	191.9 ± 9.4	194.5 ± 10.1
$\bar{p}C$	175	335.3 ± 99.6	317.6 ± 48.2	339.2 ± 41.2	336.5 ± 42.3
π^+C	70	244.7 ± 39.9	170.9 ± 6.7	210.6 ± 5.7	223.8 ± 6.2
K^+C	70	211.8 ± 53.8	135.8 ± 6.9	176.1 ± 6.2	177.0 ± 6.4
pC	70	323.3 ± 51.5	251.6 ± 10.8	326.0 ± 8.9	323.5 ± 9.3
π^-C	70	217.9 ± 44.9	222.3 ± 7.4	200.7 ± 6.9	210.5 ± 7.1
K^-C	70	231.3 ± 54.8	207.6 ± 9.5	195.1 ± 5.8	196.1 ± 6.2
$\bar{p}C$	70	329.8 ± 68.6	391.7 ± 23.1	345.8 ± 18.1	360.7 ± 19.4

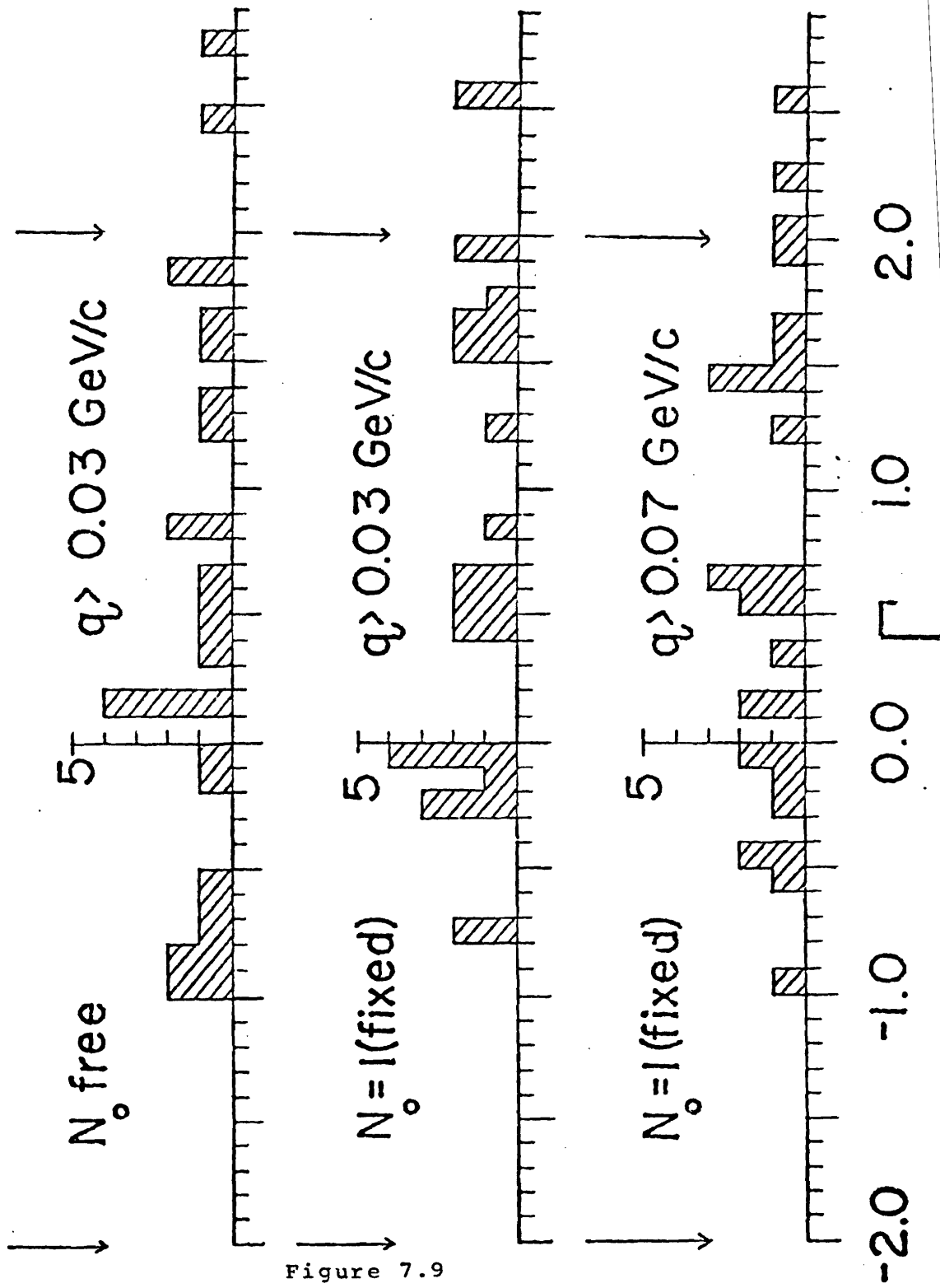


Figure 7.9

scattering data

E = statistical error on numerator

It was hoped that inspection of Figure 7.9 would give insight concerning the proper manner of treating the normalization of the elastic scattering data. However none of the results from the elastic scattering data seem to give total cross sections that are significantly more consistent with the total cross sections as measured directly. Part of this fact is due to the relatively large statistical errors on the total cross sections as measured directly. When the elastic scattering data was fit allowing the normalization to vary, a much better chi-squared per degree of freedom resulted than when the normalization was fixed to unity. In view of this fact and the above discussion of Figure 7.9, it is felt that the best way to fit the nuclear elastic scattering data is to allow the normalization to be a free parameter.

CHAPTER 8

RESULTS: HIGH-t ANALYSIS

A. Final Analysis Steps

The final analysis steps were similar to those for the nuclear target data.

The program HITRO performed the function of QRNUC (see Chap. 6, Sect. A).

The main difference in the two analyses was the application of the Monte Carlo results. For the high-t analysis only the geometric apparatus acceptance was needed, and it was used to correct the data not the theory. The following quantity was formed:

$$d\sigma/dq_{\text{data}} = D(q)/e(q)$$

where

$e(q)$ = geometric apparatus acceptance as a
function of q

All other symbols are defined in Chapter 6, Section A.

Next $d\sigma/dq_{\text{data}}$ was compared to a theoretical form of the cross section, $d\sigma/dq_{\text{th}}$, to extract the desired parameters (forward slope, etc.). The program MINUIT^{6.1} (as a subroutine in HITFT) was used in the fitting process.

However before the fits were performed, three corrections were applied to the data:

1. Coulomb scattering corrections
2. Radiative corrections
3. Correction for inelastic contamination under the elastic missing mass peak

The program HITFT performed these corrections.

B. Data Cuts

In order to extract the elastic scattering signal, a set of cuts was applied to both the target full and empty data. Table 8.1 presents the cuts used for the +200 GeV/c (π^+p , pp) and -200 GeV/c (π^-p) data. Also shown is the effect of each cut.

Table 8.1
Major Cuts to Extract Elastic Signal
High-t Data

Cut	Fractions of Events Remaining After Cut		
	π^-	π^+	p
1) Track reconstruction requirements on PWC coordinates • HFD test passed	.446	.545	.546
2) No count from VH2 and VH3	.368	.457	.447
3) HSD Test Passed	.366	.455	.447
4) Scattering angle in x and y projections $\geq .25$ mrad	.355	.444	.443
5) Track ≤ 1.5 cm from center of PWC station 4.	.352	.438	.440
6) Outgoing particle trajectory traversed the area inside of spectrometer magnet apertures	.342	.427	.430
7) Scatter vertex no more than 40cm beyond LH ₂ target ends	.293	.361	.375
8) $0.0 \leq \text{Recoil Mass Squared} \leq 1.76 \text{ (GeV/c}^2)^2$.215	.272	.287
9) Events whose trajectories were in region of $> 90\%$ efficiency in PWC station 4.	.167	.254	.269
10) Outgoing particle trajectory did not traverse the area of the counter V at the third focus.	.120	.217	.231

The first requirement was that VH2 and VH3 gave no signal in the event; this was to suppress unwanted scatters from target electrons. Next it was required that the HSD test be passed (this information was given by the HSD latch). Next the q of the scatter in the x and y projections had to be greater than 50 Mev/c.

The quantity $R4$ represented the distance of the outgoing particle from the center of the PWC at Station 4. It was defined as

$$R4 = [(x4-xc)^2 + (y4-yc)^2]^{1/2}$$

where

$x(y)4$ = measured $x(y)$ coordinate in PWC

Station 4

$x(y)c$ = $x(y)$ center of PWC Station 4

The z cut was the requirement that the scatter occur in the region of the target. A z distribution (where along the beam line the scatter occurred) is shown in Figure 8.1 with arrows indicating the cut. The dotted lines give the position of the LH_2 target.

Z DISTRIBUTION : 200 GEV/C

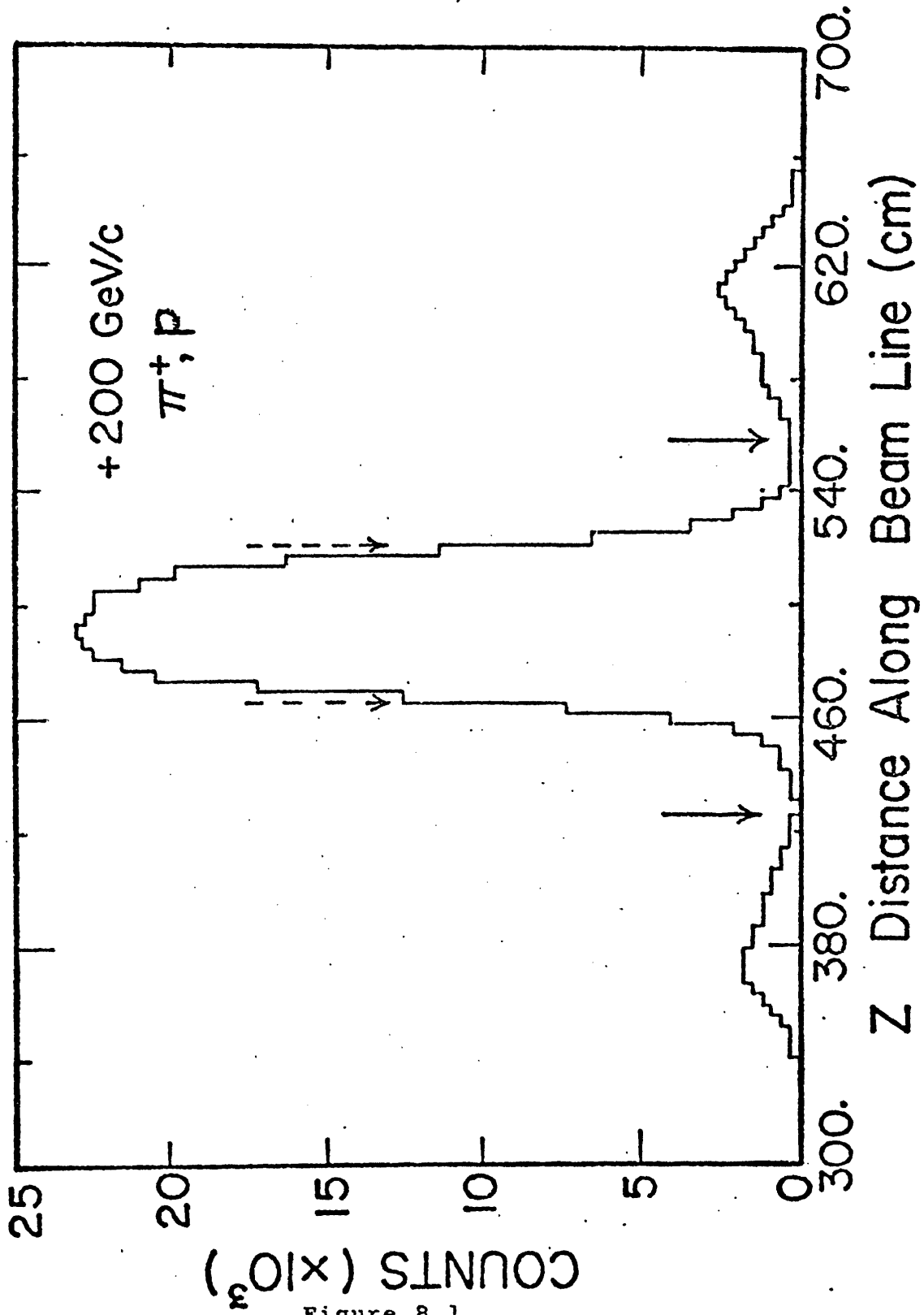


Figure 8.1

The recoil mass squared cut required that this quantity be consistent with the mass of the proton squared ($=.8804(\text{GeV}/c^2)^2$). Figure 8.2 shows a recoil mass squared distribution with arrows indicating the cut.

The requirement that the outgoing track passed within the spectrometer magnet apertures was fulfilled via the EGG cut where

$$\text{EGG} = (\text{xveto}/a)^m + (\text{yveto}/b)^m$$

where

$\text{xveto}(\text{yveto}) = \text{predicted } x(y) \text{ coordinate at the}$
veto plane

$\text{xveto}(\text{yveto})$ were calculated based on the measured outgoing track's angle and its momentum. The curve given by $\text{EGG} = 1$ represents the actual exit magnet aperture of the downstream spectrometer magnet as projected to the veto plane. Thus a curve given by $\text{EGG} < 1$ means that the outgoing track had to pass within an

RECOIL MASS SQUARED DISTRIBUTION : 200 GEV/C

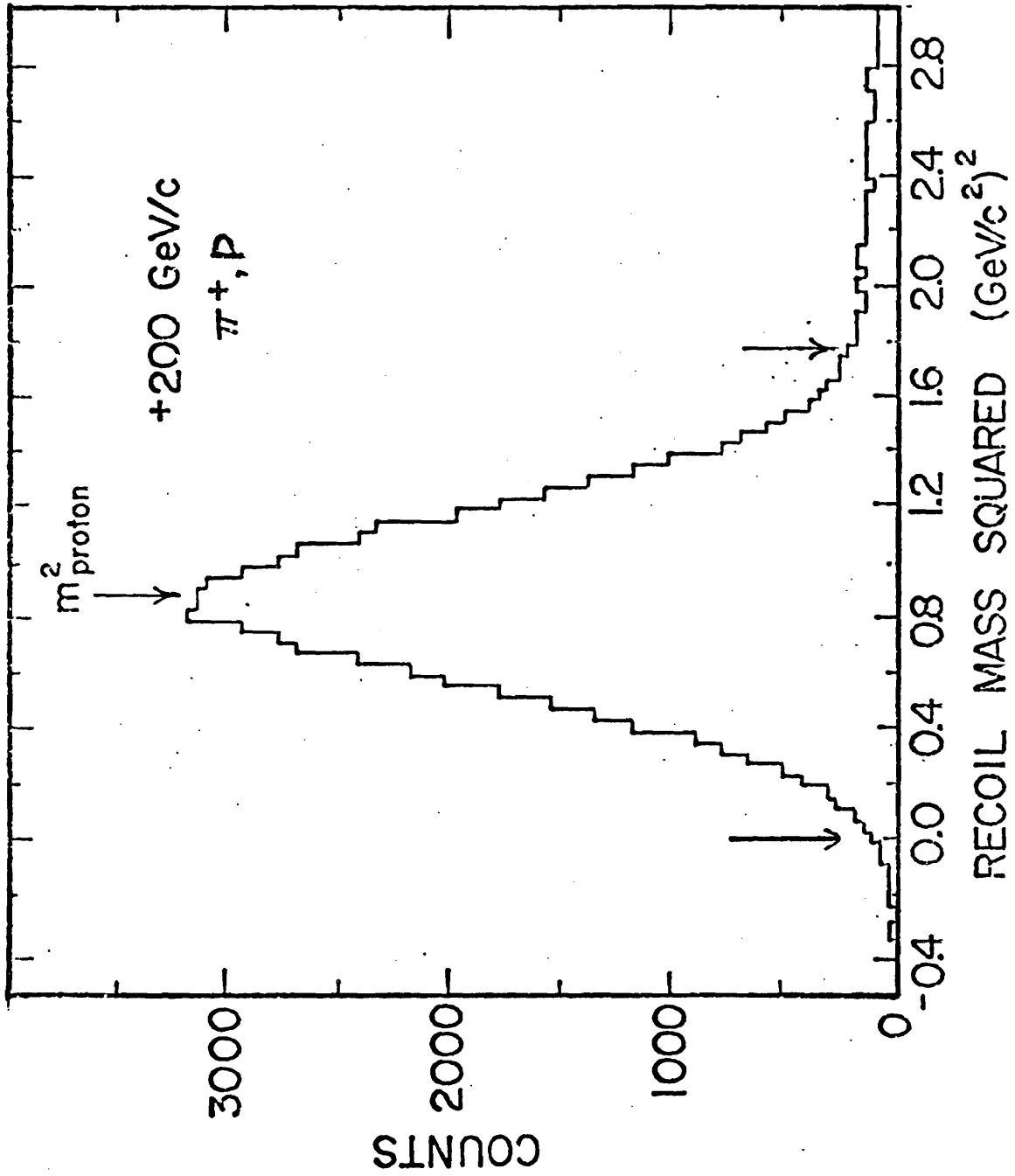


Figure 8.2

area away from the actual magnet aperture edges. Figure 8.3 shows a scattergram of the events at the veto plane and the curve represented by the EGG cut.

The OVERSIZED JAW VETO were requirements using x_{veto} and y_{veto} . The x_{veto} and y_{veto} of the event had to be outside of the OVERSIZED JAW VETO (dashed line in Figure 8.3). This cut reduced the sensitivity of the results to not knowing the exact location in space of the jaw shaped veto.

The final cuts were to take account of dead wires in PWC Station 4. Events that had x_4 or y_4 in these regions were rejected (again x_4 (y_4) are the measured x (y) coordinate in PWC Station 4).

From Table 8.1 it is seen that half of the triggers were eliminated by track reconstruction cuts imposed on the coordinates in the PWCs. The most important cuts on kinematic quantities were

1. z cut.
2. recoil mass squared cut.
3. dead wires in PWC Station 4.

CUTS MADE AT VETO PLANE FOR HIGH-T DATA

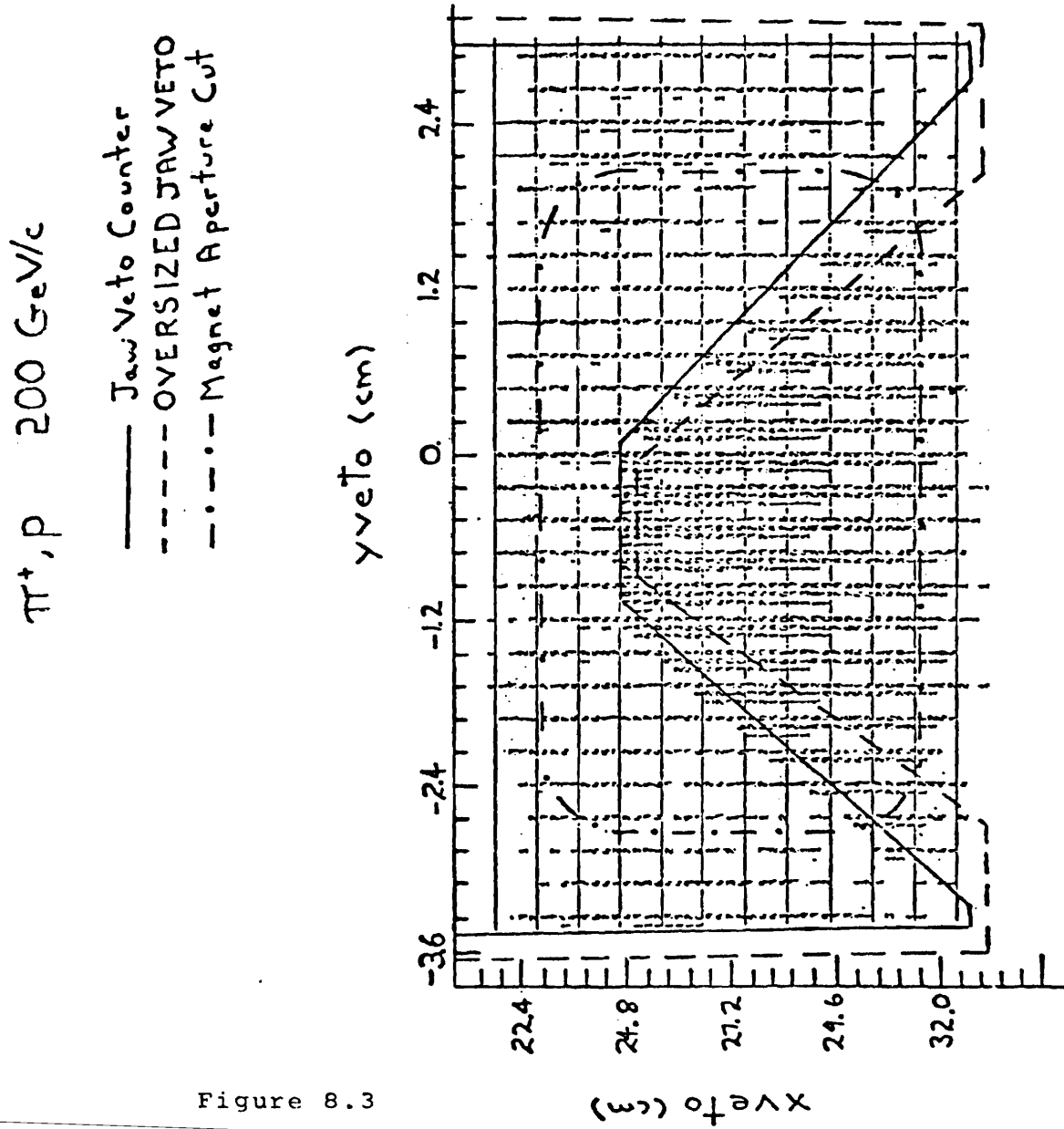


Figure 8.3

4. jaw veto cut.

C. Target Empty Subtraction And Data Normalization

The target empty subtraction was a 1% effect. To perform the subtraction, the number of incident particles in the target full and empty running had to be calculated. This number was given by the BEAM events.

Unfortunately due to an error in the hardware trigger logic, the number of incident particles was not the number of BEAM multiplied by a scale factor. The logic error caused a different amount of deadtime for SCATTER and BEAM triggers. The following formula for the number of incident particles corrected for this effect:

$$N_t^{f(mt)} = N_{Beam}^{f(mt)} * F / (F * T)$$

where

$$N_t^{f(mt)} = \text{number of incident particles for}$$

full (empty) target data
 $N_{\text{beam}}^{f(\text{mt})}$ = number of BEAM (passing cuts)
 for full (empty) target data
 F = number of SCATTER trigger passing
 HFD requirement and $(\overline{\text{VH2}} \cdot \overline{\text{VH3}})$
 $(F * T)$ = number of above SCATTER trigger that
 had BEAM latch on

The BEAM events had to pass the following cuts:

1. VH2, VH3 gave no signal
2. HFD test

D. Monte Carlo Acceptance

As described in Chapter 4, Section E there were two types of quantities involved in the Monte Carlo program, generated and reconstructed. The cuts applied to the generated quantities simulated the actual experimental apertures. The cuts applied to the reconstructed quantities were exactly the same as applied to the data. By this method, the Monte Carlo simulated the effect of the apparatus resolution.

Figures 8.4 and 8.5 present the geometric acceptance for the +200 (π^+p , pp scattering) and -200 GeV/c (π^-p scattering) data.

E. Additional Corrections

There were two effects not included in the Monte Carlo results: 1) radiative effects 2) contamination of the elastic signal by inelastic scatters. Both of these process lead to t dependent corrections which had to be explicitly calculated.

The correction for radiative effects was calculated by Sogard^{8.1}. Table 8.2 gives the formula used to derive this correction. Using Sogard's formalism and taking into account the apparatus resolution for recoil mass squared, the correction for the specific cut on recoil mass squared was calculated. The measured differential cross section was corrected as follows:

$$d\sigma/dt_{\text{corr}} = d\sigma/dt_{\text{meas}}(e^{\delta})$$

where Figure 8.6 presents $e^{\delta} - 1$. The correction for the π^-p reaction is practically identical to that for

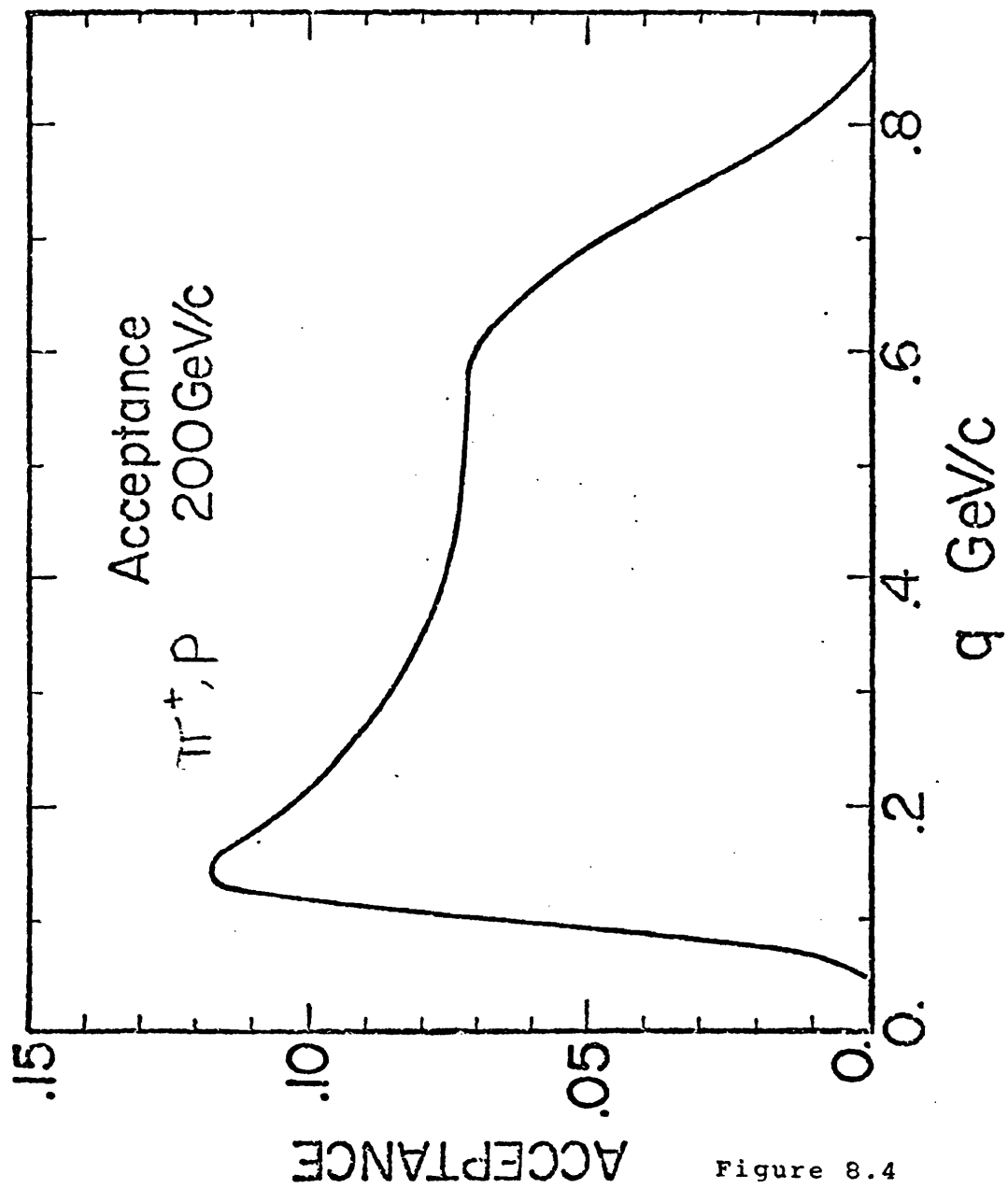


Figure 8.4

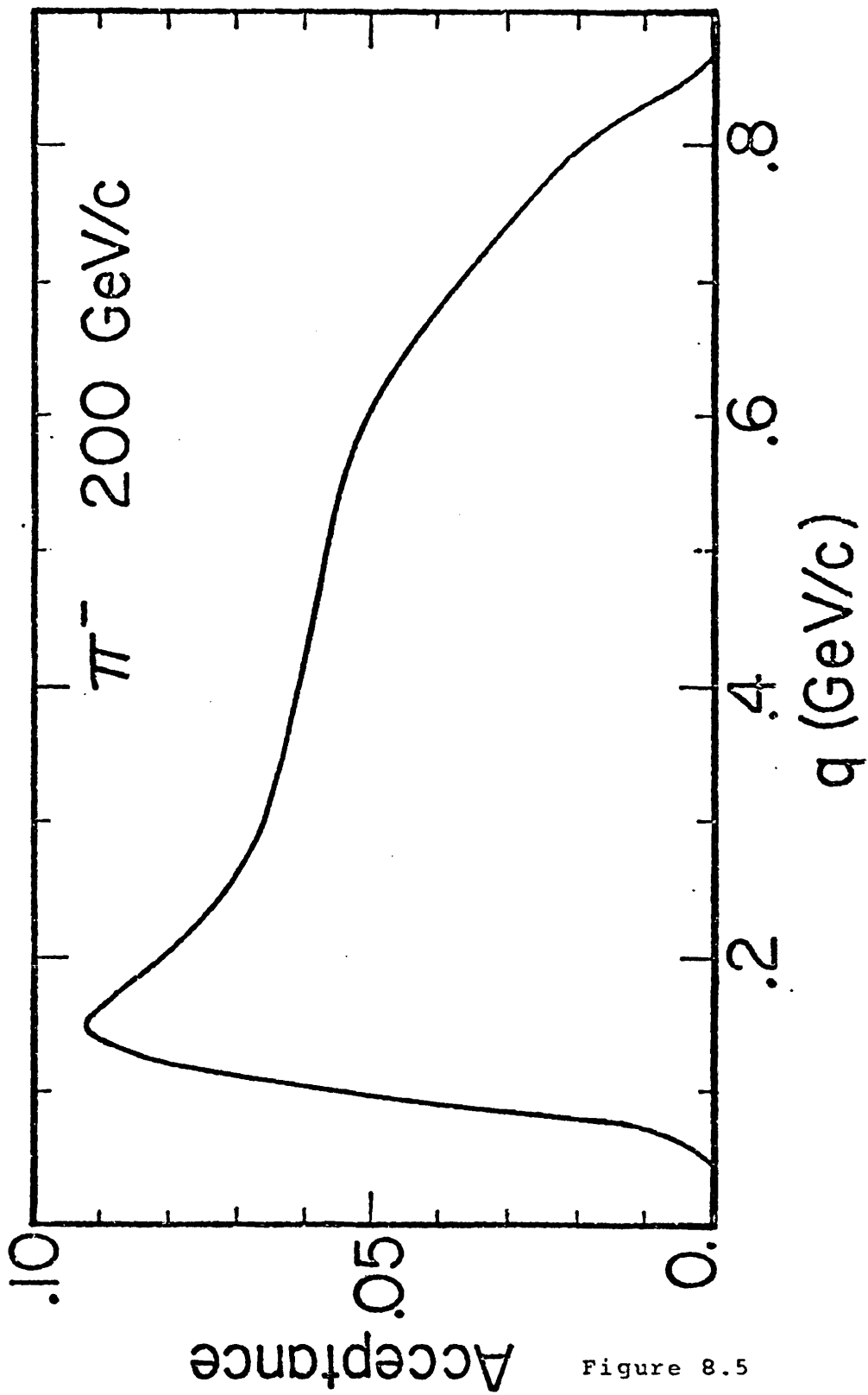


Figure 8.5

Table 8.2

Correction for Radiative Effects

$$\begin{aligned}
\delta = & \frac{\alpha}{\pi} \left\{ \left[\frac{2\mu^2 - t}{Q} \ln \left(\frac{Q-t}{Q+t} \right) - 1 + Z \left(\frac{1}{\beta_1} \ln Q_1 - \frac{1}{\beta_2} \ln Q_2 \right) \right] \left(2 \ln \frac{E_1}{\Delta E} - 3 \ln \eta \right) \right. \\
& - \frac{2\mu^2 - t}{Q} \left[\phi \left(-\frac{(E_1 - E_2)(Q-t)}{(E_1 + E_2)t - (E_1 - E_2)Q} \right) + \phi \left(\frac{(E_1 - E_2)(Q-t)}{(E_1 + E_2)t + (E_1 - E_2)Q} \right) \right. \\
& \quad - \phi \left(-\frac{(E_1 - E_2)(Q+t)}{(E_1 + E_2)t - (E_1 - E_2)Q} \right) - \phi \left(\frac{(E_1 - E_2)(Q+t)}{(E_1 + E_2)t + (E_1 - E_2)Q} \right) \\
& \quad \left. \left. - \ln \left(\frac{Q-t}{Q+t} \right) \ln \left(1 + \frac{(E_1 - E_2)^2 \mu^2}{E_1 E_2 t} \right) \right] \right\} \\
& - Z^2 \left[\ln \frac{E_1}{M} - 2 \ln \frac{M}{\eta \Delta E} \left(\frac{1}{\beta_1} \ln B_1 - 1 \right) - \frac{1}{\beta_1} \left(\ln B_1 \ln \frac{E_1 + M}{2M} - \phi(-R_1/B_1) + \phi(R_1/B_1) - \phi(R_1) + \phi(-R_1) \right) \right] \\
& + \frac{Z}{\beta_2} \left[\ln \left| \frac{M b_2^2}{E_2 \sigma_2} \frac{c_{11}}{E_1 \sigma_1} \right| \ln R_2^+ + \phi \left(\frac{E_2 - M}{\rho_2} \right) - \phi \left(-\frac{E_2 - M}{\rho_2} \right) + \phi \left(-\frac{E_2 - M}{\rho_2 R_2^+} \right) - \phi \left(\frac{E_2 - M}{\rho_2 R_2^+} \right) \right. \\
& \quad + \phi \left(\frac{M(M - E_2^+)(E_1 - E_2)}{c_{11}} \right) - \phi \left(\frac{M(M - E_2^+)(E_1 - E_2)}{c_{11}} \right) + \phi \left(\frac{(M E_2^+ - \mu^2)(E_1 - E_2)}{c_{11}} \right) \\
& \quad \left. - \phi \left(\frac{(M E_2^+ - \mu^2)(E_1 - E_2)}{c_{11}} \right) - \ln \left| \frac{M b_2^2}{E_2 \sigma_2} \frac{c_{11}}{E_1 \sigma_1} \right| \ln R_2^+ \right] \\
& - \frac{Z}{\beta_1} \left\{ \text{same expression with } 1 \leftrightarrow 3 \right\}.
\end{aligned}$$

The quantity t is the four-momentum transfer squared, $t = (\rho_1 - \rho_2)^2$; also,

$$q = E_1/E_2,$$

$$Q = (t^2 - 4\mu^2 t)^{1/2},$$

$$B_1 = \left(\frac{1 + \beta_1}{1 - \beta_1} \right)^{1/2},$$

$$R_1 = \left(\frac{E_1 - M}{E_1 + M} \right)^{1/2},$$

$$\beta_1 = \rho_1/E_1,$$

and

$$\beta_2 = \rho_2/E_2.$$

$\phi(x)$ is the Spence function

$$\phi(x) = \int_0^x -\ln|1-y| \frac{dy}{y}$$

$$Q_1 = \frac{\rho_1 + E_1 - \mu^2/M}{\rho_1 - E_1 + \mu^2/M} \frac{\rho_1 + E_1 - M}{\rho_1 - E_1 + M},$$

$$a_1^2 = M^2 + \mu^2 - 2ME_1,$$

$$b_1^2 = \rho_1(E_1^+ - M),$$

$$R_1^+ = \frac{M(M - E_1^+)}{ME_1^+ - \mu^2},$$

$$E_1^+ = E_1 + \rho_1,$$

where $i=1, 3$. Also

$$c_{11} = M^2 E_1^+ - ME_1 E_1^+ + \mu^2 E_1 - E_1 M E_1^+,$$

$$c_{12} = M^2 E_1 - ME_1 E_1^+ + \mu^2 E_1 - E_1 M E_1^+.$$

where $j=3, 1$ when $i=1, 3$.

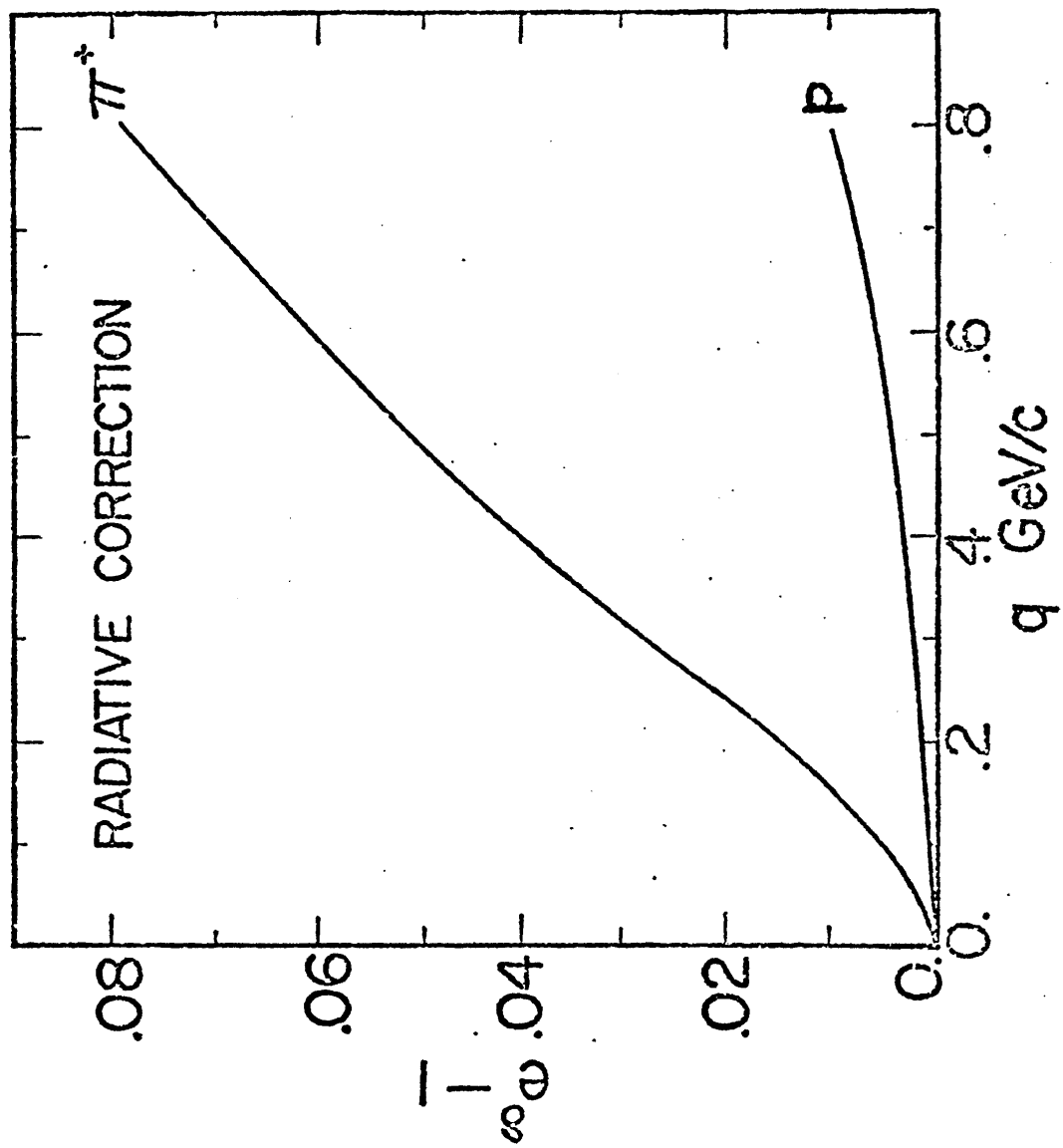


Figure 8.6

the π^+p reaction (to the fourth decimal place).

The second correction was found by fitting the recoil mass squared distribution associated with different bins of q to an elastic peak and a term representing the inelastic scattering contribution. Figure 8.7 shows a representative plot of recoil mass squared for a particular q bin, and the results of the fit. Using the fit results, the amount of inelastic contamination was derived for the specific recoil mass squared cut. Figure 8.8 presents this contamination; it is approximately 2% at the smallest scattering angles and ranges up to 6% for large angle scattering for the pion case and up to 9% for the proton case. This correction is known to 10%. The measured differential cross section was corrected for the inelastic contamination as follows:

$$d\sigma/dt_{\text{corr}} = d\sigma/dt_{\text{meas}}(1-C)$$

where C is the inelastic contamination.

It was observed that the final answers were not very sensitive to the corrections for inelastic contamination and radiative effects. Each applied

RECOIL MASS SQUARED DISTRIBUTION

$0.6 \leq q \leq 0.7 \text{ (GeV/c)}$

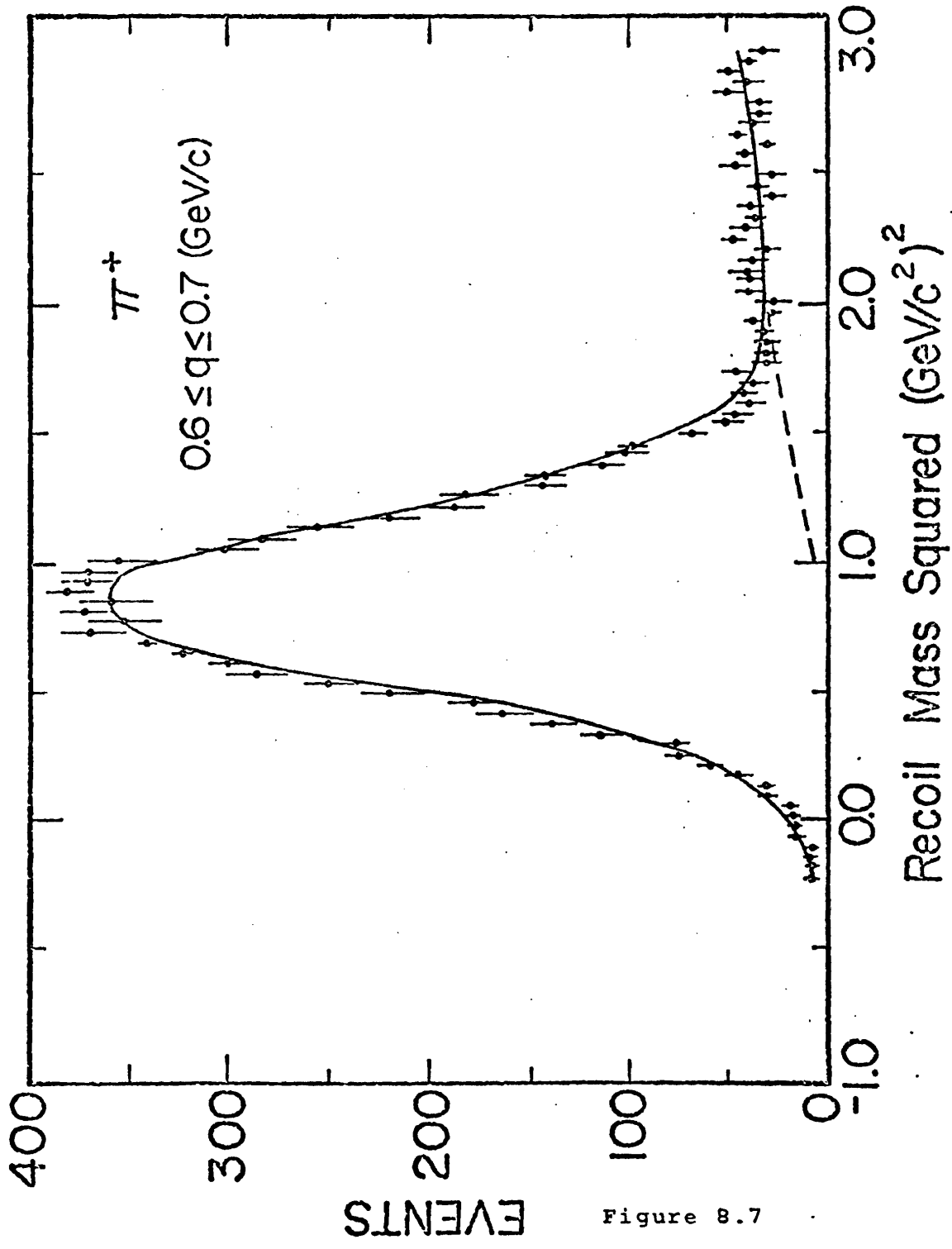


Figure 8.7

INELASTIC CONTAMINATION: HIGH-T DATA

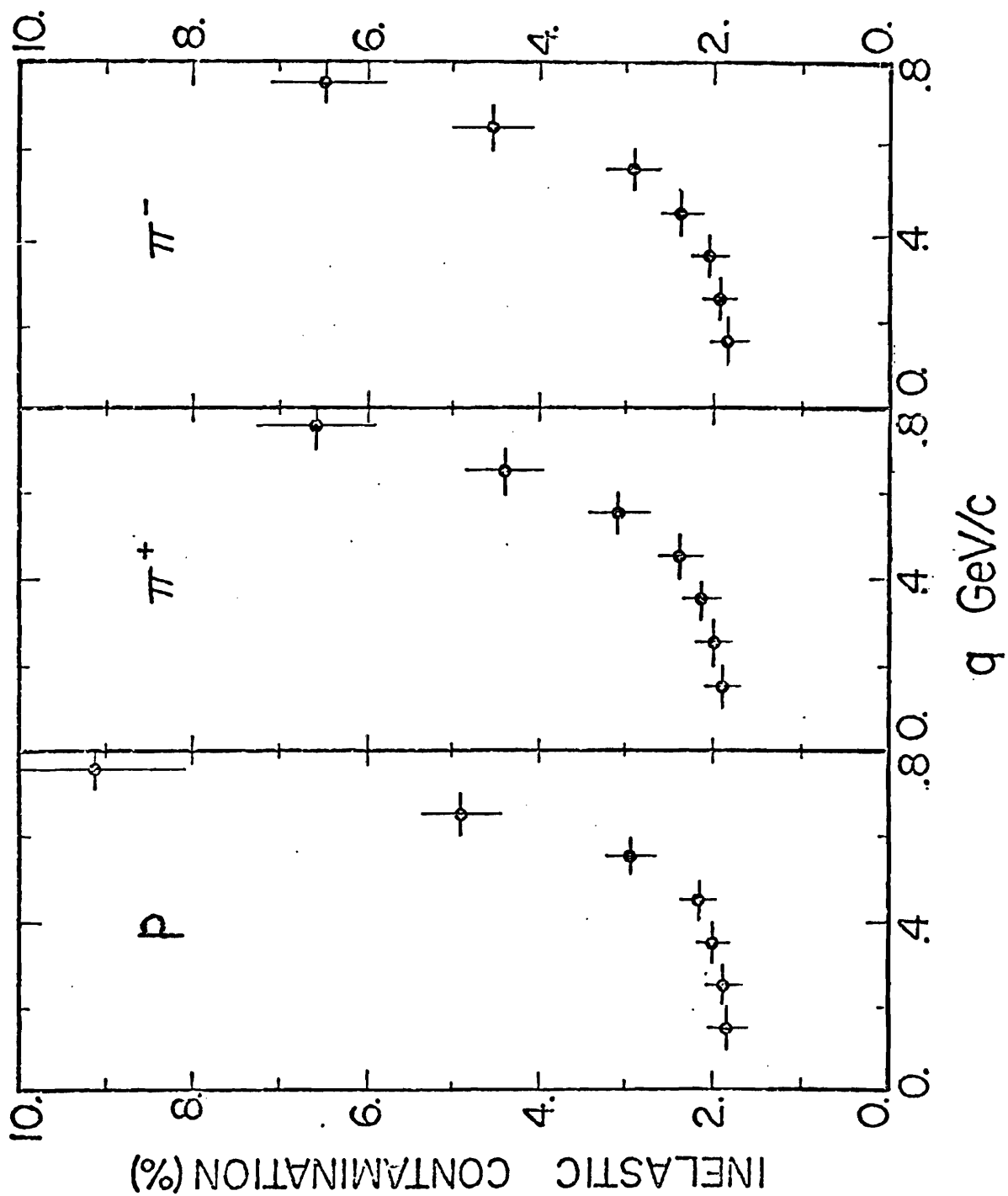


Figure 8.8

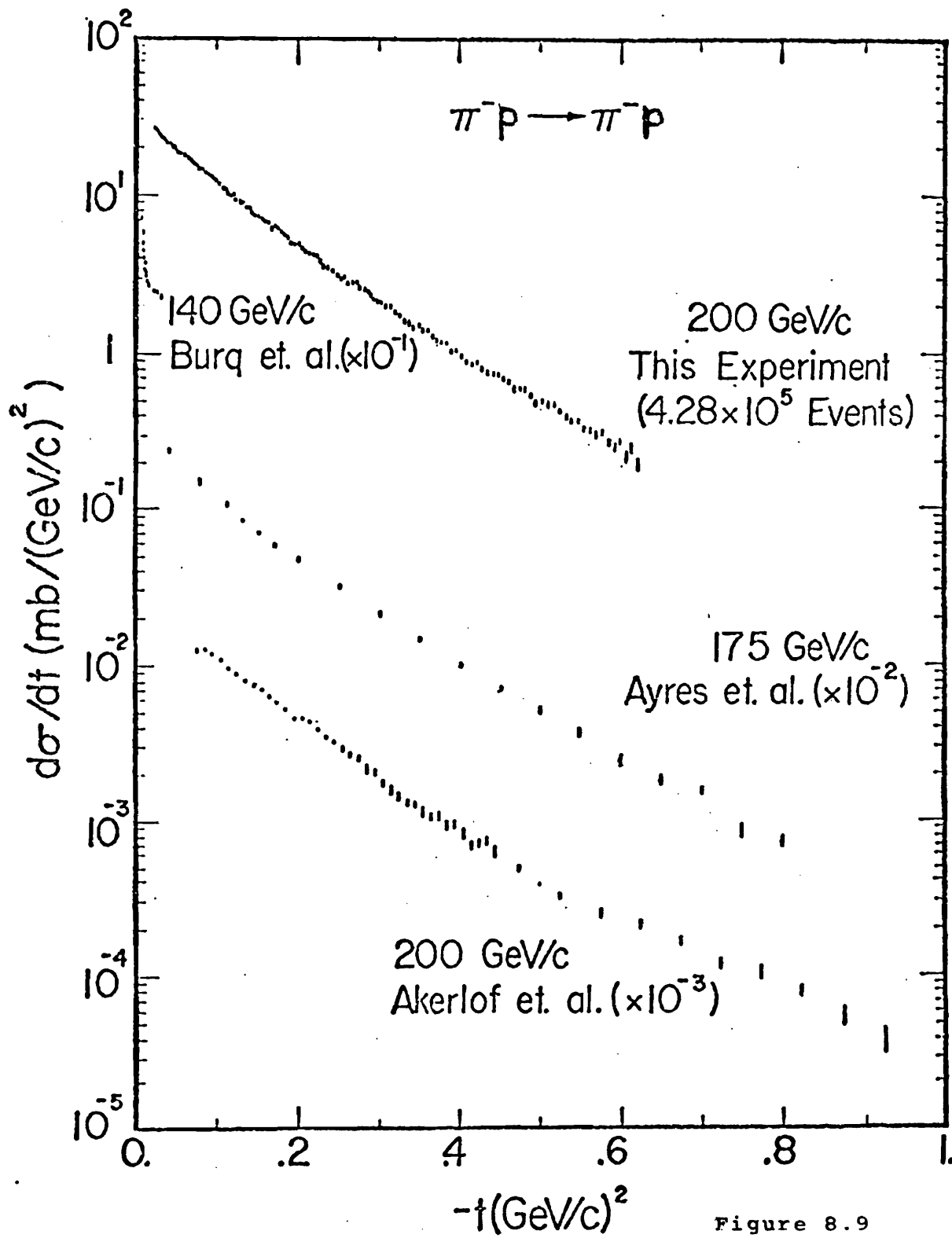
separately caused the final answers to vary by less than one standard deviation. Also the two effects act in different directions.

F. Results

After applying corrections to the data for the apparatus acceptance, radiative effects, and inelastic contamination, $d\sigma/dq$ distributions were calculated. These were transformed to $d\sigma/dt$ using the following formula:

$$d\sigma/dt = (1./2q)d\sigma/dq$$

Figures 8.9 to 8.11 show the resulting $d\sigma/dt$ distributions for π^-p , π^+p , and pp elastic scattering, respectively. Table 8.3 gives the actual values. The errors shown are statistical only; furthermore, there is an uncertainty in the overall normalization of 4%. The main contribution to this uncertainty is the statistical error involved in the method employed to calculate the incident flux. The pp distribution contains 1.16×10^6 events, π^+p 2.22×10^5 events, and π^-p 4.28×10^5 events.



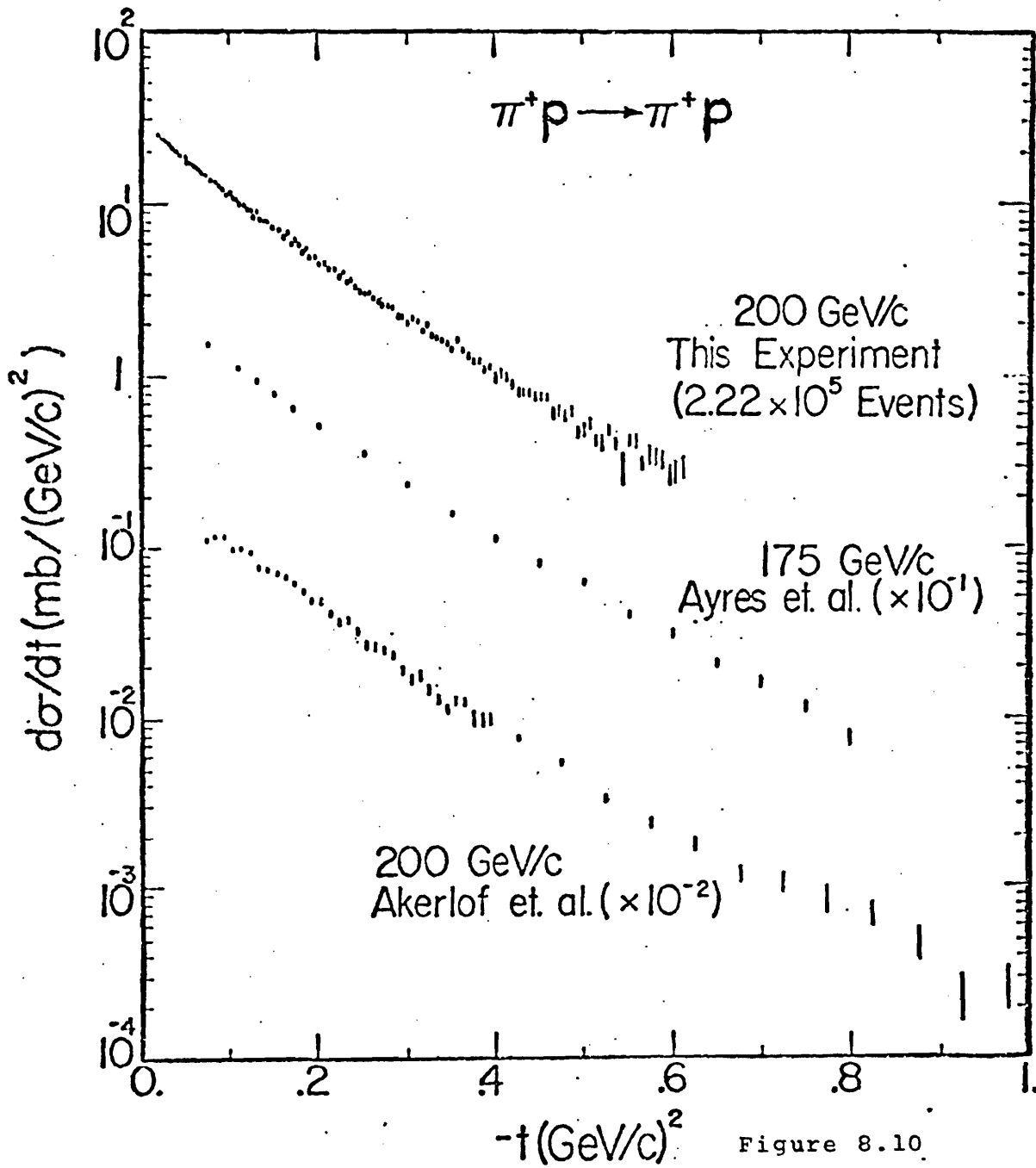


Figure 8.10

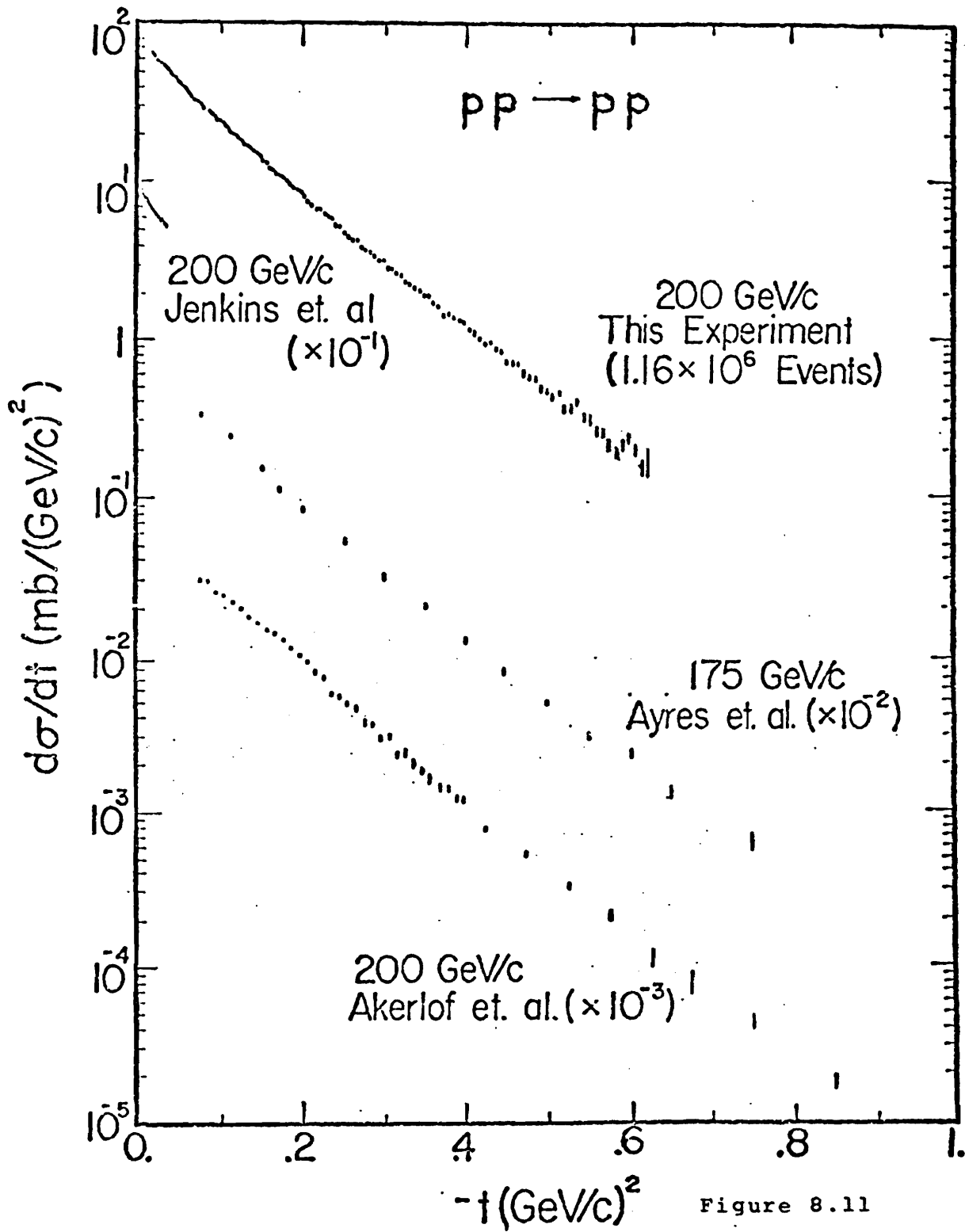


TABLE 8.3

Tabulation of differential cross sections. Errors are statistical only. Coulomb scattering contributions have been subtracted, and corrections for radiative effects, inelastic contamination, and plural nuclear scattering are included.

π^-p 200 GeV/c

$-t$ (GeV/c) ²	$d\sigma/dt$ [mb/(GeV/c) ²]		
.0206	25.38	±	.47
.0221	24.52	±	.47
.0236	24.33	±	.45
.0252	24.17	±	.44
.0268	23.90	±	.43
.0285	22.70	±	.41
.0302	22.57	±	.41
.0320	21.74	±	.39
.0338	21.81	±	.38
.0357	21.75	±	.39
.0377	20.55	±	.37
.0396	19.69	±	.35
.0417	20.58	±	.37
.0438	19.76	±	.36
.0459	19.10	±	.35
.0481	19.11	±	.35
.0503	18.78	±	.34
.0526	18.48	±	.33
.0549	18.10	±	.34
.0573	17.51	±	.33
.0598	16.86	±	.31
.0622	16.45	±	.31
.0648	15.96	±	.30
.0674	15.72	±	.30
.0700	15.58	±	.29
.0727	14.90	±	.29
.0755	14.84	±	.28
.0782	14.42	±	.27
.0811	14.28	±	.27
.0840	13.03	±	.25
.0869	14.04	±	.27
.0899	12.34	±	.24
.0930	12.94	±	.25
.0961	12.05	±	.24

$-t \text{ (GeV/c)}^2$	$d\sigma/dt \text{ [mb/(GeV/c)}^2\text{]}$		
.0992	11.77	±	.24
.1024	11.04	±	.22
.1057	11.07	±	.23
.1090	10.51	±	.21
.1123	10.13	±	.21
.1157	10.08	±	.21
.1192	9.48	±	.20
.1227	9.11	±	.19
.1263	9.39	±	.20
.1299	9.03	±	.19
.1335	8.64	±	.19
.1372	8.44	±	.18
.1410	7.84	±	.17
.1448	7.53	±	.17
.1487	7.43	±	.16
.1526	7.12	±	.16
.1565	6.82	±	.15
.1605	6.66	±	.14
.1646	6.22	±	.14
.1687	6.17	±	.14
.1729	6.19	±	.14
.1771	5.94	±	.14
.1814	5.74	±	.13
.1857	5.37	±	.12
.1901	5.08	±	.12
.1945	4.85	±	.12
.1990	4.90	±	.12
.2035	4.63	±	.11
.2081	4.42	±	.11
.2127	4.33	±	.11
.2173	4.22	±	.11
.2221	4.14	±	.10
.2268	3.89	±	.10
.2317	3.54	±	.09
.2366	3.55	±	.10
.2415	3.46	±	.09
.2465	3.17	±	.09
.2515	3.02	±	.08
.2566	3.08	±	.08
.2617	2.88	±	.08
.2669	2.82	±	.08
.2721	2.82	±	.08
.2774	2.61	±	.08
.2827	2.59	±	.07
.2881	2.51	±	.07
.2936	2.24	±	.07
.2990	2.12	±	.06
.3046	2.13	±	.06
.3102	1.98	±	.06
.3158	1.98	±	.06
.3215	1.85	±	.06

$-t \text{ (GeV/c)}^2$	$d\sigma/dt \text{ [mb/(GeV/c)}^2\text{]}$		
.3272	1.75	±	.06
.3330	1.55	±	.05
.3389	1.55	±	.05
.3448	1.49	±	.05
.3507	1.59	±	.05
.3567	1.42	±	.05
.3627	1.42	±	.05
.3688	1.30	±	.05
.3750	1.23	±	.04
.3812	1.21	±	.04
.3874	1.18	±	.04
.3937	1.04	±	.04
.4001	1.07	±	.04
.4065	.98	±	.04
.4129	.91	±	.04
.4194	.87	±	.04
.4260	.88	±	.04
.4326	.73	±	.04
.4393	.75	±	.03
.4460	.76	±	.03
.4527	.75	±	.03
.4595	.71	±	.03
.4664	.68	±	.03
.4733	.60	±	.04
.4803	.60	±	.03
.4873	.59	±	.03
.4943	.55	±	.03
.5014	.48	±	.03
.5086	.50	±	.03
.5158	.49	±	.03
.5231	.48	±	.03
.5304	.44	±	.03
.5378	.39	±	.03
.5452	.38	±	.02
.5526	.37	±	.02
.5602	.34	±	.02
.5677	.33	±	.02
.5754	.32	±	.02
.5830	.33	±	.02
.5908	.28	±	.02
.5985	.27	±	.02
.6063	.28	±	.02
.6142	.23	±	.03
.6221	.26	±	.02
.6301	.21	±	.02
.6382	.24	±	.03
.6462	.23	±	.02
.6544	.22	±	.02
.6625	.20	±	.02

$\pi^+ p$ 200 GeV/c

$-t$ (GeV/c) ²	$d\sigma/dt$ [mb/(GeV/c) ²]		
.0220	24.09	±	.46
.0235	23.53	±	.43
.0251	23.60	±	.44
.0267	23.22	±	.42
.0284	22.91	±	.40
.0301	22.32	±	.41
.0319	21.77	±	.39
.0337	22.01	±	.39
.0356	20.89	±	.38
.0375	20.65	±	.37
.0395	20.53	±	.36
.0415	19.97	±	.36
.0436	19.21	±	.35
.0457	18.70	±	.34
.0479	18.76	±	.33
.0501	18.22	±	.34
.0524	17.29	±	.32
.0547	17.18	±	.31
.0571	16.86	±	.31
.0595	16.53	±	.30
.0620	16.31	±	.30
.0645	16.23	±	.29
.0671	15.61	±	.29
.0697	15.13	±	.28
.0724	14.79	±	.28
.0752	14.44	±	.27
.0779	13.72	±	.27
.0808	13.56	±	.26
.0837	13.02	±	.26
.0866	13.35	±	.26
.0896	12.63	±	.25
.0926	12.20	±	.24
.0957	11.95	±	.24
.0988	11.20	±	.24
.1020	11.35	±	.23
.1053	10.81	±	.23
.1086	10.69	±	.22
.1119	10.02	±	.21
.1153	9.99	±	.21
.1187	9.63	±	.21
.1222	9.22	±	.21
.1258	9.00	±	.20
.1293	8.54	±	.19
.1330	8.85	±	.19
.1367	8.11	±	.19
.1404	7.96	±	.18

$-t \text{ (GeV/c)}^2$	$d\sigma/dt \text{ [mb/(GeV/c)}^2\text{]}$		
. 1442	7. 71	±	. 18
. 1481	7. 15	±	. 17
. 1520	7. 24	±	. 18
. 1559	6. 96	±	. 17
. 1599	7. 00	±	. 16
. 1640	6. 38	±	. 16
. 1681	6. 56	±	. 16
. 1722	5. 81	±	. 16
. 1764	5. 94	±	. 15
. 1807	5. 74	±	. 15
. 1850	5. 21	±	. 14
. 1893	5. 35	±	. 15
. 1937	4. 90	±	. 14
. 1982	4. 91	±	. 14
. 2027	4. 40	±	. 12
. 2072	4. 37	±	. 13
. 2118	4. 36	±	. 13
. 2165	4. 11	±	. 12
. 2212	4. 00	±	. 11
. 2259	3. 67	±	. 11
. 2308	3. 87	±	. 11
. 2356	3. 44	±	. 11
. 2405	3. 45	±	. 11
. 2455	3. 21	±	. 10
. 2505	3. 02	±	. 10
. 2556	2. 97	±	. 10
. 2607	3. 01	±	. 10
. 2658	2. 81	±	. 09
. 2710	2. 66	±	. 09
. 2763	2. 54	±	. 09
. 2816	2. 52	±	. 09
. 2870	2. 43	±	. 09
. 2924	2. 18	±	. 08
. 2979	2. 14	±	. 08
. 3034	2. 01	±	. 08
. 3089	2. 08	±	. 07
. 3146	2. 03	±	. 07
. 3202	1. 77	±	. 07
. 3259	1. 88	±	. 07
. 3317	1. 68	±	. 07
. 3375	1. 59	±	. 06
. 3434	1. 57	±	. 07
. 3493	1. 50	±	. 07
. 3553	1. 38	±	. 06
. 3613	1. 54	±	. 06
. 3674	1. 36	±	. 06
. 3735	1. 26	±	. 06
. 3797	1. 17	±	. 05
. 3859	1. 16	±	. 05

$-t \text{ (GeV/c)}^2$	$d\sigma/dt \text{ [mb/(GeV/c)}^2\text{]}$		
.3922	1.05	±	.06
.3985	1.09	±	.06
.4049	.96	±	.06
.4113	.99	±	.06
.4178	.95	±	.06
.4243	.86	±	.06
.4309	.79	±	.05
.4375	.78	±	.05
.4442	.77	±	.05
.4509	.75	±	.05
.4577	.74	±	.05
.4645	.73	±	.05
.4714	.59	±	.05
.4784	.60	±	.04
.4853	.57	±	.04
.4924	.60	±	.04
.4995	.47	±	.04
.5066	.48	±	.05
.5138	.51	±	.04
.5210	.41	±	.04
.5283	.41	±	.05
.5356	.46	±	.04
.5430	.39	±	.04
.5505	.29	±	.06
.5579	.41	±	.04
.5655	.41	±	.04
.5731	.30	±	.04
.5807	.35	±	.04
.5884	.33	±	.04
.5962	.32	±	.04
.6039	.26	±	.04
.6118	.28	±	.04
.6197	.29	±	.05
.6276	.13	±	.08
.6356	.23	±	.05
.6437	.19	±	.04
.6518	.18	±	.05
.6599	.16	±	.05

pp 200 GeV/c

$-t \text{ (GeV/c)}^2$	$d\sigma/dt \text{ [mb/(GeV/c)}^2\text{]}$		
.0206	62.33	±	.60
.0220	61.36	±	.58
.0235	59.51	±	.57
.0251	58.80	±	.57
.0267	58.17	±	.56
.0284	57.01	±	.55
.0301	55.79	±	.54
.0319	54.82	±	.53
.0337	53.27	±	.52
.0356	52.49	±	.51
.0375	51.55	±	.50
.0395	49.61	±	.49
.0415	48.54	±	.48
.0436	47.11	±	.47
.0457	46.61	±	.46
.0479	45.46	±	.46
.0501	43.71	±	.44
.0524	42.26	±	.42
.0547	41.40	±	.42
.0571	40.46	±	.41
.0595	39.40	±	.41
.0620	38.57	±	.40
.0645	36.84	±	.38
.0671	35.87	±	.37
.0697	35.11	±	.37
.0724	33.59	±	.36
.0752	32.62	±	.35
.0779	31.70	±	.34
.0808	30.59	±	.33
.0837	29.56	±	.32
.0866	29.60	±	.32
.0896	27.93	±	.31
.0926	26.78	±	.30
.0957	26.10	±	.29
.0988	24.71	±	.28
.1020	24.54	±	.28
.1053	23.74	±	.27
.1086	22.57	±	.26
.1119	22.19	±	.26
.1153	20.69	±	.25
.1187	20.11	±	.24
.1222	19.57	±	.24
.1258	18.53	±	.23
.1293	17.88	±	.22
.1330	17.09	±	.21
.1367	16.64	±	.21
.1404	16.14	±	.20

$-t \text{ (GeV/c)}^2$	$d\sigma/dt \text{ [mb/(GeV/c)}^2\text{]}$		
. 1442	15. 53	±	. 20
. 1481	14. 92	±	. 19
. 1520	14. 50	±	. 19
. 1559	13. 49	±	. 18
. 1599	13. 03	±	. 17
. 1640	12. 19	±	. 17
. 1681	11. 94	±	. 17
. 1722	11. 34	±	. 16
. 1764	10. 92	±	. 16
. 1807	10. 49	±	. 15
. 1850	10. 03	±	. 14
. 1893	9. 71	±	. 14
. 1937	9. 02	±	. 14
. 1982	8. 80	±	. 13
. 2027	8. 49	±	. 13
. 2072	8. 13	±	. 12
. 2118	7. 54	±	. 12
. 2165	7. 18	±	. 11
. 2212	6. 65	±	. 11
. 2259	6. 58	±	. 10
. 2308	6. 24	±	. 10
. 2356	5. 98	±	. 10
. 2405	5. 85	±	. 10
. 2455	5. 39	±	. 09
. 2505	5. 18	±	. 09
. 2556	4. 76	±	. 09
. 2607	4. 48	±	. 08
. 2658	4. 35	±	. 08
. 2710	4. 28	±	. 08
. 2763	3. 79	±	. 07
. 2816	3. 70	±	. 07
. 2870	3. 66	±	. 07
. 2924	3. 41	±	. 07
. 2979	3. 19	±	. 06
. 3034	3. 19	±	. 06
. 3089	2. 84	±	. 06
. 3146	2. 79	±	. 06
. 3202	2. 62	±	. 06
. 3259	2. 56	±	. 06
. 3317	2. 32	±	. 05
. 3375	2. 23	±	. 05
. 3434	2. 13	±	. 05
. 3493	2. 00	±	. 05
. 3553	1. 87	±	. 05
. 3613	1. 86	±	. 05
. 3674	1. 71	±	. 05
. 3735	1. 62	±	. 04
. 3797	1. 39	±	. 04
. 3859	1. 41	±	. 04

$-t \text{ (GeV/c)}^2$	$d\sigma/dt \text{ [mb/(GeV/c)}^2\text{]}$
.3922	1.35 ± .04
.3985	1.32 ± .04
.4049	1.25 ± .04
.4113	1.12 ± .03
.4178	1.09 ± .04
.4243	.99 ± .03
.4309	.93 ± .03
.4375	.93 ± .03
.4442	.86 ± .03
.4509	.83 ± .03
.4577	.71 ± .03
.4645	.70 ± .03
.4714	.68 ± .03
.4784	.60 ± .03
.4853	.57 ± .03
.4924	.55 ± .03
.4995	.49 ± .03
.5066	.47 ± .02
.5138	.43 ± .03
.5210	.45 ± .02
.5283	.37 ± .02
.5356	.37 ± .02
.5430	.39 ± .02
.5505	.32 ± .03
.5579	.32 ± .03
.5655	.27 ± .02
.5731	.25 ± .02
.5807	.22 ± .02
.5884	.19 ± .02
.5962	.22 ± .02
.6039	.24 ± .03
.6118	.21 ± .02
.6197	.16 ± .02
.6276	.18 ± .04
.6356	.14 ± .04
.6437	.13 ± .02
.6518	.14 ± .03
.6599	.12 ± .03

The displayed and tabulated distributions are corrected for inelastic contamination and radiative effects. Also the contribution due to Coulomb scattering (including the Coulomb - nuclear interference contribution) has been removed. Table 8.4 presents the parameters used for this subtraction. The Coulomb correction only affects $d\sigma/dt$ for $-t < 0.035 \text{ (GeV/c)}^2$ and then only slightly. Making reasonable variations of the parameters listed in Table 8.4 changed the final answers by less than one standard deviation.

A correction for plural nuclear scattering^{6.3} in the hydrogen target is also included in Table 8.3 and Figures 8.9 to 8.11. To make the correction, the data was multiplied by the following quantity:

$$[1 + K \exp(-bt/2)/b]$$

where

$$b = b(t=0) \text{ (10.9, 10.8, and 12.1 for } \pi^-p, \pi^+p, pp; \text{ see Table 8.5)}$$

$$K = \Gamma \sigma_t^2 / 64 \pi \hbar^2$$

$$\sigma_t = \text{hadron-proton total cross section}$$

$$\Gamma = N_A \rho x / A$$

$$N_A = \text{Avogadro's number}$$

$$\rho = \text{target density}$$

$$x = \text{target length}$$

Table 8.4
Parameters for Coulomb Scattering
Contribution to $d\sigma/dt$

$$\left. \frac{d\sigma}{dt} \right|_{\text{coulomb}} = \frac{4\pi\alpha^2}{\beta^2 t^2} + \sigma_{\text{hp}} e^{bt/2} \alpha\rho/\beta t$$

where α = fine structure constant

ρ = ratio of real to imaginary part of the scattering amplitude

σ_{hp} = total cross section for hadron-proton scattering

b = forward logarithmic nuclear slope

	$b(\text{GeV}/c)^{-2}$	$\sigma_{\text{hp}}(\text{mb})^{\text{a}}$	ρ^{b}
p -p	12.0	38.97	-.01
π^+ -p	10.5	23.84	.04
π^- -p	10.5	24.33	.08

^aFrom A. S. Carroll et al., Phys. Rev. Lett. 33, 928 and 932 (1974)

^bFrom R. D. Hendrick and B. L autrup, Phys. Rev. D11, 529 (1975)

A = atomic weight

At the largest t , this correction is 11% for pp scattering and 3% for $\pi^{\pm}p$ scattering. The correction is accurate to 5%. The effect of plural nuclear scattering on the data is important only when fits are performed using the entire t range measured.

The next step of the analysis was to study in detail the shape of the $d\sigma/dt$ distributions. To accomplish this study, fits were performed over small regions of t using an exponential form. Thus in the limit of infinitely small t regions, what is obtained is the forward logarithmic slope b as a function of t where

$$b(t) = d/dt[\ln(d\sigma/dt)]$$

The entire t range was split into nine to ten subregions; the errors on the measured local slopes were still reasonably small.

The fits were performed using a least squares minimization procedure; the program MINUIT^{6.1} was employed. The fitting method was such that the endpoint of the i th bin was constrained to coincide with the

beginning point of the $i+1$ th bin. This procedure of course introduced correlations between the measured local slopes. When fits were performed without the above constraint, the values of the local slopes obtained were within one standard deviation of the results from the constrained fits. The constrained fits merely reduced the statistical error of the results.

To estimate the systematic error, the local slopes were derived using a variety of cut variations. For example, the recoil mass squared cut was changed while keeping all other cuts the same. The maximum range of the values of the local slopes with respect to the different sets of cuts is the measure of the systematic error.

Another source of systematic error was the uncertainty in the absolute value of the incident beam momentum. The beam momentum was known to $\pm 1\%$. This contribution to the systematic error was added in quadrature to the other contributions to arrive at the total systematic errors given in Table 8.5.

To orient the reader, Figure 8.12 presents "b vs. t" plots for some simple cases. Figure 8.13 presents the results of the above type of analysis for the data. The errors shown are the statistical and systematic errors added in quadrature. Table 8.5 gives the values

LOCAL SLOPE VERSUS $-t$
FOR
EXAMPLES OF $d\sigma/dt$

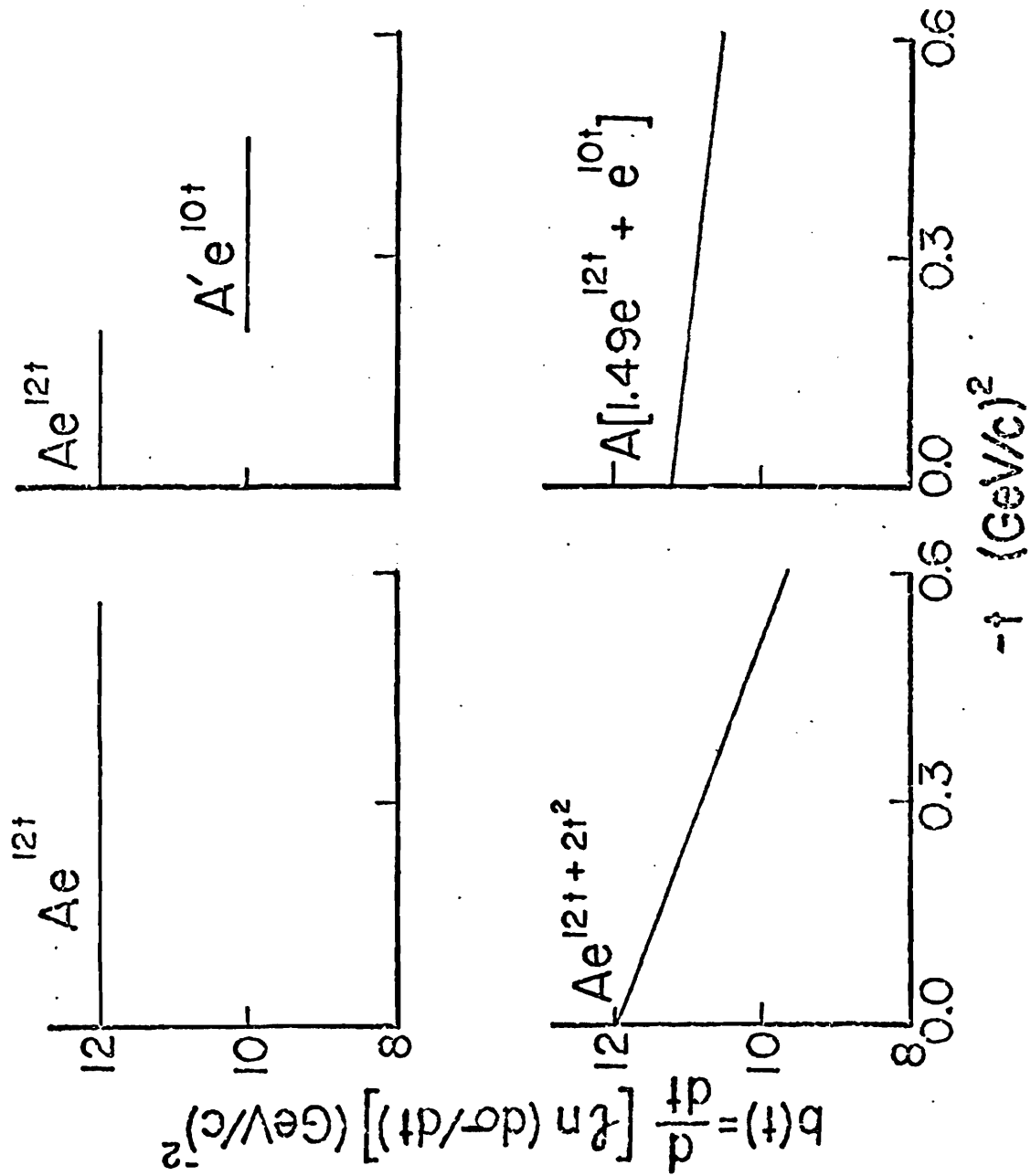


Figure 8.12

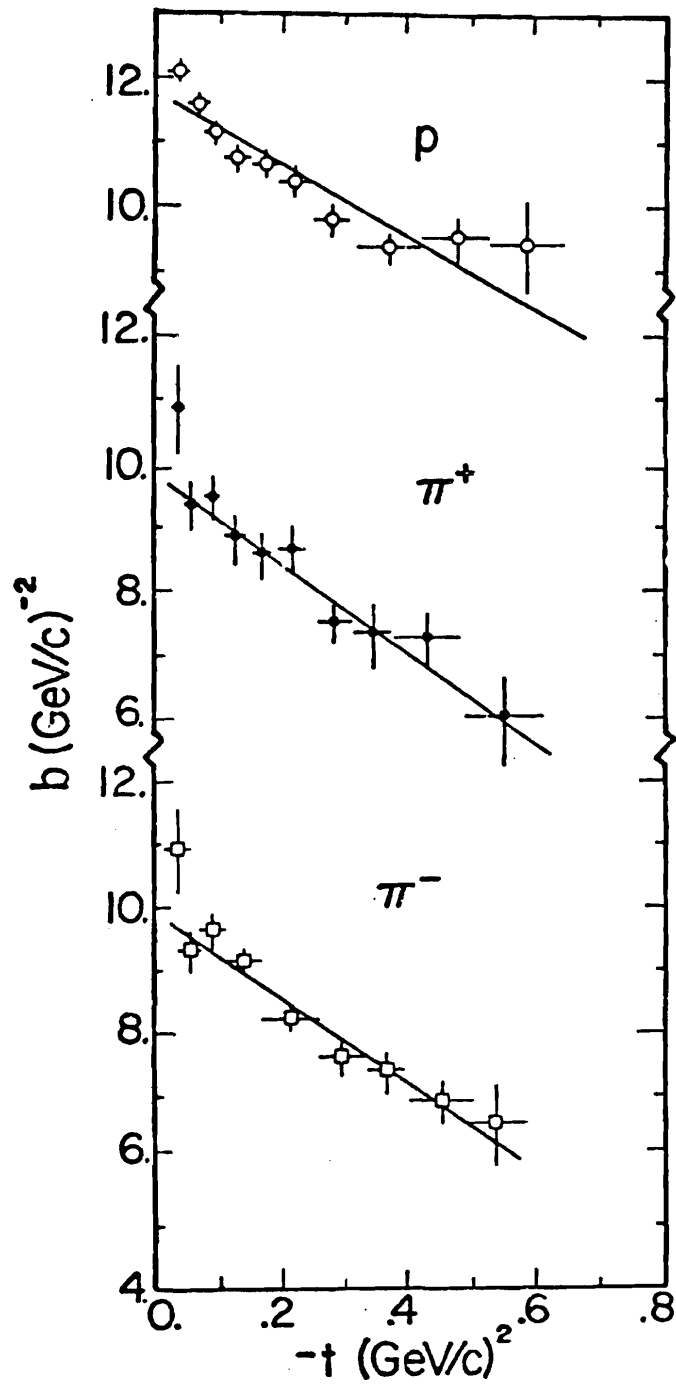
LOCAL SLOPE VERSUS $-t$: HIGH- t DATA: 200 GeV/c

Figure 8.13

TABLE 8.5
Local Slope Values and Correlations
 $\pi^- p$ 200 GeV/c

Local Slope	$ t $ Range (GeV/c) ²	Value (GeV/c) ⁻²
b_1	.022-.036	10.91 ± .55 (.25)
b_2	.036-.062	9.30 ± .29 (.18)
b_3	.062-.102	9.63 ± .23 (.17)
b_4	.102-.161	9.18 ± .17 (.10)
b_5	.161-.252	8.26 ± .11 (.08)
b_6	.252-.327	7.62 ± .16 (.18)
b_7	.327-.400	7.41 ± .24 (.22)
b_8	.400-.494	6.92 ± .27 (.23)
b_9	.494-.583	6.60 ± .49 (.43)

$$\chi^2/\text{DOF} = 130.4/113$$

Covariance Matrix Correlation Coefficients, $\rho_{b_i b_j}^a$

	b_1	b_2	b_3	b_4	b_5	b_6	b_7	b_8	
b_2		-.499							
b_3		.020	-.511						
b_4		-.102	.391	-.770					
b_5		.231	-.676	.472	-.591				
b_6		-.238	.674	-.355	.039	-.388			
b_7		.147	-.413	.200	.058	-.135	-.507		
b_8		-.067	.187	-.088	-.037	.110	.016	-.565	
b_9		.024	-.068	.032	.015	-.045	.018	.116	-.565

$\rho_{b_i b_j}^a \equiv \frac{\sigma_{b_i b_j}}{\sigma_{b_i} \sigma_{b_j}}$. $\sigma_{b_i b_j}$ is the covariance between the quantities b_i and b_j ; σ_{b_i} is the standard deviation of b_i .

TABLE 8.5 (cont.)

pp 200 GeV/c		
Local Slope	t Range (GeV/c) ²	Value (GeV/c) ⁻²
b ₁	.025-.055	12.07 ± .10 (.16)
b ₂	.055-.084	11.53 ± .12 (.08)
b ₃	.084-.109	11.12 ± .12 (.10)
b ₄	.109-.152	10.71 ± .11 (.08)
b ₅	.152-.194	10.64 ± .18 (.08)
b ₆	.194-.246	10.38 ± .18 (.20)
b ₇	.246-.315	9.72 ± .15 (.13)
b ₈	.315-.424	9.34 ± .13 (.19)
b ₉	.424-.528	9.48 ± .24 (.19)
b ₁₀	.528-.644	9.35 ± .61 (.42)

$$\chi^2/\text{DOF} = 115.1/116$$

Covariance Matrix Correlation Coefficients, $\rho_{b_i b_j}^a$

	b ₁	b ₂	b ₃	b ₄	b ₅	b ₆	b ₇	b ₈	b ₉
b ₂	.211								
b ₃	-.454	-.180							
b ₄	-.355	-.644	.110						
b ₅	.204	.221	-.316	-.559					
b ₆	.036	.044	-.162	.252	-.675				
b ₇	-.160	-.151	.410	-.287	.232	-.611			
b ₈	.141	.131	-.348	.221	-.103	.126	-.558		
b ₉	-.080	-.075	.198	-.123	.048	-.027	.122	-.530	
b ₁₀	.032	.030	-.080	-.049	-.018	.005	-.021	.109	-.497

$\rho_{b_i b_j}^a \equiv \frac{\sigma_{b_i b_j}^2}{\sigma_{b_i} \sigma_{b_j}}$ is the covariance between the quantities b_i and b_j ; σ_{b_i} is the standard deviation of b_i .

TABLE 8.5 (cont.)

$\pi^+ p$ 200 GeV/c		
Local Slope	$ t $ Range (GeV/c) ²	Value (GeV/c) ⁻²
b_1	.024-.044	10.83 ± .63 (.32)
b_2	.044-.072	9.33 ± .33 (.19)
b_3	.072-.105	9.41 ± .31 (.17)
b_4	.105-.144	8.83 ± .33 (.18)
b_5	.144-.181	8.56 ± .33 (.21)
b_6	.181-.241	8.64 ± .20 (.30)
b_7	.241-.309	7.48 ± .24 (.25)
b_8	.309-.374	7.26 ± .34 (.34)
b_9	.374-.478	7.22 ± .30 (.33)
b_{10}	.478-.604	5.96 ± .50 (.42)

$$\chi^2/\text{DOF} = 99.1/114$$

Covariance Matrix Correlation Coefficients, $\rho_{b_i b_j}^a$

	b_1	b_2	b_3	b_4	b_5	b_6	b_7	b_8	b_9
b_2	-.673								
b_3	.183	-.503							
b_4	-.029	.182	-.713						
b_5	-.025	-.379	.533	-.703					
b_6	.046	.476	-.514	.119	-.382				
b_7	-.030	-.296	.305	-.003	-.187	-.404			
b_8	.015	.142	-.145	-.008	.146	-.065	-.558		
b_9	-.006	-.054	.055	.004	-.063	.060	.083	-.582	
b_{10}	.002	.016	-.017	-.001	.020	-.022	-.013	-.124	-.523

$\rho_{b_i b_j}^a \equiv \frac{\sigma_{b_i b_j}^2}{\sigma_{b_i} \sigma_{b_j}}$. $\sigma_{b_i b_j}$ is the covariance between the quantities b_i and b_j ; σ_{b_i} is the standard deviation of b_i .

of the local slopes along with correlation coefficients. Also presented are the systematic errors in the various regions of t for $\pi^{\pm}p$ and pp scattering. It is important to note that in some cases the systematic errors are significant when compared to the statistical errors on the local slopes. Since small regions of t were used to obtain the local slopes, plural nuclear scattering has negligible effect on these results. In fact the data fit was that of Table 8.3 without (hence divided by) the plural scattering correction.

Also shown on Figure 8.13 are results of a fit to the data over the full t range using a quadratic exponential form ($\exp(bt+ct^2)$). Table 8.6 exhibits the values of b and c derived from these fits. For these fits the correction for plural nuclear scattering is included in the theory. Appendix VI gives the functional form used to fit the data.

The local slopes do depend to a degree on the bins in t chosen. Figure 8.14 presents the local slope as a function of t for several different binnings. Table 8.7 tabulates the local slopes measured for these different cases. Again it should be emphasized that the data fit was the same; what was different were the chosen subregions of t .

Table 8.6

Results from Fits of $d\sigma/dt$ to $e^{bt} + ct^2$

	$ t $ Range	b	c	χ^2/DOF
p -p	.025 - .620	11.73 \pm .04	-2.98 \pm .10	186.0/125
π^+ -p	.025 - .620	9.94 \pm .07	-3.68 \pm .16	106.0/125
π^- -p	.025 - .620	9.88 \pm .06	-3.43 \pm .13	142.4/125

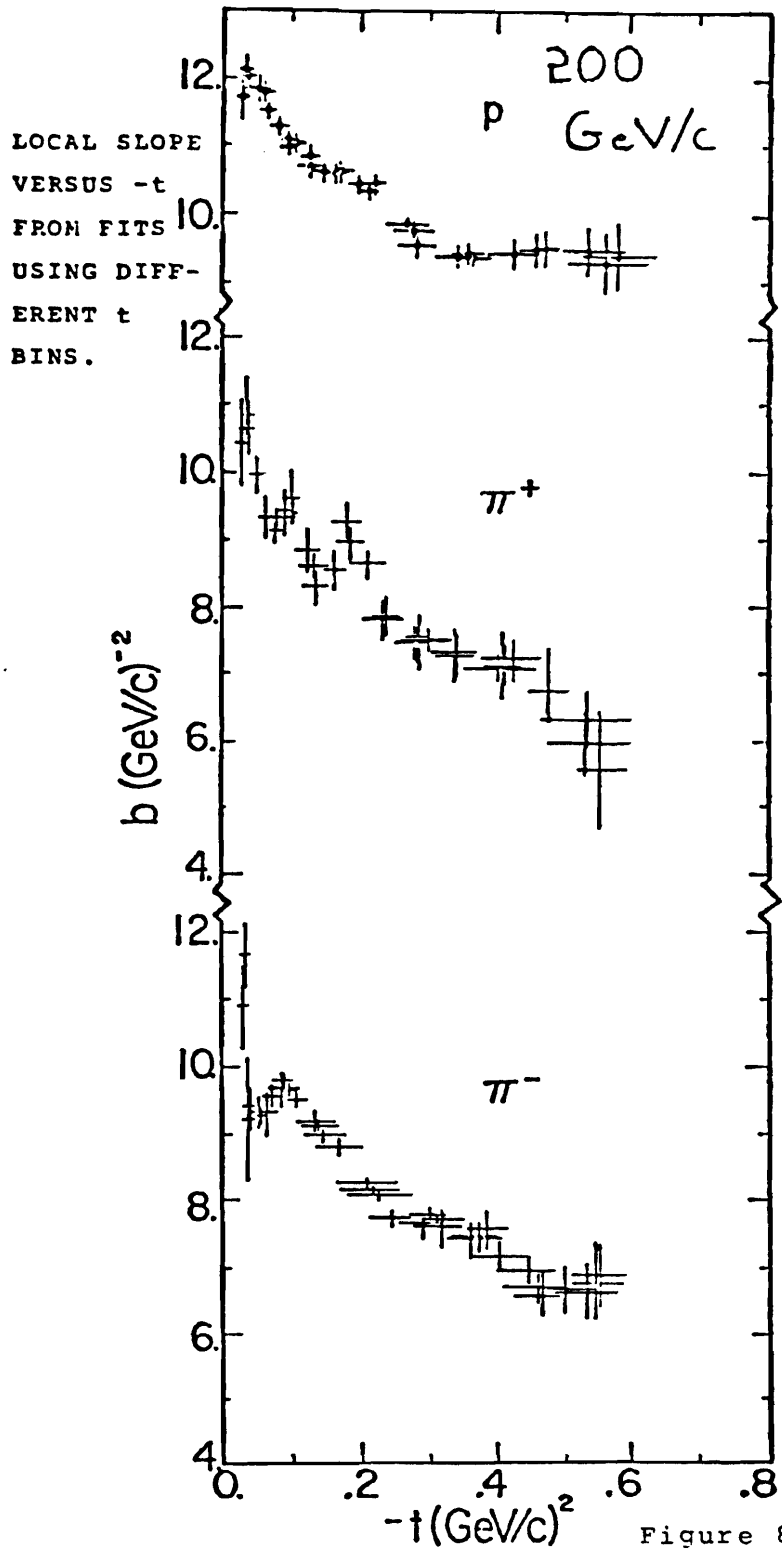


Figure 8.14

TABLE 8.7

Local Slopes using t Bins Different from those of Table 8.5 π^-p 200 GeV/c

Local Slope	$ t $ Range (GeV/c) ²	Value ^a (GeV/c) ⁻²	Local Slope	$ t $ Range (GeV/c) ²	Value ^a (GeV/c) ⁻²
b_1	.029-.044	9.52±.91	b_1	.025-.040	11.61±.54
b_2	.044-.073	9.28±.33	b_2	.040-.067	8.74±.13
b_3	.073-.116	9.64±.13	b_3	.067-.109	9.77±.12
b_4	.116-.177	8.96±.09	b_4	.109-.169	9.08±.13
b_5	.177-.272	8.02±.11	b_5	.169-.262	8.11±.08
b_6	.272-.351	7.55±.20	b_6	.262-.339	7.72±.13
b_7	.351-.426	7.53±.28	b_7	.339-.413	7.40±.23
b_8	.426-.509	6.56±.35	b_8	.413-.509	6.68±.28
b_9	.509-.583	6.75±.64	b_9	.509-.599	6.83±.48
$\chi^2/\text{DOF} = 132.5/111$			$\chi^2/\text{DOF} = 129.0/113$		

^aErrors statistical only

TABLE 8.7 (cont.)

 π^+p 200 GeV/c

Local Slope	t Range (GeV/c) ²	Value ^a (GeV/c) ⁻²	Local Slope	t Range (GeV/c) ²	Value ^a (GeV/c) ⁻²
b ₁	.025-.050	10.65±.45	b ₁	.022-.036	10.41±.67
b ₂	.050-.109	9.30±.17	b ₂	.036-.062	9.93±.29
b ₃	.109-.160	8.60±.22	b ₃	.062-.090	9.10±.16
b ₄	.160-.212	8.96±.29	b ₄	.090-.115	9.57±.37
b ₅	.212-.261	7.84±.37	b ₅	.115-.160	8.32±.28
b ₆	.261-.309	7.55±.40	b ₆	.160-.207	9.24±.30
b ₇	.309-.380	7.34±.35	b ₇	.207-.261	7.79±.30
b ₈	.380-.444	7.10±.49	b ₈	.261-.349	7.50±.18
b ₉	.444-.514	6.78±.65	b ₉	.349-.465	7.08±.22
b ₁₀	.514-.604	5.58±.90	b ₁₀	.465-.604	6.32±.41

$$\chi^2/\text{DOF} = 100.1/113$$

$$\chi^2/\text{DOF} = 103.8/115$$

^aErrors statistical only

TABLE 8.7 (cont.)

pp 200 GeV/c

Local Slope	t Range (GeV/c) ²	Value ^a (GeV/c) ⁻²	Local Slope	t Range (GeV/c) ²	Value ^a (GeV/c) ⁻²
b ₁	.024-.039	11.76±.39	b ₁	.025-.044	12.11±.26
b ₂	.039-.070	11.86±.18	b ₂	.044-.075	11.80±.13
b ₃	.070-.100	11.29±.16	b ₃	.075-.112	11.02±.12
b ₄	.100-.126	11.03±.17	b ₄	.112-.144	10.88±.18
b ₅	.126-.172	10.63±.15	b ₅	.144-.194	10.57±.15
b ₆	.172-.236	10.43±.11	b ₆	.194-.256	10.43±.15
b ₇	.236-.303	9.83±.10	b ₇	.256-.315	9.52±.18
b ₈	.303-.392	9.37±.13	b ₈	.315-.411	9.38±.15
b ₉	.392-.478	9.40±.22	b ₉	.411-.507	9.46±.24
b ₁₀	.478-.604	9.42±.36	b ₁₀	.507-.623	9.25±.47

$$\chi^2/\text{DOF} = 120.5/111$$

$$\chi^2/\text{DOF} = 115.1/113$$

^aErrors statistical only

By integrating $d\sigma/dt$ over t , the total elastic cross section is derived. To calculate the contributions of regions in t not directly measured, the results of the fits from which the local slopes were obtained were used (using the functional form of $\exp(bt)$ for the extrapolation over unmeasured t regions). It was found that when the $d\sigma/dt$ distributions were extrapolated to t equal to zero, they were consistent within the experimental errors with the optical point. Thus $d\sigma/dt$ was normalized to the optical point for the calculation of the total elastic cross sections. Table 8.8 presents the total elastic cross sections and the ratio of the total elastic cross section to the total cross section. The errors in Table 8.8 include, in addition to the statistical uncertainties, the systematic uncertainties due to extrapolating the measured $d\sigma/dt$ distributions over unmeasured t regions.

Table 8.8
Total Elastic Cross Sections
at 200 GeV/c

	σ^{Elastic} (mb)	$\sigma^{\text{Elastic}}/\sigma^{\text{Total}}$ ^a
$\nu^- p$	3.21 \pm .150	.132 \pm .006
$\pi^+ p$	3.08 \pm .061	.129 \pm .003
$p p$	6.82 \pm .136	.175 \pm .004

^aFrom A. S. Carroll et. al., Phys. Rev. Lett. 33, 928 and 932 (1974)

CHAPTER 9

HIGH- t ANALYSIS: DISCUSSION

A. Local Slopes

The results presented in Figure 8.13 clearly demonstrate the elastic scattering cross section for $\pi^\pm p$ and pp reactions at 200 GeV/c are not consistent with a simple exponential ($\exp(bt)$) (also see Table 8.6). For pp scattering the behavior is poorly parameterized by an exponential with a quadratic term ($\exp(bt+ct^2)$). However for $\pi^\pm p$ scattering, the quadratic form describes the t distributions for $-t > 0.04$ (GeV/c)².

The local slope in the pp case decreases with increasing t in the region of $0.025 < -t < 0.250$ (GeV/c)². From $0.25 < -t < 0.65$ (GeV/c)² the local slope has a constant value of approximately 9.5 (GeV/c)⁻².

For the pions, in the region $0.10 < -t < 0.60$ (GeV/c)² the local slope decreases with increasing t . From $0.03 < -t < 0.10$ (GeV/c)² the local slope is relatively flat; finally there is a sharp increase in the value of the slope in the region $0.02 < -t < 0.03$ (GeV/c)².

Figure 8.13 would indicate that in the region of approximately $0.25 < -t < 0.65$ (GeV/c)² the behavior of the local slopes as a function of t is different for pions and protons. However the data do not have sufficient statistical accuracy to conclusively prove this contention. The ratio R^\pm was formed where

$$R^\pm = [d\sigma/dt(pp)]/[d\sigma/dt(\pi^\pm p)]$$

and fit to the form of $C \exp(dt)$. Figure 9.1 shows R^\pm along with the fit; Table 9.1 presents the fit results. An exponential describes the general behavior of R^\pm (for the π^- case there is no particular region of t that dominates the contribution to the chi-squared) which would indicate similar $d\sigma/dt$ shapes for the pions and protons. Also the value of d is in good agreement with that found at 175 GeV/c in Ref. 9.1. To definitively settle the question approximately four times the present statistics in the region of $0.30 < -t < 0.60$ (GeV/c)² would be required.

Figure 9.1 shows small oscillations about the results of the fit to the R^- ratio, but none in the R^+ ratio. At the sensitivity of the measurement, it cannot be concluded whether the oscillations are real or are

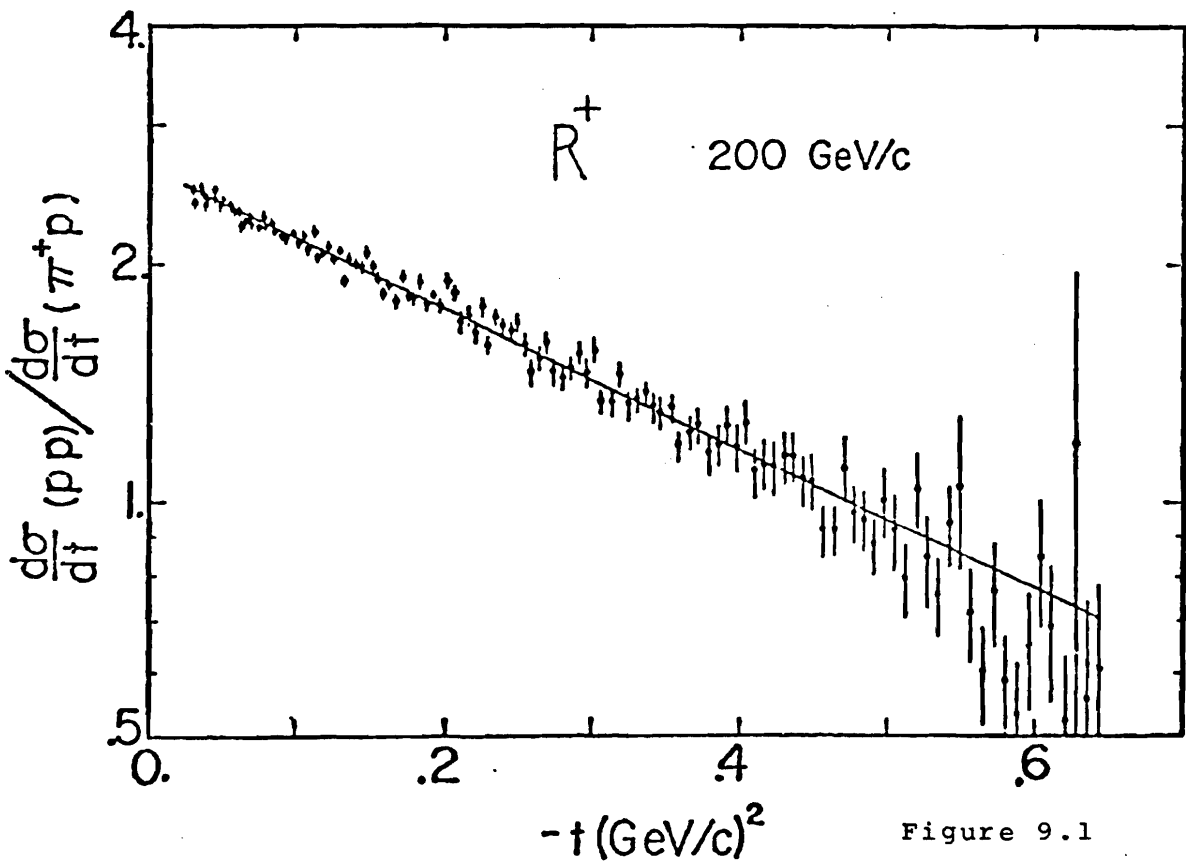
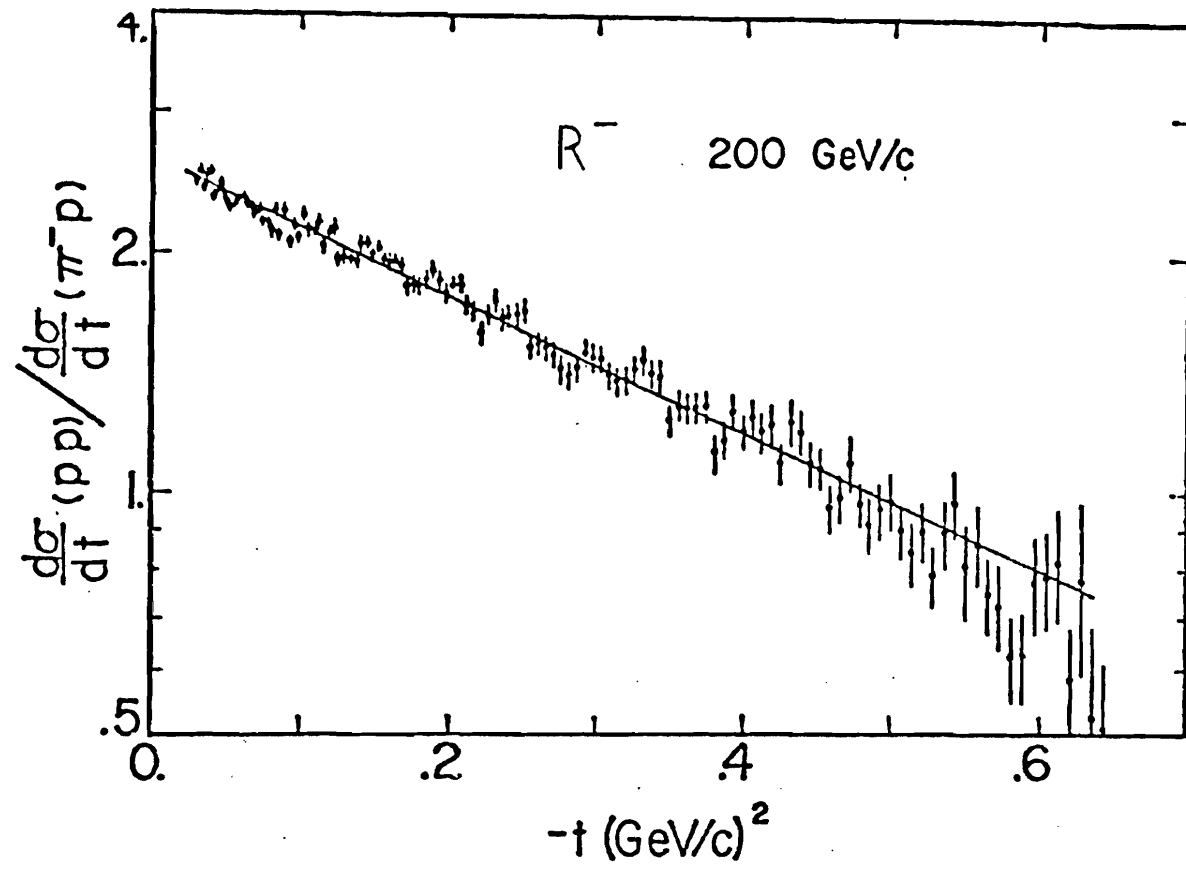


Figure 9.1

TABLE 9.1

Results of fits of R^{\pm} (as defined in text) to Ce^{dt} .

	t Range	c	d	χ^2/DOF
R^+ (p/π^+)	.022-.630	$2.67 \pm .01$	$2.08 \pm .06$	126.1/128
R^- (p/π^-)	.022-.630	$2.61 \pm .01$	$1.98 \pm .06$	165.1/128

due to instrumental effects. However it is more likely the effect is due to the latter since the R^+ ratio does not exhibit oscillations. In any case the point to point variations in the R^- ratio are too small to affect the conclusions of the analysis.

Figures 8.9 to 8.11 show a comparison of the differential cross sections for the experiments^{1.8,1.9,1.12,9.2} that have measured elastic scattering in the same kinematic region. Figure 9.2 compares measured local slopes from this experiment with those measured by others^{1.8,1.9,1.11,1.12,9.3,9.4}. It should be noted that these other measurements of the forward slopes are calculated from fits over much larger ranges of t than used in this experiment. This is especially true for references 1.8 and 1.9 where fits were performed over their full t range (-0.03 to -0.40 for Ref. 1.8; -0.07 to -0.80 for Ref. 1.9), to a quadratic form. From the fit results, the forward slope at t equal to -0.20 $(\text{GeV}/c)^2$ was calculated. It is seen that there is good agreement between all the experiments. The results from references 1.12 and 9.5 support the observation of a sharp increase in the local slope in the very small t region for π^-p scattering.

COMPARISON OF
MEASURED LOCAL
SLOPES OF
ELASTIC SCAT-
TERING

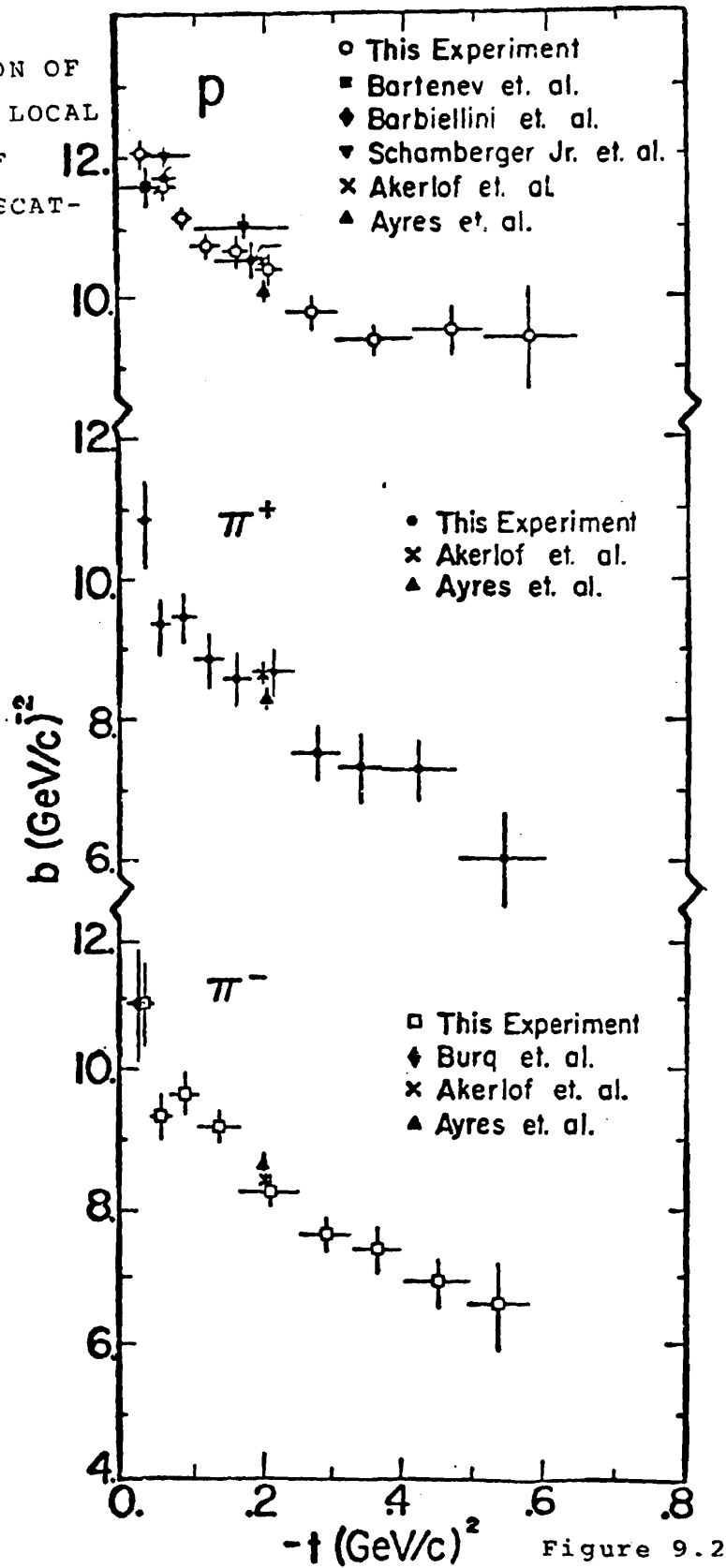


Figure 9.2

An analysis similar to the one presented here has been performed for hadron-proton elastic scattering at energies of 10.4 and 14 GeV^{1.10}. It was found that the $\pi^{\pm}p$ and pp scattering exhibit a behavior more complicated than a simple exponential in t . Thus the phenomena observed at 200 GeV are also seen in an energy regime an order of magnitude less than that of this experiment.

B. "Form Factor" Parameterization of $d\sigma/dt$

Theoretical models such as that of Chou and Yang^{9.6} and versions of the Additive Quark Model (AQM)^{9.7,9.8} attribute the major part of the small t elastic cross section variation to the hadronic form factors of the target and the projectile. These form factors are assumed to be the same as the electromagnetic ones. In the AQM the form factors describe the spatial distribution of the quarks; in the very small t region, the scattering is dominated by single quark-quark scattering. In these models, $d\sigma/dt$ is given to first order as

$$d\sigma/dt = A F^2(t)_{\text{target}} F^2(t)_{\text{projectile}} |A_{qq}(t)|^2 \quad (9.1)$$

where

$$A = N_0 \sigma^2 / 16 \pi \hbar^2$$

N_0 = normalization factor

σ = total cross section

$F(t)_{\text{target}}$ = hadronic form factor of the target

$F(t)_{\text{projectile}}$ = hadronic form factor of the
projectile

$A_{qq}(t)$ = quark-quark scattering matrix element

The following forms for the proton and pion hadronic form factors were used in this analysis:

$$F(t)_{\text{proton}} = [1 - (r_p^2 t / (12 \hbar^2))]^{-2} \quad , \text{dipole form}$$

$$F(t)_{\text{pion}} = [1 - (r_\pi^2 t / (6 \hbar^2))]^{-1} \quad , \text{monopole form}$$

where

r_p = proton electromagnetic charge radius

r_π = pion electromagnetic charge radius

The $d\sigma/dt$ distributions were fit to Eq. 9.1 using the following three forms for A_{qq} :

$$|A_{qq}|^2(t) = 1 + ut \quad , \text{linear form} \quad (9.2a)$$

$$|A_{qq}|^2(t) = \exp(ut) \quad , \text{exponential form} \quad (9.2b)$$

$$|A_{qq}|^2(t) = (1 + ut/2)^2 \quad , \text{quadratic form} \quad (9.2c)$$

The linear and quadratic forms are phenomenological; the exponential form is suggested by Bialas et. al.^{9.7} and Levin et. al.^{9.8}. In the case of the exponential form (Eq. 9.2c), one can identify u with the quark radius, r_q , where

$$r_q^2 = 2\hbar^2 u \quad (9.3)$$

Note that in the Chou - Yang model, $A_{qq}(s,t)$ is unity.

The effect of plural nuclear scattering was taken into account in the fits, again by modifying the theory. Appendix VI presents the functional forms used. The results of the fits are given in Tables 9.2, 9.3, and 9.4.

The data are well represented over the full t range ($0.025 < -t < 0.620$ (GeV/c)²) by Eq. 9.1 with the linear form for the quark-quark scattering matrix element. The fitted values of r_p and r_π are in remarkably good agreement with measured proton^{9.9} and pion^{9.10} electromagnetic charge radii. It is emphasized that the linear form for the matrix element becomes unphysical for $t > -1/u$. Hence it is surprising that this parameterization of $d\sigma/dt$ fits the data so well.

Table 9.2

Results of fits of $d\sigma/dt$ to form factor parameterization
with a linear matrix element, Eqns. 9.1 and 9.2a

Correlation Coefficients

	$ t $ Range (GeV/c) ²	A	u (GeV/c) ⁻²	r_{π} (fm)	r_p (fm)	(A,u)	(A, r_{π})	(A, r_p)	(u, r_{π})	(u, r_p)	(r_{π} , r_p)	χ^2 /DOF
pp	0.025-0.620	79.89±.24	1.18±.02	—	.81±.01	.582	—	.814	—	.910	—	119.8/122
π^+p	0.025-0.620	30.35±.18	.79±.05	.62±.04	.87±.03	.656	.112	.112	.131	.128	-.963	104.0/122
π^-p	0.025-0.620	30.98±.17	.84±.04	.62±.04	.87±.03	.639	.099	.101	.116	.112	-.971	137.0/122

Table 9.3

Results of fits of $d\sigma/dt$ to form factor parameterization
with an exponential matrix element, Eqns. 9.1 and 9.2b

Correlation Coefficients

	$ t $ Range (GeV/c) ²	A	u (GeV/c) ⁻²	r_{π} (fm)	r_p (fm)	(A,u)	(A, r_{π})	(A, r_p)	(u, r_{π})	(u, r_p)	(r_{π} , r_p)	χ^2 /DOF
pp	0.025-0.620	78.40±.27	3.32±.11	—	.72±.01	.727	—	.792	—	.992	—	154.0/122
pp	0.025-0.320	79.27±.36	2.67±.23	—	.75±.01	.807	—	.845	—	.997	—	78.4/78
π^+p	0.025-0.620	30.18±.21	1.49±.19	.65±.04	.79±.04	.703	.233	.259	-.156	.678	-.829	103.0/122
π^+p	0.025-0.320	30.11±.26	1.68±.38	.63±.04	.78±.04	.797	.412	.499	.290	.733	-.433	67.5/78
π^-p	0.025-0.620	30.78±.19	1.79±.16	.70±.03	.72±.03	.523	.304	.167	-.410	.839	-.837	136.0/122
π^-p	0.025-0.320	30.91±.37	1.26±.51	.61±.06	.84±.06	.913	.606	.590	.631	.649	-.177	97.2/78

TABLE 9.4

Results of Fits of $d\sigma/dt$ to the Form Factor Parameterization with a
Quadratic Matrix Element, Eqns. 9.1 and 9.2c

	$ t $ Range (GeV/c) ²	A	u (GeV/c) ⁻²	r_{π} (fm)	r_p (fm)	χ^2/DOF
pp	0.025-0.620	79.32±.26	-1.65±.03	—	.79±.01	124.9/122
π^+p	0.025-0.620	30.27±.19	-1.01±.08	.61±.05	.86±.04	103.0/122
π^-p	0.025-0.620	30.88±.18	-1.09±.07	.65±.04	.82±.03	136.1/122

In contrast to the linear matrix element, the quadratic form for the quark-quark scattering matrix element (Eq. 9.2c) does not become unphysical. It too gives an adequate description of the data, and the values of r_p and r_π derived are in good agreement with the measured pion and proton electromagnetic radii. It is interesting to note that Eq. 9.2c predicts a dip in the pp elastic scattering t distribution at $-t = 1.2$ $(\text{GeV}/c)^2$. Akerlof et.al.^{1,9} observe such a dip in pp scattering at 200 GeV/c incident momentum at $-t = 1.5$ $(\text{GeV}/c)^2$.

The fits using the exponential form for the matrix element were made using the full t range and a restricted t range ($0.025 < -t < 0.320$ $(\text{GeV}/c)^2$). Over the restricted t range, reasonable fits to the data were obtained. Over the full t range the pion data are well represented. However the proton data are not well represented, and value of r_p is about 10% lower than measurements of the proton electromagnetic charge radius.

Within the context of the above picture, one expects that the pion and proton electromagnetic charge radii to be the same whether extracted from the pion data or from the proton data (obviously the pp data do not measure the pion charge radius). Therefore the π^-p ,

π^+p , and pp data were fit simultaneously using a single r_π and r_p ; in some fits the u 's were constrained to be equal, in some the u 's were allowed to vary independently. Also fitting to the π^-p , π^+p , and pp data simultaneously reduced the correlation between the fitted parameters. Tables 9.5 and 9.6 present the results of these fits. Figure 9.3 shows the results using the exponential matrix element and fitting the data over the region $0.025 < -t < 0.320$ (GeV/c)².

It is observed that for fits over the full t range requiring the u 's to be equal, the data are not well represented; this fact is independent of the choice of the form for the quark-quark scattering matrix element. The data are well represented over the full t range when the linear matrix element is used, and the u 's are independent. Reasonable values of the electromagnetic charge radii are obtained; u for pp scattering is greater than u for $\pi^\pm p$ scattering. The fit to the data over the full t range using the exponential matrix element and allowing the u 's to vary independently is not as good as for the linear matrix element but still reasonable. Again u (or equivalently the quark radius) for pp scattering is greater than u for $\pi^\pm p$ scattering. The value of r_p is approximately 5% low when compared to measurements of the proton electromagnetic charge radius.

TABLE 9.5

Results of Fits of $d\sigma/dt$ to Form Factor Parameterization
Using π^-p , π^+p , pp Data Simultaneously^a

Matrix Element	$ t $ Range (GeV/c) ²	Λ_{π^-}	Λ_{π^+}	Λ_p	u_{π^-} (GeV/c) ⁻²	u_{π^+} (GeV/c) ⁻²	u_p (GeV/c) ⁻²	r_{π} (fm)	r_p (fm)	χ^2/DOF
Linear	0.025-0.620	31.02±.15	30.40±.14	79.89±.24	0.86±.02	0.82±.03	1.18±.02	.70±.01	.81±.01	360.9/370
Linear ^b	0.025-0.620	30.25±.12	29.83±.11	81.13±.23	1.03±.01	1.03±.01	1.03±.01	.63±.01	.83±.01	506.0/372
Exponential	0.025-0.620	30.63±.17	29.97±.16	80.19±.27	1.76±.08	1.71±.09	2.39±.09	.65±.02	.77±.05	446.9/370
Exponential ^b	0.025-0.620	29.89±.12	29.48±.12	80.31±.25	2.33±.07	2.33±.07	2.33±.07	.55±.01	.77±.01	510.3/372
Exponential	0.025-0.320	30.81±.25	30.25±.24	79.28±.37	1.61±.26	1.59±.26	2.67±.24	.69±.03	.75±.01	243.8/238
Exponential ^b	0.025-0.320	30.34±.15	29.87±.15	79.97±.31	2.14±.17	2.14±.17	2.14±.17	.58±.01	.78±.01	257.6/240

a r_{π} , r_p each set to a single value for pion and proton data

b u_{π^-} , u_{π^+} , u_p constrained to be equal for pion and proton data.

TABLE 9.6 (Cont.)

Matrix Element	t Range (GeV/c) ²	Correlation Coefficients					
		A _{π-}	A _{π+}	A _p	u	r _π	
Linear (u _{π-} = u _{π+} = u _p = u)	0.025-0.620	A _{π+}	.407				
		A _p	.774	.615			
		u	.352	.876	.390		
		r _π	.643	.430	.741	.373	
		r _p	.193	.489	.075	.781	.204
Exponential (u _{π-} = u _{π+} = u _p = u)	0.025-0.620	A _{π+}	.528				
		A _p	.729	.911			
		u	.519	.983	.867		
		r _π	.676	.549	.723	.539	
		r _p	.327	.623	.462	.731	.341
Exponential (u _{π-} = u _{π+} = u _p = u)	0.025-0.320	A _{π+}	.617				
		A _p	.756	.960			
		u	.613	.994	.943		
		r _π	.760	.629	.757	.625	
		r _p	.447	.726	.636	.786	.455

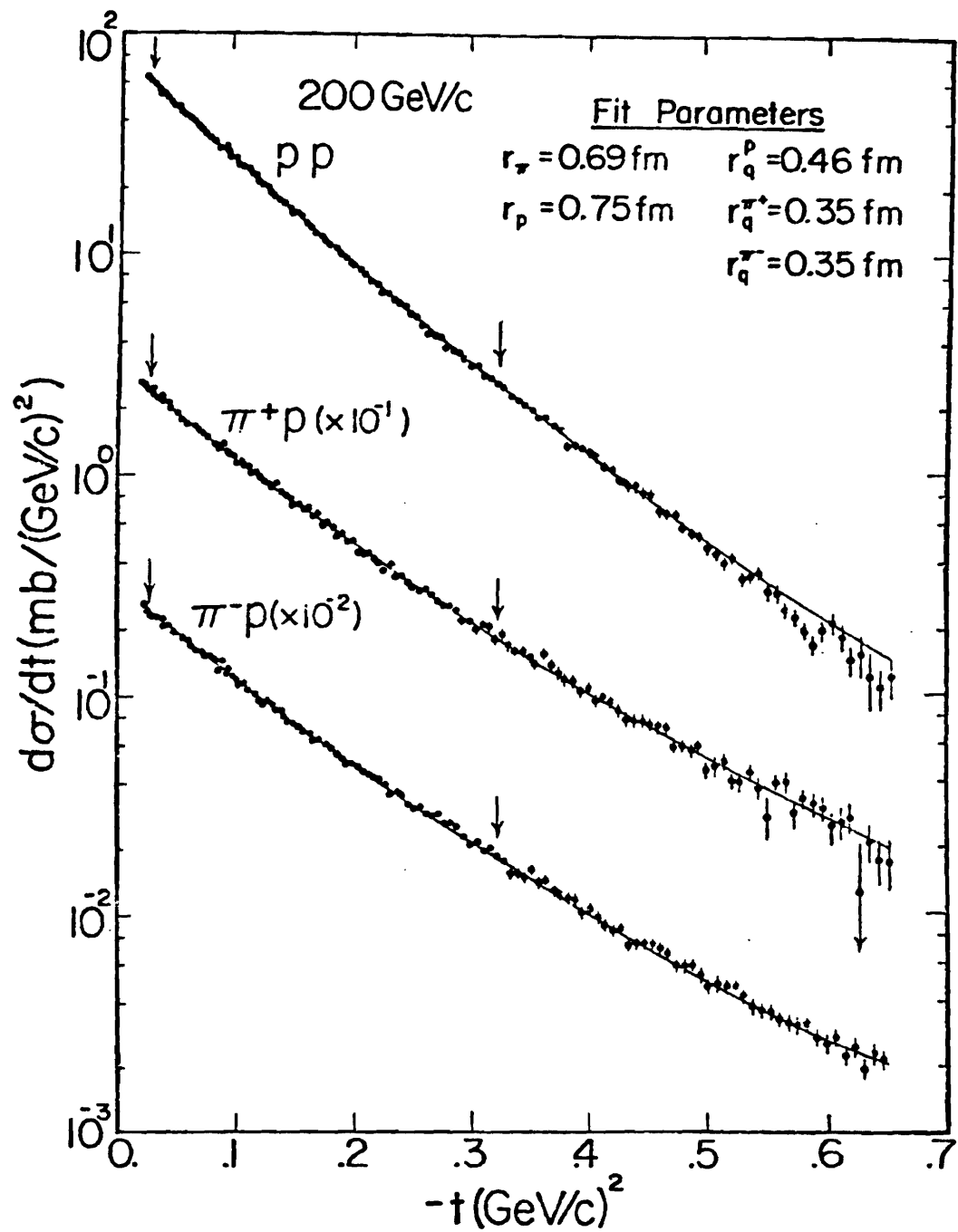


Figure 9.3

Over the region $0.025 < -t < 0.320$ (GeV/c)² the data are well represented by the fits using the exponential matrix element. This conclusion is true whether the u 's were constrained to be equal or were allowed to vary independently (though with independent u 's the fit is slightly improved). Again r_p is approximately 5% low when compared to measurements of the proton electromagnetic charge radius.

There is general agreement between the $\pi^\pm p$ and pp elastic scattering data and the AQM predictions. The fit results show that the shape of $d\sigma/dt$ in the region $0.025 < -t < 0.620$ (GeV/c)² is described by the product of the electromagnetic form factors of the projectile and the target. This is especially true in the region $0.025 < -t < 0.320$ (GeV/c)² where good fits to the data were found when using the intuitively appealing exponential form for the quark-quark scattering matrix element. The fitted values for r_p and r_π are remarkably close to their electromagnetic counterparts. The derived values of the quark radius (using Eq. 9.3) is $\sim 0.35 \pm 0.03$ fm from $\pi^\pm p$ elastic scattering and $\sim 0.45 \pm 0.02$ fm from pp elastic scattering. Within the the context of the AQM, there is evidence that the hadronic and electromagnetic form factors of elementary particles are very similiar.

It is not claimed that the analysis tests the above theoretical ideas in a strict sense. First Eq. 9.1 represents only the first order form for $d\sigma/dt$; higher order terms have been neglected. Also there were technical difficulties with the fitting procedure, since the results are very sensitive to the values of the proton and pion electromagnetic charge radii. For example constraining r_p to be 0.81 fm caused the fit to the pp data using an exponential matrix element to be quite poor. The spread in the published values of both the proton and pion electromagnetic charge radii is just too great to allow the data to definitively test the above theoretical ideas.

C. Bounds on $d\sigma/dt$

Upper limits on the ratio of the scattering amplitude at a given t to the scattering amplitude at t equal zero can be calculated^{1.13,9.11}. These limits assume unitarity and analyticity of the scattering amplitude in the complex s -plane (where s is the center of mass energy squared). Figure 9.4 shows how the data compare to one such upper bound, Eq. 1.3 of reference 9.11. It is seen that there is no violation of the bounds; however the data are close to saturating them. This behavior has been also observed at energies of

COMPARISON
OF HIGH-T DATA
WITH BOUND ON
SCATTERING
AMPLITUDE AS
DERIVED IN
REF. 1.13

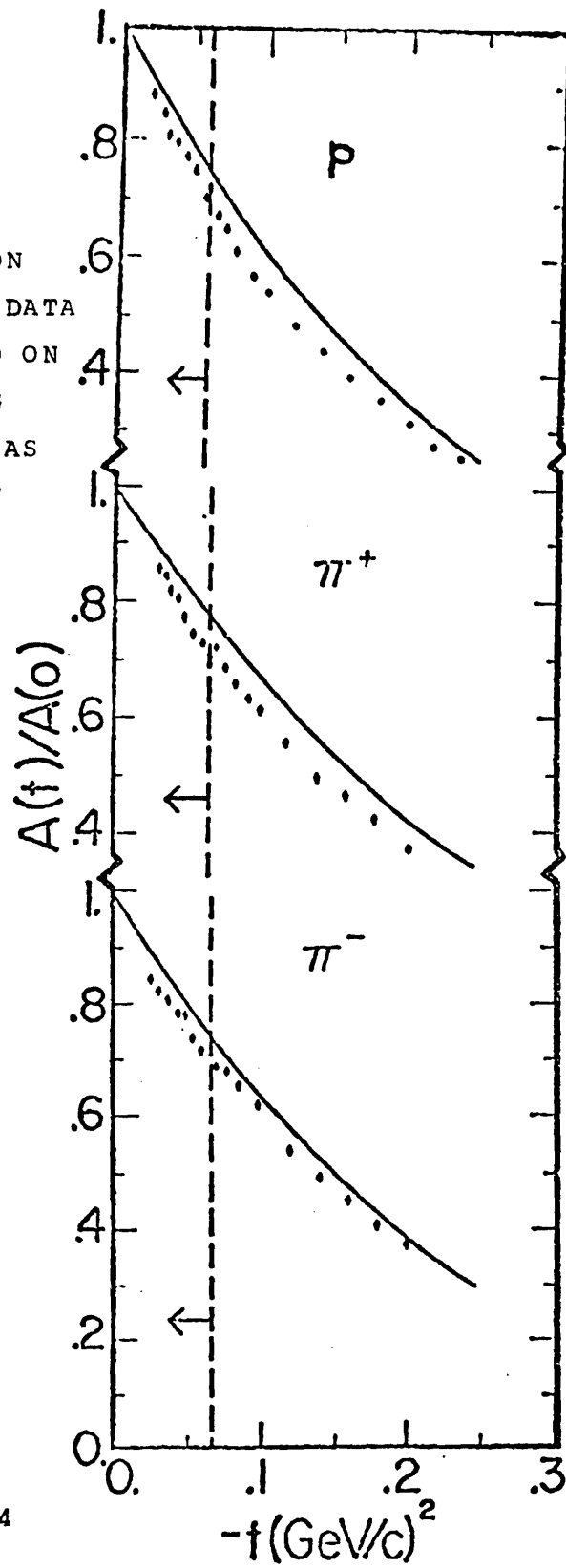


Figure 9.4

20-30 GeV^{1.13}.

S. M. Roy in reference 1.14 derives the following bound on $d\sigma/dt$ for pion-nucleon elastic scattering:

$$|b(t)| (f(t))^{1/2} > \frac{[b(0)/2] [f(t)]^{1/2} [3(f(t_1)b^2(t_1))/(f(0)b^2(0)) - 1]}{1} \quad (9.4)$$

where

$$f(t) = d\sigma/dt(t)$$

$$t = 3t_1(1+ct_1)$$

$$c = (8m_{\text{proton}}E)^{-1}$$

E = incident beam energy

$$b(t) = d/dt[\ln(d\sigma/dt)]$$

In Figure 9.5 the right hand side minus the left hand side of Eq. 9.4 is plotted. For this study the data were parameterized by Eq. 9.1 with the linear form for the matrix element. Figure 9.5 demonstrates that the data satisfy the bound, in contrast to the conclusions of reference 1.14^{9.12}. It is interesting that the bound is not violated for the pp scattering data; reference 1.14 does not address nucleon-nucleon elastic scattering. Strictly speaking the data test the bound only for $-t > 0.075$ (GeV/c)². For $-t > 0.25$ (GeV/c)² the right hand side of Eq. 9.4 is negative, and the

(RIGHT HAND SIDE) - (LEFT HAND SIDE) OF EQUATION 9.4

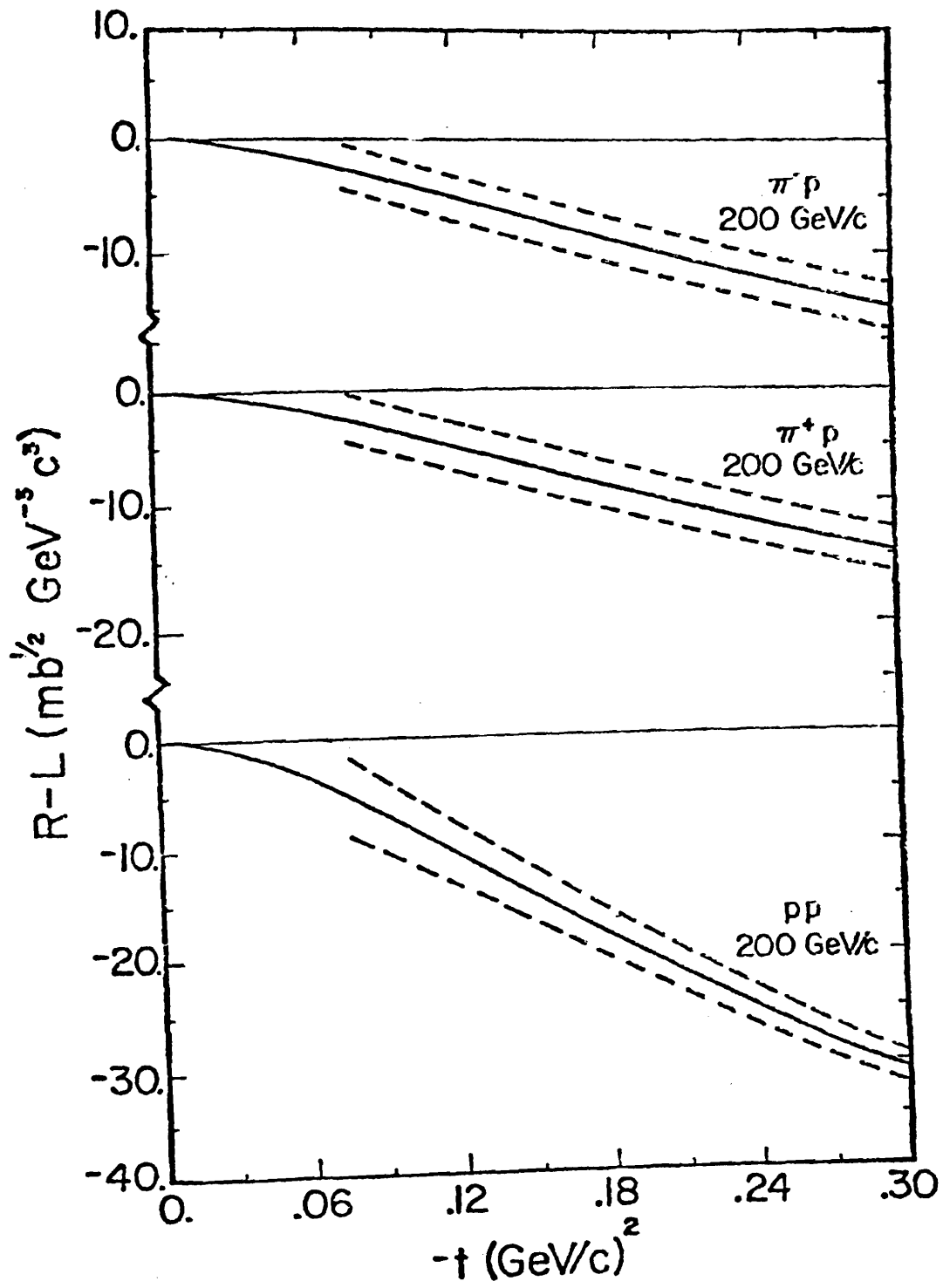


Figure 9.5

bound is not useful. At $t=t_1=0$ the two sides of the bound are by definition equal; thus at small t it is not surprising that the bound appears saturated.

Finally Appendix V shows on general grounds that if $d\sigma/dt$ is parameterized by Eq. 9.1 with an exponential matrix element and u , r_p , r_π are all greater than zero, then it is impossible to violate the bound at any t .

D. Conclusions

In the region $0.025 < -t < 0.600$ (GeV/c)² at an incident momentum of 200 GeV/c the shape of the $d\sigma/dt$ distributions for π^-p , π^+p , and pp elastic scattering have been studied in detail. The variation of the local slope as a function of t is similar for π^+p and π^-p elastic scattering, while there is indication that the variation is different in pp elastic scattering.

Over the entire t range measured, $d\sigma/dt$ for all three particles is inconsistent with the form of $\exp(bt)$ or $\exp(bt+ct^2)$. However functional forms involving the product of the electromagnetic form factors of the projectile and the target describe the data, especially for $-t < 0.30$ (GeV/c)². The Additive Quark Model leads to such functional forms for the elastic cross sections.

Finally no violations of bounds on the elastic scattering amplitude were found.

APPENDIX I

ALIGNMENT PROCEDURE

To calculate the alignment parameters (relative offsets) of the PWCs in the experiment, a sample of BEAM events was used. It was required that each PWC had one and only one coordinate. The BEAM events were used because the majority of these triggers traversed the apparatus without scattering.

The first step was to assign the nominal beam momentum to the center of the beam distribution in the momentum tagging PWC at the momentum dispersed second focus. Second a straight line was fit, in the x and y projections, to the coordinates in the high resolution chambers Stations 1 through 4 on the concrete block (the u and v chambers in Station 3 were not used). Using the parameters of these fitted tracks and tracing through the magnetic field as required, coordinates were predicted at the u and v chambers at Station 3 and at the chambers at Station 5 and 6. Residuals, the difference between the actual and predicted coordinates, were then calculated. Finally a chi-squared for each chamber was formed using all the events in an iteration

(typically 500 to 3000 BEAMS). The average residual was used to correct the PWC offsets.

It was found that the above procedure had to be performed in a particular manner to avoid systematic effects. First a prealignment using the above method was performed on the first 500 BEAM events in each run. Survey results were used to supply the starting offsets; each successive iteration used the corrected offsets. Events that failed a residual cut test at any PWC were eliminated; the test required that the residual be less than three times the chi-squared associated with a chamber. New chi-squares were calculated for each iteration. This prealignment terminated when the chi-squared change was less than twice the error matrix component for each chamber. Usually convergence was reached in three or four iterations. Note that the x and y chambers at Station 1 were kept fixed as the coordinate system origin.

Next, starting at the beginning of the run, the run was divided into typically ten segments containing 1000 to 3000 BEAM events each. One iteration then determined the alignment parameters for that segment (since the prealignment offsets were used as starting values, only one iteration was needed to have convergence). Again, the x and y chambers at Station 1 remained fixed as the

origin. Also the offset of Station 6 remained constant; instead the magnetic field of the spectrometer magnets was varied. The final alignment parameters (chamber offsets and spectrometer magnetic field) were calculated by averaging the results of each segment. Care was taken to check the consistency of the parameters associated with each segment before the averaging was performed. Again, the alignment parameters were derived on a run by run basis.

APPENDIX II

PWC CHAMBER RESOLUTION AND ROTATIONS

A. Chamber Rotations

This appendix deals with PWC Stations 3 and 4 (the high resolution chambers downstream of the target). We want $\theta_x^I(y)$ for each station where

$\theta_x^I(y)$ = rotation angle of PWC as
measured from the BEAM axis

To calculate this rotation, one studies events of cluster type 5 (see Chap. 4, Sect. B). Label alternate wirespaces even and odd; an event is classified as even or odd depending on the wirespace that the particle passed through.

Next define

$\theta_x(y)$ = the angle in the x (y) plane as measured
from the axis perpendicular to Station 3

$\theta_{x(y)}$ is measured within a constant using the information from the x (y) planes of Stations 3 and 4.

To derive the constant, β is calculated where

$$\beta = \ln[(\text{even labeled events}) / (\text{odd labeled events})]$$

as a function of $\theta_{x(y)}$. At $\theta_{x(y)}$ of 0 mr, $\beta_{x(y)}$ will be zero.

Figures A2.1 to A2.2 show plots of $\beta_{x(y)}$ versus $\theta_{x(y)}$. The angle of the beam is determined by where the BEAM events lie in the distribution. $\theta_{x(y)}^r$ is the difference between the point where the BEAM events lie in the $\beta_{x(y)}$ vs. $\theta_{x(y)}$ plot and the point where $\beta_{x(y)}$ is zero. The rotation angles, $\theta_{x(y)}^r$, are the following:

1. PWC 3X Rotation = 0.8 mrad
2. PWC 3Y Rotation = 0.0 mrad
3. PWC 4X Rotation = 1.7 mrad
4. PWC 4Y Rotation = 0.0 mrad

where PWC i refers to the PWC at Station i.

BETA (see text for definition) VERSUS SCATTERING ANGLE

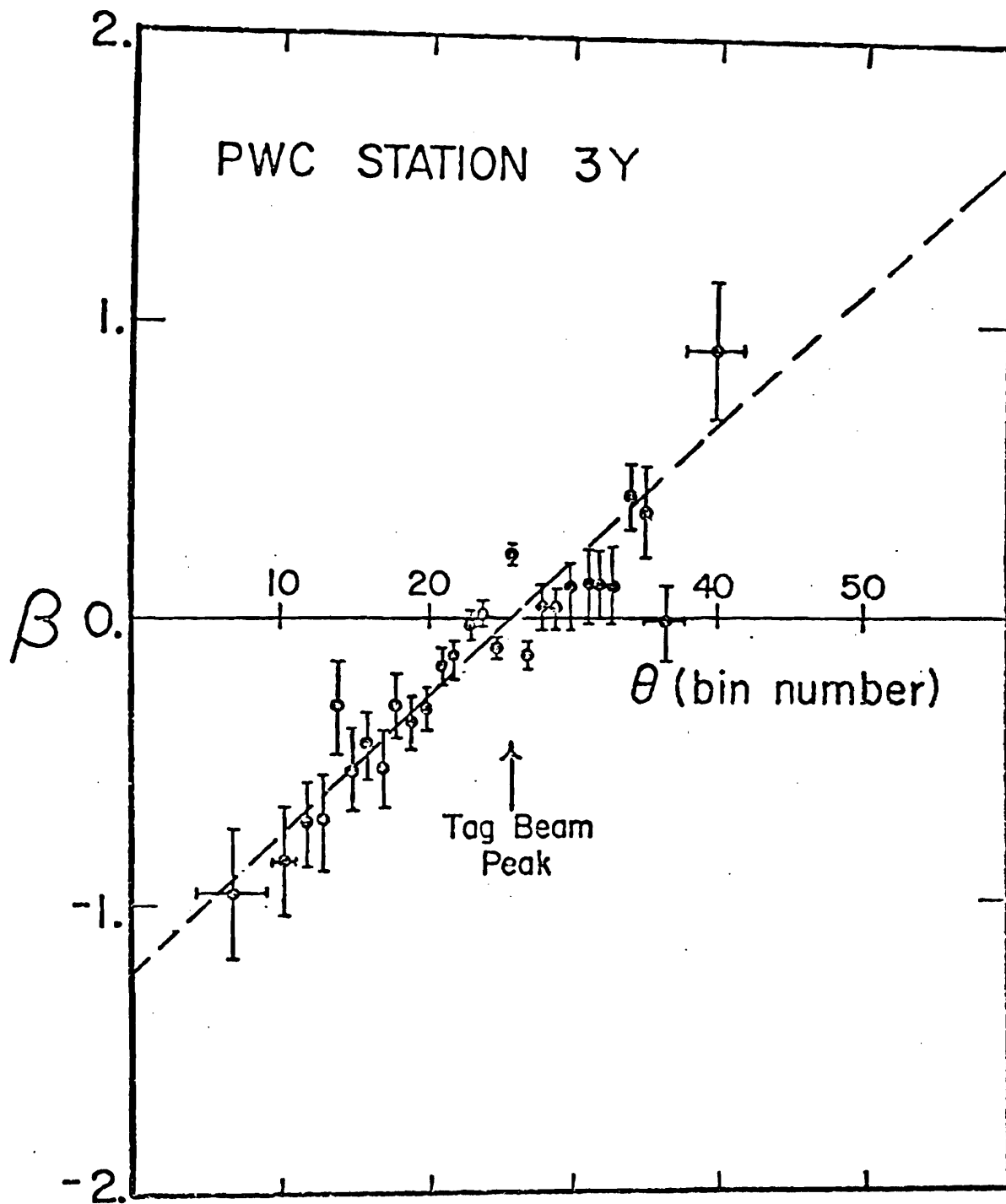


Figure A2.1

BETA (see text for definition) VERSUS SCATTERING ANGLE

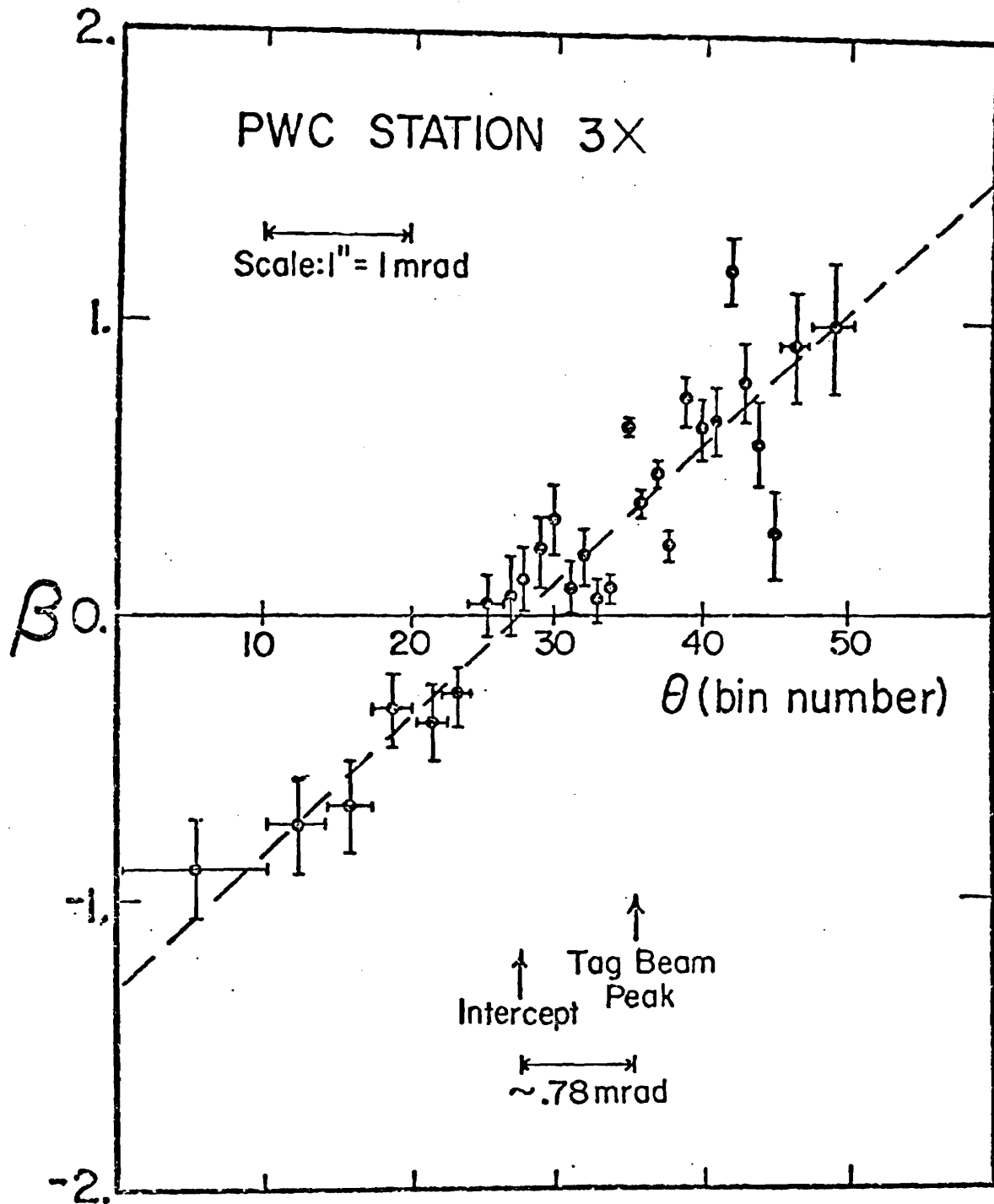
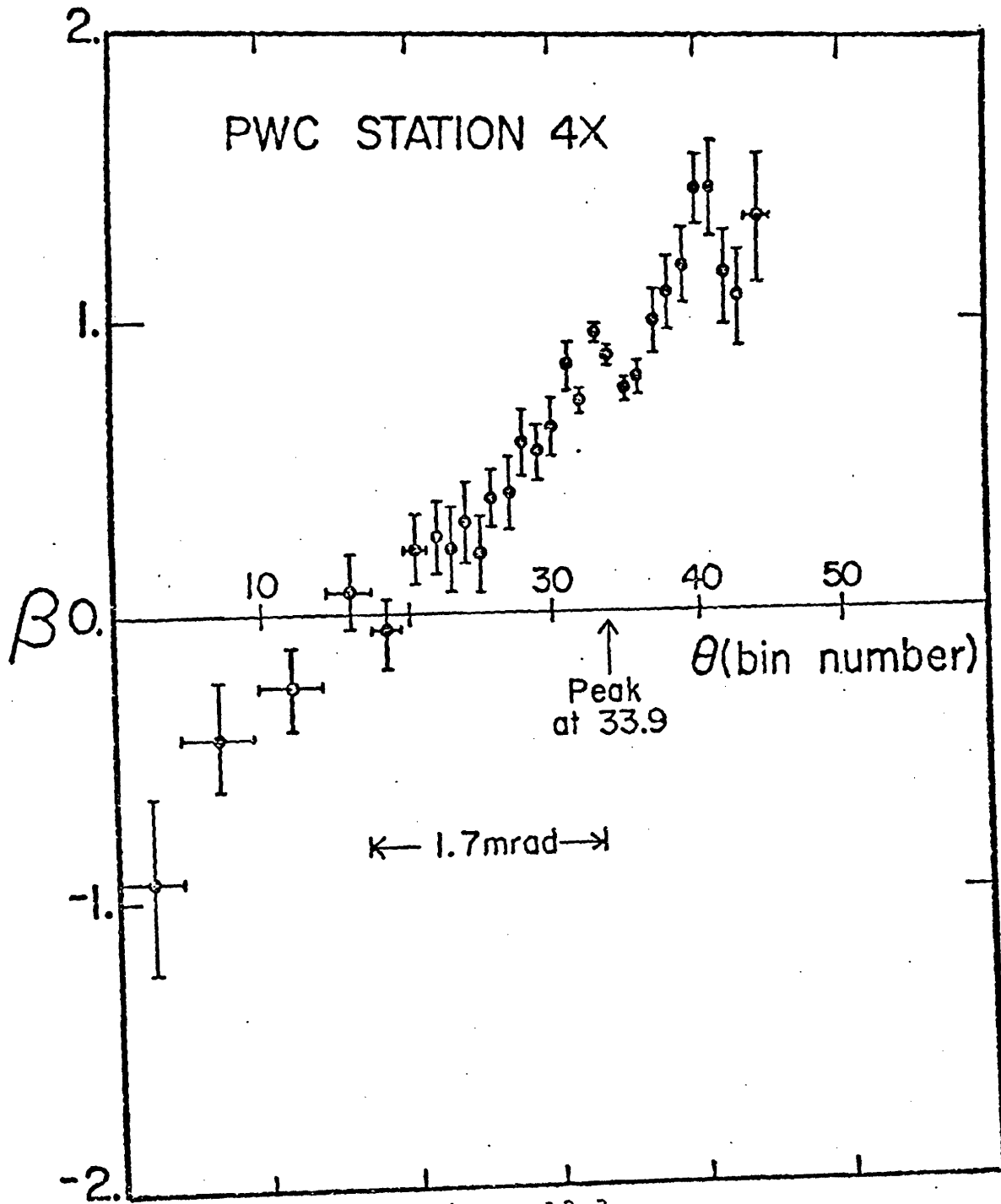


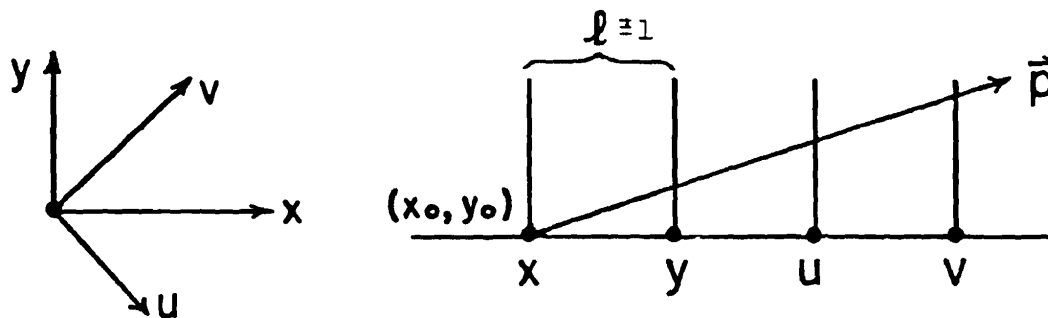
Figure A2.2

BETA (see text for definition) VERSUS SCATTERING ANGLE



B. Chamber Resolution

Consider the four planes of PWCs at Station 3 and the x and y coordinates of the track at each plane. Schematically the situation is as follows:



where p is the track trajectory. Then it is easily seen that

$$\begin{array}{ll}
 x_x = x_0 & Y_x = y_0 \\
 x_y = x_0 + 1\theta_x & Y_y = y_0 + 1\theta_y \\
 x_u = x_0 + 21\theta_x & Y_u = y_0 + 21\theta_y \\
 x_v = x_0 + 31\theta_x & Y_v = y_0 + 31\theta_y
 \end{array}$$

where

$$x_i (y_i) = x (y) \text{ coordinate at the } i\text{th plane,}$$

$$i = x, y, u, v$$

$$\theta_x (y) = \text{angle of trajectory in the } x (y) \text{ projection}$$

There are two unknowns, x_0 and y_0 , but four measured quantities:

$$1. \quad x = x_x$$

$$2. \quad y = y_y$$

$$3. \quad u = u_u$$

$$4. \quad v = v_v$$

where u_u and v_v are defined in a manner similar to x_i . Thus u and v can be used to predict x and y , and by comparing the predictions with the measured values of x and y , the chamber resolutions can be derived.

Thus

$$u = (x_u - y_u) / \sqrt{2} = (x - y + 21\theta_x - 1\theta_y) / \sqrt{2}$$

$$v = (x_v + y_v) / \sqrt{2} = (x + y + 31\theta_x + 21\theta_y) / \sqrt{2}$$

and solving for x and y

$$x^* = [(u+v)/\sqrt{2}] - [1(5\theta_x + \theta_y)/2]$$

$$y^* = [(v-u)/\sqrt{2}] - [1(\theta_x + 3\theta_y)/2]$$

where starred quantities are predicted values.

Define

$$s = x - x^*$$

$$t = y - y^*$$

and thus

$$\sigma_s^2 = \sigma_x^2 + (.5)\sigma_u^2 + (.5)\sigma_v^2$$

$$\sigma_t^2 = \sigma_y^2 + (.5)\sigma_u^2 + (.5)\sigma_v^2$$

We now consider the two major cases of cluster types.

CASE 1: Cluster Type 5:

Look at events where the coordinates in each of the planes in Station 3 are cluster type 5. Assume each plane has identical resolution which can be parameterized as

$$\sigma_x^2 = a + b\theta_x^2$$

The u, v, y planes have a similar form with the same "a" and "b". Then σ_s^2 , σ_t^2 are functions of θ_u and θ_v as well as of θ_x and θ_y . But

$$\theta_u = (\theta_x - \theta_y) / \sqrt{2}$$

$$\theta_v = (\theta_x + \theta_y) / \sqrt{2}$$

leading to

$$\sigma_s^2 = 2a + (b/2)(3\theta_x^2 + \theta_y^2) = 2a + (b/2)\theta_s$$

$$\sigma_t^2 = 2a + (b/2)(3\theta_y^2 + \theta_x^2) = 2a + (b/2)\theta_t$$

Plots of $\sigma_s^2(t)$ versus $\theta_s(t)$ are given in Figures A2.4.

A linear regression fit to the data gives

$$a = (51.90 \mu\text{m} \pm .25 \mu\text{m})^2$$

$$b = (23.66 \mu\text{m} \pm 1.01 \mu\text{m})^2 \times 10^6$$

$$\rho_{ab} = -.768$$

$$\chi^2/\text{DOF} = 15.86/15$$

Therefore for cluster type 5 events we have

$$\sigma_x^2 = (51.90 \pm .25)^2 + (23.7 \pm 1.0)^2 (\theta_x - \theta_x^r)^2$$

and similarly for σ_y^2 . The units of σ and θ are microns and milliradians respectively.

CASE 2: Cluster Type 6:

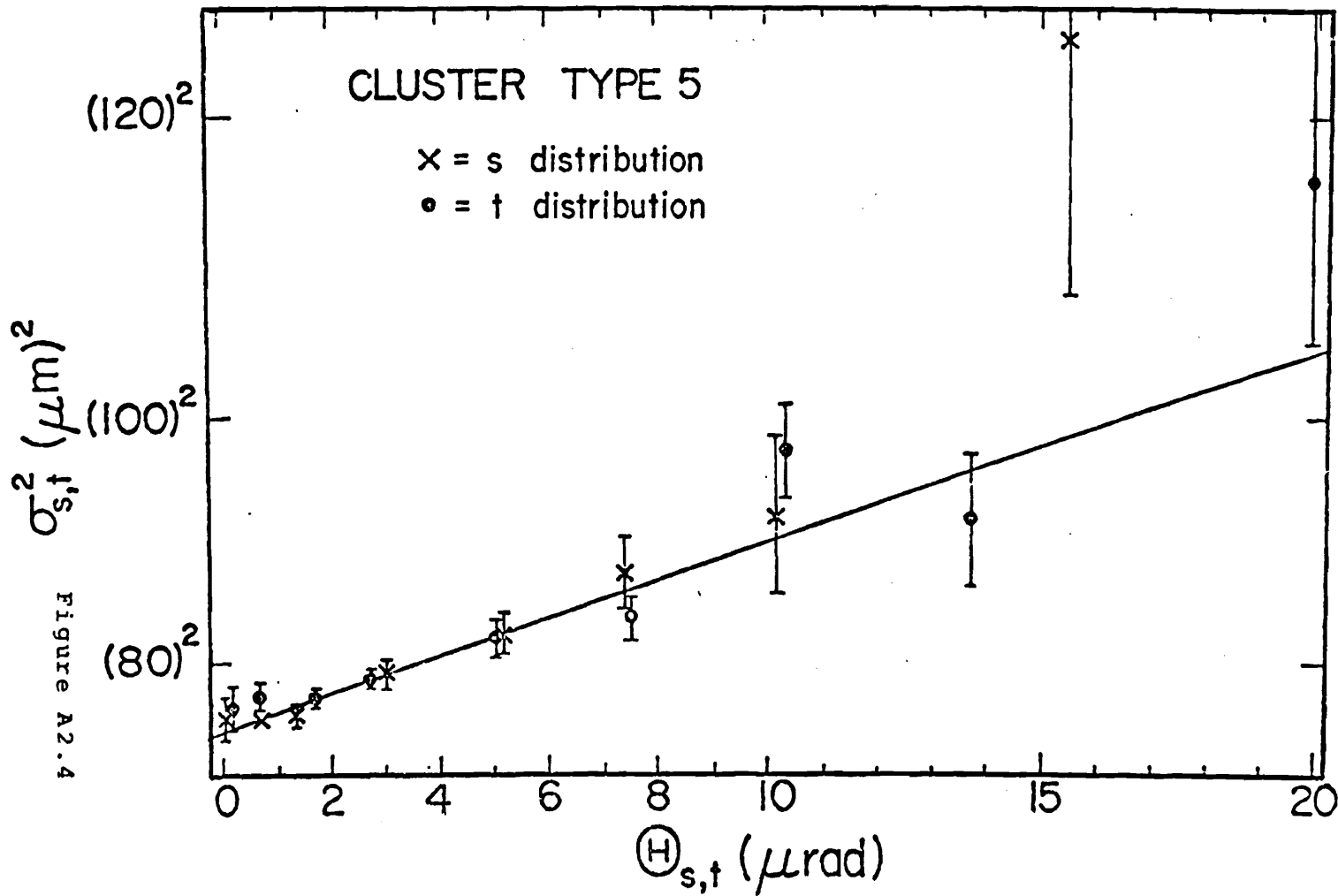


Figure A2.4

Due to a lack of statistics, a mixture of cluster types must be made for this case. Assume the following parameterizations:

$$\sigma_i^2 = a + b\theta_i^2, \quad \text{cluster type 5}$$

$$\sigma_i^2 = a' + b'\theta_i^2, \quad \text{cluster type 6}$$

where $i = x, y, u, v$.

There are two cases for mixing the cluster types.

CASE A: x, y hits are cluster type 6

u, v hits are cluster type 5

Here

$$\sigma_{s,A}^2 = (a+a') + (b'-b)\theta_x^2 + (b/2)(3\theta_x^2 + \theta_y^2)$$

$$\sigma_{t,A}^2 = (a+a') + (b'-b)\theta_y^2 + (b/2)(3\theta_y^2 + \theta_x^2)$$

CASE B: x, y hits are cluster type 5

u, v hits are cluster type 6

Here

$$\sigma_{s,B}^2 = (a+a') + (b-b') \theta_x^2 + (b'/2) (3\theta_x^2 + \theta_y^2)$$

$$\sigma_{t,B}^2 = (a+a') + (b-b') \theta_y^2 + (b'/2) (3\theta_y^2 + \theta_x^2)$$

CASE A is related to CASE B by $a \longleftrightarrow a'$ and $b \longleftrightarrow b'$.

Then

$$\sigma_{s,A}^2 + \sigma_{s,B}^2 = 2(a+a') + (.5)(b+b') \theta_s$$

$$\sigma_{t,A}^2 + \sigma_{t,B}^2 = 2(a+a') + (.5)(b+b') \theta_t$$

These two functions are plotted in Figure A2.5 along with the best fit to the data. This best fit gives

$$(a + a') = (60.47 \mu\text{m} \pm 1.42 \mu\text{m})^2$$

$$(b + b') = (37.32 \mu\text{m} \pm 4.57 \mu\text{m})^2 \times 10^6$$

$$\rho = -.784$$

$$\chi^2/\text{DOF} = 4.04/12$$

Using the results from CASE I, one derives that for cluster type 6 events

$$\sigma_i^2 = (31.0 \pm 2.8)^2 + (28.9 \pm 6.0)^2 (\theta_i - \theta_i^r)^2$$

where $i = x, y$ and the units are as for CASE I.

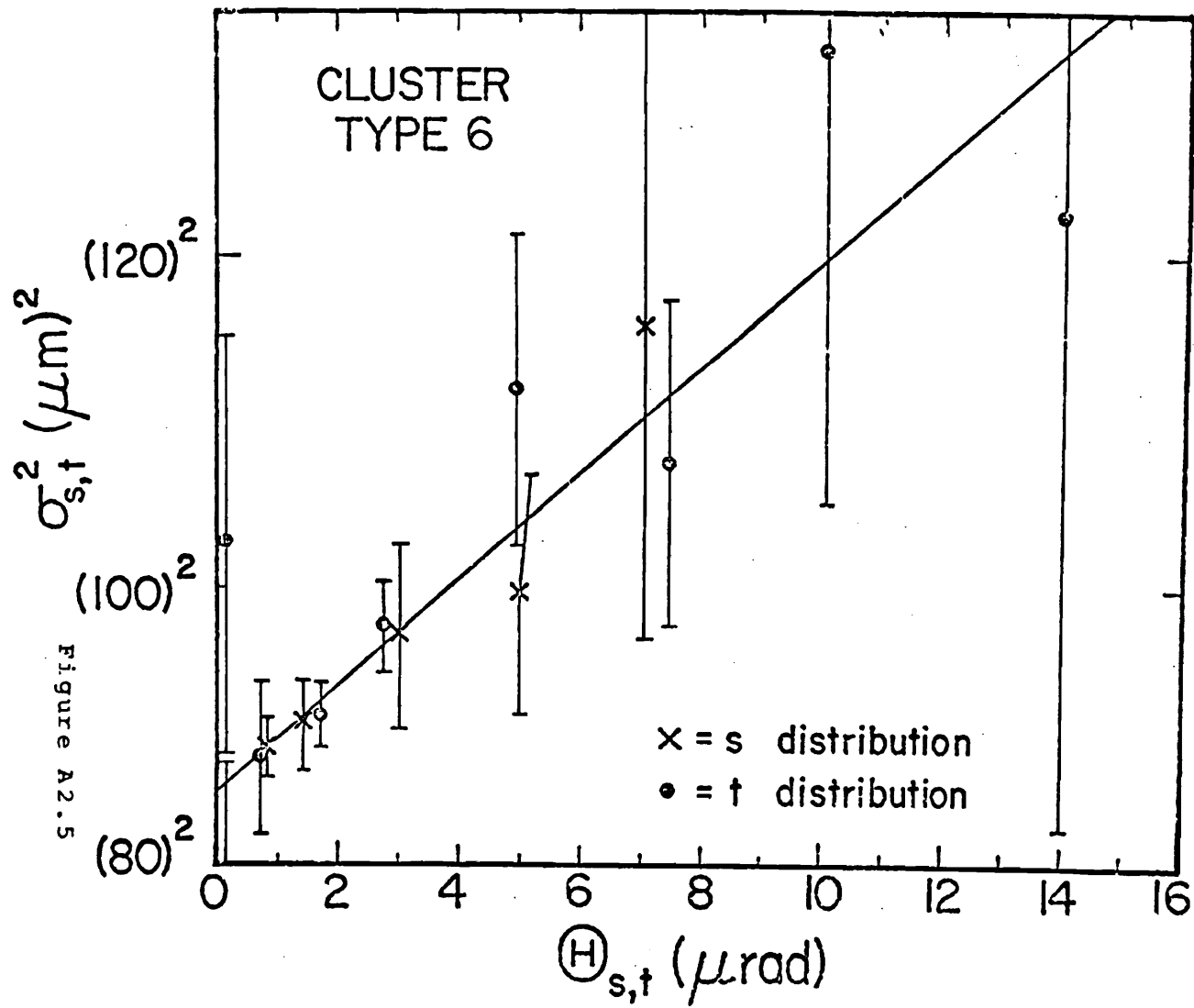


Figure A2.5

APPENDIX III

NUCLEAR TARGET DATA

This appendix presents tables and plots of the differential cross sections, $d\sigma/dt$, for the measured hadron-nucleus reactions. The solid line in the plots is the result of the fit to the data using Eq. 6.6, as presented in Table 6.5.

The data have been corrected only for effects described in Chapter 6. Hence no corrections have been performed for plural nuclear scattering effects, radiative effects, or for inelastic contamination (where the inelastic process involves particle production).

PIPLUS - BE: 175 GEV/C
 UNITS: T: (GEV/C)**2; DSIGMA/DT: MILLIBARNS/((GEV/C)**2)

-T	DSIGMA/DT	ERROR	-T	DSIGMA/DT	ERROR
.0015	3374.	125.	.0805	87.	12.
.0021	2213.	85.	.0927	61.	10.
.0028	1836.	68.	.0970	42.	8.
.0035	1488.	56.	.1014	57.	10.
.0044	1332.	49.	.1060	58.	11.
.0054	1218.	44.	.1106	37.	8.
.0065	1124.	41.	.1153	40.	9.
.0077	1010.	37.	.1201	36.	9.
.0089	960.	34.	.1250	37.	9.
.0103	904.	32.	.1300	23.	7.
.0118	732.	29.	.1351	45.	10.
.0133	674.	26.	.1403	15.	6.
.0150	644.	25.	.1455	35.	8.
.0168	532.	22.	.1509	30.	8.
.0186	504.	21.	.1564	33.	9.
.0206	453.	20.	.1620	18.	6.
.0227	428.	19.	.1677	21.	6.
.0248	372.	18.	.1735	27.	7.
.0271	315.	16.	.1794	9.	4.
.0294	323.	16.	.1853	13.	5.
.0319	257.	15.	.1914	10.	4.
.0344	258.	15.	.1976	18.	6.
.0371	222.	14.	.2039	26.	8.
.0398	205.	14.	.2102	19.	6.
.0426	177.	13.	.2167	9.	4.
.0456	158.	13.	.2233	3.	2.
.0486	147.	12.	.2299	21.	6.
.0518	142.	13.	.2367	8.	4.
.0550	129.	11.	.2435	14.	5.
.0583	101.	10.	.2505	3.	2.
.0618	112.	11.	.2576	5.	3.
.0653	101.	10.	.2647	16.	5.
.0689	78.	10.	.2720	10.	4.
.0726	80.	10.	.2793	8.	4.
.0765	67.	10.	.2868	6.	3.
.0804	94.	12.	.2943	4.	3.
.0844	77.	11.	.3020	4.	3.

KPLUS - BE: 175 GEV/C
 UNITS: T: (GEV/C)**2; DSIGMA/DT: MILLIBARNS/((GEV/C)**2)

-T	DSIGMA/DT	ERROR	-T	DSIGMA/DT	ERROR
.0015	2979.	151.	.0805	57.	13.
.0021	1919.	100.	.0927	60.	13.
.0028	1153.	69.	.0970	43.	11.
.0035	1179.	63.	.1014	27.	9.
.0044	959.	53.	.1060	38.	11.
.0054	920.	49.	.1106	41.	11.
.0065	797.	43.	.1153	25.	9.
.0077	744.	40.	.1201	48.	13.
.0089	672.	37.	.1250	37.	11.
.0103	591.	33.	.1300	40.	14.
.0118	533.	30.	.1351	33.	11.
.0133	554.	30.	.1403	31.	10.
.0150	450.	26.	.1455	27.	9.
.0168	417.	25.	.1509	15.	8.
.0186	385.	24.	.1564	34.	11.
.0206	367.	23.	.1620	22.	9.
.0227	349.	22.	.1677	30.	10.
.0248	289.	20.	.1735	18.	7.
.0271	228.	18.	.1794	21.	8.
.0294	209.	17.	.1853	7.	5.
.0319	206.	17.	.1914	25.	9.
.0344	175.	16.	.1976	11.	6.
.0371	176.	16.	.2039	15.	8.
.0398	164.	16.	.2102	6.	4.
.0426	150.	15.	.2167	10.	6.
.0456	144.	15.	.2233	8.	5.
.0486	93.	12.	.2299	19.	8.
.0518	92.	12.	.2367	9.	5.
.0550	111.	14.	.2435	9.	5.
.0583	83.	12.	.2505	8.	5.
.0618	90.	12.	.2576	9.	5.
.0653	83.	12.	.2647	3.	3.
.0689	85.	13.	.2720	10.	6.
.0726	56.	11.	.2793	7.	5.
.0765	57.	11.	.2868	1.	4.
.0804	59.	12.	.2943	0.	0.
.0844	43.	11.	.3020	6.	5.

PPLUS - BE: 175 GEV/C
 UNITS: T: (GEV/C)**2; DSIGMA/DT: MILLIBARNS/((GEV/C)**2)

-T	DSIGMA/DT	ERROR	-T	DSIGMA/DT	ERROR
.0015	5821.	151.	.0885	125.	14.
.0021	4354.	111.	.0927	96.	12.
.0028	3772.	92.	.0970	101.	12.
.0035	3205.	78.	.1014	89.	12.
.0044	2907.	69.	.1060	79.	12.
.0054	2749.	63.	.1106	66.	11.
.0065	2504.	57.	.1153	70.	11.
.0077	2167.	51.	.1201	94.	13.
.0089	2002.	47.	.1250	71.	12.
.0103	1951.	45.	.1300	57.	10.
.0118	1722.	41.	.1351	81.	13.
.0133	1496.	37.	.1403	66.	11.
.0150	1458.	35.	.1455	54.	10.
.0168	1266.	32.	.1509	54.	11.
.0186	1079.	27.	.1564	47.	10.
.0206	991.	28.	.1620	37.	9.
.0227	839.	25.	.1677	39.	8.
.0248	777.	24.	.1735	24.	4.
.0271	667.	22.	.1794	46.	9.
.0294	582.	21.	.1853	36.	8.
.0319	531.	20.	.1914	35.	8.
.0344	501.	20.	.1974	40.	9.
.0371	437.	19.	.2039	32.	8.
.0398	397.	19.	.2102	31.	7.
.0426	353.	18.	.2167	21.	6.
.0456	336.	17.	.2233	9.	4.
.0486	309.	17.	.2299	16.	5.
.0518	276.	16.	.2367	19.	6.
.0550	240.	15.	.2435	23.	6.
.0583	223.	14.	.2505	26.	6.
.0618	186.	13.	.2576	16.	5.
.0653	177.	13.	.2647	13.	5.
.0689	145.	13.	.2720	9.	4.
.0726	150.	13.	.2793	5.	3.
.0765	158.	14.	.2868	12.	5.
.0804	147.	14.	.2943	10.	4.
.0844	110.	13.	.3020	9.	4.

PIPLUS - C: 175 GEV/C
 UNITS: T: (GEV/C)**2; DSIGMA/DT: MILLIBARNS/((GEV/C)**2)

-T	DSIGMA/DT	ERROR	-T	DSIGMA/DT	ERROR
.0015	6467.	205.	.0885	59.	11.
.0021	4264.	140.	.0927	49.	11.
.0028	3156.	106.	.0970	56.	12.
.0035	2634.	88.	.1014	74.	13.
.0044	2316.	77.	.1060	42.	10.
.0054	1991.	67.	.1106	40.	10.
.0065	1774.	60.	.1153	55.	11.
.0077	1588.	54.	.1201	27.	8.
.0089	1601.	52.	.1250	52.	12.
.0103	1353.	46.	.1300	21.	7.
.0118	1262.	43.	.1351	32.	9.
.0133	1144.	40.	.1403	53.	12.
.0150	1040.	37.	.1455	23.	9.
.0168	965.	35.	.1509	12.	6.
.0186	844.	32.	.1564	24.	9.
.0206	684.	29.	.1620	23.	8.
.0227	577.	26.	.1677	33.	10.
.0248	558.	25.	.1735	27.	9.
.0271	482.	24.	.1794	8.	5.
.0294	422.	22.	.1853	15.	6.
.0319	331.	20.	.1914	11.	5.
.0344	306.	20.	.1974	23.	8.
.0371	272.	19.	.2039	30.	9.
.0398	258.	19.	.2102	12.	5.
.0426	225.	18.	.2167	7.	4.
.0456	154.	15.	.2233	13.	6.
.0486	173.	16.	.2299	16.	7.
.0518	136.	14.	.2367	15.	6.
.0550	105.	12.	.2435	11.	5.
.0583	115.	13.	.2505	3.	3.
.0618	92.	12.	.2576	8.	4.
.0653	94.	12.	.2647	16.	6.
.0689	76.	11.	.2720	8.	5.
.0726	100.	13.	.2793	21.	7.
.0765	88.	14.	.2868	9.	5.
.0804	66.	12.	.2943	10.	6.
.0844	60.	12.	.3020	7.	5.

KPLUS - C: 175 GEV/C
 UNITS: T: (GEV/C)**2; DSIGMA/DT: MILLIBARNS/((GEV/C)**2)

-T	DSIGMA/DT	ERROR	-T	DSIGMA/DT	ERROR
.0015	5960.	253.	.0885	36.	11.
.0021	3604.	161.	.0927	35.	12.
.0028	2483.	119.	.0970	48.	16.
.0035	2109.	99.	.1014	46.	13.
.0044	1625.	81.	.1060	28.	11.
.0054	1526.	74.	.1106	24.	10.
.0065	1462.	69.	.1153	33.	11.
.0077	1273.	61.	.1201	16.	8.
.0089	1080.	54.	.1250	42.	14.
.0103	999.	51.	.1300	38.	12.
.0118	784.	43.	.1351	34.	12.
.0133	877.	44.	.1403	57.	16.
.0150	794.	41.	.1455	21.	10.
.0168	675.	37.	.1509	50.	16.
.0186	633.	35.	.1564	5.	5.
.0206	560.	33.	.1620	21.	9.
.0227	491.	31.	.1677	22.	10.
.0248	435.	29.	.1735	15.	9.
.0271	383.	27.	.1794	18.	9.
.0294	327.	25.	.1853	16.	8.
.0319	294.	24.	.1914	15.	7.
.0344	239.	22.	.1976	29.	11.
.0371	242.	23.	.2039	13.	8.
.0398	205.	21.	.2102	20.	9.
.0426	160.	19.	.2167	7.	5.
.0456	109.	16.	.2233	12.	7.
.0486	159.	19.	.2299	17.	9.
.0518	111.	16.	.2367	8.	6.
.0550	123.	17.	.2435	11.	6.
.0583	116.	16.	.2505	13.	7.
.0618	92.	15.	.2576	4.	4.
.0653	103.	16.	.2647	4.	4.
.0689	60.	13.	.2720	4.	4.
.0726	59.	13.	.2793	13.	7.
.0765	54.	14.	.2868	10.	9.
.0804	63.	15.	.2943	5.	5.
.0844	86.	18.	.3020	0.	0.

PPLUS - C: 175 GEV/C
 UNITS: T: (GEV/C)**2; DSIGMA/DT: MILLIBARNS/((GEV/C)**2)

-T	DSIGMA/DT	ERROR	-T	DSIGMA/DT	ERROR
.0015	9793.	232.	.0885	84.	13.
.0021	7110.	166.	.0927	117.	16.
.0028	5892.	135.	.0970	88.	14.
.0035	5344.	116.	.1014	62.	11.
.0044	4656.	101.	.1060	103.	15.
.0054	4157.	90.	.1106	66.	12.
.0065	3656.	80.	.1153	100.	14.
.0077	3426.	74.	.1201	52.	11.
.0089	3211.	69.	.1250	53.	12.
.0103	2891.	63.	.1300	43.	9.
.0118	2504.	57.	.1351	37.	9.
.0133	2365.	53.	.1403	64.	13.
.0150	2144.	50.	.1455	48.	12.
.0168	1913.	46.	.1509	52.	12.
.0186	1591.	41.	.1564	48.	11.
.0206	1415.	38.	.1620	40.	9.
.0227	1226.	36.	.1677	14.	6.
.0248	1059.	33.	.1735	27.	8.
.0271	924.	30.	.1794	27.	8.
.0294	830.	29.	.1853	30.	8.
.0319	711.	27.	.1914	30.	8.
.0344	564.	25.	.1976	13.	5.
.0371	514.	24.	.2039	33.	9.
.0398	476.	24.	.2102	15.	6.
.0426	387.	22.	.2167	18.	6.
.0456	314.	19.	.2233	13.	5.
.0486	294.	19.	.2299	28.	8.
.0518	227.	16.	.2367	33.	9.
.0550	206.	16.	.2435	20.	6.
.0583	186.	15.	.2505	35.	9.
.0618	160.	14.	.2576	9.	4.
.0653	159.	15.	.2647	7.	4.
.0689	148.	14.	.2720	12.	5.
.0726	137.	15.	.2793	7.	4.
.0765	163.	17.	.2868	15.	6.
.0804	120.	15.	.2943	9.	5.
.0844	112.	15.	.3020	6.	4.

PIPLUS - AL: 175 GEV/C
 UNITS: T: (GEV/C)**2; DSIGMA/DT: MILLIBARNS/((GEV/C)**2)

-T	DSIGMA/DT	ERROR	-T	DSIGMA/DT	ERROR
.0015	26987.	838.	.0890	102.	29.
.0021	15731.	544.	.0933	114.	31.
.0028	10437.	393.	.0976	79.	28.
.0036	9138.	329.	.1021	70.	25.
.0044	7095.	270.	.1066	97.	31.
.0054	6736.	247.	.1112	118.	34.
.0065	5582.	215.	.1160	44.	22.
.0077	4808.	183.	.1208	45.	23.
.0090	4353.	172.	.1257	44.	22.
.0104	3559.	150.	.1307	51.	23.
.0118	2976.	132.	.1359	45.	22.
.0134	2761.	123.	.1411	108.	36.
.0151	2115.	105.	.1464	46.	23.
.0169	1817.	95.	.1518	33.	19.
.0187	1407.	82.	.1574	33.	19.
.0207	1235.	76.	.1630	12.	12.
.0228	927.	65.	.1687	12.	12.
.0250	708.	56.	.1745	36.	21.
.0272	659.	54.	.1804	41.	20.
.0296	492.	47.	.1864	93.	33.
.0321	422.	44.	.1926	0.	0.
.0346	257.	36.	.1988	0.	0.
.0373	232.	34.	.2051	20.	14.
.0400	210.	33.	.2115	13.	13.
.0429	136.	27.	.2180	19.	14.
.0459	172.	31.	.2246	30.	17.
.0489	153.	29.	.2313	43.	19.
.0521	85.	21.	.2381	10.	10.
.0553	106.	24.	.2450	43.	21.
.0587	120.	26.	.2520	30.	17.
.0621	95.	23.	.2591	21.	15.
.0657	145.	30.	.2663	10.	10.
.0693	114.	26.	.2736	18.	13.
.0731	98.	26.	.2810	22.	16.
.0769	68.	23.	.2885	12.	12.
.0809	110.	30.	.2961	11.	11.
.0849	51.	21.	.3038	0.	0.

KPLUS - AL: 175 GEV/C
 UNITS: T: (GEV/C)**2; DSIGMA/DT: MILLIBARNS/((GEV/C)**2)

-T	DSIGMA/DT	ERROR	-T	DSIGMA/DT	ERROR
.0015	25522.	1058.	.0890	116.	41.
.0021	14573.	644.	.0933	59.	30.
.0028	9947.	495.	.0976	134.	48.
.0036	7707.	391.	.1021	90.	37.
.0044	5634.	312.	.1066	16.	16.
.0054	5994.	300.	.1112	33.	24.
.0065	4715.	253.	.1160	93.	42.
.0077	3761.	216.	.1208	58.	33.
.0090	3055.	186.	.1257	38.	27.
.0104	3000.	181.	.1307	52.	36.
.0118	2618.	160.	.1359	76.	38.
.0134	1852.	133.	.1411	41.	29.
.0151	1831.	126.	.1464	78.	39.
.0169	1363.	107.	.1518	37.	24.
.0187	1020.	92.	.1574	19.	19.
.0207	856.	82.	.1630	43.	30.
.0228	824.	80.	.1687	20.	20.
.0250	629.	69.	.1745	41.	29.
.0272	580.	66.	.1804	0.	0.
.0296	343.	53.	.1864	40.	28.
.0321	262.	46.	.1926	37.	26.
.0346	219.	42.	.1988	19.	19.
.0373	168.	38.	.2051	0.	0.
.0400	227.	45.	.2115	0.	0.
.0429	116.	32.	.2180	16.	16.
.0459	75.	27.	.2246	17.	17.
.0489	87.	29.	.2313	14.	14.
.0521	171.	39.	.2381	0.	0.
.0553	95.	30.	.2450	0.	0.
.0587	130.	35.	.2520	0.	0.
.0621	133.	35.	.2591	0.	0.
.0657	72.	27.	.2663	0.	0.
.0693	123.	35.	.2736	31.	22.
.0731	119.	38.	.2810	19.	19.
.0769	77.	32.	.2885	0.	0.
.0809	43.	25.	.2961	0.	0.
.0849	58.	29.	.3038	23.	23.

PPLUS - AL: 175 GEV/C
 UNITS: T: (GEV/C)**2; DSIGMA/DT: MILLIBARNS/((GEV/C)**2)

-T	DSIGMA/DT	ERROR	-T	DSIGMA/DT	ERROR
.0015	35710.	886.	.0890	207.	39.
.0021	23840.	620.	.0933	137.	32.
.0028	19139.	488.	.0976	172.	38.
.0036	16753.	414.	.1021	130.	32.
.0044	13231.	344.	.1066	177.	39.
.0054	11792.	303.	.1112	128.	33.
.0065	10382.	270.	.1160	124.	34.
.0077	9232.	243.	.1208	118.	34.
.0090	7667.	211.	.1257	47.	26.
.0104	6507.	189.	.1307	115.	32.
.0118	6044.	175.	.1359	29.	17.
.0134	4544.	148.	.1411	52.	23.
.0151	3997.	134.	.1464	60.	24.
.0169	3059.	115.	.1518	76.	27.
.0187	2643.	106.	.1574	67.	25.
.0207	2154.	93.	.1630	54.	24.
.0228	1507.	78.	.1687	31.	18.
.0250	1159.	67.	.1745	10.	10.
.0272	1038.	64.	.1804	53.	22.
.0296	744.	54.	.1864	10.	10.
.0321	584.	48.	.1926	48.	21.
.0346	452.	44.	.1988	48.	21.
.0373	382.	42.	.2051	43.	19.
.0400	368.	42.	.2115	33.	19.
.0429	324.	38.	.2180	42.	19.
.0459	328.	40.	.2246	52.	21.
.0489	236.	34.	.2313	30.	15.
.0521	230.	33.	.2381	35.	17.
.0553	203.	31.	.2450	9.	9.
.0587	166.	28.	.2520	26.	15.
.0621	276.	37.	.2591	28.	16.
.0657	236.	35.	.2663	42.	19.
.0693	188.	31.	.2736	8.	8.
.0731	201.	35.	.2810	10.	10.
.0769	172.	34.	.2885	0.	0.
.0809	176.	36.	.2961	19.	14.
.0849	118.	30.	.3038	0.	0.

PIPLUS - CU: 175 GEV/C
 UNITS: T: (GEV/C)**2; DSIGMA/DT: MILLIBARNS/((GEV/C)**2)

-T	DSIGMA/DT	ERROR	-T	DSIGMA/DT	ERROR
.0015	118382.	3307.	.0885	137.	69.
.0021	60055.	2141.	.0927	209.	95.
.0028	44079.	1545.	.0970	169.	76.
.0035	31493.	1199.	.1014	220.	90.
.0044	24841.	984.	.1060	37.	37.
.0054	21209.	852.	.1106	113.	65.
.0065	15699.	701.	.1153	121.	70.
.0077	13002.	607.	.1201	83.	59.
.0089	9931.	500.	.1250	0.	0.
.0103	7636.	429.	.1300	42.	42.
.0118	5042.	336.	.1351	0.	0.
.0133	4402.	302.	.1403	43.	43.
.0150	2677.	233.	.1455	85.	60.
.0168	2148.	203.	.1509	189.	95.
.0186	1489.	166.	.1564	0.	0.
.0206	743.	119.	.1620	49.	49.
.0227	755.	117.	.1677	49.	49.
.0248	307.	72.	.1735	43.	43.
.0271	319.	73.	.1794	40.	40.
.0294	222.	64.	.1853	0.	0.
.0319	309.	73.	.1914	40.	40.
.0344	272.	73.	.1976	81.	58.
.0371	485.	95.	.2039	42.	42.
.0398	271.	72.	.2102	0.	0.
.0426	306.	79.	.2167	114.	66.
.0456	341.	85.	.2233	112.	65.
.0486	322.	81.	.2299	0.	0.
.0518	305.	79.	.2367	38.	38.
.0550	308.	80.	.2435	0.	0.
.0583	328.	82.	.2505	79.	56.
.0618	248.	72.	.2576	0.	0.
.0653	171.	60.	.2647	0.	0.
.0689	121.	54.	.2720	38.	38.
.0726	129.	58.	.2793	0.	0.
.0765	237.	84.	.2868	0.	0.
.0804	126.	63.	.2943	46.	46.
.0844	95.	55.	.3020	0.	0.

XPLUS - CU: 175 GEV/C
 UNITS: T: (GEV/C)**2; DSIGMA/DT: MILLIBARNS/((GEV/C)**2)

-T	DSIGMA/DT	ERROR	-T	DSIGMA/DT	ERROR
.0015	106595.	3982.	.0885	108.	76.
.0021	57242.	2428.	.0927	110.	78.
.0028	38021.	1788.	.0970	0.	0.
.0035	25495.	1334.	.1014	173.	100.
.0044	18851.	1064.	.1060	0.	0.
.0054	15168.	893.	.1106	60.	60.
.0065	11890.	756.	.1153	127.	90.
.0077	9632.	650.	.1201	0.	0.
.0089	6912.	529.	.1250	132.	93.
.0103	5223.	452.	.1300	66.	66.
.0118	3849.	367.	.1351	141.	100.
.0133	3006.	357.	.1403	68.	68.
.0150	2004.	249.	.1455	0.	0.
.0168	1675.	224.	.1509	75.	75.
.0186	1053.	178.	.1564	0.	0.
.0206	803.	149.	.1620	0.	0.
.0227	353.	102.	.1677	0.	0.
.0248	404.	104.	.1735	0.	0.
.0271	270.	90.	.1794	126.	89.
.0294	275.	96.	.1853	0.	0.
.0319	195.	79.	.1914	0.	0.
.0344	197.	74.	.1976	64.	64.
.0371	294.	93.	.2039	66.	66.
.0398	275.	92.	.2102	0.	0.
.0426	161.	72.	.2167	0.	0.
.0456	253.	90.	.2233	0.	0.
.0486	286.	95.	.2299	58.	58.
.0518	192.	79.	.2367	0.	0.
.0550	130.	65.	.2435	0.	0.
.0583	97.	56.	.2505	0.	0.
.0618	65.	46.	.2576	0.	0.
.0653	67.	48.	.2647	0.	0.
.0689	229.	94.	.2720	0.	0.
.0726	203.	91.	.2793	61.	61.
.0765	47.	47.	.2868	14.	83.
.0804	99.	70.	.2943	0.	0.
.0844	0.	0.	.3020	0.	0.

PPLUS - CU: 175 GEV/C
 UNITS: T: (GEV/C)**2; DSIGMA/DT: MILLIBARNS/((GEV/C)**2)

-T	DSIGMA/DT	ERROR	-T	DSIGMA/DT	ERROR
.0015	131897.	3181.	.0885	56.	40.
.0021	83163.	2148.	.0927	200.	76.
.0028	60732.	1651.	.0970	194.	73.
.0035	48548.	1345.	.1014	120.	60.
.0044	38722.	1108.	.1060	214.	81.
.0054	29975.	915.	.1106	124.	62.
.0065	26494.	819.	.1153	165.	74.
.0077	20515.	688.	.1201	68.	48.
.0089	14009.	545.	.1250	110.	74.
.0103	11105.	470.	.1300	103.	60.
.0118	7778.	379.	.1351	147.	73.
.0133	5712.	317.	.1403	71.	50.
.0150	3827.	254.	.1455	140.	70.
.0168	2472.	199.	.1509	78.	55.
.0186	1497.	154.	.1564	0.	0.
.0206	848.	113.	.1620	120.	69.
.0227	803.	110.	.1677	0.	0.
.0248	496.	87.	.1735	35.	35.
.0271	449.	84.	.1794	66.	46.
.0294	350.	73.	.1853	0.	0.
.0319	623.	95.	.1914	33.	33.
.0344	604.	96.	.1976	100.	58.
.0371	588.	98.	.2039	34.	34.
.0398	397.	79.	.2102	0.	0.
.0426	820.	117.	.2167	0.	0.
.0456	626.	102.	.2233	31.	31.
.0486	513.	92.	.2299	0.	0.
.0518	334.	75.	.2367	0.	0.
.0550	489.	91.	.2435	0.	0.
.0583	471.	89.	.2505	0.	0.
.0618	255.	66.	.2576	0.	0.
.0653	280.	70.	.2647	0.	0.
.0689	159.	56.	.2720	31.	31.
.0726	211.	67.	.2793	0.	0.
.0765	121.	54.	.2868	34.	34.
.0804	258.	82.	.2943	38.	38.
.0844	156.	64.	.3020	35.	35.

PIPLUS - SN: 175 GEV/C
 UNITS: T: (GEV/C)**2; DSIGMA/DT: MILLIBARNS/((GEV/C)**2)

-T	DSIGMA/DT	ERROR	-T	DSIGMA/DT	ERROR
.0015	293203.	6323.	.0890	119.	69.
.0021	167807.	4013.	.0933	135.	78.
.0028	103211.	2800.	.0974	44.	44.
.0034	74063.	2139.	.1021	134.	77.
.0044	51085.	1649.	.1066	52.	52.
.0054	36323.	1303.	.1112	160.	92.
.0065	27535.	1105.	.1160	0.	0.
.0077	19739.	878.	.1208	0.	0.
.0090	12201.	671.	.1257	113.	80.
.0104	9039.	557.	.1307	106.	75.
.0118	4123.	365.	.1359	0.	0.
.0134	2611.	271.	.1411	66.	66.
.0151	1489.	214.	.1464	69.	69.
.0169	900.	170.	.1518	125.	88.
.0187	418.	129.	.1574	0.	0.
.0207	521.	135.	.1630	72.	72.
.0228	506.	121.	.1687	129.	91.
.0250	892.	143.	.1745	58.	58.
.0272	784.	135.	.1804	57.	57.
.0294	1145.	171.	.1864	0.	0.
.0321	777.	135.	.1924	56.	56.
.0346	678.	138.	.1988	49.	49.
.0373	614.	125.	.2051	0.	0.
.0400	629.	128.	.2115	0.	0.
.0429	433.	108.	.2180	0.	0.
.0459	675.	144.	.2244	53.	53.
.0489	408.	109.	.2313	0.	0.
.0521	225.	79.	.2381	0.	0.
.0553	345.	100.	.2450	57.	57.
.0587	270.	85.	.2520	0.	0.
.0621	318.	96.	.2591	0.	0.
.0657	90.	52.	.2663	0.	0.
.0693	183.	75.	.2736	94.	66.
.0731	206.	84.	.2810	53.	53.
.0769	213.	87.	.2885	0.	0.
.0809	279.	105.	.2961	0.	0.
.0849	0.	0.	.3038	0.	0.

KPLUS - SN: 175 GEV/C
 UNITS: T: (GEV/C)**2; DSIGMA/DT: MILLIBARNS/((GEV/C)**2)

-T	DSIGMA/DT	ERROR	-T	DSIGMA/DT	ERROR
.0015	292382.	7982.	.0890	64.	64.
.0021	157657.	4037.	.0933	73.	73.
.0028	89927.	3283.	.0974	71.	71.
.0034	60214.	2437.	.1021	145.	102.
.0044	43911.	1923.	.1066	0.	0.
.0054	32085.	1540.	.1112	347.	174.
.0065	23166.	1252.	.1160	0.	0.
.0077	15580.	981.	.1208	169.	119.
.0090	12055.	824.	.1257	0.	0.
.0104	6437.	634.	.1307	173.	122.
.0118	3714.	420.	.1359	87.	87.
.0134	1445.	291.	.1411	108.	108.
.0151	1412.	246.	.1464	112.	112.
.0169	1002.	221.	.1518	203.	143.
.0187	384.	153.	.1574	103.	103.
.0207	512.	142.	.1630	117.	117.
.0228	632.	176.	.1687	105.	105.
.0250	484.	134.	.1745	0.	0.
.0272	825.	176.	.1804	92.	92.
.0294	629.	191.	.1864	0.	0.
.0321	625.	175.	.1924	91.	91.
.0346	448.	135.	.1988	80.	80.
.0373	624.	161.	.2051	0.	0.
.0400	469.	141.	.2115	0.	0.
.0429	352.	125.	.2180	0.	0.
.0459	399.	141.	.2244	0.	0.
.0489	277.	106.	.2313	90.	90.
.0521	365.	129.	.2381	0.	0.
.0553	140.	81.	.2450	0.	0.
.0587	220.	98.	.2520	0.	0.
.0621	469.	148.	.2591	0.	0.
.0657	243.	109.	.2663	75.	75.
.0693	49.	49.	.2736	0.	0.
.0731	56.	56.	.2810	0.	0.
.0769	346.	141.	.2885	0.	0.
.0809	194.	112.	.2961	98.	98.
.0849	291.	145.	.3038	0.	0.

PPLUS - SN: 175 GEV/C
 UNITS: T: (GEV/C)**2; DSIGMA/DT: MILLIBARNS/((GEV/C)**2)

-T	DSIGMA/DT	ERROR	-T	DSIGMA/DT	ERROR
.0015	319263.	6106.	.0890	47.	47.
.0021	199043.	4063.	.0933	342.	114.
.0028	131338.	2914.	.0976	185.	83.
.0034	97976.	2278.	.1021	113.	65.
.0044	73705.	1832.	.1066	130.	75.
.0054	53025.	1445.	.1112	225.	101.
.0065	37091.	1162.	.1160	170.	85.
.0077	24403.	901.	.1208	307.	116.
.0090	16161.	698.	.1257	12.	107.
.0104	9984.	546.	.1307	0.	0.
.0118	5880.	407.	.1359	135.	78.
.0134	3142.	301.	.1411	112.	79.
.0151	1579.	211.	.1464	58.	58.
.0169	1183.	190.	.1518	105.	74.
.0187	1053.	183.	.1574	107.	75.
.0207	1411.	170.	.1630	0.	0.
.0228	1140.	169.	.1687	109.	77.
.0250	1801.	191.	.1745	98.	69.
.0272	1549.	184.	.1804	48.	48.
.0294	1516.	178.	.1864	112.	79.
.0321	1531.	175.	.1926	47.	47.
.0346	1220.	163.	.1988	83.	58.
.0373	918.	156.	.2051	93.	66.
.0400	752.	129.	.2115	138.	79.
.0429	663.	123.	.2180	0.	0.
.0459	492.	113.	.2246	0.	0.
.0489	517.	113.	.2313	0.	0.
.0521	522.	111.	.2381	0.	0.
.0553	316.	88.	.2450	0.	0.
.0587	342.	88.	.2520	0.	0.
.0621	341.	91.	.2591	0.	0.
.0657	252.	80.	.2663	39.	39.
.0693	334.	93.	.2736	0.	0.
.0731	463.	116.	.2810	0.	0.
.0769	90.	52.	.2885	0.	0.
.0809	269.	95.	.2961	0.	0.
.0849	302.	107.	.3038	44.	44.

PIPLUS - PB: 175 GEV/C
 UNITS: T: (GEV/C)**2; DSIGMA/DT: MILLIBARNS/((GEV/C)**2)

-T	DSIGMA/DT	ERROR	-T	DSIGMA/DT	ERROR
.0015	690070.	14568.	.0885	171.	121.
.0021	373660.	9024.	.0927	95.	95.
.0028	208730.	5994.	.0970	95.	95.
.0035	143020.	4456.	.1014	319.	184.
.0044	91314.	3317.	.1060	333.	192.
.0054	56595.	2445.	.1106	108.	108.
.0065	32943.	1678.	.1153	117.	117.
.0077	18935.	1375.	.1201	111.	111.
.0089	11833.	1024.	.1250	465.	232.
.0103	5773.	739.	.1300	114.	114.
.0118	3568.	546.	.1351	0.	0.
.0133	1743.	344.	.1403	115.	115.
.0150	1159.	383.	.1455	0.	0.
.0168	1674.	349.	.1509	126.	126.
.0186	2426.	389.	.1564	134.	134.
.0206	1829.	348.	.1620	0.	0.
.0227	2062.	333.	.1677	0.	0.
.0248	1993.	300.	.1735	0.	0.
.0271	1966.	296.	.1794	256.	181.
.0294	1019.	247.	.1853	0.	0.
.0319	928.	207.	.1914	0.	0.
.0344	571.	214.	.1974	101.	101.
.0371	396.	140.	.2039	0.	0.
.0398	410.	145.	.2102	107.	107.
.0426	444.	157.	.2167	193.	137.
.0456	272.	122.	.2233	0.	0.
.0486	481.	160.	.2299	0.	0.
.0518	345.	141.	.2367	94.	94.
.0550	429.	152.	.2435	106.	106.
.0583	378.	143.	.2505	90.	90.
.0618	403.	152.	.2576	0.	0.
.0653	174.	100.	.2647	0.	0.
.0689	132.	93.	.2720	0.	0.
.0726	223.	129.	.2793	0.	0.
.0765	523.	198.	.2868	119.	119.
.0804	360.	180.	.2943	0.	0.
.0844	90.	90.	.3020	0.	0.

KPLUS - PB: 175 GEV/C
 UNITS: T: (GEV/C)**2; DSIGMA/DT: MILLIBARNS/((GEV/C)**2)

-T	DSIGMA/DT	ERROR	-T	DSIGMA/DT	ERROR
.0015	674398.	18421.	.0885	280.	198.
.0021	358701.	10745.	.0927	155.	155.
.0028	211202.	7344.	.0970	0.	0.
.0035	122969.	5086.	.1014	347.	246.
.0044	78657.	3756.	.1060	544.	314.
.0054	52902.	2879.	.1106	0.	0.
.0065	32541.	2186.	.1153	383.	271.
.0077	17410.	1521.	.1201	544.	314.
.0089	12711.	1262.	.1250	0.	0.
.0103	4278.	956.	.1300	187.	187.
.0118	2634.	575.	.1351	0.	0.
.0133	2206.	569.	.1403	187.	187.
.0150	2060.	425.	.1455	0.	0.
.0168	1414.	426.	.1509	412.	291.
.0186	2257.	472.	.1564	0.	0.
.0204	1865.	381.	.1620	0.	0.
.0227	2389.	471.	.1677	367.	259.
.0248	1479.	331.	.1735	0.	0.
.0271	1221.	358.	.1794	0.	0.
.0294	840.	375.	.1853	160.	160.
.0319	662.	304.	.1914	0.	0.
.0344	398.	178.	.1976	0.	0.
.0371	81.	81.	.2039	0.	0.
.0398	418.	187.	.2102	0.	0.
.0426	453.	203.	.2167	0.	0.
.0456	621.	235.	.2233	0.	0.
.0486	436.	195.	.2299	0.	0.
.0518	470.	210.	.2367	153.	153.
.0550	175.	124.	.2435	173.	173.
.0583	353.	176.	.2505	0.	0.
.0618	94.	94.	.2576	0.	0.
.0653	0.	0.	.2647	0.	0.
.0689	216.	152.	.2720	0.	0.
.0726	0.	0.	.2793	0.	0.
.0765	366.	211.	.2868	0.	0.
.0804	0.	0.	.2943	0.	0.
.0844	146.	146.	.3020	0.	0.

PPLUS - PB: 175 GEV/C
 UNITS: T: (GEV/C)**2; DSIGMA/DT: MILLIBARNS/((GEV/C)**2)

-T	DSIGMA/DT	ERROR	-T	DSIGMA/DT	ERROR
.0015	744506.	14111.	.0885	221.	127.
.0021	416289.	8939.	.0927	326.	163.
.0028	255668.	6271.	.0970	164.	116.
.0035	174645.	4640.	.1014	183.	129.
.0044	111067.	3400.	.1060	382.	191.
.0054	69897.	2513.	.1106	186.	131.
.0065	38732.	1856.	.1153	0.	0.
.0077	23734.	1417.	.1201	0.	0.
.0089	14167.	1026.	.1250	0.	0.
.0103	5749.	757.	.1300	589.	241.
.0118	3517.	584.	.1351	0.	0.
.0133	3582.	548.	.1403	197.	139.
.0150	4258.	535.	.1455	101.	101.
.0168	4459.	510.	.1509	108.	108.
.0186	4437.	509.	.1564	0.	0.
.0204	4700.	438.	.1620	111.	111.
.0227	3690.	425.	.1677	96.	96.
.0248	3402.	393.	.1735	195.	138.
.0271	1744.	298.	.1794	330.	190.
.0294	1068.	228.	.1853	253.	146.
.0319	1065.	233.	.1914	89.	89.
.0344	617.	197.	.1976	0.	0.
.0371	445.	214.	.2039	184.	130.
.0398	572.	159.	.2102	0.	0.
.0426	762.	191.	.2167	166.	117.
.0456	793.	192.	.2233	0.	0.
.0486	1010.	215.	.2299	189.	133.
.0518	741.	191.	.2367	80.	80.
.0550	691.	178.	.2435	0.	0.
.0583	603.	167.	.2505	0.	0.
.0618	346.	131.	.2576	0.	0.
.0653	497.	157.	.2647	0.	0.
.0689	454.	160.	.2720	87.	87.
.0726	320.	143.	.2793	0.	0.
.0765	513.	182.	.2868	102.	102.
.0804	77.	77.	.2943	0.	0.
.0844	231.	133.	.3020	0.	0.

PIMINUS - BE: 175 GEV/C
 UNITS: T: (GEV/C)**2; DSIGMA/DT: MILLIBARNS/((GEV/C)**2)

-T	DSIGMA/DT	ERROR	-T	DSIGMA/DT	ERROR
.0015	3361.	145.	.0894	79.	12.
.0021	2272.	100.	.0936	52.	10.
.0028	1717.	76.	.0980	47.	9.
.0036	1488.	64.	.1025	63.	12.
.0045	1437.	59.	.1070	49.	10.
.0055	1228.	52.	.1117	45.	10.
.0065	1135.	47.	.1164	49.	10.
.0077	974.	42.	.1213	50.	11.
.0090	875.	38.	.1262	40.	9.
.0104	841.	36.	.1313	29.	8.
.0119	725.	32.	.1364	29.	8.
.0135	634.	29.	.1417	39.	10.
.0152	568.	27.	.1470	30.	9.
.0169	537.	26.	.1524	39.	9.
.0188	447.	24.	.1580	22.	7.
.0208	461.	24.	.1636	27.	8.
.0229	416.	22.	.1694	24.	8.
.0251	339.	20.	.1752	16.	6.
.0273	339.	20.	.1812	5.	4.
.0297	289.	18.	.1872	18.	6.
.0322	283.	18.	.1933	23.	8.
.0348	252.	18.	.1996	22.	8.
.0374	208.	16.	.2059	13.	6.
.0402	195.	16.	.2123	17.	6.
.0431	182.	16.	.2189	15.	6.
.0460	158.	15.	.2255	8.	5.
.0491	134.	14.	.2322	5.	4.
.0523	124.	13.	.2391	2.	2.
.0555	122.	13.	.2460	8.	5.
.0589	121.	13.	.2530	3.	3.
.0624	104.	12.	.2601	15.	7.
.0659	108.	12.	.2674	13.	6.
.0696	89.	12.	.2747	11.	5.
.0734	87.	12.	.2821	6.	4.
.0772	61.	10.	.2896	9.	5.
.0812	66.	11.	.2973	10.	6.
.0852	73.	12.	.3050	9.	5.

KMINUS - BE: 175 GEV/C
 UNITS: T: (GEV/C)**2; DSIGMA/DT: MILLIBARNS/((GEV/C)**2)

-T	DSIGMA/DT	ERROR	-T	DSIGMA/DT	ERROR
.0015	3726.	219.	.0894	59.	16.
.0021	2192.	145.	.0936	51.	15.
.0028	1574.	108.	.0980	48.	14.
.0036	1167.	84.	.1025	52.	16.
.0045	1161.	78.	.1070	61.	17.
.0055	911.	66.	.1117	28.	12.
.0065	857.	61.	.1164	38.	13.
.0077	801.	56.	.1213	26.	12.
.0090	691.	51.	.1262	32.	12.
.0104	645.	47.	.1313	45.	14.
.0119	611.	44.	.1364	29.	12.
.0135	536.	40.	.1417	20.	10.
.0152	437.	35.	.1470	30.	13.
.0169	419.	34.	.1524	10.	7.
.0188	457.	35.	.1580	11.	8.
.0208	380.	32.	.1636	25.	11.
.0229	304.	28.	.1694	26.	12.
.0251	301.	28.	.1752	11.	8.
.0273	252.	25.	.1812	17.	10.
.0297	241.	25.	.1872	10.	7.
.0322	181.	22.	.1933	17.	10.
.0348	158.	21.	.1996	30.	13.
.0374	142.	20.	.2059	18.	10.
.0402	183.	23.	.2123	32.	13.
.0431	143.	21.	.2189	11.	8.
.0460	148.	21.	.2255	36.	15.
.0491	113.	19.	.2322	0.	0.
.0523	130.	20.	.2391	10.	7.
.0555	145.	21.	.2460	6.	6.
.0589	94.	17.	.2530	7.	7.
.0624	101.	18.	.2601	14.	10.
.0659	46.	12.	.2674	17.	10.
.0696	85.	17.	.2747	12.	8.
.0734	73.	17.	.2821	0.	0.
.0772	75.	17.	.2896	6.	6.
.0812	47.	14.	.2973	7.	7.
.0852	49.	15.	.3050	35.	15.

PIMINUS - BE: 175 GEV/C
 UNITS: T: (GEV/C)**2; DSIGMA/DT: MILLIBARNS/((GEV/C)**2)

-T	DSIGMA/DT	ERROR	-T	DSIGMA/DT	ERROR
.0015	6778.	804.	.0894	96.	56.
.0021	5189.	605.	.0936	96.	56.
.0028	3340.	427.	.0980	120.	60.
.0036	3033.	372.	.1025	289.	102.
.0045	3216.	358.	.1070	178.	80.
.0055	2530.	301.	.1117	0.	0.
.0065	2264.	271.	.1164	0.	0.
.0077	2202.	256.	.1213	120.	69.
.0090	2220.	247.	.1262	0.	0.
.0104	1786.	214.	.1313	34.	34.
.0119	1589.	196.	.1364	0.	0.
.0135	1689.	196.	.1417	0.	0.
.0152	1231.	165.	.1470	46.	46.
.0169	1136.	155.	.1524	37.	37.
.0188	1155.	154.	.1580	41.	41.
.0208	919.	136.	.1636	38.	38.
.0229	761.	122.	.1694	40.	40.
.0251	794.	124.	.1752	0.	0.
.0273	810.	125.	.1812	43.	43.
.0297	584.	107.	.1872	0.	0.
.0322	577.	107.	.1933	44.	44.
.0348	453.	77.	.1994	45.	45.
.0374	493.	103.	.2059	0.	0.
.0402	513.	107.	.2123	0.	0.
.0431	322.	86.	.2189	0.	0.
.0460	490.	107.	.2255	46.	46.
.0491	255.	77.	.2322	0.	0.
.0523	368.	92.	.2391	40.	40.
.0555	297.	82.	.2460	47.	47.
.0589	160.	61.	.2530	53.	53.
.0624	272.	82.	.2601	0.	0.
.0659	70.	40.	.2674	0.	0.
.0696	242.	81.	.2747	0.	0.
.0734	232.	82.	.2821	0.	0.
.0772	89.	51.	.2896	0.	0.
.0812	97.	56.	.2973	0.	0.
.0852	170.	76.	.3050	0.	0.

PIMINUS - C: 175 GEV/C
 UNITS: T: (GEV/C)**2; DSIGMA/DT: MILLIBARNS/((GEV/C)**2)

-T	DSIGMA/DT	ERROR	-T	DSIGMA/DT	ERROR
.0015	6720.	289.	.0894	55.	15.
.0021	4094.	192.	.0936	79.	19.
.0028	3179.	148.	.0980	61.	16.
.0036	2693.	124.	.1025	50.	16.
.0045	2176.	105.	.1070	46.	14.
.0055	1923.	92.	.1117	56.	15.
.0065	1854.	86.	.1164	62.	16.
.0077	1624.	77.	.1213	24.	10.
.0090	1616.	74.	.1262	35.	12.
.0104	1320.	64.	.1313	50.	15.
.0119	1250.	61.	.1364	36.	13.
.0135	1135.	57.	.1417	9.	6.
.0152	1007.	52.	.1470	14.	8.
.0169	945.	49.	.1524	51.	15.
.0188	759.	44.	.1580	52.	15.
.0208	588.	38.	.1636	45.	15.
.0229	671.	40.	.1694	16.	9.
.0251	524.	36.	.1752	22.	10.
.0273	469.	33.	.1812	4.	4.
.0297	397.	31.	.1872	32.	13.
.0322	376.	30.	.1933	22.	11.
.0348	298.	27.	.1994	25.	11.
.0374	308.	28.	.2059	21.	10.
.0402	275.	27.	.2123	32.	13.
.0431	214.	24.	.2189	16.	9.
.0460	171.	22.	.2255	5.	5.
.0491	172.	22.	.2322	16.	9.
.0523	172.	22.	.2391	12.	8.
.0555	127.	19.	.2460	5.	5.
.0589	113.	18.	.2530	35.	14.
.0624	104.	18.	.2601	26.	13.
.0659	81.	16.	.2674	10.	7.
.0696	88.	16.	.2747	6.	6.
.0734	61.	14.	.2821	6.	6.
.0772	73.	16.	.2896	12.	9.
.0812	60.	15.	.2973	12.	9.
.0852	60.	16.	.3050	0.	0.

KMINUS - C: 175 GEV/C
 UNITS: T: (GEV/C)**2; DSIGMA/DT: MILLIBARNS/((GEV/C)**2)

-T	DSIGMA/DT	ERROR	-T	DSIGMA/DT	ERROR
.0015	7503.	444.	.0094	44.	20.
.0021	3777.	274.	.0936	39.	19.
.0028	2629.	202.	.0980	78.	28.
.0036	2096.	163.	.1025	30.	17.
.0045	1806.	140.	.1070	10.	10.
.0055	1643.	127.	.1117	29.	17.
.0065	1484.	115.	.1164	28.	16.
.0077	1409.	107.	.1213	36.	18.
.0090	1240.	98.	.1262	49.	22.
.0104	966.	83.	.1313	30.	18.
.0119	951.	80.	.1364	10.	10.
.0135	891.	75.	.1417	31.	18.
.0152	755.	67.	.1470	10.	10.
.0169	523.	55.	.1524	10.	10.
.0188	568.	56.	.1580	23.	16.
.0208	509.	53.	.1636	11.	11.
.0229	404.	47.	.1694	24.	17.
.0251	449.	49.	.1752	10.	10.
.0273	328.	42.	.1812	38.	19.
.0297	356.	43.	.1872	12.	12.
.0322	276.	39.	.1933	0.	0.
.0348	251.	38.	.1996	0.	0.
.0374	208.	41.	.2059	46.	23.
.0402	195.	34.	.2123	12.	12.
.0431	165.	32.	.2189	0.	0.
.0460	124.	28.	.2255	20.	14.
.0491	89.	24.	.2322	12.	12.
.0523	105.	26.	.2391	0.	0.
.0555	158.	32.	.2460	24.	17.
.0589	82.	23.	.2530	13.	13.
.0624	102.	26.	.2601	0.	0.
.0659	107.	27.	.2674	0.	0.
.0696	50.	19.	.2747	0.	0.
.0734	68.	23.	.2821	0.	0.
.0772	98.	28.	.2896	40.	23.
.0812	53.	22.	.2973	0.	0.
.0852	76.	27.	.3050	13.	13.

KMINUS - C: 175 GEV/C
 UNITS: T: (GEV/C)**2; DSIGMA/DT: MILLIBARNS/((GEV/C)**2)

-T	DSIGMA/DT	ERROR	-T	DSIGMA/DT	ERROR
.0015	9982.	1397.	.0894	197.	114.
.0021	9520.	1170.	.0936	147.	104.
.0028	5761.	804.	.0980	147.	104.
.0036	5239.	702.	.1025	76.	76.
.0045	4102.	582.	.1070	153.	108.
.0055	4976.	605.	.1117	72.	72.
.0065	3962.	512.	.1164	0.	0.
.0077	4565.	527.	.1213	67.	47.
.0090	2318.	362.	.1262	74.	74.
.0104	2948.	394.	.1313	76.	76.
.0119	2129.	394.	.1364	76.	76.
.0135	2435.	338.	.1417	0.	0.
.0152	1941.	297.	.1470	79.	79.
.0169	1467.	252.	.1524	0.	0.
.0188	1563.	257.	.1580	87.	87.
.0208	1365.	238.	.1636	84.	84.
.0229	770.	177.	.1694	88.	88.
.0251	1287.	227.	.1752	0.	0.
.0273	1152.	214.	.1812	72.	72.
.0297	978.	187.	.1872	0.	0.
.0322	692.	168.	.1933	0.	0.
.0348	635.	164.	.1996	84.	84.
.0374	441.	140.	.2059	87.	87.
.0402	457.	144.	.2123	0.	0.
.0431	138.	80.	.2189	92.	92.
.0460	279.	114.	.2255	0.	0.
.0491	478.	151.	.2322	0.	0.
.0523	418.	139.	.2391	195.	138.
.0555	190.	95.	.2460	0.	0.
.0589	190.	95.	.2530	0.	0.
.0624	51.	51.	.2601	0.	0.
.0659	50.	50.	.2674	0.	0.
.0696	47.	47.	.2747	0.	0.
.0734	170.	98.	.2821	0.	0.
.0772	0.	0.	.2896	0.	0.
.0812	200.	115.	.2973	0.	0.
.0852	143.	101.	.3050	0.	0.

PIMINUS - AL: 175 GEV/C
 UNITS: T: (GEV/C)**2; DSIGMA/DT: MILLIBARNS/((GEV/C)**2)

-T	DSIGMA/DT	ERROR	-T	DSIGMA/DT	ERROR
.0015	27309.	1251.	.0894	58.	34.
.0021	15009.	790.	.0936	55.	32.
.0028	12391.	617.	.0980	18.	18.
.0034	8826.	475.	.1025	114.	51.
.0045	7728.	414.	.1070	83.	42.
.0055	6065.	347.	.1117	83.	41.
.0065	5472.	312.	.1164	41.	29.
.0077	4252.	264.	.1213	102.	46.
.0090	4265.	255.	.1262	82.	41.
.0104	3885.	235.	.1313	41.	29.
.0119	2958.	200.	.1364	68.	39.
.0135	2348.	175.	.1417	45.	32.
.0152	2322.	170.	.1470	80.	40.
.0169	1654.	142.	.1524	84.	42.
.0188	1288.	125.	.1580	118.	53.
.0208	1106.	118.	.1636	42.	30.
.0229	860.	99.	.1694	66.	38.
.0251	836.	98.	.1752	22.	22.
.0273	678.	87.	.1812	0.	0.
.0297	433.	69.	.1872	0.	0.
.0322	516.	76.	.1933	0.	0.
.0348	370.	65.	.1996	24.	24.
.0374	261.	56.	.2059	24.	24.
.0402	234.	54.	.2123	0.	0.
.0431	138.	42.	.2189	25.	25.
.0460	261.	58.	.2255	0.	0.
.0491	122.	41.	.2322	26.	26.
.0523	178.	48.	.2391	24.	24.
.0555	51.	26.	.2460	51.	34.
.0589	78.	32.	.2530	55.	39.
.0624	125.	42.	.2601	25.	25.
.0659	41.	24.	.2674	30.	30.
.0696	58.	29.	.2747	0.	0.
.0734	80.	36.	.2821	0.	0.
.0772	66.	33.	.2896	0.	0.
.0812	69.	35.	.2973	0.	0.
.0852	35.	25.	.3050	0.	0.

KMINUS - AL: 175 GEV/C
 UNITS: T: (GEV/C)**2; DSIGMA/DT: MILLIBARNS/((GEV/C)**2)

-T	DSIGMA/DT	ERROR	-T	DSIGMA/DT	ERROR
.0015	28623.	1910.	.0894	91.	64.
.0021	15340.	1201.	.0936	130.	75.
.0028	9247.	823.	.0980	84.	59.
.0036	8135.	697.	.1025	107.	75.
.0045	6291.	568.	.1070	49.	49.
.0055	5388.	496.	.1117	0.	0.
.0065	4670.	440.	.1164	48.	48.
.0077	3724.	376.	.1213	96.	68.
.0090	4034.	382.	.1262	96.	68.
.0104	2848.	309.	.1313	49.	49.
.0119	2265.	269.	.1364	0.	0.
.0135	2103.	254.	.1417	0.	0.
.0152	1785.	229.	.1470	94.	64.
.0169	1398.	200.	.1524	49.	49.
.0198	1349.	193.	.1580	55.	55.
.0208	1151.	178.	.1636	49.	49.
.0229	825.	149.	.1694	52.	52.
.0251	759.	141.	.1752	0.	0.
.0273	574.	122.	.1812	56.	56.
.0297	546.	119.	.1872	58.	58.
.0322	448.	109.	.1933	0.	0.
.0348	298.	90.	.1996	114.	81.
.0374	167.	68.	.2059	0.	0.
.0402	145.	63.	.2123	0.	0.
.0431	176.	72.	.2189	0.	0.
.0460	184.	75.	.2255	40.	60.
.0491	150.	67.	.2322	124.	88.
.0523	0.	0.	.2391	0.	0.
.0555	30.	30.	.2460	0.	0.
.0589	153.	68.	.2530	0.	0.
.0624	163.	73.	.2601	0.	0.
.0659	64.	45.	.2674	0.	0.
.0696	68.	48.	.2747	0.	0.
.0734	38.	38.	.2821	0.	0.
.0772	155.	78.	.2896	0.	0.
.0812	41.	41.	.2973	0.	0.
.0852	0.	0.	.3050	63.	63.

PIMINUS - AL: 175 GEV/C
 UNITS: T: (GEV/C)**2; DSIGMA/DT: MILLIBARNS/((GEV/C)**2)

-T	DSIGMA/DT	ERROR	-T	DSIGMA/DT	ERROR
.0015	27608.	4939.	.0894	303.	303.
.0021	19777.	3667.	.0936	0.	0.
.0028	13346.	2555.	.0980	840.	485.
.0036	11502.	2150.	.1025	0.	0.
.0045	17761.	2472.	.1070	0.	0.
.0055	13962.	2059.	.1117	324.	324.
.0065	11810.	1801.	.1164	0.	0.
.0077	8879.	1501.	.1213	0.	0.
.0090	9014.	1462.	.1262	0.	0.
.0104	5782.	1134.	.1313	325.	325.
.0119	5920.	1119.	.1364	0.	0.
.0135	4646.	969.	.1417	0.	0.
.0152	2824.	764.	.1470	0.	0.
.0169	1904.	602.	.1524	0.	0.
.0188	1125.	459.	.1580	0.	0.
.0208	2195.	634.	.1636	0.	0.
.0229	713.	357.	.1694	0.	0.
.0251	1223.	462.	.1752	0.	0.
.0273	1392.	492.	.1812	0.	0.
.0297	521.	301.	.1872	0.	0.
.0322	352.	249.	.1933	0.	0.
.0348	362.	256.	.1996	0.	0.
.0374	186.	186.	.2059	0.	0.
.0402	193.	193.	.2123	0.	0.
.0431	589.	340.	.2189	0.	0.
.0460	204.	204.	.2255	0.	0.
.0491	201.	201.	.2322	0.	0.
.0523	0.	0.	.2391	0.	0.
.0555	0.	0.	.2460	0.	0.
.0589	0.	0.	.2530	0.	0.
.0624	218.	218.	.2601	0.	0.
.0659	0.	0.	.2674	0.	0.
.0696	228.	228.	.2747	0.	0.
.0734	0.	0.	.2821	0.	0.
.0772	259.	259.	.2896	0.	0.
.0812	271.	271.	.2973	0.	0.
.0852	0.	0.	.3050	0.	0.

PIMINUS - CU: 175 GEV/C
 UNITS: T: (GEV/C)**2; DSIGMA/DT: MILLIBARNS/((GEV/C)**2)

-T	DSIGMA/DT	ERROR	-T	DSIGMA/DT	ERROR
.0015	102959.	3467.	.0894	123.	71.
.0021	61994.	2306.	.0936	181.	81.
.0028	41773.	1657.	.0980	79.	56.
.0036	30248.	1273.	.1025	125.	72.
.0045	24696.	1082.	.1070	81.	57.
.0055	18799.	888.	.1117	76.	54.
.0065	15354.	760.	.1164	0.	0.
.0077	11872.	642.	.1213	155.	77.
.0090	9220.	538.	.1262	78.	55.
.0104	7276.	462.	.1313	40.	40.
.0119	5397.	387.	.1364	42.	42.
.0135	4287.	335.	.1417	97.	68.
.0152	2629.	263.	.1470	136.	78.
.0169	1820.	207.	.1524	150.	87.
.0188	1245.	170.	.1580	0.	0.
.0208	859.	140.	.1636	50.	50.
.0229	528.	118.	.1694	134.	77.
.0251	679.	128.	.1752	47.	47.
.0273	275.	81.	.1812	139.	80.
.0297	214.	73.	.1872	0.	0.
.0322	285.	79.	.1933	86.	68.
.0348	327.	87.	.1996	44.	44.
.0374	328.	88.	.2059	0.	0.
.0402	221.	80.	.2123	0.	0.
.0431	230.	77.	.2189	0.	0.
.0460	242.	76.	.2255	51.	51.
.0491	459.	113.	.2322	0.	0.
.0523	266.	84.	.2391	0.	0.
.0555	294.	89.	.2460	51.	51.
.0589	261.	83.	.2530	50.	50.
.0624	158.	64.	.2601	49.	49.
.0659	52.	37.	.2674	50.	50.
.0696	147.	66.	.2747	136.	79.
.0734	152.	68.	.2821	0.	0.
.0772	140.	70.	.2896	0.	0.
.0812	186.	83.	.2973	0.	0.
.0852	114.	66.	.3050	0.	0.

KMINUS - CU: 175 GEV/C
 UNITS: T: (GEV/C)**2; DSIGMA/DT: MILLIBARNS/((GEV/C)**2)

-T	DSIGMA/DT	ERROR	-T	DSIGMA/DT	ERROR
.0015	105076.	5074.	.0894	460.	206.
.0021	65126.	3494.	.0936	163.	115.
.0028	35305.	2302.	.0980	0.	0.
.0036	29167.	1867.	.1025	0.	0.
.0045	21974.	1519.	.1070	182.	129.
.0055	16432.	1234.	.1117	171.	121.
.0065	11293.	968.	.1164	97.	97.
.0077	10672.	892.	.1213	0.	0.
.0090	6890.	718.	.1262	88.	88.
.0104	4986.	574.	.1313	0.	0.
.0119	4420.	526.	.1364	190.	134.
.0135	3304.	449.	.1417	0.	0.
.0152	1981.	330.	.1470	0.	0.
.0169	1870.	318.	.1524	0.	0.
.0188	1118.	238.	.1580	0.	0.
.0208	939.	215.	.1636	112.	112.
.0229	391.	138.	.1694	0.	0.
.0251	245.	110.	.1752	0.	0.
.0273	330.	125.	.1812	0.	0.
.0297	238.	107.	.1872	0.	0.
.0322	197.	99.	.1933	0.	0.
.0348	0.	0.	.1996	0.	0.
.0374	264.	118.	.2059	0.	0.
.0402	218.	109.	.2123	0.	0.
.0431	230.	115.	.2189	0.	0.
.0460	217.	109.	.2255	115.	115.
.0491	114.	81.	.2322	0.	0.
.0523	419.	159.	.2391	0.	0.
.0555	420.	159.	.2460	0.	0.
.0589	59.	59.	.2530	0.	0.
.0624	118.	84.	.2601	0.	0.
.0659	59.	59.	.2674	0.	0.
.0696	331.	148.	.2747	0.	0.
.0734	137.	97.	.2821	111.	111.
.0772	78.	78.	.2896	0.	0.
.0812	0.	0.	.2973	0.	0.
.0852	171.	121.	.3050	0.	0.

PHINUS - CU: 175 GEV/C
 UNITS: T: (GEV/C)**2; DSIGMA/DT: MILLIBARNS/((GEV/C)**2)

-T	DSIGMA/DT	ERROR	-T	DSIGMA/DT	ERROR
.0015	132141.	15608.	.0894	0.	0.
.0021	81712.	10815.	.0936	611.	611.
.0028	54109.	7745.	.0980	0.	0.
.0036	45731.	6460.	.1025	707.	707.
.0045	50348.	6221.	.1070	0.	0.
.0055	31833.	4862.	.1117	0.	0.
.0065	20698.	3550.	.1164	0.	0.
.0077	19049.	3267.	.1213	0.	0.
.0090	16090.	2890.	.1262	0.	0.
.0104	13589.	2568.	.1313	0.	0.
.0119	10121.	2158.	.1364	0.	0.
.0135	4816.	1548.	.1417	0.	0.
.0152	3452.	1508.	.1470	0.	0.
.0169	1555.	777.	.1524	0.	0.
.0188	1145.	661.	.1580	0.	0.
.0208	2227.	909.	.1636	0.	0.
.0229	734.	519.	.1694	0.	0.
.0251	736.	520.	.1752	0.	0.
.0273	1416.	708.	.1812	0.	0.
.0297	716.	506.	.1872	0.	0.
.0322	0.	0.	.1933	0.	0.
.0348	1579.	790.	.1996	747.	747.
.0374	1586.	793.	.2059	0.	0.
.0402	1639.	820.	.2123	0.	0.
.0431	864.	611.	.2189	0.	0.
.0460	816.	577.	.2255	0.	0.
.0491	1286.	743.	.2322	0.	0.
.0523	900.	636.	.2391	0.	0.
.0555	902.	638.	.2460	0.	0.
.0589	442.	442.	.2530	851.	851.
.0624	444.	444.	.2601	0.	0.
.0659	441.	441.	.2674	0.	0.
.0696	497.	497.	.2747	0.	0.
.0734	0.	0.	.2821	0.	0.
.0772	0.	0.	.2896	0.	0.
.0812	0.	0.	.2973	0.	0.
.0852	0.	0.	.3050	0.	0.

PIMINUS - SN: 175 GEV/C
 UNITS: T: (GEV/C)**2; DSIGMA/DT: MILLIBARNS/((GEV/C)**2)

-T	DSIGMA/DT	ERROR	-T	DSIGMA/DT	ERROR
.0015	256826.	6809.	.0894	109.	77.
.0021	148449.	4343.	.0936	54.	54.
.0028	96900.	3060.	.0980	160.	92.
.0036	64658.	2251.	.1025	122.	86.
.0045	48959.	1835.	.1070	353.	144.
.0055	35809.	1488.	.1117	0.	0.
.0065	24464.	1162.	.1164	58.	58.
.0077	17672.	954.	.1213	108.	77.
.0090	11059.	721.	.1262	66.	66.
.0104	6760.	548.	.1313	183.	106.
.0119	5624.	482.	.1364	128.	91.
.0135	3192.	366.	.1417	220.	127.
.0152	1559.	254.	.1470	60.	60.
.0169	850.	191.	.1524	0.	0.
.0188	439.	165.	.1580	123.	87.
.0208	714.	169.	.1636	0.	0.
.0229	493.	142.	.1694	184.	106.
.0251	708.	175.	.1752	60.	60.
.0273	1103.	192.	.1812	124.	88.
.0297	745.	159.	.1872	213.	123.
.0322	1054.	189.	.1933	124.	88.
.0348	761.	166.	.1996	65.	65.
.0374	683.	157.	.2059	59.	59.
.0402	551.	147.	.2123	0.	0.
.0431	463.	134.	.2189	69.	69.
.0460	531.	142.	.2255	0.	0.
.0491	219.	116.	.2322	0.	0.
.0523	154.	77.	.2391	0.	0.
.0555	402.	127.	.2460	0.	0.
.0589	346.	115.	.2530	68.	68.
.0624	360.	120.	.2601	0.	0.
.0659	249.	102.	.2674	0.	0.
.0696	268.	110.	.2747	89.	89.
.0734	87.	62.	.2821	0.	0.
.0772	261.	117.	.2896	0.	0.
.0812	160.	93.	.2973	0.	0.
.0852	54.	54.	.3050	0.	0.

KMINUS - SN: 175 GEV/C
 UNITS: T: (GEV/C)**2; DSIGMA/DT: MILLIBARNS/((GEV/C)**2)

-T	DSIGMA/DT	ERROR	-T	DSIGMA/DT	ERROR
.0015	268684.	10080.	.0894	123.	123.
.0021	132849.	6085.	.0936	0.	0.
.0028	90089.	4429.	.0980	239.	169.
.0036	62246.	3268.	.1025	273.	193.
.0045	48677.	2682.	.1070	0.	0.
.0055	31660.	2059.	.1117	0.	0.
.0065	20862.	1598.	.1164	130.	130.
.0077	16553.	1343.	.1213	122.	122.
.0090	9674.	1067.	.1262	0.	0.
.0104	6779.	824.	.1313	0.	0.
.0119	4335.	655.	.1364	0.	0.
.0135	2907.	548.	.1417	0.	0.
.0152	1637.	376.	.1470	405.	234.
.0169	590.	223.	.1524	264.	186.
.0188	488.	199.	.1580	0.	0.
.0208	700.	233.	.1636	0.	0.
.0229	227.	131.	.1694	0.	0.
.0251	822.	248.	.1752	0.	0.
.0273	525.	199.	.1812	0.	0.
.0297	684.	228.	.1872	0.	0.
.0322	1069.	286.	.1933	139.	139.
.0348	244.	141.	.1996	0.	0.
.0374	889.	268.	.2059	0.	0.
.0402	619.	234.	.2123	0.	0.
.0431	173.	122.	.2189	0.	0.
.0460	426.	191.	.2255	0.	0.
.0491	175.	123.	.2322	0.	0.
.0523	173.	122.	.2391	0.	0.
.0555	180.	126.	.2460	171.	171.
.0589	86.	86.	.2530	0.	0.
.0624	0.	0.	.2601	0.	0.
.0659	279.	161.	.2674	0.	0.
.0696	201.	142.	.2747	0.	0.
.0734	196.	138.	.2821	241.	241.
.0772	234.	166.	.2896	0.	0.
.0812	480.	240.	.2973	0.	0.
.0852	121.	121.	.3050	0.	0.

PHINUS - SM: 175 GEV/C
 UNITS: T: (GEV/C)**2; DSIGMA/DT: MILLIBARNS/((GEV/C)**2)

-T	DSIGMA/DT	ERROR	-T	DSIGMA/DT	ERROR
.0015	303116.	28925.	.0894	0.	0.
.0021	158153.	18627.	.0936	0.	0.
.0028	131790.	15050.	.0980	851.	851.
.0036	97535.	10953.	.1025	0.	0.
.0045	66648.	8511.	.1070	0.	0.
.0055	61841.	7771.	.1117	895.	895.
.0065	37848.	5642.	.1164	0.	0.
.0077	29422.	4773.	.1213	0.	0.
.0090	11537.	2884.	.1262	0.	0.
.0104	10912.	2728.	.1313	0.	0.
.0119	5942.	1981.	.1364	0.	0.
.0135	1859.	1073.	.1417	0.	0.
.0152	0.	0.	.1470	0.	0.
.0169	1199.	848.	.1524	0.	0.
.0188	1157.	818.	.1580	0.	0.
.0208	1659.	958.	.1636	0.	0.
.0229	1075.	760.	.1694	0.	0.
.0251	1063.	752.	.1752	0.	0.
.0273	533.	533.	.1812	0.	0.
.0297	1081.	765.	.1872	1133.	1133.
.0322	543.	543.	.1933	0.	0.
.0348	579.	579.	.1996	0.	0.
.0374	3446.	1407.	.2059	0.	0.
.0402	3144.	1406.	.2123	0.	0.
.0431	616.	616.	.2189	0.	0.
.0460	606.	606.	.2255	0.	0.
.0491	0.	0.	.2322	1112.	1112.
.0523	1844.	1065.	.2391	0.	0.
.0555	0.	0.	.2460	0.	0.
.0589	0.	0.	.2530	0.	0.
.0624	639.	639.	.2601	0.	0.
.0659	0.	0.	.2674	0.	0.
.0696	0.	0.	.2747	0.	0.
.0734	0.	0.	.2821	0.	0.
.0772	0.	0.	.2896	0.	0.
.0812	0.	0.	.2973	0.	0.
.0852	0.	0.	.3050	0.	0.

PHINUS - PB: 175 GEV/C
 UNITS: T: (GEV/C)**2; DSIGMA/DT: MILLIBARNS/((GEV/C)**2)

-T	DSIGMA/DT	ERROR	-T	DSIGMA/DT	ERROR
.0015	640216.	16824.	.0894	105.	105.
.0021	329285.	10102.	.0936	225.	159.
.0028	198570.	6625.	.0980	110.	110.
.0036	135334.	4859.	.1025	218.	154.
.0045	84198.	3692.	.1070	131.	131.
.0055	54750.	2813.	.1117	0.	0.
.0065	31576.	2014.	.1164	125.	125.
.0077	21137.	1659.	.1213	243.	172.
.0090	11517.	1157.	.1262	405.	234.
.0104	5825.	790.	.1313	136.	136.
.0119	3915.	610.	.1364	121.	121.
.0135	1565.	574.	.1417	135.	135.
.0152	1979.	442.	.1470	123.	123.
.0169	2016.	502.	.1524	0.	0.
.0188	2799.	491.	.1580	131.	131.
.0208	3357.	490.	.1636	129.	129.
.0229	1684.	437.	.1694	135.	135.
.0251	1783.	450.	.1752	0.	0.
.0273	1349.	302.	.1812	0.	0.
.0297	1033.	267.	.1872	276.	195.
.0322	770.	232.	.1933	0.	0.
.0348	631.	210.	.1996	146.	146.
.0374	226.	130.	.2059	0.	0.
.0402	73.	73.	.2123	0.	0.
.0431	238.	138.	.2189	0.	0.
.0460	614.	217.	.2255	0.	0.
.0491	269.	265.	.2322	0.	0.
.0523	700.	233.	.2391	153.	153.
.0555	318.	159.	.2460	0.	0.
.0589	358.	160.	.2530	0.	0.
.0624	157.	111.	.2601	0.	0.
.0659	500.	204.	.2674	0.	0.
.0696	337.	169.	.2747	0.	0.
.0734	470.	210.	.2821	0.	0.
.0772	298.	172.	.2896	0.	0.
.0812	110.	110.	.2973	0.	0.
.0852	411.	205.	.3050	0.	0.

KMINUS - PD: 175 GEV/C
 UNITS: T: (GEV/C)**2; DSIGMA/DT: MILLIBARNS/((GEV/C)**2)

-T	DSIGMA/DT	ERROR	-T	DSIGMA/DT	ERROR
.0015	720334.	25170.	.0894	0.	0.
.0021	338280.	15047.	.0936	253.	253.
.0028	204095.	9976.	.0980	0.	0.
.0036	131845.	7044.	.1025	245.	245.
.0045	84564.	5119.	.1070	294.	294.
.0053	54607.	3929.	.1117	0.	0.
.0065	37225.	3140.	.1164	280.	280.
.0077	17949.	1994.	.1213	0.	0.
.0090	6491.	1838.	.1262	0.	0.
.0104	4538.	1083.	.1313	918.	530.
.0119	2713.	966.	.1364	271.	271.
.0135	2403.	964.	.1417	302.	302.
.0152	2178.	604.	.1470	0.	0.
.0169	1805.	544.	.1524	0.	0.
.0188	1656.	763.	.1580	0.	0.
.0208	2022.	730.	.1636	0.	0.
.0229	1661.	501.	.1694	0.	0.
.0251	922.	376.	.1752	0.	0.
.0273	1666.	502.	.1812	0.	0.
.0297	928.	379.	.1872	310.	310.
.0322	786.	352.	.1933	0.	0.
.0348	0.	0.	.1996	0.	0.
.0374	338.	239.	.2059	332.	332.
.0402	163.	163.	.2123	0.	0.
.0431	0.	0.	.2189	0.	0.
.0460	344.	244.	.2255	0.	0.
.0491	0.	0.	.2322	0.	0.
.0523	0.	0.	.2391	0.	0.
.0555	0.	0.	.2460	0.	0.
.0589	161.	161.	.2530	0.	0.
.0624	529.	305.	.2601	0.	0.
.0659	0.	0.	.2674	0.	0.
.0696	189.	189.	.2747	0.	0.
.0734	211.	211.	.2821	0.	0.
.0772	0.	0.	.2896	0.	0.
.0812	0.	0.	.2973	0.	0.
.0852	231.	231.	.3050	0.	0.

PHINUS - PB: 175 GEV/C
 UNITS: T: (GEV/C)**2; DSIGMA/DT: MILLIBARNS/((GEV/C)**2)

-T	DSIGMA/DT	ERROR	-T	DSIGMA/DT	ERROR
.0015	661885.	66354.	.0894	0.	0.
.0021	417429.	46973.	.0936	0.	0.
.0028	231613.	28128.	.0980	0.	0.
.0036	219261.	23914.	.1025	0.	0.
.0045	100638.	15775.	.1070	0.	0.
.0055	65807.	12408.	.1117	0.	0.
.0065	37371.	7968.	.1164	0.	0.
.0077	29821.	6841.	.1213	0.	0.
.0090	18885.	5238.	.1262	2147.	2147.
.0104	8170.	3335.	.1313	0.	0.
.0119	6416.	2869.	.1364	0.	0.
.0135	3712.	2143.	.1417	0.	0.
.0152	1693.	3867.	.1470	0.	0.
.0169	5813.	2599.	.1524	0.	0.
.0188	3380.	1951.	.1580	2070.	2070.
.0208	7954.	3006.	.1636	2051.	2051.
.0229	3208.	1852.	.1694	0.	0.
.0251	7619.	2880.	.1752	0.	0.
.0273	0.	0.	.1812	0.	0.
.0297	0.	0.	.1872	0.	0.
.0322	2227.	1575.	.1933	0.	0.
.0348	0.	0.	.1996	0.	0.
.0374	1198.	1198.	.2059	0.	0.
.0402	1157.	1157.	.2123	0.	0.
.0431	0.	0.	.2189	0.	0.
.0460	0.	0.	.2255	0.	0.
.0491	1214.	1214.	.2322	0.	0.
.0523	2473.	1749.	.2391	0.	0.
.0555	0.	0.	.2460	0.	0.
.0589	1139.	1139.	.2530	0.	0.
.0624	0.	0.	.2601	0.	0.
.0659	2653.	1876.	.2674	0.	0.
.0696	0.	0.	.2747	0.	0.
.0734	0.	0.	.2821	0.	0.
.0772	0.	0.	.2896	0.	0.
.0812	1749.	1749.	.2973	0.	0.
.0852	0.	0.	.3050	0.	0.

PIPLUS - BE: 125 GEV/C
 UNITS: T: (GEV/C)**2; DSIGMA/DT: MILLIBARNS/((GEV/C)**2)

-T	DSIGMA/DT	ERROR	-T	DSIGMA/DT	ERROR
.0014	3403.	163.	.0495	144.	25.
.0018	2398.	125.	.0518	106.	22.
.0023	1946.	103.	.0541	151.	26.
.0028	1787.	92.	.0564	132.	26.
.0033	1530.	82.	.0588	103.	24.
.0039	1460.	76.	.0613	76.	20.
.0046	1460.	72.	.0638	125.	28.
.0053	1146.	62.	.0663	147.	30.
.0060	1111.	59.	.0689	96.	25.
.0068	1053.	55.	.0714	95.	24.
.0077	1076.	54.	.0743	98.	27.
.0086	695.	48.	.0770	59.	20.
.0095	1005.	50.	.0798	113.	28.
.0105	780.	44.	.0827	54.	19.
.0116	779.	43.	.0856	60.	19.
.0127	711.	40.	.0885	61.	19.
.0138	750.	41.	.0915	99.	25.
.0150	700.	39.	.0946	55.	17.
.0163	515.	34.	.0977	52.	16.
.0176	560.	35.	.1008	30.	12.
.0189	516.	34.	.1040	55.	17.
.0203	506.	34.	.1073	83.	21.
.0218	412.	31.	.1106	39.	15.
.0233	401.	31.	.1139	55.	17.
.0248	390.	32.	.1173	61.	18.
.0264	325.	30.	.1208	71.	20.
.0281	311.	31.	.1243	30.	12.
.0298	235.	28.	.1278	49.	16.
.0315	274.	31.	.1314	18.	9.
.0333	286.	33.	.1351	41.	15.
.0352	248.	30.	.1388	32.	12.
.0371	216.	29.	.1425	32.	13.
.0390	227.	30.	.1463	32.	12.
.0410	170.	26.	.1502	40.	14.
.0431	157.	26.	.1541	15.	9.
.0452	212.	32.	.1580	14.	8.
.0473	132.	25.	.1620	39.	15.

KPLUS - BE: 125 GEV/C
 UNITS: T: (GEV/C)**2; DSIGMA/DT: MILLIBARNS/((GEV/C)**2)

-T	DSIGMA/DT	ERROR	-T	DSIGMA/DT	ERROR
.0014	3049.	183.	.0495	103.	25.
.0018	2098.	133.	.0518	112.	26.
.0023	1828.	116.	.0541	92.	24.
.0028	1338.	93.	.0564	121.	29.
.0033	1002.	77.	.0588	88.	25.
.0039	1003.	73.	.0613	109.	27.
.0046	943.	68.	.0638	76.	25.
.0053	903.	63.	.0663	99.	29.
.0060	857.	60.	.0689	69.	25.
.0068	696.	52.	.0714	56.	21.
.0077	734.	52.	.0743	61.	25.
.0086	694.	49.	.0770	60.	27.
.0095	643.	47.	.0798	38.	19.
.0105	519.	41.	.0827	64.	24.
.0116	554.	42.	.0856	56.	21.
.0127	581.	42.	.0885	8.	8.
.0138	478.	38.	.0915	36.	18.
.0150	449.	37.	.0946	40.	16.
.0163	403.	35.	.0977	28.	14.
.0176	402.	34.	.1008	48.	18.
.0189	370.	33.	.1040	59.	21.
.0203	427.	36.	.1073	52.	20.
.0218	328.	32.	.1106	52.	20.
.0233	265.	30.	.1139	54.	19.
.0248	251.	30.	.1173	38.	17.
.0264	205.	28.	.1208	44.	18.
.0281	257.	32.	.1243	14.	10.
.0298	194.	29.	.1278	37.	16.
.0315	214.	32.	.1314	6.	6.
.0333	180.	30.	.1351	14.	10.
.0352	138.	26.	.1388	44.	16.
.0371	169.	29.	.1425	29.	14.
.0390	186.	32.	.1463	31.	14.
.0410	142.	28.	.1502	20.	12.
.0431	164.	31.	.1541	7.	7.
.0452	145.	30.	.1580	45.	17.
.0473	98.	25.	.1620	8.	8.

PPLUS - BE: 125 GEV/C
 UNITS: T: (GEV/C)**2; DSIGMA/DT: MILLIBARNS/((GEV/C)**2)

-T	DSIGMA/DT	ERROR	-T	DSIGMA/DT	ERROR
.0014	5153.	184.	.0495	308.	34.
.0018	4937.	162.	.0518	263.	32.
.0023	3983.	136.	.0541	234.	30.
.0028	3635.	121.	.0564	311.	37.
.0033	3361.	112.	.0588	259.	35.
.0039	3145.	103.	.0613	207.	30.
.0046	2865.	94.	.0638	209.	33.
.0053	2794.	89.	.0663	167.	30.
.0060	2386.	80.	.0689	220.	35.
.0068	2543.	80.	.0716	203.	32.
.0077	2323.	74.	.0743	167.	33.
.0086	2142.	69.	.0770	141.	28.
.0095	1910.	64.	.0798	139.	29.
.0105	1833.	62.	.0827	162.	31.
.0116	1771.	60.	.0856	143.	27.
.0127	1688.	58.	.0885	140.	27.
.0138	1615.	56.	.0915	112.	25.
.0150	1367.	51.	.0946	107.	21.
.0163	1171.	47.	.0977	89.	20.
.0176	1268.	49.	.1008	116.	22.
.0189	1140.	46.	.1040	127.	24.
.0203	1058.	45.	.1073	118.	24.
.0218	968.	44.	.1106	90.	21.
.0233	824.	41.	.1139	47.	14.
.0248	882.	44.	.1173	105.	22.
.0264	721.	42.	.1208	65.	17.
.0281	656.	41.	.1243	78.	18.
.0298	627.	42.	.1278	107.	22.
.0315	592.	43.	.1314	55.	15.
.0333	533.	41.	.1351	62.	16.
.0352	517.	40.	.1388	75.	17.
.0371	337.	33.	.1425	29.	12.
.0390	364.	36.	.1463	58.	15.
.0410	370.	36.	.1502	47.	14.
.0431	349.	36.	.1541	26.	11.
.0452	411.	41.	.1580	41.	13.
.0473	307.	35.	.1620	63.	14.

PIPLUS - AL: 125 GEV/C
 UNITS: T: (GEV/C)**2; DSIGMA/DT: MILLIBARNS/((GEV/C)**2)

-T	DSIGMA/DT	ERROR	-T	DSIGMA/DT	ERROR
.0014	28114.	930.	.0495	209.	60.
.0018	19198.	697.	.0518	98.	44.
.0023	14725.	560.	.0541	115.	47.
.0028	11733.	467.	.0564	108.	44.
.0033	10347.	421.	.0588	333.	86.
.0039	8131.	356.	.0613	152.	62.
.0046	7289.	318.	.0638	60.	34.
.0053	7081.	302.	.0663	86.	50.
.0060	6377.	276.	.0689	57.	40.
.0068	5531.	248.	.0716	54.	38.
.0077	4997.	229.	.0743	225.	75.
.0086	4451.	212.	.0770	84.	48.
.0095	4264.	203.	.0798	182.	64.
.0105	4047.	192.	.0827	176.	66.
.0116	3431.	174.	.0856	146.	60.
.0127	3147.	164.	.0885	17.	43.
.0138	2715.	152.	.0915	98.	44.
.0150	2371.	140.	.0946	103.	46.
.0163	2021.	129.	.0977	91.	45.
.0176	1825.	122.	.1008	71.	36.
.0189	1423.	108.	.1040	80.	40.
.0203	1341.	105.	.1073	61.	35.
.0218	1065.	96.	.1106	175.	55.
.0233	951.	92.	.1139	59.	30.
.0248	852.	92.	.1173	19.	19.
.0264	599.	79.	.1208	117.	48.
.0281	542.	78.	.1243	50.	29.
.0298	364.	68.	.1278	41.	29.
.0315	406.	73.	.1314	93.	42.
.0333	357.	70.	.1351	49.	28.
.0352	363.	71.	.1388	77.	38.
.0371	204.	55.	.1425	66.	38.
.0390	244.	61.	.1463	0.	0.
.0410	191.	55.	.1502	20.	20.
.0431	145.	46.	.1541	41.	29.
.0452	197.	70.	.1580	22.	22.
.0473	220.	61.	.1620	0.	0.

KPLUS - AL: 125 GEV/C
 UNITS: T: (GEV/C)**2; DSIGMA/DT: MILLIBARNS/((GEV/C)**2)

-T	DSIGMA/DT	ERROR	-T	DSIGMA/DT	ERROR
.0014	24025.	1041.	.0495	169.	44.
.0018	14424.	764.	.0518	82.	47.
.0023	13111.	619.	.0541	106.	53.
.0028	9250.	488.	.0564	150.	61.
.0033	8053.	434.	.0588	92.	53.
.0039	6937.	386.	.0613	140.	70.
.0044	5962.	339.	.0638	55.	39.
.0053	5379.	308.	.0663	80.	56.
.0060	5019.	291.	.0699	40.	40.
.0068	4034.	250.	.0716	0.	0.
.0077	3829.	230.	.0743	35.	35.
.0086	4151.	239.	.0770	116.	67.
.0095	3077.	203.	.0798	63.	45.
.0105	2822.	189.	.0827	139.	70.
.0114	2208.	165.	.0856	68.	48.
.0127	2082.	157.	.0885	108.	54.
.0138	1991.	154.	.0915	54.	38.
.0150	1591.	138.	.0944	86.	50.
.0163	1630.	136.	.0977	63.	44.
.0174	1237.	118.	.1008	99.	50.
.0189	1067.	111.	.1040	56.	39.
.0203	1057.	110.	.1073	113.	56.
.0218	1048.	112.	.1104	145.	59.
.0233	867.	106.	.1139	21.	21.
.0248	673.	96.	.1173	103.	51.
.0264	597.	93.	.1208	27.	27.
.0281	580.	95.	.1243	69.	40.
.0298	418.	85.	.1278	141.	63.
.0315	345.	79.	.1314	77.	45.
.0333	229.	66.	.1351	45.	32.
.0352	194.	61.	.1388	27.	27.
.0371	223.	67.	.1425	0.	0.
.0390	233.	70.	.1463	57.	40.
.0410	221.	70.	.1502	28.	28.
.0431	321.	80.	.1541	86.	49.
.0452	232.	77.	.1580	0.	0.
.0473	24.	24.	.1620	0.	0.

PPLUS - AL: 125 GEV/C
 UNITS: T: (GEV/C)**2; DSIGMA/DT: MILLIBARNS/((GEV/C)**2)

-T	DSIGMA/DT	ERROR	-T	DSIGMA/DT	ERROR
.0014	34332.	936.	.0495	244.	59.
.0018	28704.	759.	.0518	178.	54.
.0023	23039.	635.	.0541	268.	65.
.0028	19007.	537.	.0564	178.	51.
.0033	16829.	485.	.0588	256.	68.
.0039	15033.	434.	.0613	229.	69.
.0044	14229.	406.	.0638	147.	49.
.0053	12307.	365.	.0663	260.	78.
.0060	11547.	338.	.0689	258.	78.
.0068	11042.	319.	.0716	290.	81.
.0077	8925.	280.	.0743	185.	62.
.0086	8361.	262.	.0770	115.	51.
.0095	7871.	248.	.0798	206.	62.
.0105	6502.	221.	.0827	227.	69.
.0114	5789.	207.	.0856	201.	63.
.0127	5391.	196.	.0885	80.	36.
.0138	4500.	178.	.0915	129.	46.
.0150	3948.	164.	.0944	187.	56.
.0163	3502.	154.	.0977	168.	56.
.0174	2697.	135.	.1008	88.	36.
.0189	2735.	139.	.1040	132.	47.
.0203	2153.	121.	.1073	151.	50.
.0218	1841.	115.	.1104	101.	38.
.0233	1542.	107.	.1139	122.	38.
.0248	1353.	105.	.1173	46.	26.
.0264	1037.	95.	.1208	112.	42.
.0281	1143.	103.	.1243	95.	36.
.0298	744.	88.	.1278	167.	53.
.0315	517.	75.	.1314	107.	40.
.0333	463.	72.	.1351	107.	38.
.0352	471.	74.	.1388	95.	39.
.0371	336.	64.	.1425	10.	37.
.0390	251.	56.	.1463	64.	38.
.0410	249.	57.	.1502	49.	28.
.0431	309.	61.	.1541	51.	29.
.0452	276.	65.	.1580	37.	26.
.0473	321.	67.	.1620	37.	26.

PIPLUS - PB: 125 GEV/C
 UNITS: T: (GEV/C)**2; DSIGMA/DT: MILLIBARNS/((GEV/C)**2)

-T	DSIGMA/DT	ERROR	-T	DSIGMA/DT	ERROR
.0014	672511.	16978.	.0495	868.	434.
.0018	430193.	12213.	.0518	455.	321.
.0023	310240.	9360.	.0541	499.	353.
.0028	224398.	7329.	.0564	263.	263.
.0033	156499.	6050.	.0588	275.	275.
.0039	117113.	4991.	.0613	532.	376.
.0046	86478.	3929.	.0638	584.	413.
.0053	63589.	3263.	.0663	332.	332.
.0060	43050.	2642.	.0689	601.	425.
.0068	29708.	2071.	.0716	315.	315.
.0077	21152.	1652.	.0743	0.	0.
.0086	13856.	1382.	.0770	280.	280.
.0095	7241.	1117.	.0798	0.	0.
.0105	6421.	958.	.0827	0.	0.
.0116	4208.	674.	.0856	637.	451.
.0127	2149.	481.	.0885	302.	302.
.0138	1679.	420.	.0915	264.	264.
.0150	2722.	534.	.0946	487.	344.
.0163	2833.	535.	.0977	259.	259.
.0176	2296.	490.	.1008	465.	329.
.0189	3443.	590.	.1040	0.	0.
.0203	1138.	343.	.1073	232.	232.
.0218	2660.	532.	.1106	0.	0.
.0233	3324.	617.	.1139	0.	0.
.0248	2315.	531.	.1173	0.	0.
.0264	2867.	626.	.1208	214.	214.
.0281	1682.	486.	.1243	0.	0.
.0298	566.	283.	.1278	218.	218.
.0315	1166.	441.	.1314	241.	241.
.0333	1030.	420.	.1351	241.	241.
.0352	934.	418.	.1388	0.	0.
.0371	386.	273.	.1425	0.	0.
.0390	845.	423.	.1463	0.	0.
.0410	0.	0.	.1502	0.	0.
.0431	196.	196.	.1541	470.	332.
.0452	0.	0.	.1580	0.	0.
.0473	395.	279.	.1620	0.	0.

KPLUS - PB: 125 GEV/C
 UNITS: T: (GEV/C)**2; DSIGMA/DT: MILLIBARNS/((GEV/C)**2)

-T	DSIGMA/DT	ERROR	-T	DSIGMA/DT	ERROR
.0014	692076.	20559.	.0495	1185.	592.
.0018	451760.	14474.	.0518	310.	310.
.0023	289600.	10389.	.0541	1363.	682.
.0028	222858.	8311.	.0564	0.	0.
.0033	141527.	6523.	.0588	751.	531.
.0039	112382.	5602.	.0613	363.	363.
.0046	78759.	4421.	.0638	0.	0.
.0053	59053.	3548.	.0663	453.	453.
.0060	44756.	3255.	.0689	0.	0.
.0068	28967.	2408.	.0716	430.	430.
.0077	17732.	1984.	.0743	984.	697.
.0086	12984.	1470.	.0770	383.	383.
.0095	7485.	1092.	.0798	0.	0.
.0105	5573.	929.	.0827	0.	0.
.0116	3094.	675.	.0856	435.	435.
.0127	1467.	464.	.0895	0.	0.
.0138	1862.	517.	.0915	0.	0.
.0150	550.	589.	.0946	0.	0.
.0163	1105.	391.	.0977	0.	0.
.0176	1425.	451.	.1008	317.	317.
.0189	1659.	479.	.1040	339.	339.
.0203	1836.	509.	.1073	0.	0.
.0218	2470.	599.	.1106	282.	282.
.0233	1722.	519.	.1139	284.	284.
.0248	832.	372.	.1173	0.	0.
.0264	1491.	527.	.1208	0.	0.
.0281	1531.	541.	.1243	0.	0.
.0298	386.	273.	.1278	0.	0.
.0315	1365.	557.	.1314	329.	329.
.0333	469.	331.	.1351	0.	0.
.0352	510.	361.	.1388	561.	397.
.0371	0.	0.	.1425	0.	0.
.0390	289.	289.	.1463	361.	361.
.0410	0.	0.	.1502	0.	0.
.0431	0.	0.	.1541	0.	0.
.0452	0.	0.	.1580	0.	0.
.0473	539.	381.	.1620	389.	389.

PPLUS - PB: 125 DEV/C
 UNITS: T: (GEV/C)²; DSIGMA/DT: MILLIBARNS/((GEV/C)²)

-T	DSIGMA/DT	ERROR	-T	DSIGMA/DT	ERROR
.0014	740074.	16498.	.0435	547.	316.
.0018	508566.	11607.	.0518	956.	428.
.0023	365031.	9443.	.0541	1050.	470.
.0028	263466.	7342.	.0564	443.	313.
.0033	207326.	6393.	.0588	0.	0.
.0039	153291.	5095.	.0613	447.	316.
.0046	110047.	4198.	.0638	491.	347.
.0053	75455.	3582.	.0663	558.	394.
.0060	56072.	2834.	.0689	0.	0.
.0068	37301.	2231.	.0716	0.	0.
.0077	21509.	1825.	.0743	304.	304.
.0086	16279.	1340.	.0770	943.	472.
.0095	9096.	1014.	.0798	591.	418.
.0105	6239.	923.	.0827	0.	0.
.0116	5264.	691.	.0856	0.	0.
.0127	4041.	693.	.0885	254.	254.
.0138	4185.	768.	.0915	445.	315.
.0150	5724.	710.	.0946	205.	205.
.0163	4426.	614.	.0977	218.	218.
.0176	4979.	739.	.1008	0.	0.
.0189	3138.	823.	.1040	209.	209.
.0203	5046.	663.	.1073	195.	195.
.0218	4628.	726.	.1106	174.	174.
.0233	4821.	682.	.1139	0.	0.
.0248	3484.	598.	.1173	197.	197.
.0264	3101.	597.	.1208	180.	180.
.0281	2476.	540.	.1243	172.	172.
.0298	1547.	429.	.1278	183.	183.
.0315	701.	313.	.1314	608.	351.
.0333	433.	250.	.1351	0.	0.
.0352	786.	351.	.1388	0.	0.
.0371	487.	281.	.1425	0.	0.
.0390	1245.	470.	.1463	223.	223.
.0410	818.	366.	.1502	222.	222.
.0431	1156.	437.	.1541	197.	197.
.0452	1494.	528.	.1580	0.	0.
.0473	994.	407.	.1620	240.	240.

PIPLUS - BE: 70 GEV/C
 UNITS: T: (GEV/C)**2; DSIGMA/DT: MILLIBARNS/((GEV/C)**2)

-T	DSIGMA/DT	ERROR	-T	DSIGMA/DT	ERROR
.0012	4295.	197.	.0239	352.	60.
.0014	3768.	177.	.0248	400.	66.
.0016	3096.	154.	.0258	498.	72.
.0019	2591.	135.	.0267	356.	62.
.0022	2266.	124.	.0277	371.	64.
.0025	2078.	116.	.0287	310.	59.
.0028	1899.	108.	.0298	305.	59.
.0031	1687.	100.	.0308	297.	59.
.0034	1653.	98.	.0319	425.	71.
.0038	1616.	96.	.0329	293.	60.
.0042	1364.	87.	.0340	314.	63.
.0046	1475.	90.	.0352	342.	65.
.0050	1303.	83.	.0363	174.	45.
.0054	1216.	80.	.0374	241.	55.
.0059	1221.	81.	.0396	262.	55.
.0063	1080.	76.	.0398	193.	46.
.0068	1208.	81.	.0410	159.	40.
.0073	1092.	78.	.0422	147.	41.
.0078	1012.	76.	.0435	219.	49.
.0084	1125.	83.	.0447	190.	46.
.0089	924.	78.	.0460	158.	42.
.0095	942.	80.	.0473	233.	52.
.0101	912.	82.	.0486	128.	37.
.0107	849.	82.	.0500	177.	42.
.0113	720.	78.	.0513	97.	32.
.0120	793.	80.	.0527	153.	41.
.0127	688.	76.	.0541	142.	39.
.0133	826.	87.	.0555	117.	35.
.0140	666.	72.	.0569	199.	50.
.0148	651.	73.	.0583	132.	40.
.0155	689.	78.	.0598	71.	29.
.0163	615.	73.	.0613	136.	41.
.0170	631.	76.	.0628	224.	50.
.0178	597.	73.	.0643	81.	31.
.0186	517.	69.	.0658	62.	28.
.0195	418.	61.	.0673	39.	22.
.0203	411.	59.	.0689	125.	42.
.0212	460.	67.	.0705	133.	44.
.0221	535.	71.	.0721	31.	22.
.0230	401.	62.	.0737	197.	62.

KPLUS - BE: 70 GEV/C
 UNITS: T: (GEV/C)**2; DSIGMA/DT: MILLIBARNS/((GEV/C)**2)

-T	DSIGMA/DT	ERROR	-T	DSIGMA/DT	ERROR
.0012	4067.	237.	.0239	354.	74.
.0014	3176.	197.	.0248	241.	62.
.0016	2642.	173.	.0258	262.	64.
.0019	2199.	154.	.0267	289.	68.
.0022	1841.	129.	.0277	260.	65.
.0025	1397.	116.	.0287	379.	79.
.0028	1281.	108.	.0298	269.	67.
.0031	1300.	108.	.0308	212.	61.
.0034	1382.	109.	.0319	193.	58.
.0038	1228.	102.	.0329	163.	54.
.0042	1242.	101.	.0340	107.	59.
.0046	833.	82.	.0352	127.	48.
.0050	950.	86.	.0363	69.	35.
.0054	893.	84.	.0374	170.	57.
.0059	633.	81.	.0396	136.	48.
.0063	854.	82.	.0398	160.	51.
.0068	737.	77.	.0410	69.	36.
.0073	642.	73.	.0422	185.	56.
.0078	654.	75.	.0435	82.	36.
.0084	700.	80.	.0447	116.	44.
.0089	770.	87.	.0460	34.	24.
.0095	624.	80.	.0473	139.	49.
.0101	689.	87.	.0486	79.	36.
.0107	518.	79.	.0500	102.	39.
.0113	710.	94.	.0513	144.	48.
.0120	542.	81.	.0527	162.	51.
.0127	444.	74.	.0541	98.	40.
.0133	478.	81.	.0555	95.	39.
.0140	466.	74.	.0569	74.	37.
.0148	270.	57.	.0583	125.	47.
.0155	384.	87.	.0598	19.	18.
.0163	458.	76.	.0613	129.	49.
.0170	408.	74.	.0628	33.	24.
.0178	242.	57.	.0643	52.	30.
.0186	412.	75.	.0658	55.	32.
.0195	344.	67.	.0673	96.	43.
.0203	293.	61.	.0689	41.	29.
.0212	364.	73.	.0705	132.	54.
.0221	384.	74.	.0721	23.	23.
.0230	227.	57.	.0737	59.	42.

PPLUS - BE: 70 GEV/C
 UNITS: T: (GEV/C)**2; DSIGMA/DT: MILLIBARNS/((GEV/C)**2)

-T	DSIGMA/DT	ERROR	-T	DSIGMA/DT	ERROR
.0012	6483.	267.	.0239	923.	107.
.0014	6160.	246.	.0248	849.	105.
.0016	4820.	211.	.0258	826.	101.
.0019	4448.	194.	.0267	835.	104.
.0022	4287.	186.	.0277	767.	100.
.0025	3789.	170.	.0287	765.	100.
.0028	3477.	160.	.0298	621.	93.
.0031	3983.	165.	.0308	680.	98.
.0034	3516.	155.	.0319	519.	85.
.0036	3144.	146.	.0329	566.	91.
.0042	3242.	145.	.0340	538.	90.
.0046	3131.	142.	.0352	451.	81.
.0050	2816.	133.	.0363	414.	76.
.0054	2783.	132.	.0374	665.	100.
.0059	2578.	127.	.0386	434.	77.
.0063	2541.	127.	.0398	524.	82.
.0066	2387.	125.	.0410	425.	71.
.0073	2079.	113.	.0422	336.	67.
.0078	2312.	126.	.0435	222.	54.
.0084	2168.	126.	.0447	358.	69.
.0089	2213.	131.	.0460	376.	71.
.0095	2029.	129.	.0473	208.	54.
.0101	2013.	133.	.0486	343.	66.
.0107	1926.	134.	.0500	328.	62.
.0113	2071.	144.	.0513	358.	68.
.0120	1637.	126.	.0527	169.	47.
.0127	1608.	126.	.0541	338.	66.
.0133	1725.	137.	.0555	329.	65.
.0140	1371.	113.	.0569	282.	65.
.0148	1470.	120.	.0583	171.	49.
.0155	1432.	122.	.0598	269.	62.
.0163	1444.	121.	.0613	323.	69.
.0170	1370.	122.	.0628	227.	55.
.0178	1226.	115.	.0643	234.	57.
.0186	1253.	117.	.0658	221.	57.
.0195	1216.	113.	.0673	184.	53.
.0203	1071.	105.	.0689	232.	62.
.0212	943.	105.	.0705	141.	50.
.0221	773.	94.	.0721	204.	62.
.0230	841.	98.	.0737	188.	66.

PIPLUS - C: 70 GEV/C
 UNITS: T: (GEV/C)**2; DSIGMA/DT: MILLIBARNS/((GEV/C)**2)

-T	DSIGMA/DT	ERROR	-T	DSIGMA/DT	ERROR
.0012	8606.	378.	.0239	476.	90.
.0014	6302.	310.	.0248	610.	110.
.0016	5467.	277.	.0258	701.	117.
.0019	4677.	250.	.0267	777.	131.
.0022	3692.	212.	.0277	454.	99.
.0025	3413.	201.	.0287	437.	95.
.0028	3158.	190.	.0298	517.	113.
.0031	2625.	169.	.0308	543.	106.
.0034	2599.	165.	.0319	480.	100.
.0036	2431.	158.	.0329	544.	116.
.0042	2121.	145.	.0340	355.	89.
.0046	2485.	157.	.0352	220.	70.
.0050	2151.	144.	.0363	269.	75.
.0054	2033.	139.	.0374	255.	74.
.0059	2148.	144.	.0386	237.	71.
.0063	1845.	134.	.0398	346.	89.
.0068	1810.	133.	.0410	224.	67.
.0073	1801.	135.	.0422	273.	76.
.0078	1698.	134.	.0435	88.	39.
.0084	1773.	144.	.0447	105.	47.
.0089	1635.	141.	.0460	150.	57.
.0095	1691.	146.	.0473	121.	46.
.0101	1668.	152.	.0486	125.	47.
.0107	1428.	141.	.0500	177.	59.
.0113	1215.	130.	.0513	91.	41.
.0120	1319.	140.	.0527	90.	40.
.0127	1152.	129.	.0541	110.	45.
.0133	1322.	144.	.0555	114.	51.
.0140	1075.	131.	.0569	74.	38.
.0148	1173.	133.	.0583	133.	60.
.0155	948.	119.	.0598	86.	43.
.0163	960.	129.	.0613	112.	50.
.0170	901.	119.	.0628	167.	68.
.0178	1057.	138.	.0643	44.	31.
.0186	718.	110.	.0658	132.	54.
.0195	609.	106.	.0673	123.	55.
.0203	658.	113.	.0689	60.	43.
.0212	733.	111.	.0705	214.	76.
.0221	530.	97.	.0721	51.	36.
.0230	619.	107.	.0737	158.	79.

KPLUS - C: 70 GEV/C
 UNITS: T: (GEV/C)**2; DSIGMA/DT: MILLIBARNS/((GEV/C)**2)

-T	DSIGMA/DT	ERROR	-T	DSIGMA/DT	ERROR
.0012	8436.	475.	.0239	421.	105.
.0014	7266.	410.	.0248	487.	122.
.0016	5217.	335.	.0258	241.	85.
.0019	4107.	289.	.0267	343.	108.
.0022	3223.	246.	.0277	200.	82.
.0025	2876.	230.	.0287	450.	120.
.0028	2636.	215.	.0298	266.	101.
.0031	2018.	186.	.0308	419.	116.
.0034	2012.	181.	.0319	258.	91.
.0038	1786.	169.	.0329	306.	108.
.0042	1649.	162.	.0340	171.	77.
.0046	1483.	150.	.0352	238.	90.
.0050	1363.	143.	.0363	320.	101.
.0054	1476.	147.	.0374	164.	74.
.0059	1415.	144.	.0386	100.	58.
.0063	1539.	152.	.0398	107.	62.
.0068	1330.	142.	.0410	94.	54.
.0073	1001.	125.	.0422	260.	92.
.0078	1253.	143.	.0435	273.	86.
.0084	1262.	151.	.0447	196.	80.
.0089	1263.	154.	.0460	165.	74.
.0095	871.	130.	.0473	133.	60.
.0101	1129.	155.	.0486	248.	83.
.0107	948.	145.	.0500	122.	61.
.0113	885.	138.	.0513	28.	28.
.0120	1030.	154.	.0527	84.	48.
.0127	778.	132.	.0541	85.	49.
.0133	729.	133.	.0555	35.	35.
.0140	644.	126.	.0569	59.	42.
.0148	744.	131.	.0583	165.	82.
.0155	778.	133.	.0598	66.	47.
.0163	675.	135.	.0613	103.	60.
.0170	806.	140.	.0628	129.	75.
.0178	554.	124.	.0643	34.	34.
.0186	568.	121.	.0658	0.	0.
.0195	798.	151.	.0673	0.	0.
.0203	747.	149.	.0689	47.	47.
.0212	566.	121.	.0705	83.	58.
.0221	491.	116.	.0721	118.	68.
.0230	508.	123.	.0737	122.	86.

PPLUS - C: 70 GEV/C
 UNITS: T: (GEV/C)**2; DSIGMA/DT: MILLIBARNS/((GEV/C)**2)

-T	DSIGMA/DT	ERROR	-T	DSIGMA/DT	ERROR
.0012	12201.	496.	.0239	1027.	144.
.0014	10176.	429.	.0248	1281.	173.
.0016	8901.	387.	.0258	1082.	158.
.0019	7560.	343.	.0267	998.	162.
.0022	6678.	312.	.0277	1049.	164.
.0025	5935.	288.	.0287	911.	150.
.0028	6128.	207.	.0298	939.	169.
.0031	5314.	262.	.0308	791.	140.
.0034	5546.	263.	.0319	618.	124.
.0038	5180.	252.	.0329	966.	168.
.0042	4796.	237.	.0340	551.	120.
.0046	4208.	221.	.0352	735.	140.
.0050	4378.	225.	.0363	515.	112.
.0054	3965.	211.	.0374	479.	110.
.0059	4328.	222.	.0386	434.	105.
.0063	3571.	203.	.0398	601.	128.
.0068	3504.	203.	.0410	385.	96.
.0073	3868.	215.	.0422	423.	103.
.0078	3391.	206.	.0435	292.	78.
.0084	3179.	210.	.0447	375.	97.
.0089	3393.	221.	.0460	380.	98.
.0095	3380.	224.	.0473	122.	50.
.0101	3231.	230.	.0486	232.	70.
.0107	3003.	222.	.0500	420.	99.
.0113	2545.	205.	.0513	216.	68.
.0120	2911.	226.	.0527	257.	74.
.0127	2572.	209.	.0541	259.	75.
.0133	2495.	216.	.0555	244.	81.
.0140	2620.	223.	.0569	158.	60.
.0148	2332.	204.	.0583	347.	105.
.0155	2051.	190.	.0598	204.	72.
.0163	2190.	213.	.0613	211.	75.
.0170	1982.	193.	.0628	395.	114.
.0178	1993.	206.	.0643	130.	58.
.0186	1582.	177.	.0658	78.	45.
.0195	1441.	177.	.0673	87.	51.
.0203	1900.	209.	.0689	178.	80.
.0212	1223.	155.	.0705	221.	84.
.0221	962.	142.	.0721	301.	95.
.0230	1327.	174.	.0737	186.	93.

PIPLUS - AL: 70 GEV/C
 UNITS: T: (GEV/C)**2; DSIGMA/DT: MILLIBARNS/((GEV/C)**2)

-T	DSIGMA/DT	ERROR	-T	DSIGMA/DT	ERROR
.0012	36312.	1121.	.0239	927.	202.
.0014	27860.	933.	.0248	1024.	218.
.0016	22727.	807.	.0258	507.	163.
.0019	17070.	679.	.0267	946.	212.
.0022	14857.	612.	.0277	460.	141.
.0025	13618.	571.	.0287	824.	200.
.0028	11724.	515.	.0298	491.	155.
.0031	11464.	500.	.0308	535.	154.
.0034	9329.	443.	.0319	467.	148.
.0038	8954.	426.	.0329	362.	128.
.0042	8362.	407.	.0340	136.	78.
.0046	7782.	388.	.0352	389.	129.
.0050	6820.	358.	.0363	298.	112.
.0054	7084.	365.	.0374	259.	106.
.0059	6420.	347.	.0386	484.	146.
.0063	6405.	351.	.0398	163.	82.
.0058	5049.	314.	.0410	251.	102.
.0073	5584.	341.	.0422	367.	130.
.0078	4519.	313.	.0435	217.	97.
.0084	5428.	357.	.0447	129.	75.
.0089	4396.	330.	.0460	130.	75.
.0095	3215.	285.	.0473	88.	62.
.0101	4057.	343.	.0486	241.	99.
.0107	3480.	322.	.0500	217.	97.
.0113	3051.	313.	.0513	88.	63.
.0120	3147.	315.	.0527	49.	49.
.0127	2824.	310.	.0541	48.	48.
.0133	2552.	299.	.0555	98.	70.
.0140	2354.	288.	.0569	216.	108.
.0148	2446.	286.	.0583	53.	53.
.0155	2241.	287.	.0598	60.	60.
.0163	2056.	277.	.0613	121.	85.
.0170	1715.	253.	.0628	58.	58.
.0178	1485.	235.	.0643	226.	131.
.0186	1695.	261.	.0658	65.	65.
.0195	1224.	227.	.0673	166.	117.
.0203	1180.	219.	.0689	102.	102.
.0212	1294.	240.	.0705	0.	0.
.0221	912.	199.	.0721	105.	105.
.0230	1216.	218.	.0737	115.	115.

KPLUS - AL: 70 GEV/C
 UNITS: T: (GEV/C)**2; DSIGMA/DT: MILLIBARNS/((GEV/C)**2)

-T	DSIGMA/DT	ERROR	-T	DSIGMA/DT	ERROR
.0012	34168.	1369.	.0239	685.	217.
.0014	25711.	1113.	.0248	722.	228.
.0016	19627.	931.	.0258	280.	140.
.0019	16791.	836.	.0267	661.	220.
.0022	13495.	728.	.0277	396.	162.
.0025	11105.	640.	.0287	526.	199.
.0028	9619.	581.	.0298	915.	264.
.0031	8179.	528.	.0308	553.	196.
.0034	7611.	502.	.0319	145.	102.
.0038	7147.	475.	.0329	140.	99.
.0042	6136.	441.	.0340	560.	198.
.0046	6295.	432.	.0352	201.	116.
.0050	6108.	422.	.0363	66.	66.
.0054	5114.	387.	.0374	201.	116.
.0059	4324.	353.	.0386	68.	68.
.0063	5221.	395.	.0398	63.	63.
.0068	3931.	345.	.0410	130.	92.
.0073	4007.	360.	.0422	71.	71.
.0078	3421.	339.	.0435	202.	116.
.0084	3609.	363.	.0447	67.	67.
.0089	3544.	370.	.0460	0.	0.
.0095	2199.	294.	.0473	69.	69.
.0101	2967.	365.	.0486	187.	188.
.0107	2055.	320.	.0500	0.	0.
.0113	2591.	359.	.0513	69.	69.
.0120	3075.	387.	.0527	0.	0.
.0127	2269.	346.	.0541	75.	75.
.0133	2440.	364.	.0555	76.	76.
.0140	1798.	313.	.0569	168.	119.
.0148	1611.	289.	.0583	165.	117.
.0155	1254.	267.	.0598	92.	92.
.0163	1508.	296.	.0613	187.	132.
.0170	1273.	271.	.0628	180.	127.
.0178	1613.	305.	.0643	0.	0.
.0186	1377.	294.	.0658	0.	0.
.0195	1179.	278.	.0673	0.	0.
.0203	821.	228.	.0689	0.	0.
.0212	1039.	248.	.0705	0.	0.
.0221	607.	202.	.0721	0.	0.
.0230	852.	228.	.0737	0.	0.

PPLUS - AL: 70 GEV/C
 UNITS: T: (GEV/C)**2; DSIGMA/DT: MILLIBARNS/((GEV/C)**2)

-T	DSIGMA/DT	ERROR	-T	DSIGMA/DT	ERROR
.0012	44456.	1417.	.0239	1686.	308.
.0014	39542.	1258.	.0248	1481.	296.
.0016	29689.	1052.	.0258	1266.	270.
.0019	27348.	964.	.0267	843.	225.
.0022	25063.	901.	.0277	1353.	271.
.0025	22032.	819.	.0207	987.	247.
.0028	19753.	756.	.0298	665.	233.
.0031	19760.	738.	.0308	681.	197.
.0034	15807.	652.	.0319	297.	133.
.0038	16102.	645.	.0329	460.	163.
.0042	14772.	610.	.0340	172.	100.
.0046	14816.	601.	.0352	494.	165.
.0050	12885.	559.	.0363	704.	195.
.0054	11320.	521.	.0374	439.	155.
.0059	10943.	511.	.0386	561.	177.
.0063	11924.	540.	.0398	519.	164.
.0068	10736.	518.	.0410	319.	130.
.0073	10397.	525.	.0422	117.	83.
.0078	9799.	519.	.0435	441.	156.
.0084	8913.	516.	.0447	219.	110.
.0089	8663.	523.	.0460	221.	110.
.0095	7315.	486.	.0473	337.	138.
.0101	6936.	506.	.0486	205.	102.
.0107	6777.	507.	.0500	166.	96.
.0113	6664.	522.	.0513	225.	113.
.0120	4647.	431.	.0527	186.	107.
.0127	5630.	494.	.0541	184.	106.
.0133	5695.	503.	.0555	313.	140.
.0140	4874.	467.	.0569	138.	97.
.0148	3796.	402.	.0583	204.	118.
.0155	3975.	431.	.0598	0.	0.
.0163	3331.	398.	.0613	77.	77.
.0170	2991.	377.	.0628	222.	128.
.0178	2553.	347.	.0643	0.	0.
.0186	2414.	352.	.0658	83.	83.
.0195	3063.	406.	.0673	106.	106.
.0203	2643.	370.	.0689	130.	130.
.0212	2671.	390.	.0705	129.	129.
.0221	1770.	313.	.0721	0.	0.
.0230	1748.	295.	.0737	146.	146.

PIPLUS - CU: 70 GEV/C
 UNITS: T: (GEV/C)**2; DSIGMA/DT: MILLIBARNS/((GEV/C)**2)

-T	DSIGMA/DT	ERROR	-T	DSIGMA/DT	ERROR
.0012	156701.	4318.	.0239	465.	268.
.0014	120801.	3630.	.0248	299.	212.
.0016	91589.	3013.	.0258	475.	275.
.0019	75521.	2663.	.0267	276.	195.
.0022	60050.	2294.	.0277	153.	153.
.0025	47768.	1993.	.0287	286.	202.
.0028	45240.	1885.	.0298	370.	262.
.0031	39376.	1735.	.0308	330.	233.
.0034	33666.	1570.	.0319	301.	213.
.0038	29674.	1465.	.0329	161.	161.
.0042	28767.	1419.	.0340	167.	167.
.0046	25703.	1329.	.0352	312.	220.
.0050	22853.	1236.	.0363	172.	172.
.0054	19863.	1155.	.0374	185.	185.
.0059	18597.	1113.	.0386	502.	290.
.0063	19171.	1130.	.0398	492.	284.
.0068	17289.	1087.	.0410	130.	130.
.0073	13760.	998.	.0422	175.	175.
.0078	11196.	923.	.0435	157.	157.
.0084	11370.	958.	.0447	569.	285.
.0089	9368.	900.	.0460	301.	213.
.0095	8568.	888.	.0473	389.	225.
.0101	6938.	796.	.0486	417.	241.
.0107	7258.	861.	.0500	335.	237.
.0113	5893.	780.	.0513	185.	185.
.0120	6833.	905.	.0527	412.	238.
.0127	4323.	692.	.0541	0.	0.
.0133	3411.	613.	.0555	308.	218.
.0140	2737.	547.	.0569	348.	246.
.0148	3424.	647.	.0583	332.	234.
.0155	2117.	499.	.0598	0.	0.
.0163	2990.	610.	.0613	0.	0.
.0170	2084.	505.	.0628	224.	224.
.0178	1739.	465.	.0643	200.	200.
.0186	691.	282.	.0658	223.	223.
.0195	2091.	540.	.0673	425.	301.
.0203	1119.	396.	.0689	214.	214.
.0212	0.	0.	.0705	0.	0.
.0221	269.	190.	.0721	0.	0.
.0230	676.	301.	.0737	0.	0.

KPLUS - CU: 70 GEV/C
 UNITS: T: (GEV/C)**2; DSIGMA/DT: MILLIBARNS/((GEV/C)**2)

-T	DSIGMA/DT	ERROR	-T	DSIGMA/DT	ERROR
.0012	155253.	5297.	.0239	1388.	567.
.0014	104432.	4114.	.0248	671.	387.
.0016	92988.	3702.	.0258	473.	335.
.0019	61011.	2924.	.0267	0.	0.
.0022	51316.	2598.	.0277	229.	229.
.0025	48360.	2443.	.0287	0.	0.
.0028	37074.	2086.	.0298	277.	277.
.0031	31752.	1911.	.0308	246.	246.
.0034	27045.	1734.	.0319	0.	0.
.0038	24541.	1629.	.0329	0.	0.
.0042	22977.	1579.	.0340	0.	0.
.0046	20395.	1439.	.0352	466.	329.
.0050	19464.	1394.	.0363	513.	363.
.0054	18344.	1356.	.0374	276.	276.
.0059	15489.	1232.	.0386	0.	0.
.0063	13224.	1147.	.0398	0.	0.
.0068	12351.	1123.	.0410	0.	0.
.0073	9520.	1015.	.0422	0.	0.
.0078	10467.	1091.	.0435	0.	0.
.0084	8914.	1036.	.0447	0.	0.
.0089	7407.	981.	.0460	224.	224.
.0095	6743.	963.	.0473	194.	194.
.0101	6818.	964.	.0486	208.	208.
.0107	6014.	1008.	.0500	0.	0.
.0113	4633.	846.	.0513	552.	391.
.0120	5372.	981.	.0527	0.	0.
.0127	3973.	811.	.0541	673.	388.
.0133	2630.	657.	.0555	230.	230.
.0140	2780.	674.	.0569	260.	260.
.0148	3471.	796.	.0583	248.	248.
.0155	1757.	556.	.0598	0.	0.
.0163	1303.	492.	.0613	267.	267.
.0170	1465.	518.	.0628	0.	0.
.0178	928.	415.	.0643	298.	298.
.0186	1377.	487.	.0658	0.	0.
.0195	1249.	510.	.0673	318.	318.
.0203	627.	362.	.0689	320.	320.
.0212	872.	436.	.0705	343.	343.
.0221	402.	284.	.0721	440.	440.
.0230	0.	0.	.0737	856.	605.

PPLUS - CU: 70 GEV/C
 UNITS: T: (GEV/C)**2; DSIGMA/DT: MILLIBARNS/((GEV/C)**2)

-T	DSIGMA/DT	ERROR	-T	DSIGMA/DT	ERROR
.0012	173969.	5042.	.0239	922.	412.
.0014	134087.	4198.	.0248	356.	252.
.0016	113712.	3707.	.0258	755.	377.
.0019	88252.	3133.	.0267	657.	329.
.0022	86680.	3027.	.0277	731.	365.
.0025	64650.	2529.	.0287	340.	241.
.0028	61670.	2409.	.0298	977.	641.
.0031	57953.	2287.	.0308	393.	278.
.0034	51152.	2111.	.0319	537.	310.
.0038	46104.	1993.	.0329	1731.	577.
.0042	41336.	1856.	.0340	398.	282.
.0046	39793.	1794.	.0352	371.	263.
.0050	35156.	1688.	.0363	614.	354.
.0054	33399.	1634.	.0374	879.	440.
.0059	33320.	1621.	.0386	597.	345.
.0063	25917.	1433.	.0398	390.	276.
.0068	26072.	1466.	.0410	309.	219.
.0073	20954.	1344.	.0422	1461.	552.
.0078	21040.	1381.	.0435	1124.	459.
.0084	17667.	1302.	.0447	339.	240.
.0089	15536.	1269.	.0460	895.	400.
.0095	14041.	1241.	.0473	463.	267.
.0101	13478.	1210.	.0486	828.	371.
.0107	11198.	1167.	.0500	200.	200.
.0113	10832.	1155.	.0513	220.	220.
.0120	9849.	1186.	.0527	818.	366.
.0127	7390.	988.	.0541	894.	400.
.0133	6813.	945.	.0555	734.	367.
.0140	5735.	865.	.0569	207.	207.
.0148	4514.	811.	.0583	395.	279.
.0155	2661.	611.	.0598	495.	350.
.0163	2670.	629.	.0613	638.	369.
.0170	2190.	565.	.0628	0.	0.
.0178	2810.	645.	.0643	0.	0.
.0186	2195.	549.	.0658	265.	265.
.0195	2656.	664.	.0673	253.	253.
.0203	999.	408.	.0689	255.	255.
.0212	2432.	650.	.0705	273.	273.
.0221	962.	393.	.0721	351.	351.
.0230	801.	358.	.0737	0.	0.

PIPLUS - SM: 70 GEV/C
 UNITS: T: (GEV/C)**2; DSIGMA/DT: MILLIBARNS/((GEV/C)**2)

-T	DSIGMA/DT	ERROR	-T	DSIGMA/DT	ERROR
.0012	411919.	8730.	.0239	240.	240.
.0014	312454.	7234.	.0248	1284.	574.
.0016	226888.	5907.	.0258	854.	427.
.0019	183813.	5156.	.0267	1429.	583.
.0022	148477.	4496.	.0277	1303.	532.
.0025	124277.	3992.	.0287	462.	327.
.0028	104115.	3577.	.0298	514.	363.
.0031	97376.	3417.	.0308	942.	471.
.0034	74649.	2923.	.0319	446.	316.
.0038	68153.	2735.	.0329	718.	414.
.0042	57401.	2496.	.0340	708.	409.
.0046	52940.	2399.	.0352	497.	352.
.0050	47387.	2229.	.0363	471.	333.
.0054	36547.	1996.	.0374	917.	458.
.0059	34609.	1907.	.0386	387.	273.
.0063	29373.	1755.	.0398	1437.	587.
.0068	26359.	1684.	.0410	902.	451.
.0073	23263.	1629.	.0422	465.	329.
.0078	21439.	1623.	.0435	878.	439.
.0084	16100.	1440.	.0447	252.	252.
.0089	13200.	1340.	.0460	439.	311.
.0095	12127.	1339.	.0473	0.	0.
.0101	7943.	1102.	.0486	201.	201.
.0107	7620.	1111.	.0500	244.	244.
.0113	5900.	933.	.0513	217.	217.
.0120	4705.	889.	.0527	0.	0.
.0127	2722.	660.	.0541	318.	318.
.0133	3520.	787.	.0555	0.	0.
.0140	1598.	565.	.0569	255.	255.
.0148	1563.	553.	.0583	325.	325.
.0155	745.	372.	.0598	561.	397.
.0163	997.	446.	.0613	0.	0.
.0170	384.	271.	.0628	0.	0.
.0178	1889.	630.	.0643	0.	0.
.0186	1429.	540.	.0658	0.	0.
.0195	0.	0.	.0673	414.	414.
.0203	643.	371.	.0689	0.	0.
.0212	596.	344.	.0705	519.	519.
.0221	663.	383.	.0721	460.	460.
.0230	507.	358.	.0737	508.	508.

KPLUS - SM: 70 GEV/C
 UNITS: T: (GEV/C)**2; DSIGMA/DT: MILLIBARNS/((GEV/C)**2)

-T	DSIGMA/DT	ERROR	-T	DSIGMA/DT	ERROR
.0012	416151.	10760.	.0239	362.	362.
.0014	289511.	8485.	.0248	0.	0.
.0016	219869.	7096.	.0258	643.	454.
.0019	171396.	6110.	.0267	717.	507.
.0022	127052.	5097.	.0277	327.	327.
.0025	116338.	4748.	.0287	348.	348.
.0028	91543.	4115.	.0298	0.	0.
.0031	80506.	3855.	.0308	1417.	708.
.0034	70623.	3468.	.0319	336.	336.
.0038	52011.	2930.	.0329	0.	0.
.0042	48722.	2890.	.0340	1065.	615.
.0046	44318.	2653.	.0352	748.	529.
.0050	39747.	2504.	.0363	354.	354.
.0054	32495.	2248.	.0374	345.	345.
.0059	27990.	2000.	.0386	0.	0.
.0063	25252.	1996.	.0398	721.	510.
.0068	21670.	1874.	.0410	0.	0.
.0073	20931.	1895.	.0422	350.	350.
.0078	16508.	1712.	.0435	330.	330.
.0084	14921.	1700.	.0447	759.	537.
.0089	14741.	1737.	.0460	0.	0.
.0095	10457.	1525.	.0473	311.	311.
.0101	7125.	1280.	.0486	302.	302.
.0107	4567.	1248.	.0500	0.	0.
.0113	5326.	1087.	.0513	654.	463.
.0120	4550.	1072.	.0527	356.	356.
.0127	2650.	799.	.0541	0.	0.
.0133	1854.	701.	.0555	0.	0.
.0140	2103.	795.	.0569	383.	383.
.0148	1176.	588.	.0583	978.	691.
.0155	2521.	840.	.0598	0.	0.
.0163	1200.	600.	.0613	421.	421.
.0170	577.	408.	.0628	428.	428.
.0178	0.	0.	.0643	0.	0.
.0186	0.	0.	.0658	0.	0.
.0195	1188.	594.	.0673	0.	0.
.0203	645.	456.	.0689	0.	0.
.0212	299.	299.	.0705	1560.	1103.
.0221	333.	333.	.0721	0.	0.
.0230	0.	0.	.0737	0.	0.

PPLUS - SN: 70 GEV/C
 UNITS: T: (GEV/C)**2; DSIGMA/DT: MILLIBARNS/((GEV/C)**2)

-T	DSIGMA/DT	ERROR	-T	DSIGMA/DT	ERROR
.0012	443606.	10017.	.0239	1420.	635.
.0014	332200.	8178.	.0248	910.	525.
.0016	266034.	7000.	.0258	1009.	504.
.0019	207402.	5935.	.0267	844.	487.
.0022	169890.	5261.	.0277	1539.	628.
.0025	146621.	4711.	.0287	4092.	1056.
.0028	133225.	4415.	.0298	1444.	1051.
.0031	122859.	4169.	.0308	1668.	681.
.0034	105057.	3769.	.0319	1318.	590.
.0038	95389.	3516.	.0329	1696.	692.
.0042	75732.	3115.	.0340	1393.	623.
.0046	71444.	2985.	.0352	1468.	656.
.0050	63702.	2848.	.0363	1112.	556.
.0054	51257.	2501.	.0374	812.	469.
.0059	45976.	2385.	.0386	1141.	510.
.0063	43236.	2314.	.0398	1131.	566.
.0068	33101.	2107.	.0410	533.	377.
.0073	26261.	1881.	.0422	2746.	868.
.0078	24801.	1859.	.0435	518.	366.
.0084	21143.	1793.	.0447	298.	298.
.0089	17196.	1662.	.0460	519.	367.
.0095	14496.	1591.	.0473	733.	423.
.0101	9922.	1338.	.0486	475.	336.
.0107	11105.	1458.	.0500	288.	288.
.0113	6968.	1102.	.0513	257.	257.
.0120	6151.	1105.	.0527	0.	0.
.0127	3026.	756.	.0541	1501.	750.
.0133	2910.	778.	.0555	836.	483.
.0140	2830.	817.	.0569	301.	301.
.0148	3230.	863.	.0583	384.	384.
.0155	1979.	660.	.0598	0.	0.
.0163	1648.	623.	.0613	331.	331.
.0170	906.	453.	.0628	336.	336.
.0178	992.	496.	.0643	424.	424.
.0186	964.	482.	.0658	1123.	648.
.0195	233.	233.	.0673	488.	488.
.0203	1771.	669.	.0689	552.	552.
.0212	1409.	575.	.0705	1837.	1061.
.0221	2351.	784.	.0721	1087.	769.
.0230	3292.	993.	.0737	599.	599.

PIPLUS - PB: 70 GEV/C
 UNITS: T: (GEV/C)**2; DSIGMA/DT: MILLIBARNS/((GEV/C)**2)

-T	DSIGMA/DT	ERROR	-T	DSIGMA/DT	ERROR
.0012	1012490.	25157.	.0239	2953.	1476.
.0014	699965.	19919.	.0248	1498.	1059.
.0016	530502.	16490.	.0258	3294.	1647.
.0019	416727.	14379.	.0267	937.	937.
.0022	344836.	12517.	.0277	3645.	1823.
.0025	286874.	11192.	.0287	2588.	1494.
.0028	224845.	9596.	.0298	1425.	1008.
.0031	178572.	8474.	.0308	819.	819.
.0034	165175.	7910.	.0319	2395.	1383.
.0038	126998.	6877.	.0329	802.	802.
.0042	112670.	6379.	.0340	0.	0.
.0046	90673.	5757.	.0352	985.	985.
.0050	77035.	5182.	.0363	0.	0.
.0054	61929.	4629.	.0374	0.	0.
.0059	51509.	4348.	.0386	0.	0.
.0063	41467.	3817.	.0398	0.	0.
.0068	39050.	3758.	.0410	0.	0.
.0073	27020.	3184.	.0422	2978.	1200.
.0078	18004.	2684.	.0435	837.	837.
.0084	16186.	2698.	.0447	0.	0.
.0089	10402.	2080.	.0460	0.	0.
.0095	8466.	1995.	.0473	0.	0.
.0101	6108.	1842.	.0486	0.	0.
.0107	4772.	1591.	.0500	0.	0.
.0113	2731.	1221.	.0513	765.	765.
.0120	1617.	934.	.0527	0.	0.
.0127	1782.	1029.	.0541	1712.	1210.
.0133	2385.	1192.	.0555	831.	831.
.0140	3131.	1400.	.0569	0.	0.
.0148	1127.	797.	.0583	0.	0.
.0155	1263.	893.	.0598	1767.	1250.
.0163	1271.	899.	.0613	0.	0.
.0170	4238.	1730.	.0628	1050.	1050.
.0178	2443.	1222.	.0643	0.	0.
.0186	3184.	1592.	.0658	1292.	1292.
.0195	4556.	1722.	.0673	0.	0.
.0203	6584.	2082.	.0689	0.	0.
.0212	2959.	1479.	.0705	1643.	1643.
.0221	2835.	1418.	.0721	0.	0.
.0230	2900.	1450.	.0737	0.	0.

KPLUS - PB: 70 GEV/C
 UNITS: T: (GEV/C)**2; DSIGMA/DT: MILLIBARNS/((GEV/C)**2)

-T	DSIGMA/DT	ERROR	-T	DSIGMA/DT	ERROR
.0012	1024274.	31911.	.0239	1146.	1146.
.0014	725595.	25090.	.0248	2326.	1645.
.0016	543116.	20706.	.0258	1279.	1279.
.0019	398691.	17404.	.0267	0.	0.
.0022	326931.	15232.	.0277	1415.	1415.
.0025	262382.	13252.	.0287	1339.	1339.
.0028	220042.	11830.	.0298	0.	0.
.0031	167661.	10205.	.0308	2543.	1798.
.0034	142134.	9296.	.0319	1240.	1240.
.0038	119131.	8300.	.0329	0.	0.
.0042	79193.	7035.	.0340	0.	0.
.0046	81097.	6666.	.0352	0.	0.
.0050	64411.	5905.	.0363	0.	0.
.0054	64468.	5885.	.0374	0.	0.
.0059	35005.	4342.	.0386	0.	0.
.0063	42017.	4788.	.0398	0.	0.
.0068	33126.	4313.	.0410	1313.	1313.
.0073	26224.	3909.	.0422	0.	0.
.0078	20502.	3569.	.0435	0.	0.
.0084	16359.	3275.	.0447	0.	0.
.0089	11630.	2741.	.0460	0.	0.
.0095	10955.	2829.	.0473	0.	0.
.0101	3449.	1725.	.0486	0.	0.
.0107	6268.	3262.	.0500	1170.	1170.
.0113	9330.	2613.	.0513	0.	0.
.0120	3348.	1674.	.0527	0.	0.
.0127	2767.	1597.	.0541	0.	0.
.0133	2777.	1603.	.0555	1291.	1291.
.0140	3889.	1945.	.0569	0.	0.
.0148	1751.	1238.	.0583	0.	0.
.0155	1961.	1386.	.0598	0.	0.
.0163	2961.	1710.	.0613	0.	0.
.0170	3290.	1899.	.0628	0.	0.
.0178	948.	948.	.0643	0.	0.
.0186	2472.	1748.	.0658	2007.	2007.
.0195	2021.	1429.	.0673	0.	0.
.0203	0.	0.	.0689	0.	0.
.0212	1149.	1149.	.0705	0.	0.
.0221	3302.	1906.	.0721	0.	0.
.0230	0.	0.	.0737	2561.	2561.

PPLUS - PB: 70 GEV/C
 UNITS: T: (GEV/C)**2; DSIGMA/DT: MILLIBARNS/((GEV/C)**2)

-T	DSIGMA/DT	ERROR	-T	DSIGMA/DT	ERROR
.0012	1028753.	28843.	.0239	5421.	2213.
.0014	782617.	23522.	.0248	0.	0.
.0016	572163.	19420.	.0258	3023.	1746.
.0019	450948.	16475.	.0267	4587.	2293.
.0022	354458.	14295.	.0277	1115.	1115.
.0025	300516.	12677.	.0287	3167.	1828.
.0028	253951.	11369.	.0298	0.	0.
.0031	233745.	10625.	.0308	0.	0.
.0034	191946.	9434.	.0319	0.	0.
.0038	157702.	8478.	.0329	0.	0.
.0042	129934.	7578.	.0340	1040.	1040.
.0046	95874.	6435.	.0352	1206.	1206.
.0050	94415.	6567.	.0363	1235.	1235.
.0054	64359.	5220.	.0374	0.	0.
.0059	54184.	4940.	.0386	0.	0.
.0063	49080.	4632.	.0398	3081.	1779.
.0068	37463.	4255.	.0410	1034.	1034.
.0073	29394.	3674.	.0422	0.	0.
.0078	23503.	3392.	.0435	1025.	1025.
.0084	18708.	3208.	.0447	0.	0.
.0089	12731.	2546.	.0460	0.	0.
.0095	11512.	2574.	.0473	0.	0.
.0101	6116.	2039.	.0486	0.	0.
.0107	6489.	2052.	.0500	0.	0.
.0113	3343.	1495.	.0513	0.	0.
.0120	3958.	1616.	.0527	0.	0.
.0127	5988.	1923.	.0541	2095.	1481.
.0133	5107.	1930.	.0555	1017.	1017.
.0140	5364.	2027.	.0569	0.	0.
.0148	2759.	1380.	.0583	0.	0.
.0155	5409.	2044.	.0598	0.	0.
.0163	4668.	1906.	.0613	0.	0.
.0170	5186.	2117.	.0628	1286.	1286.
.0178	2243.	1295.	.0643	0.	0.
.0186	4871.	2178.	.0658	0.	0.
.0195	5575.	2107.	.0673	1440.	1440.
.0203	5641.	2132.	.0689	0.	0.
.0212	7242.	2560.	.0705	0.	0.
.0221	3470.	1735.	.0721	0.	0.
.0230	3549.	1774.	.0737	0.	0.

PIMINUS - BE: 70 GEV/C
 UNITS: T: (GEV/C)**2; DSIGMA/DT: MILLIBARNS/((GEV/C)**2)

-T	DSIGMA/DT	ERROR	-T	DSIGMA/DT	ERROR
.0012	4365.	174.	.0239	477.	65.
.0014	3638.	152.	.0248	334.	53.
.0016	2751.	126.	.0258	440.	64.
.0019	2243.	111.	.0267	413.	58.
.0022	1964.	100.	.0277	403.	61.
.0025	1845.	95.	.0287	262.	46.
.0028	1644.	88.	.0298	356.	56.
.0031	1663.	87.	.0308	273.	48.
.0034	1558.	82.	.0319	232.	47.
.0038	1460.	78.	.0329	273.	46.
.0042	1207.	70.	.0340	328.	56.
.0046	1343.	73.	.0352	251.	48.
.0050	1271.	71.	.0363	232.	46.
.0054	1241.	69.	.0374	190.	42.
.0059	1210.	68.	.0386	221.	44.
.0063	1050.	64.	.0398	235.	45.
.0068	1064.	65.	.0410	157.	38.
.0073	989.	64.	.0422	255.	47.
.0078	1061.	68.	.0435	190.	41.
.0084	892.	65.	.0447	175.	40.
.0089	959.	69.	.0460	118.	32.
.0095	772.	64.	.0473	158.	36.
.0101	781.	67.	.0486	116.	33.
.0107	794.	69.	.0500	148.	37.
.0113	882.	75.	.0513	122.	33.
.0120	846.	74.	.0527	104.	33.
.0127	647.	65.	.0541	189.	44.
.0133	674.	68.	.0555	77.	27.
.0140	685.	70.	.0569	151.	42.
.0148	675.	71.	.0583	154.	43.
.0155	635.	65.	.0598	146.	41.
.0163	569.	65.	.0613	80.	30.
.0170	594.	67.	.0628	136.	41.
.0178	456.	60.	.0643	87.	36.
.0186	520.	64.	.0658	76.	34.
.0195	559.	67.	.0673	115.	41.
.0203	406.	59.	.0689	92.	37.
.0212	482.	62.	.0705	89.	45.
.0221	383.	56.	.0721	182.	61.
.0230	467.	64.	.0737	68.	39.

KMINUS - BE: 70 GEV/C
 UNITS: T: (GEV/C)**2; DSIGMA/DT: MILLIBARNS/((GEV/C)**2)

-T	DSIGMA/DT	ERROR	-T	DSIGMA/DT	ERROR
.0012	3976.	222.	.0239	394.	79.
.0014	3253.	192.	.0248	238.	60.
.0016	2437.	161.	.0258	117.	44.
.0019	1823.	134.	.0267	265.	63.
.0022	1799.	128.	.0277	284.	69.
.0025	1534.	116.	.0287	298.	65.
.0028	1134.	98.	.0298	223.	60.
.0031	1512.	110.	.0308	274.	65.
.0034	1153.	94.	.0319	155.	52.
.0038	1067.	90.	.0329	195.	52.
.0042	1027.	86.	.0340	172.	54.
.0046	1012.	85.	.0352	83.	37.
.0050	1058.	86.	.0363	182.	55.
.0054	871.	77.	.0374	129.	46.
.0059	830.	75.	.0386	111.	42.
.0063	800.	74.	.0398	171.	52.
.0068	794.	75.	.0410	82.	37.
.0073	792.	76.	.0422	157.	50.
.0078	735.	75.	.0435	194.	56.
.0084	717.	77.	.0447	198.	57.
.0089	634.	86.	.0460	151.	48.
.0095	795.	87.	.0473	74.	33.
.0101	534.	74.	.0486	103.	42.
.0107	544.	76.	.0500	166.	52.
.0113	473.	73.	.0513	141.	47.
.0120	535.	79.	.0527	130.	49.
.0127	711.	91.	.0541	168.	56.
.0133	454.	75.	.0555	68.	34.
.0140	580.	85.	.0569	62.	36.
.0148	415.	75.	.0583	85.	42.
.0155	482.	76.	.0598	60.	35.
.0163	491.	80.	.0613	123.	50.
.0170	567.	71.	.0628	88.	44.
.0178	491.	83.	.0643	52.	37.
.0186	300.	65.	.0658	27.	27.
.0195	257.	61.	.0673	77.	45.
.0203	211.	57.	.0689	27.	27.
.0212	268.	62.	.0705	40.	40.
.0221	218.	56.	.0721	34.	36.
.0230	283.	67.	.0737	40.	40.

PHINUS - BE: 70 GEV/C
 UNITS: T: (GEV/C)**2; DSIGMA/DT: MILLIBARNS/((GEV/C)**2)

-T	DSIGMA/DT	ERROR	-T	DSIGMA/DT	ERROR
.0012	7022.	368.	.0239	1055.	161.
.0014	5400.	307.	.0248	1113.	161.
.0016	4504.	272.	.0258	1092.	168.
.0019	5059.	277.	.0267	711.	128.
.0022	4705.	261.	.0277	781.	142.
.0025	3964.	232.	.0287	718.	127.
.0028	3769.	221.	.0298	718.	133.
.0031	4293.	232.	.0308	545.	114.
.0034	3660.	209.	.0319	484.	114.
.0038	3560.	204.	.0329	412.	94.
.0042	3354.	194.	.0340	697.	137.
.0046	3115.	185.	.0352	438.	106.
.0050	3111.	185.	.0363	516.	115.
.0054	2824.	174.	.0374	579.	121.
.0059	2944.	177.	.0386	516.	113.
.0063	2885.	176.	.0398	387.	97.
.0068	2893.	176.	.0410	436.	106.
.0073	2315.	162.	.0422	269.	81.
.0078	2503.	174.	.0435	351.	94.
.0084	2361.	175.	.0447	410.	103.
.0089	2444.	184.	.0460	352.	91.
.0095	2339.	187.	.0473	392.	95.
.0101	2099.	183.	.0486	349.	97.
.0107	2239.	193.	.0500	361.	96.
.0113	1874.	181.	.0513	364.	94.
.0120	2061.	193.	.0527	405.	108.
.0127	1978.	189.	.0541	175.	71.
.0133	1605.	175.	.0555	186.	70.
.0140	1863.	191.	.0569	193.	79.
.0148	1647.	185.	.0583	230.	87.
.0155	1257.	154.	.0598	313.	99.
.0163	1663.	186.	.0613	64.	45.
.0170	1649.	187.	.0628	241.	91.
.0178	1573.	185.	.0643	242.	99.
.0186	1777.	199.	.0658	211.	94.
.0195	1044.	152.	.0673	200.	90.
.0203	1198.	168.	.0689	254.	104.
.0212	1449.	178.	.0705	249.	124.
.0221	1041.	153.	.0721	56.	56.
.0230	857.	145.	.0737	252.	126.

PHINUS - C: 70 GEV/C
 UNITS: T: (GEV/C)**2; DSIGMA/DT: MILLIBARNS/((GEV/C)**2)

-T	DSIGMA/DT	ERROR	-T	DSIGMA/DT	ERROR
.0012	8612.	335.	.0239	712.	106.
.0014	6347.	275.	.0248	623.	105.
.0016	5282.	241.	.0258	481.	84.
.0019	4367.	212.	.0267	481.	93.
.0022	3586.	186.	.0277	573.	100.
.0025	3213.	172.	.0287	656.	104.
.0028	2780.	156.	.0298	396.	81.
.0031	2508.	146.	.0308	455.	91.
.0034	2484.	142.	.0319	450.	92.
.0038	2556.	142.	.0329	357.	73.
.0042	2131.	128.	.0340	346.	77.
.0046	2108.	126.	.0352	307.	77.
.0050	2399.	133.	.0363	241.	62.
.0054	2002.	121.	.0374	406.	85.
.0059	1809.	115.	.0386	265.	64.
.0063	1872.	117.	.0398	263.	68.
.0068	1630.	110.	.0410	449.	86.
.0073	1639.	114.	.0422	202.	61.
.0078	1802.	121.	.0435	186.	56.
.0084	1605.	119.	.0447	119.	45.
.0089	1250.	107.	.0460	230.	64.
.0095	1431.	119.	.0473	158.	53.
.0101	1541.	130.	.0486	151.	48.
.0107	1364.	126.	.0500	134.	47.
.0113	1083.	114.	.0513	193.	56.
.0120	1073.	114.	.0527	93.	42.
.0127	1071.	117.	.0541	104.	43.
.0133	1256.	127.	.0555	140.	53.
.0140	1205.	125.	.0569	44.	31.
.0148	1129.	122.	.0583	44.	31.
.0155	924.	114.	.0598	185.	62.
.0163	831.	106.	.0613	0.	0.
.0170	770.	106.	.0628	146.	55.
.0178	1085.	135.	.0643	137.	56.
.0186	712.	101.	.0658	55.	39.
.0195	944.	123.	.0673	128.	64.
.0203	797.	116.	.0689	46.	46.
.0212	781.	109.	.0705	89.	63.
.0221	619.	95.	.0721	113.	65.
.0230	656.	102.	.0737	119.	69.

KMINUS - C: 70 GEV/C
 UNITS: T: (GEV/C)**2; DSIGMA/DT: MILLIBARNS/((GEV/C)**2)

-T	DSIGMA/DT	ERROR	-T	DSIGMA/DT	ERROR
.0012	8404.	456.	.0239	330.	99.
.0014	5900.	365.	.0248	236.	89.
.0016	5583.	341.	.0258	359.	100.
.0019	3993.	280.	.0267	203.	83.
.0022	4034.	271.	.0277	658.	147.
.0025	3446.	246.	.0287	466.	120.
.0028	2791.	216.	.0298	501.	125.
.0031	2566.	202.	.0308	448.	124.
.0034	2083.	179.	.0319	319.	106.
.0038	2236.	183.	.0329	149.	69.
.0042	2113.	176.	.0340	360.	109.
.0046	1634.	152.	.0352	435.	126.
.0050	1928.	165.	.0363	213.	80.
.0054	1683.	152.	.0374	267.	95.
.0059	1913.	162.	.0386	207.	78.
.0063	1510.	145.	.0398	232.	88.
.0068	1544.	148.	.0410	220.	83.
.0073	1239.	136.	.0422	313.	104.
.0078	1117.	132.	.0435	128.	64.
.0084	1611.	164.	.0447	323.	102.
.0089	1288.	150.	.0460	168.	75.
.0095	1066.	141.	.0473	100.	58.
.0101	901.	138.	.0486	86.	49.
.0107	1270.	167.	.0500	127.	64.
.0113	1140.	161.	.0513	305.	96.
.0120	845.	139.	.0527	213.	87.
.0127	869.	145.	.0541	66.	47.
.0133	850.	144.	.0555	152.	76.
.0140	957.	153.	.0569	126.	72.
.0148	920.	151.	.0583	83.	59.
.0155	663.	133.	.0598	155.	78.
.0163	697.	134.	.0613	143.	82.
.0170	990.	165.	.0628	40.	40.
.0178	885.	167.	.0643	86.	61.
.0186	756.	143.	.0658	104.	74.
.0195	758.	152.	.0673	304.	136.
.0203	867.	167.	.0689	86.	86.
.0212	580.	130.	.0705	84.	84.
.0221	558.	125.	.0721	142.	101.
.0230	758.	152.	.0737	75.	75.

PHINUS - C: 70 GEV/C
 UNITS: T: (GEV/C)**2; DSIGMA/DT: MILLIBARNS/((GEV/C)**2)

-T	DSIGMA/DT	ERROR	-T	DSIGMA/DT	ERROR
.0012	12388.	673.	.0239	1376.	247.
.0014	10534.	591.	.0248	1696.	291.
.0016	7941.	493.	.0258	818.	183.
.0019	7851.	474.	.0267	1399.	244.
.0022	7265.	443.	.0277	973.	218.
.0025	7100.	429.	.0287	991.	216.
.0028	6512.	399.	.0298	787.	191.
.0031	6274.	385.	.0308	969.	222.
.0034	5434.	352.	.0319	683.	187.
.0038	5024.	333.	.0329	459.	138.
.0042	5263.	337.	.0340	582.	168.
.0046	5951.	354.	.0352	430.	152.
.0050	5069.	323.	.0363	855.	196.
.0054	4134.	291.	.0374	396.	140.
.0059	4807.	313.	.0386	175.	87.
.0063	4552.	306.	.0398	638.	177.
.0068	5009.	324.	.0410	326.	123.
.0073	4331.	309.	.0422	309.	126.
.0078	4316.	315.	.0435	426.	142.
.0084	3516.	294.	.0447	479.	151.
.0089	3297.	291.	.0460	547.	165.
.0095	4151.	339.	.0473	98.	70.
.0101	3357.	322.	.0486	84.	60.
.0107	3921.	356.	.0500	141.	82.
.0113	2634.	309.	.0513	406.	135.
.0120	2365.	283.	.0527	315.	128.
.0127	2574.	303.	.0541	195.	97.
.0133	2838.	319.	.0555	450.	159.
.0140	2870.	323.	.0569	434.	164.
.0148	2245.	287.	.0583	62.	62.
.0155	1688.	257.	.0598	58.	58.
.0163	2369.	301.	.0613	211.	122.
.0170	1751.	267.	.0628	292.	131.
.0178	2666.	353.	.0643	192.	111.
.0186	2037.	285.	.0658	77.	77.
.0195	2198.	314.	.0673	270.	156.
.0203	2186.	322.	.0689	511.	256.
.0212	1417.	247.	.0705	250.	177.
.0221	1487.	248.	.0721	105.	105.
.0230	1211.	233.	.0737	111.	111.

PIMINUS - AL: 70 GEV/C
 UNITS: T: (GEV/C)**2; DSIGMA/DT: MILLIBARNS/((GEV/C)**2)

-T	DSIGMA/DT	ERROR	-T	DSIGMA/DT	ERROR
.0012	33897.	946.	.0239	808.	165.
.0014	27197.	609.	.0248	889.	174.
.0016	20178.	463.	.0258	737.	165.
.0019	15730.	376.	.0267	782.	156.
.0022	14210.	325.	.0277	594.	136.
.0025	12181.	275.	.0287	687.	158.
.0028	10928.	240.	.0298	521.	134.
.0031	10112.	217.	.0308	395.	110.
.0034	8398.	169.	.0319	348.	105.
.0038	8202.	159.	.0329	95.	55.
.0042	8027.	153.	.0340	334.	106.
.0046	7165.	129.	.0352	256.	91.
.0050	6637.	113.	.0363	151.	68.
.0054	6356.	104.	.0374	194.	87.
.0059	5711.	79.	.0386	164.	73.
.0063	5764.	79.	.0398	271.	96.
.0068	5104.	61.	.0410	221.	90.
.0073	4971.	61.	.0422	160.	71.
.0078	4594.	57.	.0435	96.	55.
.0084	4095.	47.	.0447	154.	69.
.0089	4464.	53.	.0460	62.	44.
.0095	3685.	47.	.0473	109.	63.
.0101	3702.	61.	.0486	201.	82.
.0107	3471.	57.	.0500	193.	79.
.0113	3654.	61.	.0513	146.	65.
.0120	2351.	47.	.0527	91.	53.
.0127	2811.	66.	.0541	61.	43.
.0133	2772.	66.	.0555	213.	87.
.0140	2382.	57.	.0569	191.	85.
.0148	2365.	57.	.0583	75.	53.
.0155	2262.	63.	.0598	195.	97.
.0163	1784.	47.	.0613	132.	76.
.0170	1933.	53.	.0628	161.	93.
.0178	1199.	37.	.0643	55.	55.
.0186	1641.	47.	.0658	104.	74.
.0195	1370.	37.	.0673	338.	151.
.0203	1154.	37.	.0689	106.	75.
.0212	972.	37.	.0705	138.	97.
.0221	1081.	47.	.0721	376.	153.
.0230	905.	37.	.0737	78.	78.

KMINUS - AL: 70 GEV/C
 UNITS: T: (GEV/C)**2; DSIGMA/DT: MILLIBARNS/((GEV/C)**2)

-T	DSIGMA/DT	ERROR	-T	DSIGMA/DT	ERROR
.0012	33355.	911.	.0239	657.	143.
.0014	25975.	760.	.0248	794.	159.
.0016	19817.	635.	.0258	685.	153.
.0019	15697.	559.	.0267	756.	148.
.0022	13848.	499.	.0277	407.	109.
.0025	11811.	455.	.0287	639.	146.
.0028	9862.	405.	.0298	484.	125.
.0031	9899.	393.	.0308	650.	136.
.0034	7669.	340.	.0319	441.	114.
.0038	7534.	334.	.0329	235.	83.
.0042	6984.	319.	.0340	218.	82.
.0046	6293.	298.	.0352	327.	99.
.0050	5949.	286.	.0363	112.	56.
.0054	5407.	270.	.0374	216.	88.
.0059	5088.	264.	.0386	274.	91.
.0063	4462.	248.	.0398	157.	70.
.0068	4729.	261.	.0410	240.	91.
.0073	4547.	259.	.0422	119.	59.
.0078	4038.	250.	.0435	89.	51.
.0084	3940.	257.	.0447	143.	64.
.0089	3076.	235.	.0460	58.	41.
.0095	2885.	232.	.0473	101.	58.
.0101	2564.	231.	.0486	156.	70.
.0107	2491.	226.	.0500	269.	90.
.0113	2480.	249.	.0513	27.	27.
.0120	2477.	227.	.0527	57.	40.
.0127	2006.	216.	.0541	143.	64.
.0133	1687.	199.	.0555	132.	66.
.0140	2021.	221.	.0569	142.	71.
.0148	1862.	219.	.0583	105.	61.
.0155	2244.	253.	.0598	136.	78.
.0163	1312.	180.	.0613	82.	58.
.0170	1237.	184.	.0628	100.	70.
.0178	1728.	219.	.0643	152.	88.
.0186	1215.	177.	.0658	97.	68.
.0195	1565.	204.	.0673	126.	89.
.0203	831.	149.	.0689	0.	0.
.0212	1186.	183.	.0705	192.	111.
.0221	883.	164.	.0721	58.	58.
.0230	1160.	189.	.0737	72.	72.

PIMINUS - AL: 70 GEV/C
 UNITS: T: (GEV/C)**2; DSIGMA/DT: MILLIBARNS/((GEV/C)**2)

-T	DSIGMA/DT	ERROR	-T	DSIGMA/DT	ERROR
.0012	42873.	1228.	.0239	1971.	297.
.0014	35144.	1049.	.0248	1273.	241.
.0016	30782.	944.	.0258	637.	177.
.0019	26504.	852.	.0267	1206.	224.
.0022	23755.	786.	.0277	873.	190.
.0025	21320.	726.	.0287	963.	245.
.0028	20337.	691.	.0298	739.	185.
.0031	18509.	646.	.0308	728.	172.
.0034	19553.	650.	.0319	926.	197.
.0038	16793.	595.	.0329	588.	157.
.0042	16799.	588.	.0340	801.	189.
.0046	15453.	558.	.0352	383.	128.
.0050	14943.	546.	.0363	442.	133.
.0054	13214.	510.	.0374	361.	136.
.0059	12267.	491.	.0386	393.	131.
.0063	11746.	481.	.0398	450.	142.
.0068	10792.	472.	.0410	245.	110.
.0073	10732.	476.	.0422	340.	120.
.0078	10141.	474.	.0435	340.	120.
.0084	9430.	476.	.0447	327.	116.
.0089	8701.	472.	.0460	249.	102.
.0095	8578.	478.	.0473	241.	108.
.0101	7031.	453.	.0486	268.	109.
.0107	6838.	447.	.0500	343.	121.
.0113	7440.	496.	.0513	271.	103.
.0120	6553.	442.	.0527	284.	107.
.0127	5708.	436.	.0541	245.	100.
.0133	4325.	381.	.0555	284.	116.
.0140	4958.	413.	.0569	203.	102.
.0148	4330.	400.	.0583	250.	112.
.0155	5326.	465.	.0598	519.	183.
.0163	3295.	342.	.0613	175.	101.
.0170	3461.	369.	.0628	428.	175.
.0178	4507.	424.	.0643	581.	205.
.0186	2035.	274.	.0658	138.	98.
.0195	2809.	326.	.0673	360.	180.
.0203	2265.	295.	.0689	141.	100.
.0212	1818.	271.	.0705	183.	129.
.0221	1830.	282.	.0721	167.	118.
.0230	2037.	307.	.0737	309.	179.

PIMINUS - CU: 70 GEV/C
 UNITS: T: (GEV/C)**2; DSIGMA/DT: MILLIBARNS/((GEV/C)**2)

-T	DSIGMA/DT	ERROR	-T	DSIGMA/DT	ERROR
.0012	149306.	4688.	.0239	772.	386.
.0014	108656.	3817.	.0248	342.	242.
.0016	79130.	3126.	.0258	524.	303.
.0019	61537.	2679.	.0267	0.	0.
.0022	53757.	2411.	.0277	574.	332.
.0025	46506.	2200.	.0287	362.	256.
.0028	39500.	1966.	.0298	0.	0.
.0031	35021.	1843.	.0308	158.	158.
.0034	33189.	1742.	.0319	0.	0.
.0038	31822.	1673.	.0329	0.	0.
.0042	24002.	1432.	.0340	0.	0.
.0046	23987.	1423.	.0352	525.	303.
.0050	21826.	1341.	.0363	195.	195.
.0054	18900.	1238.	.0374	509.	294.
.0059	17167.	1182.	.0386	376.	266.
.0063	17785.	1202.	.0398	186.	186.
.0068	14323.	1092.	.0410	358.	253.
.0073	14659.	1124.	.0422	0.	0.
.0078	11872.	1049.	.0435	0.	0.
.0084	11074.	1046.	.0447	180.	180.
.0089	10950.	1084.	.0460	525.	303.
.0095	9303.	1034.	.0473	0.	0.
.0101	6736.	884.	.0486	357.	252.
.0107	6548.	899.	.0500	783.	391.
.0113	6155.	888.	.0513	0.	0.
.0120	5605.	865.	.0527	772.	446.
.0127	3215.	670.	.0541	667.	385.
.0133	4080.	800.	.0555	185.	185.
.0140	5394.	939.	.0569	0.	0.
.0148	3536.	772.	.0583	250.	250.
.0155	3677.	767.	.0598	523.	370.
.0163	2852.	672.	.0613	253.	253.
.0170	1565.	495.	.0628	0.	0.
.0178	2703.	676.	.0643	0.	0.
.0186	1925.	581.	.0658	0.	0.
.0195	1107.	418.	.0673	816.	577.
.0203	1184.	447.	.0689	428.	428.
.0212	169.	169.	.0705	360.	360.
.0221	988.	442.	.0721	0.	0.
.0230	571.	330.	.0737	0.	0.

KMINUS - CU: 70 GEV/C
 UNITS: T: (GEV/C)**2; DSIGMA/DT: MILLIBARNS/((GEV/C)**2)

-T	DSIGMA/DT	ERROR	-T	DSIGMA/DT	ERROR
.0012	149993.	4525.	.0239	712.	356.
.0014	105302.	3606.	.0248	790.	353.
.0016	85667.	3130.	.0258	161.	161.
.0019	62302.	2609.	.0267	0.	0.
.0022	52459.	2295.	.0277	177.	177.
.0025	42840.	2042.	.0287	334.	236.
.0028	37485.	1846.	.0298	322.	228.
.0031	32666.	1678.	.0308	0.	0.
.0034	27415.	1521.	.0319	0.	0.
.0038	27548.	1501.	.0329	0.	0.
.0042	22303.	1326.	.0340	851.	381.
.0046	20650.	1269.	.0352	162.	162.
.0050	17630.	1157.	.0363	359.	254.
.0054	17438.	1142.	.0374	157.	157.
.0059	14487.	1043.	.0386	347.	246.
.0063	13637.	1011.	.0398	0.	0.
.0068	12984.	999.	.0410	0.	0.
.0073	12650.	1003.	.0422	369.	261.
.0078	10696.	957.	.0435	508.	293.
.0084	9031.	908.	.0447	0.	0.
.0089	8716.	929.	.0460	0.	0.
.0095	7206.	874.	.0473	358.	253.
.0101	7037.	888.	.0486	329.	233.
.0107	7295.	912.	.0500	542.	313.
.0113	4851.	758.	.0513	175.	175.
.0120	4679.	759.	.0527	0.	0.
.0127	4127.	730.	.0541	410.	290.
.0133	4053.	766.	.0555	513.	296.
.0140	3167.	691.	.0569	190.	190.
.0148	3884.	777.	.0583	693.	400.
.0155	2508.	608.	.0598	0.	0.
.0163	2193.	566.	.0613	0.	0.
.0170	2165.	559.	.0628	215.	215.
.0178	935.	382.	.0643	0.	0.
.0186	1292.	457.	.0658	0.	0.
.0195	875.	357.	.0673	0.	0.
.0203	936.	302.	.0689	395.	395.
.0212	1249.	442.	.0705	0.	0.
.0221	1276.	482.	.0721	0.	0.
.0230	527.	304.	.0737	0.	0.

PMINUS - CU: 70 GEV/C
 UNITS: T: (GEV/C)**2; DSIGMA/DT: MILLIBARNS/((GEV/C)**2)

-T	DSIGMA/DT	ERROR	-T	DSIGMA/DT	ERROR
.0012	165648.	5722.	.0239	1032.	516.
.0014	126148.	4724.	.0248	457.	323.
.0016	107058.	4203.	.0258	0.	0.
.0019	93994.	3815.	.0267	242.	242.
.0022	85095.	3515.	.0277	256.	256.
.0025	71649.	3164.	.0287	0.	0.
.0028	67451.	2967.	.0298	1166.	521.
.0031	56425.	2654.	.0308	211.	211.
.0034	49603.	2462.	.0319	1147.	513.
.0038	50245.	2437.	.0329	780.	451.
.0042	44287.	2248.	.0340	1232.	551.
.0046	38148.	2075.	.0352	468.	331.
.0050	36403.	2010.	.0363	1300.	581.
.0054	36502.	1997.	.0374	1568.	600.
.0059	33268.	1902.	.0386	252.	252.
.0063	27347.	1723.	.0398	1246.	557.
.0068	25816.	1695.	.0410	479.	338.
.0073	22124.	1597.	.0422	1069.	534.
.0078	21555.	1635.	.0435	0.	0.
.0084	18496.	1563.	.0447	0.	0.
.0089	18648.	1636.	.0460	936.	468.
.0095	14274.	1480.	.0473	777.	448.
.0101	12531.	1419.	.0486	0.	0.
.0107	13867.	1513.	.0500	261.	261.
.0113	8739.	1224.	.0513	508.	359.
.0120	8203.	1209.	.0527	688.	486.
.0127	5043.	971.	.0541	0.	0.
.0133	7548.	1258.	.0555	990.	495.
.0140	5897.	1135.	.0569	276.	276.
.0148	6975.	1253.	.0583	0.	0.
.0155	2991.	799.	.0598	350.	350.
.0163	2964.	792.	.0613	0.	0.
.0170	5645.	1086.	.0628	0.	0.
.0178	2483.	749.	.0643	656.	464.
.0186	1403.	573.	.0658	0.	0.
.0195	211.	211.	.0673	0.	0.
.0203	1130.	505.	.0689	0.	0.
.0212	1131.	506.	.0705	0.	0.
.0221	1584.	646.	.0721	0.	0.
.0230	763.	441.	.0737	711.	711.

PIMINUS - SN: 70 GEV/C
 UNITS: T: (GEV/C)**2; DSIGMA/DT: MILLIBARNS/((GEV/C)**2)

-T	DSIGMA/DT	ERROR	-T	DSIGMA/DT	ERROR
.0012	393679.	8115.	.0239	414.	293.
.0014	270373.	6435.	.0218	595.	344.
.0016	204138.	5341.	.0258	883.	441.
.0019	156820.	4581.	.0267	1428.	540.
.0022	125098.	3939.	.0277	1160.	522.
.0025	111697.	3636.	.0287	819.	410.
.0028	91302.	3219.	.0298	1322.	540.
.0031	79860.	2968.	.0308	1397.	570.
.0034	70503.	2708.	.0319	889.	445.
.0038	62408.	2508.	.0329	994.	497.
.0042	51021.	2231.	.0340	1655.	626.
.0046	45736.	2090.	.0352	1062.	531.
.0050	43855.	2038.	.0363	428.	303.
.0054	37997.	1888.	.0374	1581.	598.
.0059	31974.	1712.	.0386	206.	206.
.0063	25643.	1546.	.0398	0.	0.
.0068	22698.	1407.	.0410	1312.	536.
.0073	19897.	1414.	.0422	1175.	526.
.0078	15428.	1290.	.0435	198.	198.
.0084	13173.	1202.	.0447	621.	359.
.0089	12287.	1193.	.0460	0.	0.
.0095	12167.	1229.	.0473	476.	337.
.0101	9112.	1097.	.0486	234.	234.
.0107	6987.	988.	.0500	233.	233.
.0113	3931.	771.	.0513	247.	247.
.0120	4729.	799.	.0527	504.	356.
.0127	4517.	839.	.0541	705.	407.
.0133	2610.	674.	.0555	0.	0.
.0140	1835.	553.	.0569	0.	0.
.0148	1106.	452.	.0583	564.	399.
.0155	1846.	584.	.0598	487.	344.
.0163	980.	400.	.0613	0.	0.
.0170	802.	401.	.0628	0.	0.
.0178	1139.	465.	.0643	0.	0.
.0186	423.	299.	.0658	859.	496.
.0195	784.	392.	.0673	0.	0.
.0203	376.	266.	.0689	0.	0.
.0212	1291.	527.	.0705	0.	0.
.0221	1361.	514.	.0721	0.	0.
.0230	992.	444.	.0737	0.	0.

KMINUS - SN: 70 GEV/C
 UNITS: T: (GEV/C)**2; DSIGMA/DT: MILLIBARNS/((GEV/C)**2)

-T	DSIGMA/DT	ERROR	-T	DSIGMA/DT	ERROR
.0012	413922.	8080.	.0239	387.	274.
.0014	294046.	6469.	.0248	556.	321.
.0016	223038.	5411.	.0258	825.	413.
.0019	158041.	4475.	.0267	572.	330.
.0022	129742.	3878.	.0277	437.	309.
.0025	101364.	3383.	.0287	1340.	507.
.0028	89064.	3090.	.0298	412.	291.
.0031	76900.	2784.	.0308	453.	377.
.0034	67097.	2554.	.0319	832.	416.
.0038	56894.	2333.	.0329	2325.	735.
.0042	46384.	2075.	.0340	221.	221.
.0046	43841.	1979.	.0352	497.	351.
.0050	38620.	1850.	.0363	600.	347.
.0054	31761.	1669.	.0374	634.	366.
.0059	31700.	1648.	.0386	771.	386.
.0063	26509.	1520.	.0398	557.	322.
.0068	21681.	1405.	.0410	204.	204.
.0073	18325.	1312.	.0422	1319.	538.
.0078	17757.	1338.	.0435	370.	262.
.0084	14372.	1215.	.0447	581.	335.
.0089	9431.	1011.	.0460	537.	310.
.0095	9636.	1058.	.0473	445.	315.
.0101	8946.	1115.	.0486	0.	0.
.0107	3659.	692.	.0500	218.	218.
.0113	5514.	883.	.0513	0.	0.
.0120	3538.	669.	.0527	0.	0.
.0127	3496.	714.	.0541	0.	0.
.0133	1464.	488.	.0555	188.	188.
.0140	2964.	680.	.0569	481.	340.
.0148	1379.	488.	.0583	264.	264.
.0155	1208.	437.	.0598	227.	227.
.0163	917.	374.	.0613	0.	0.
.0170	750.	375.	.0628	384.	384.
.0178	1243.	470.	.0643	562.	397.
.0186	1187.	485.	.0658	0.	0.
.0195	367.	259.	.0673	0.	0.
.0203	351.	248.	.0689	553.	391.
.0212	0.	0.	.0705	402.	402.
.0221	545.	315.	.0721	0.	0.
.0230	928.	415.	.0737	0.	0.

MINUS - SM: 70 GEV/C
 UNITS: T: (GEV/C)**2; DSIGMA/DT: MILLIBARNS/((GEV/C)**2)

-T	DSIGMA/DT	ERROR	-T	DSIGMA/DT	ERROR
.0012	424412.	9767.	.0239	2218.	784.
.0014	324850.	8081.	.0248	2124.	751.
.0016	267069.	7067.	.0258	2363.	835.
.0019	207081.	6036.	.0267	2184.	772.
.0022	165635.	5285.	.0277	1876.	766.
.0025	149578.	4808.	.0287	975.	948.
.0028	138520.	4581.	.0298	1179.	590.
.0031	113448.	4067.	.0308	1870.	763.
.0034	106737.	3854.	.0319	1488.	665.
.0038	90341.	3513.	.0329	2329.	880.
.0042	78854.	3209.	.0340	633.	448.
.0046	72068.	3035.	.0352	1777.	795.
.0050	61114.	2831.	.0363	2005.	758.
.0054	56767.	2719.	.0374	1814.	740.
.0059	46346.	2304.	.0386	1104.	552.
.0063	45548.	2384.	.0398	797.	460.
.0068	37416.	2209.	.0410	1463.	654.
.0073	27972.	1940.	.0422	1573.	703.
.0078	26422.	1953.	.0435	1323.	592.
.0084	19685.	1701.	.0447	277.	277.
.0089	16133.	1582.	.0460	1026.	513.
.0095	15784.	1619.	.0473	637.	450.
.0101	8581.	1334.	.0486	313.	313.
.0107	8603.	1268.	.0500	936.	540.
.0113	5058.	1012.	.0513	0.	0.
.0120	4339.	886.	.0527	337.	337.
.0127	3127.	807.	.0541	943.	544.
.0133	2794.	807.	.0555	539.	381.
.0140	1339.	547.	.0569	688.	487.
.0148	1481.	604.	.0583	0.	0.
.0155	1976.	699.	.0598	326.	326.
.0163	1093.	489.	.0613	0.	0.
.0170	1877.	710.	.0628	0.	0.
.0178	508.	359.	.0643	402.	402.
.0186	1415.	633.	.0658	766.	542.
.0195	2887.	870.	.0673	449.	449.
.0203	1257.	562.	.0689	0.	0.
.0212	2016.	762.	.0705	575.	575.
.0221	780.	451.	.0721	520.	520.
.0230	1859.	702.	.0737	0.	0.

MINUS - PB: 70 GEV/C
 UNITS: T: (GEV/C)**2; DSIGMA/DT: MILLIBARNS/((GEV/C)**2)

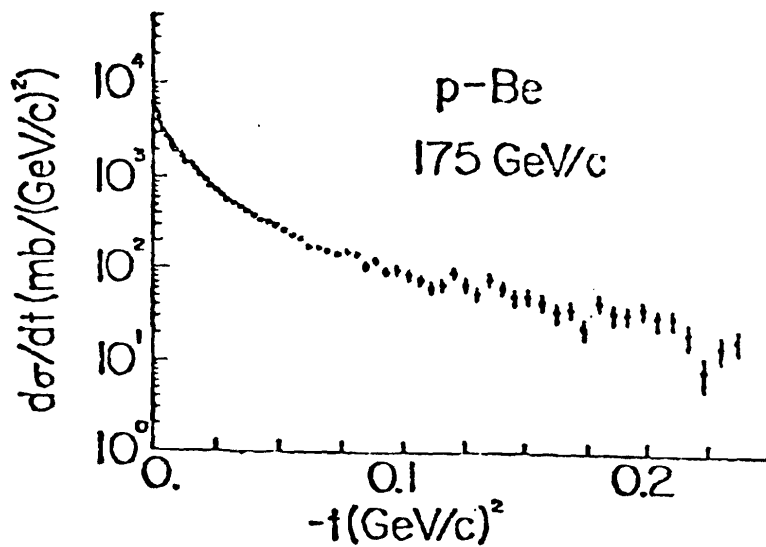
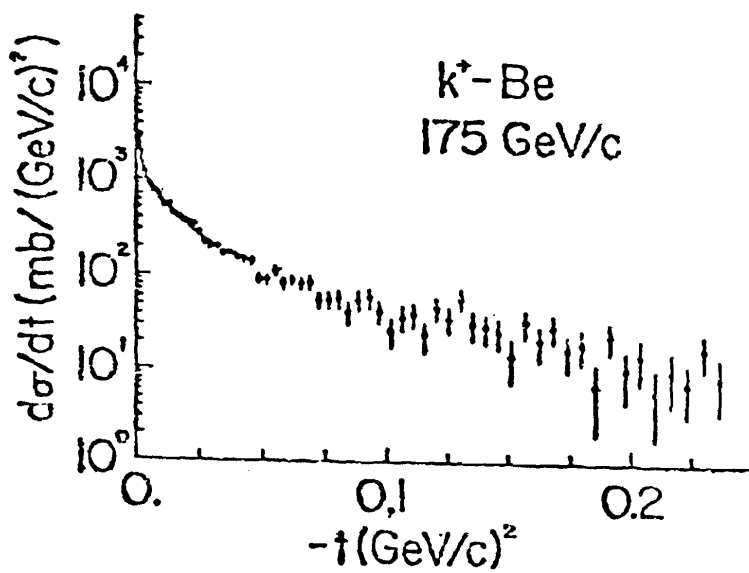
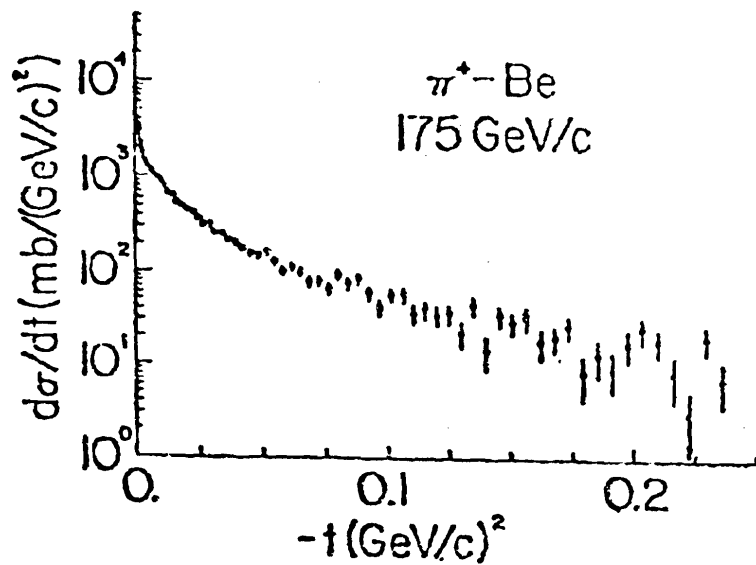
-T	DSIGMA/DT	ERROR	-T	DSIGMA/DT	ERROR
.0012	923296.	26400.	.0239	2457.	1419.
.0014	651080.	21236.	.0248	1017.	1017.
.0016	490502.	17578.	.0258	0.	0.
.0019	360660.	14747.	.0267	3719.	1860.
.0022	294151.	12790.	.0277	0.	0.
.0025	221181.	10729.	.0287	0.	0.
.0028	196891.	10044.	.0298	1027.	1027.
.0031	161473.	8983.	.0308	2040.	1443.
.0034	134501.	7926.	.0319	0.	0.
.0038	119947.	7354.	.0329	0.	0.
.0042	95106.	6471.	.0340	0.	0.
.0046	80695.	5870.	.0352	1893.	1338.
.0050	65854.	5290.	.0363	1109.	1109.
.0054	55809.	4858.	.0374	968.	968.
.0059	40756.	4182.	.0386	910.	910.
.0063	43000.	4300.	.0398	936.	936.
.0068	26168.	3350.	.0410	0.	0.
.0073	22084.	3221.	.0422	914.	914.
.0078	17709.	2911.	.0435	0.	0.
.0084	17781.	3006.	.0447	943.	943.
.0089	9439.	2225.	.0460	946.	946.
.0095	8865.	2289.	.0473	0.	0.
.0101	9584.	2396.	.0486	0.	0.
.0107	6114.	2038.	.0500	1177.	1177.
.0113	3821.	1709.	.0513	2254.	1594.
.0120	2684.	1342.	.0527	0.	0.
.0127	0.	0.	.0541	0.	0.
.0133	2835.	1418.	.0555	0.	0.
.0140	1533.	1084.	.0569	0.	0.
.0148	2104.	1215.	.0583	0.	0.
.0155	2362.	1363.	.0598	0.	0.
.0163	3326.	1663.	.0613	0.	0.
.0170	1567.	1108.	.0628	0.	0.
.0178	4917.	2007.	.0643	0.	0.
.0186	3545.	1585.	.0658	1754.	1754.
.0195	1026.	1026.	.0673	0.	0.
.0203	3603.	1802.	.0689	0.	0.
.0212	0.	0.	.0705	0.	0.
.0221	3155.	1577.	.0721	0.	0.
.0230	1853.	1310.	.0737	0.	0.

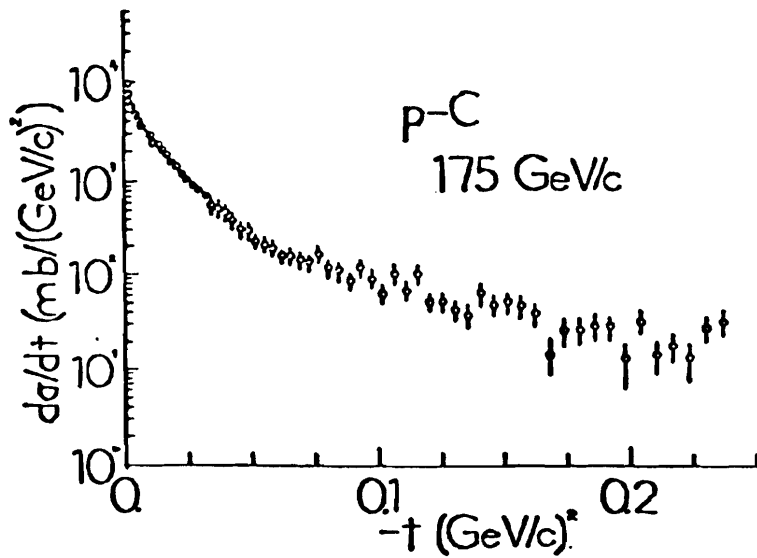
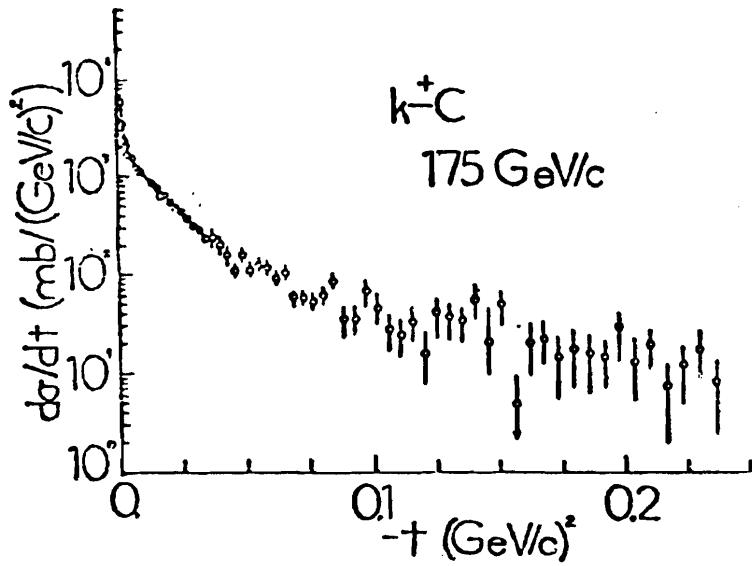
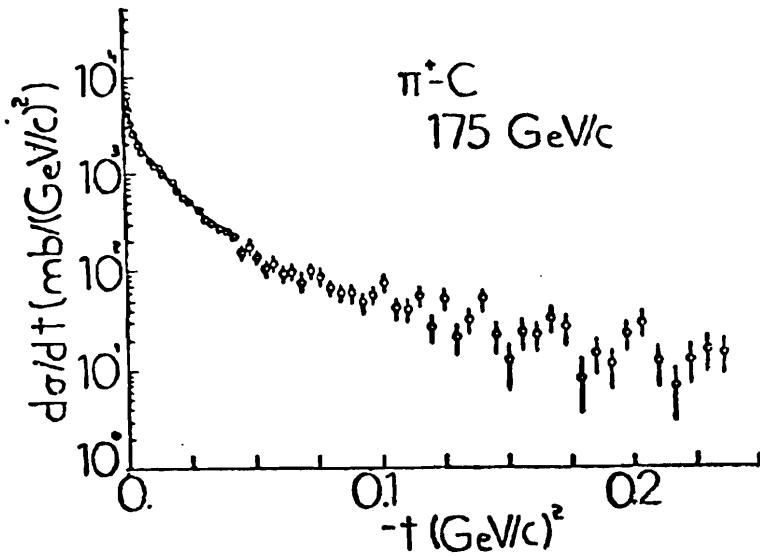
KMINUS - PB: 70 GEV/C
 UNITS: T: (GEV/C)**2; DSIGMA/DT: MILLIBARNS/((GEV/C)**2)

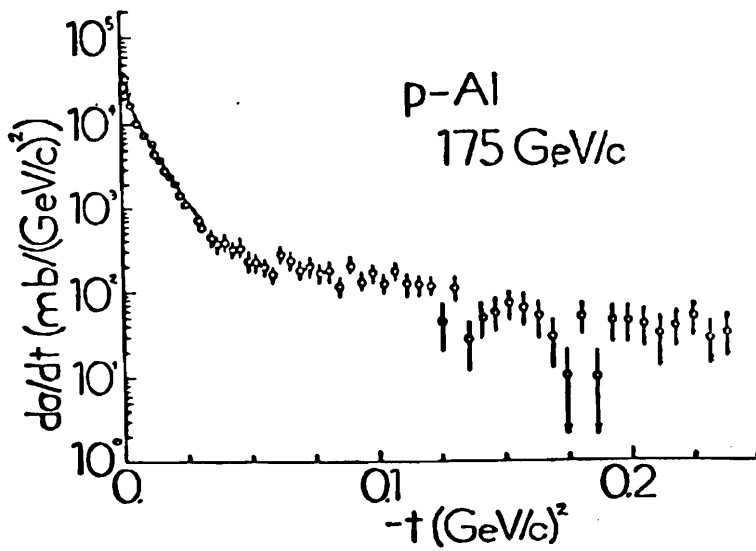
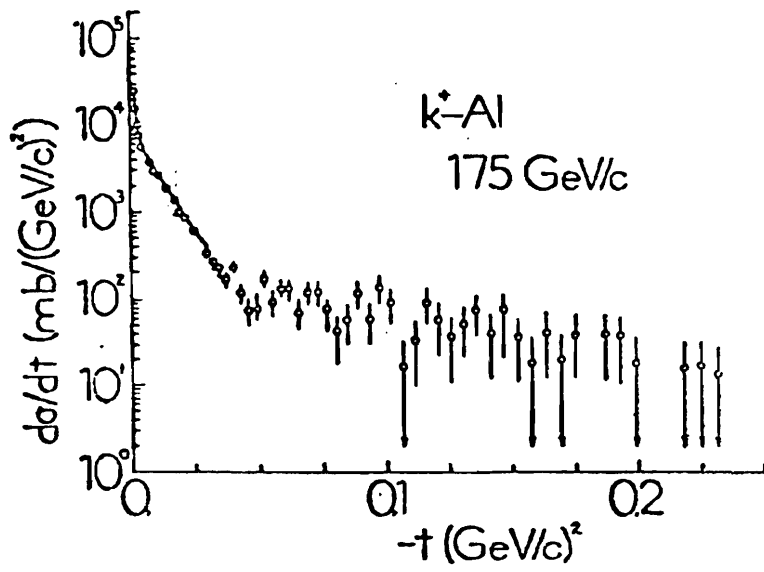
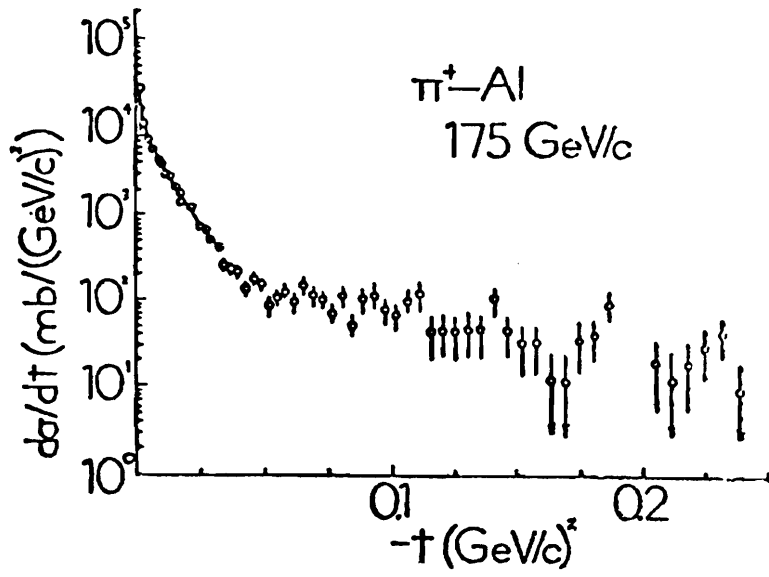
-T	DSIGMA/DT	ERROR	-T	DSIGMA/DT	ERROR
.0012	911995.	25394.	.0239	3038.	1717.
.0014	687516.	20924.	.0248	1906.	1347.
.0016	485537.	16993.	.0258	849.	849.
.0019	362581.	14505.	.0267	1743.	1233.
.0022	297848.	12457.	.0277	0.	0.
.0025	226246.	10718.	.0287	1812.	1281.
.0028	193401.	9711.	.0290	0.	0.
.0031	143688.	8058.	.0308	0.	0.
.0034	121252.	7285.	.0319	868.	868.
.0038	116626.	7101.	.0329	800.	800.
.0042	106963.	6721.	.0340	804.	804.
.0046	77236.	5560.	.0352	1774.	1255.
.0050	66504.	5146.	.0363	0.	0.
.0054	59046.	4837.	.0374	0.	0.
.0059	37799.	3899.	.0386	853.	853.
.0063	37483.	3887.	.0398	0.	0.
.0068	30156.	3482.	.0410	851.	851.
.0073	30388.	3658.	.0422	0.	0.
.0078	21084.	3075.	.0435	0.	0.
.0084	14235.	2608.	.0447	0.	0.
.0089	9339.	2142.	.0460	0.	0.
.0095	8309.	2145.	.0473	0.	0.
.0101	2211.	1797.	.0486	0.	0.
.0107	5094.	1801.	.0500	0.	0.
.0113	5731.	2026.	.0513	0.	0.
.0120	3145.	1407.	.0527	0.	0.
.0127	1312.	928.	.0541	0.	0.
.0133	2658.	1329.	.0555	876.	876.
.0140	2156.	1245.	.0569	1211.	1211.
.0148	657.	657.	.0583	1043.	1043.
.0155	1476.	1043.	.0598	0.	0.
.0163	1559.	1102.	.0613	2723.	1925.
.0170	2203.	1272.	.0628	0.	0.
.0178	768.	768.	.0643	1135.	1135.
.0186	3987.	1628.	.0658	0.	0.
.0195	1923.	1360.	.0673	1550.	1550.
.0203	2533.	1462.	.0689	0.	0.
.0212	3726.	1666.	.0705	0.	0.
.0221	2957.	1478.	.0721	0.	0.
.0230	2606.	1504.	.0737	0.	0.

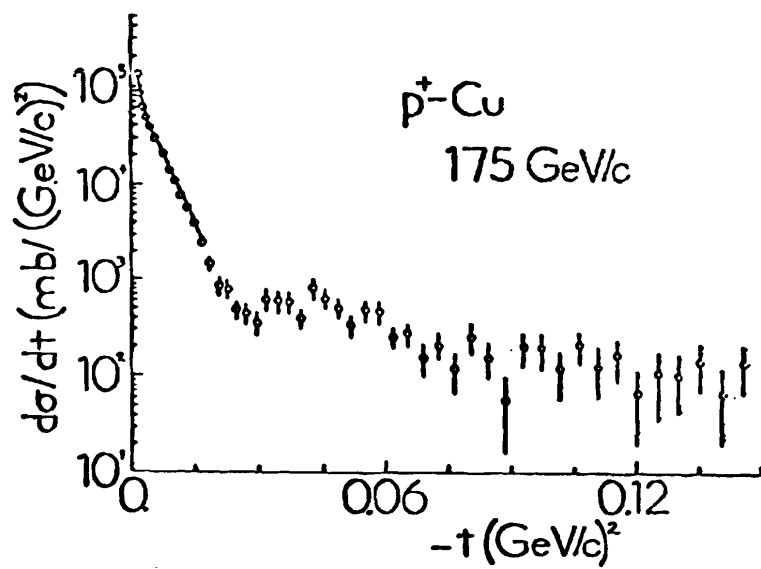
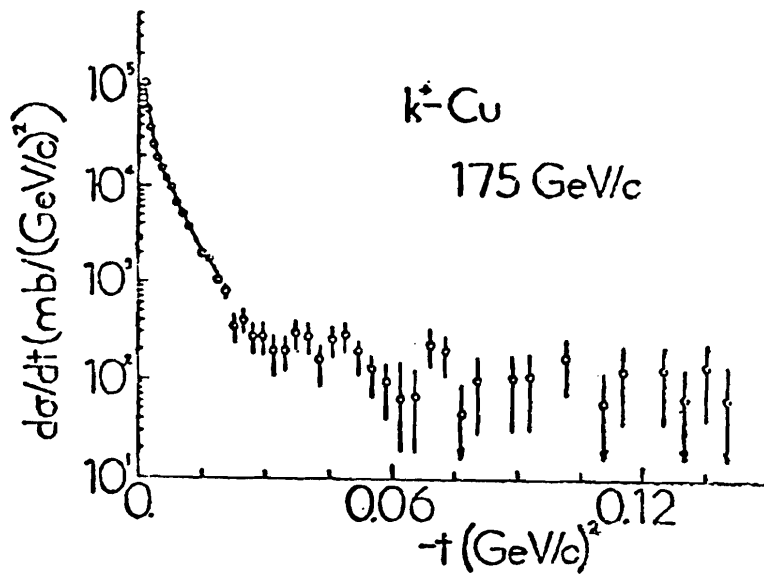
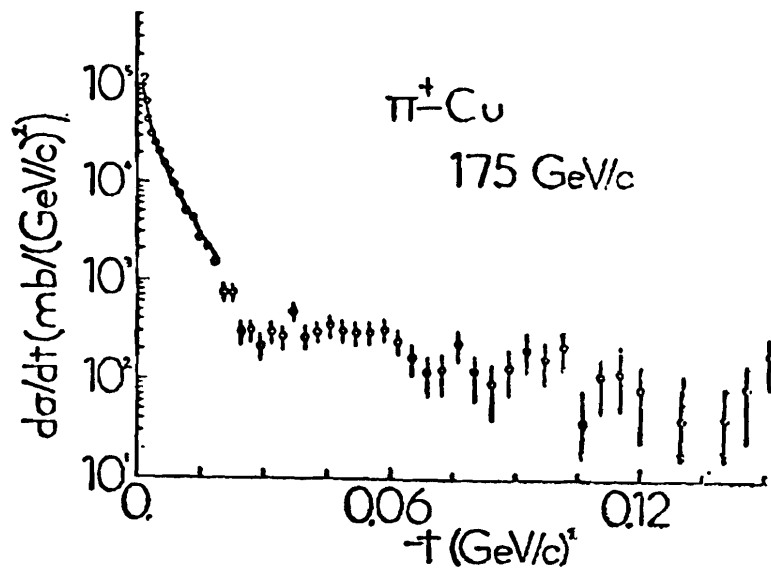
PHINUS - PB: 70 GEV/C
 UNITS: T: (GEV/C)**2; DSIGMA/DT: MILLIBARNS/((GEV/C)**2)

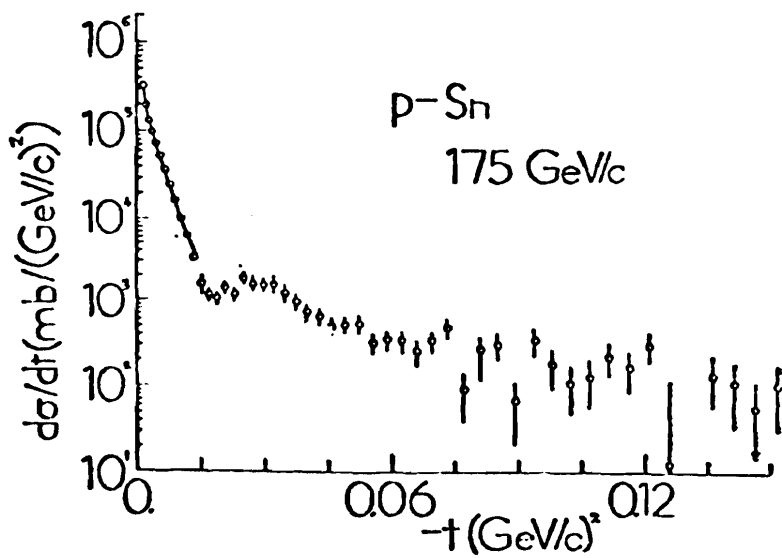
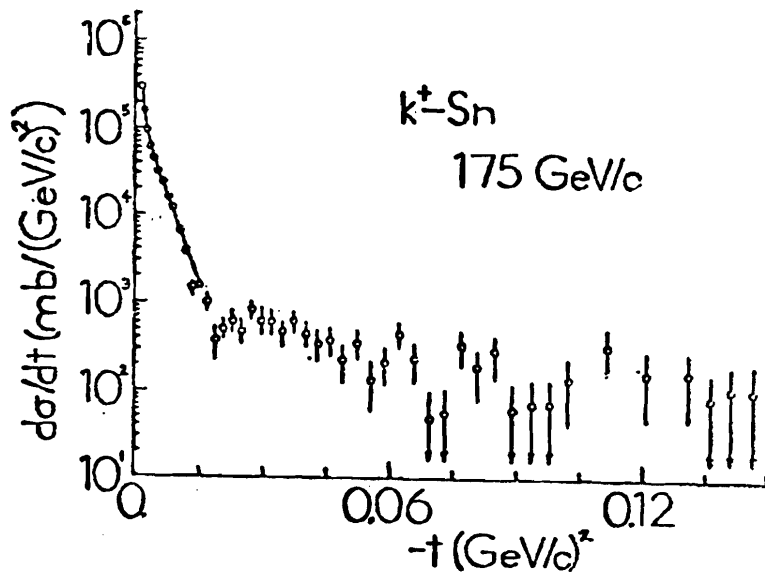
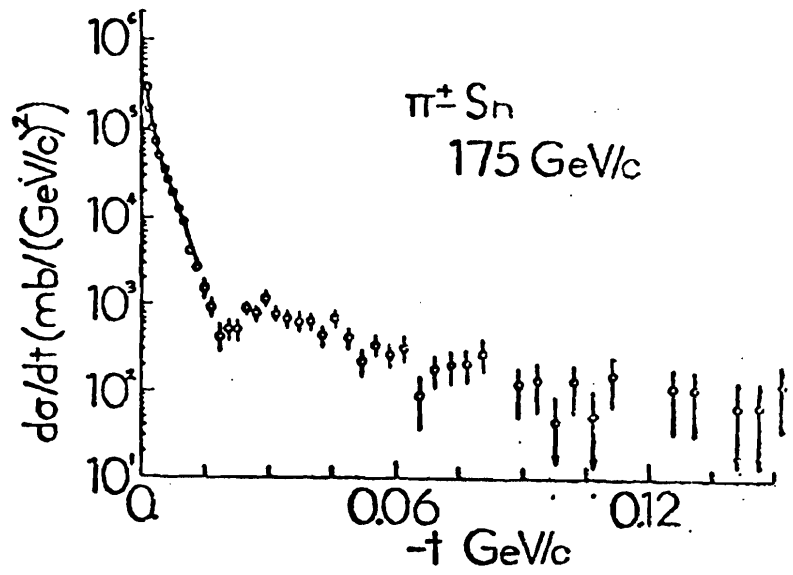
-T	DSIGMA/DT	ERROR	-T	DSIGMA/DT	ERROR
.0012	920240.	30493.	.0239	4349.	2175.
.0014	699464.	25045.	.0248	0.	0.
.0016	522716.	20825.	.0258	2405.	1700.
.0019	447009.	18737.	.0267	4938.	2469.
.0022	330704.	15840.	.0277	3695.	2133.
.0025	295731.	14491.	.0287	0.	0.
.0028	233150.	12605.	.0298	2728.	1929.
.0031	225292.	12109.	.0308	1354.	1354.
.0034	180424.	10577.	.0319	3686.	2128.
.0038	165835.	10070.	.0329	2265.	1602.
.0042	127432.	8631.	.0340	1138.	1138.
.0046	114500.	8056.	.0352	0.	0.
.0050	92519.	7481.	.0363	0.	0.
.0054	67932.	6471.	.0374	1285.	1285.
.0059	56956.	5696.	.0386	0.	0.
.0063	54233.	5564.	.0398	0.	0.
.0068	35310.	4484.	.0410	0.	0.
.0073	33061.	4541.	.0422	0.	0.
.0078	20333.	3594.	.0435	2586.	1829.
.0084	12140.	2862.	.0447	2504.	1771.
.0089	6266.	2089.	.0460	0.	0.
.0095	10984.	2936.	.0473	1458.	1458.
.0101	5576.	2862.	.0486	1260.	1260.
.0107	4510.	2017.	.0500	1562.	1562.
.0113	5073.	2269.	.0513	0.	0.
.0120	4455.	1992.	.0527	1142.	1142.
.0127	7436.	2629.	.0541	1721.	1721.
.0133	2823.	1630.	.0555	0.	0.
.0140	4071.	2036.	.0569	1715.	1715.
.0148	10240.	3008.	.0583	0.	0.
.0155	7315.	2765.	.0598	0.	0.
.0163	4415.	2208.	.0613	0.	0.
.0170	7280.	2752.	.0628	0.	0.
.0178	0.	0.	.0643	1608.	1608.
.0186	6589.	2490.	.0658	2329.	2329.
.0195	8172.	3336.	.0673	2195.	2195.
.0203	3588.	2072.	.0689	2304.	2304.
.0212	4222.	2111.	.0705	0.	0.
.0221	4188.	2094.	.0721	0.	0.
.0230	7381.	3013.	.0737	0.	0.

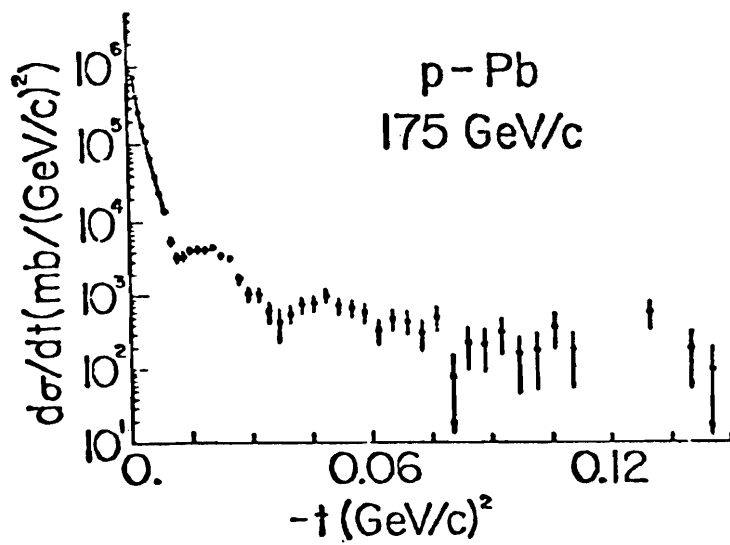
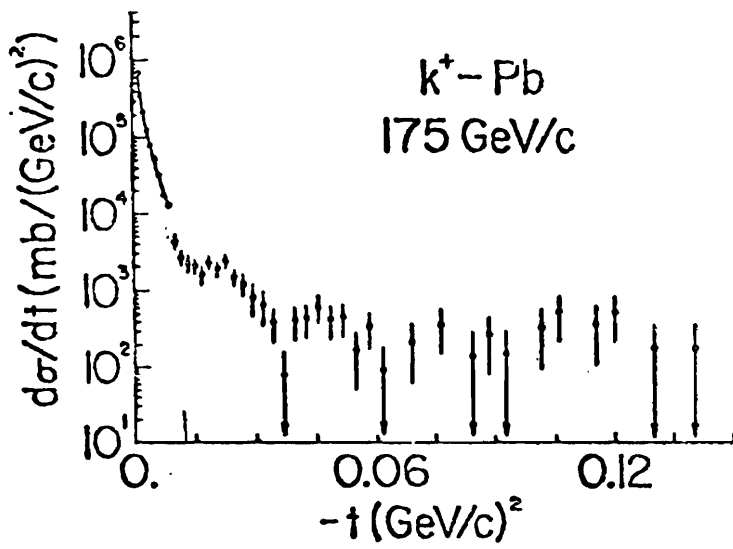
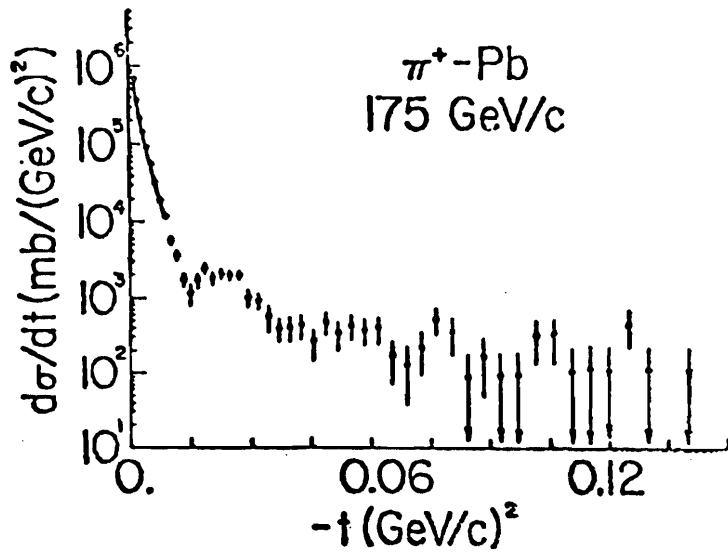


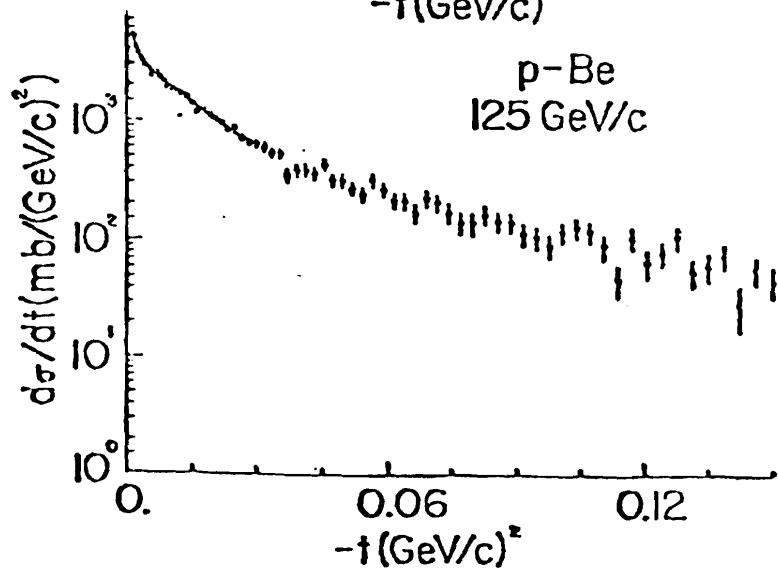
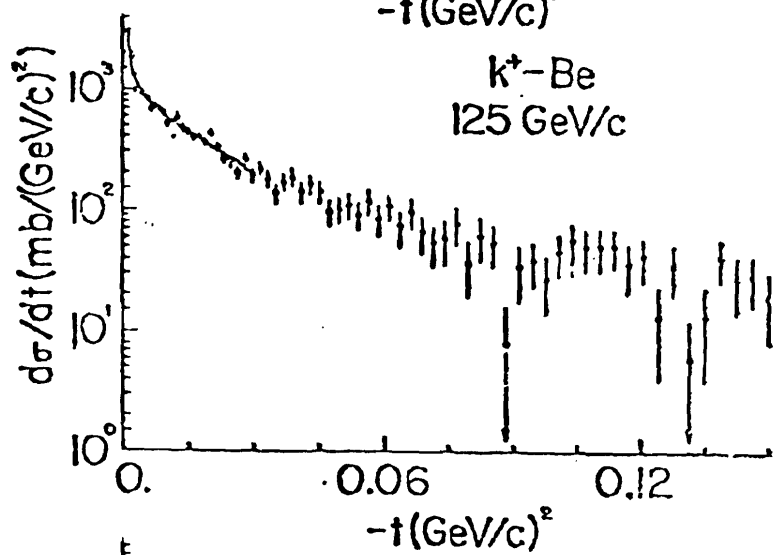
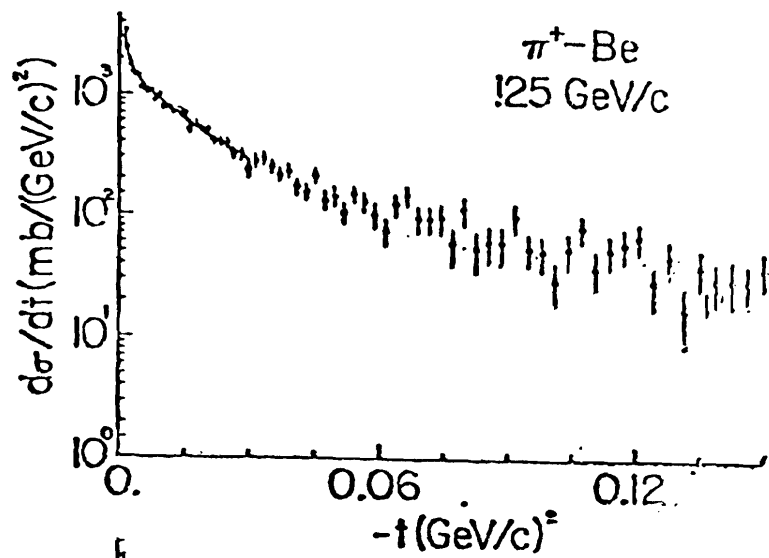


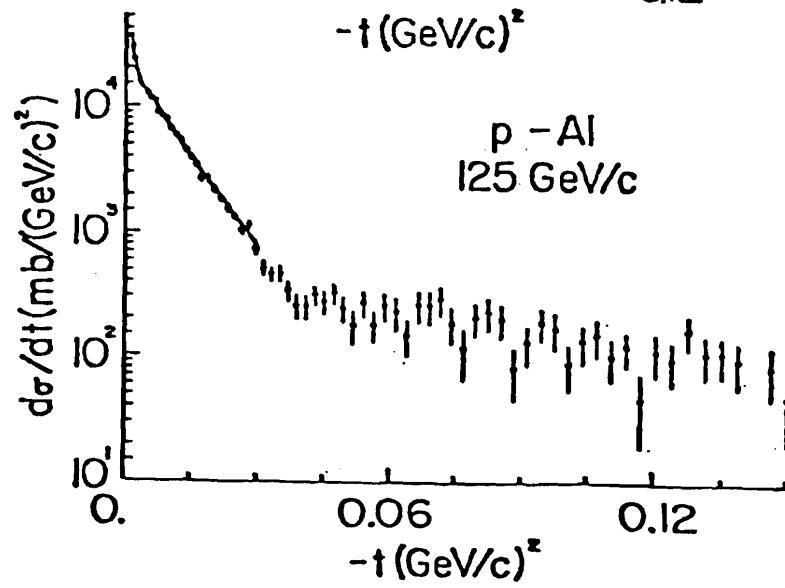
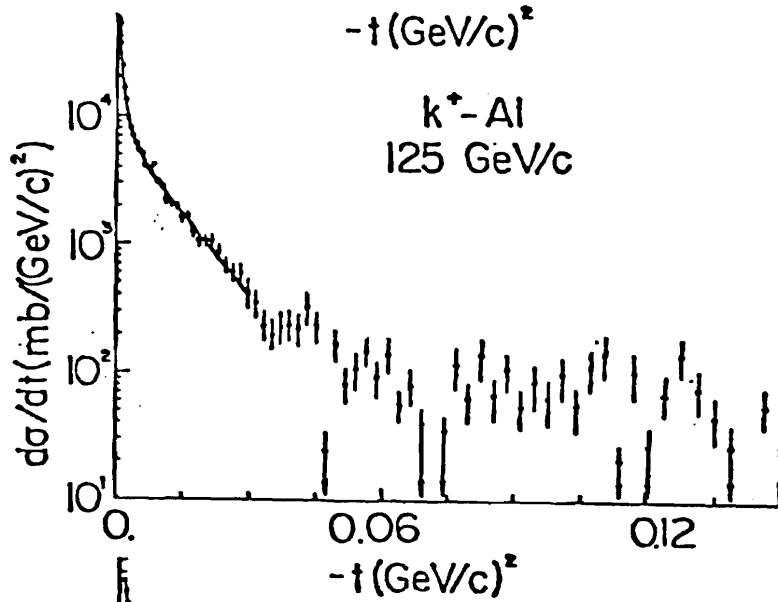
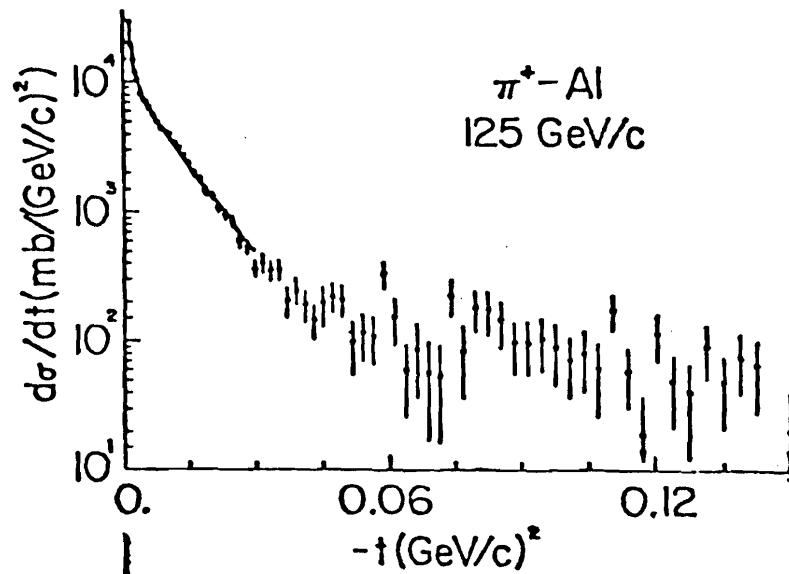


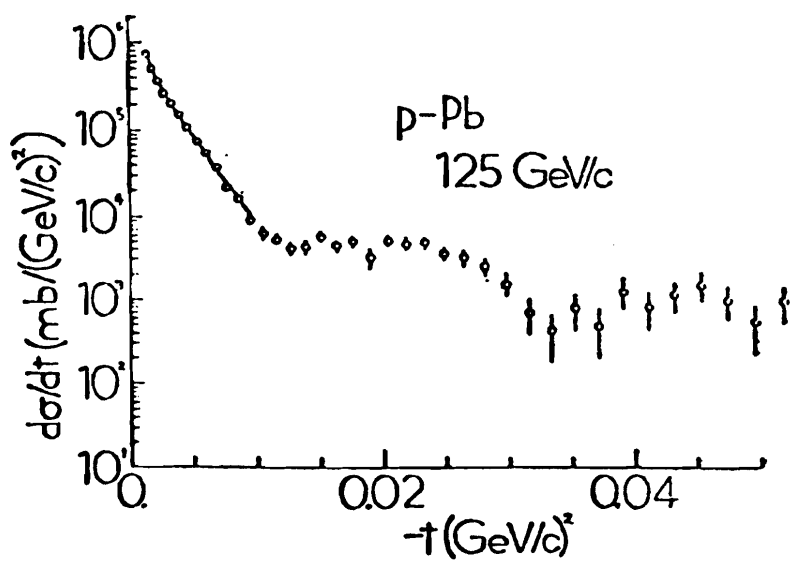
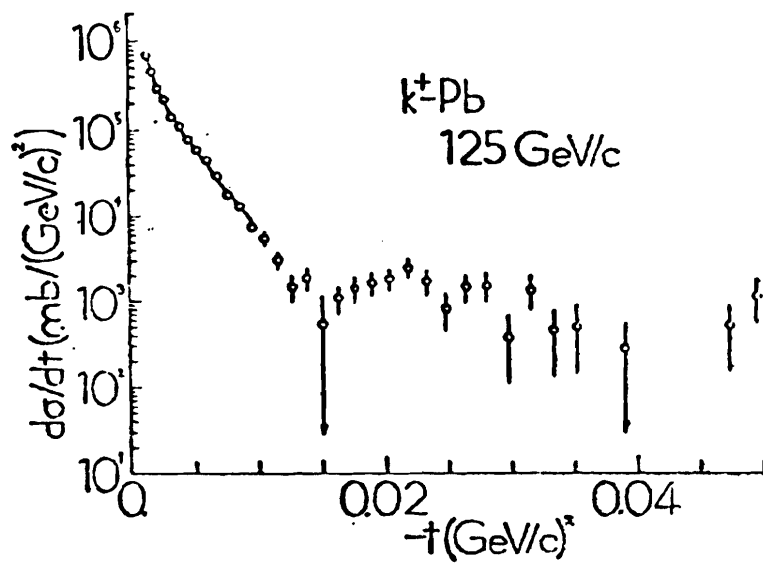
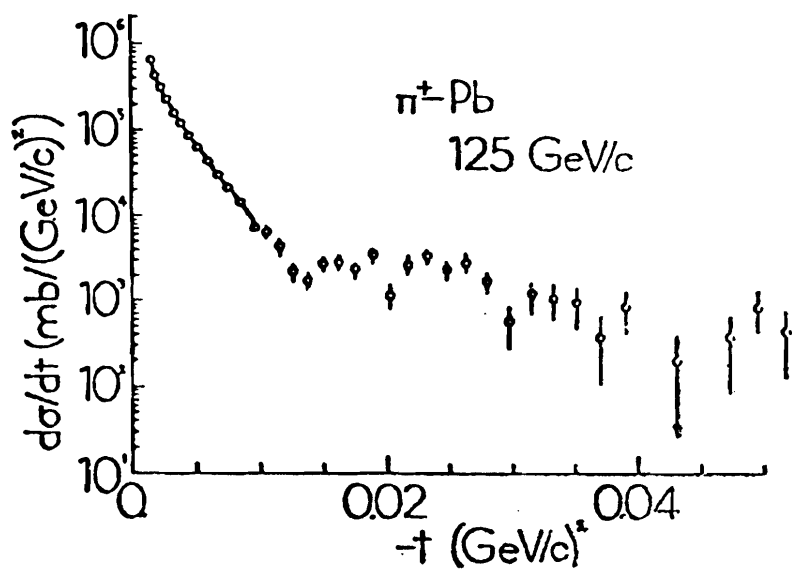


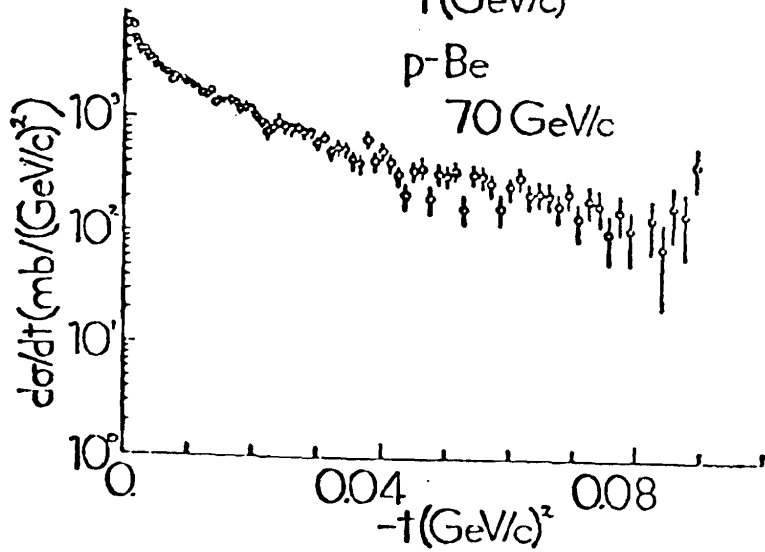
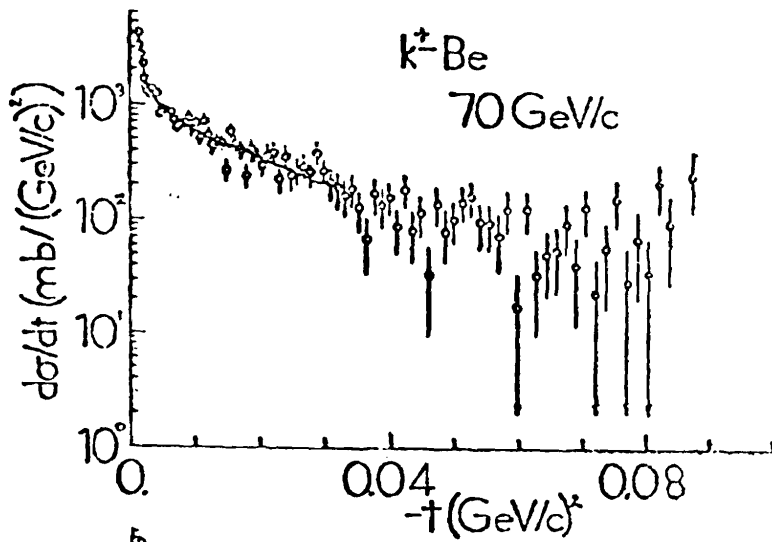
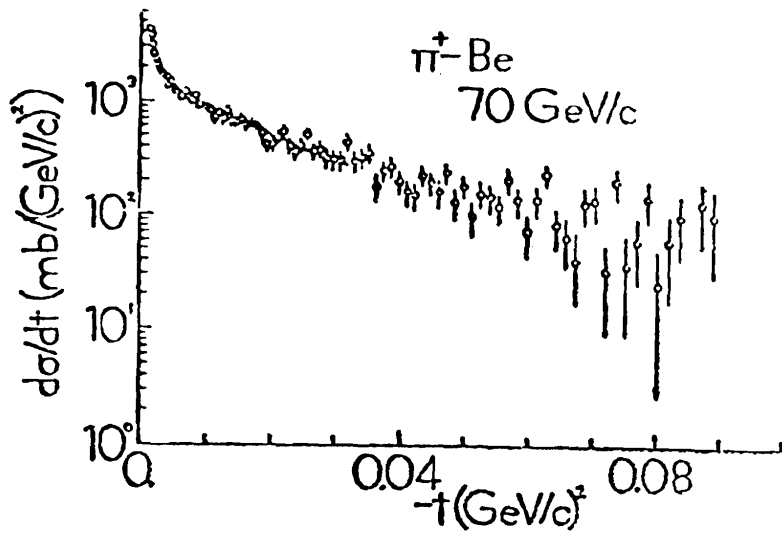


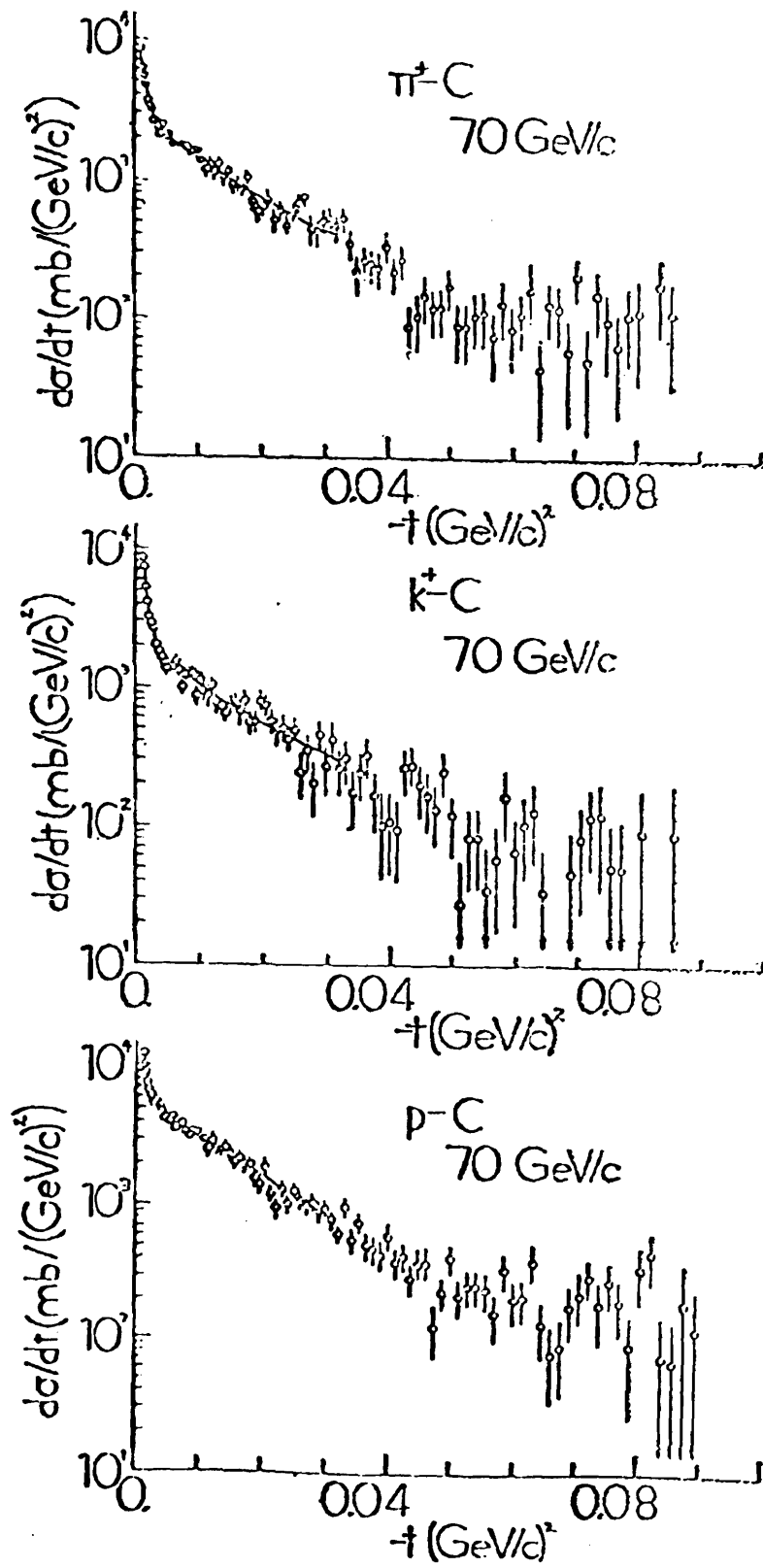


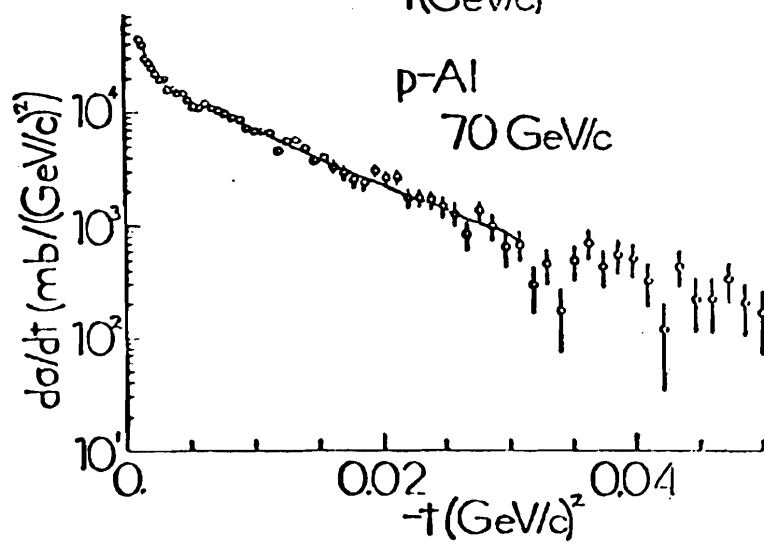
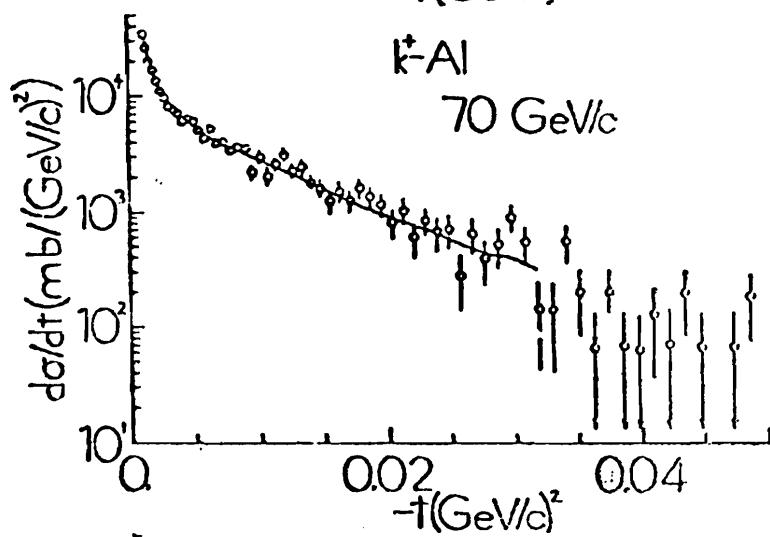
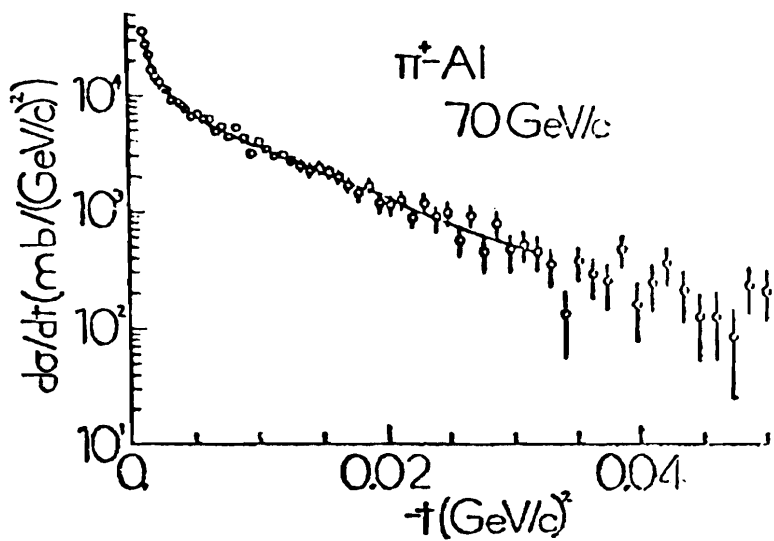


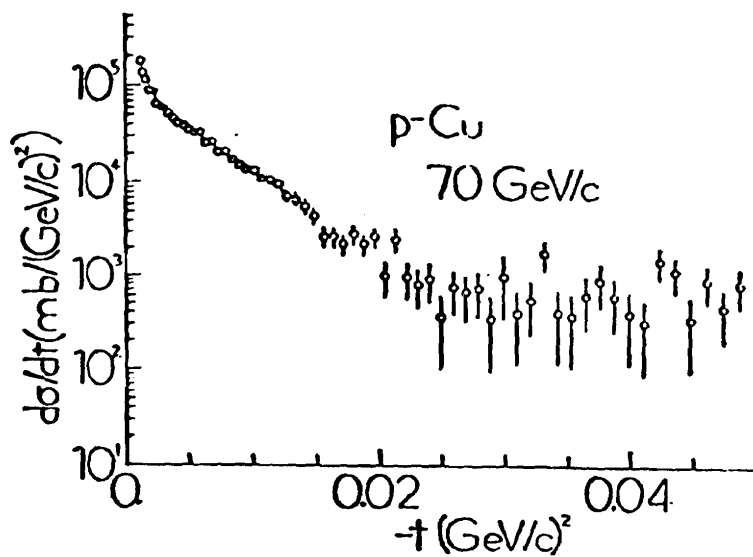
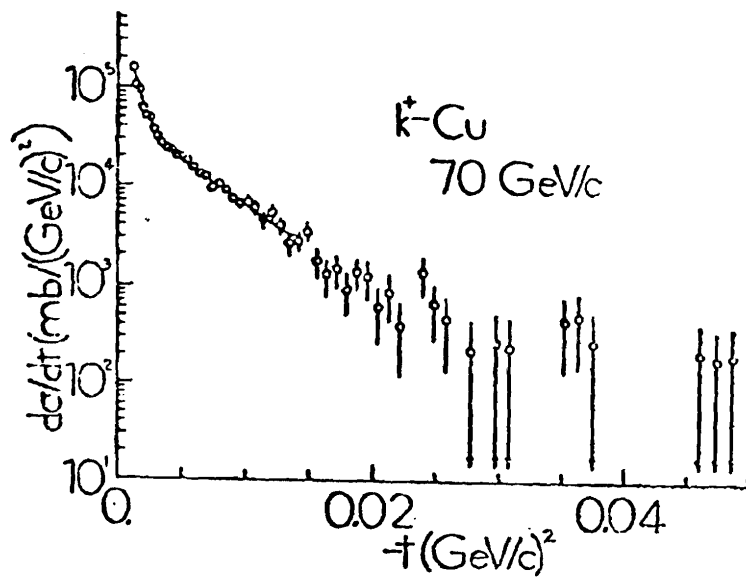
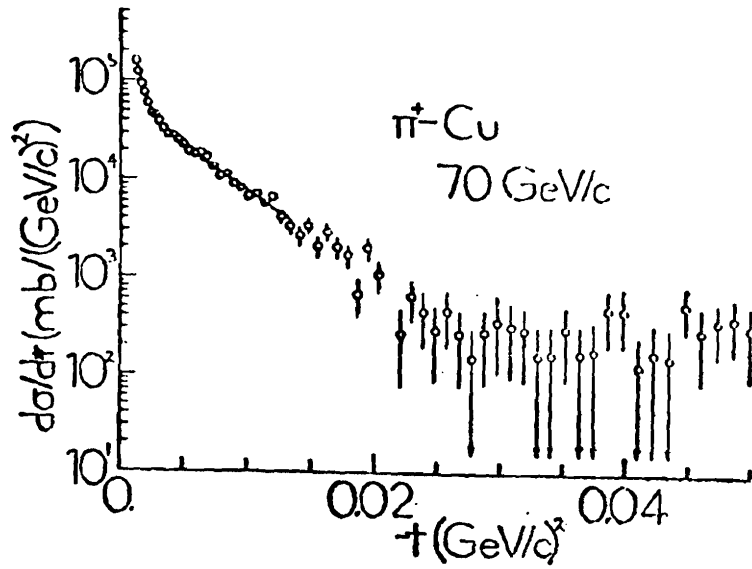


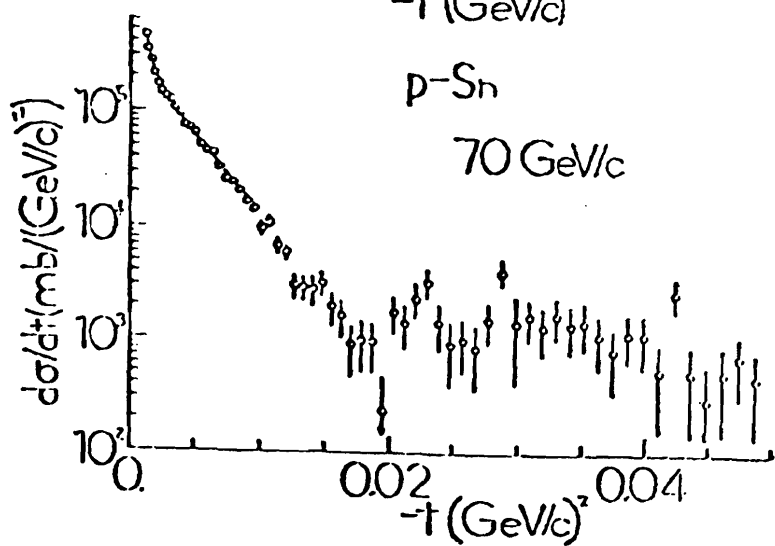
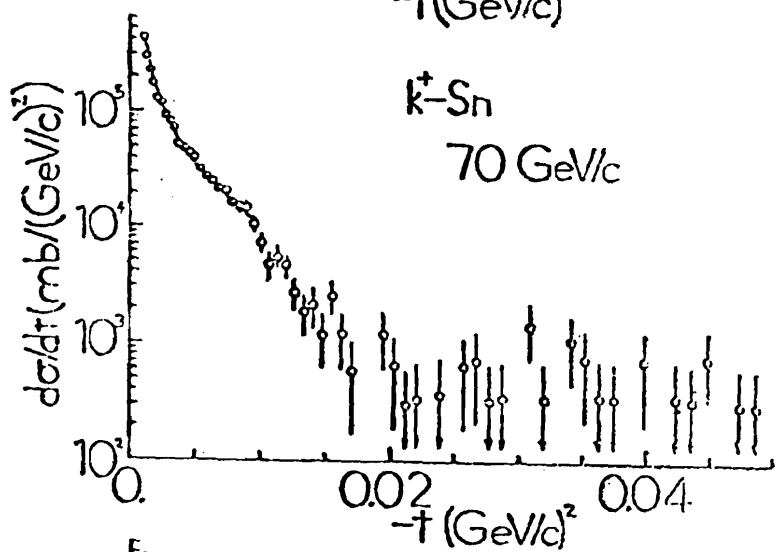
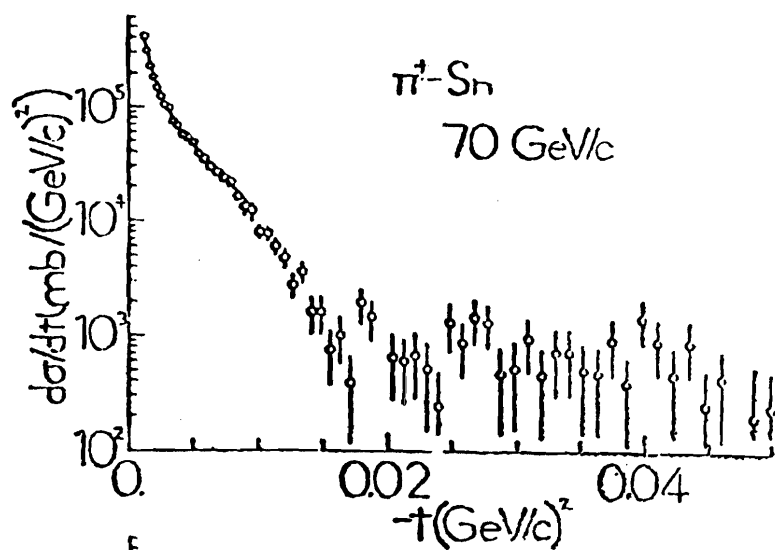


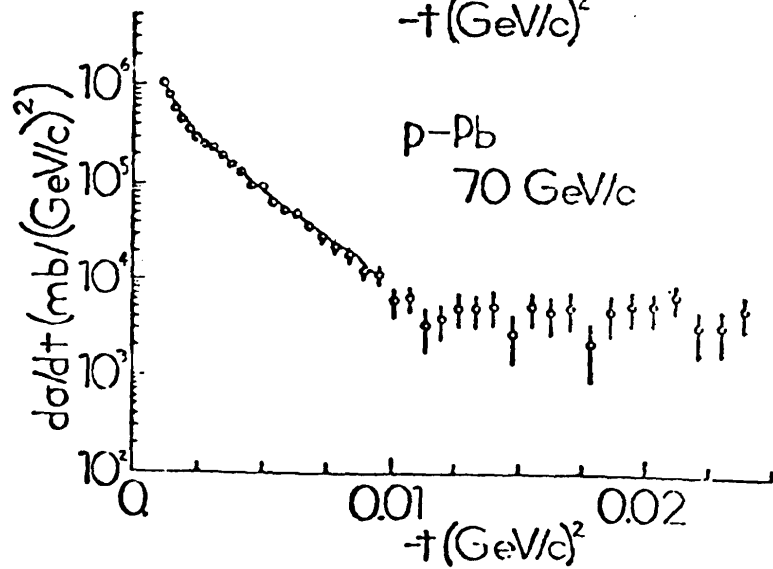
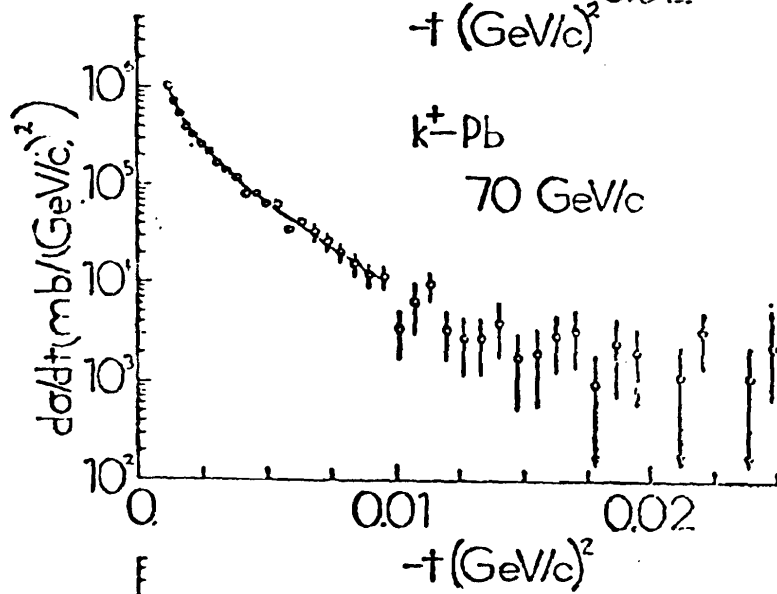
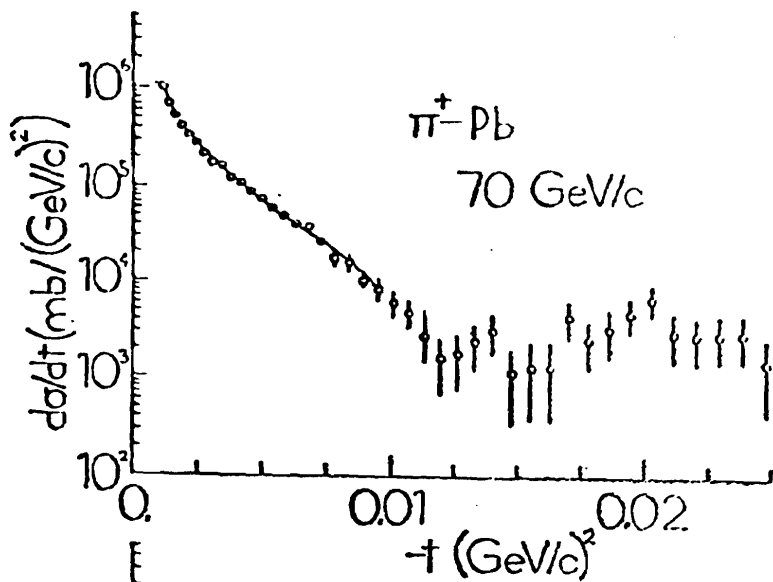


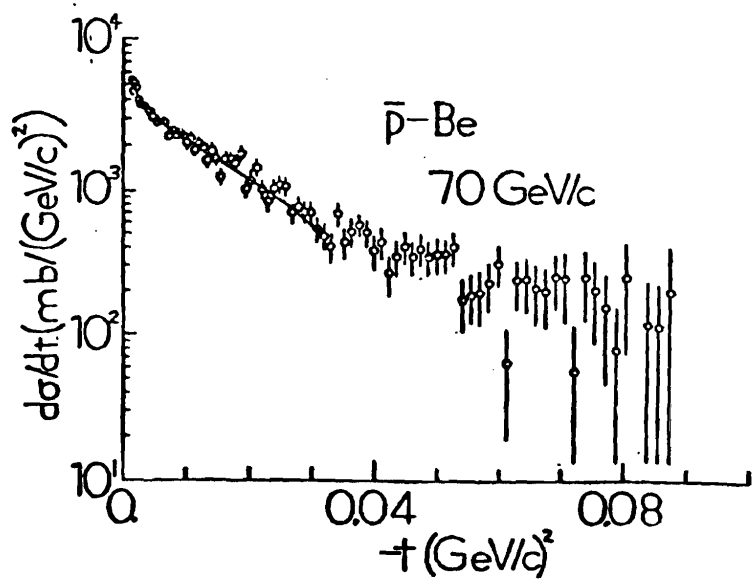
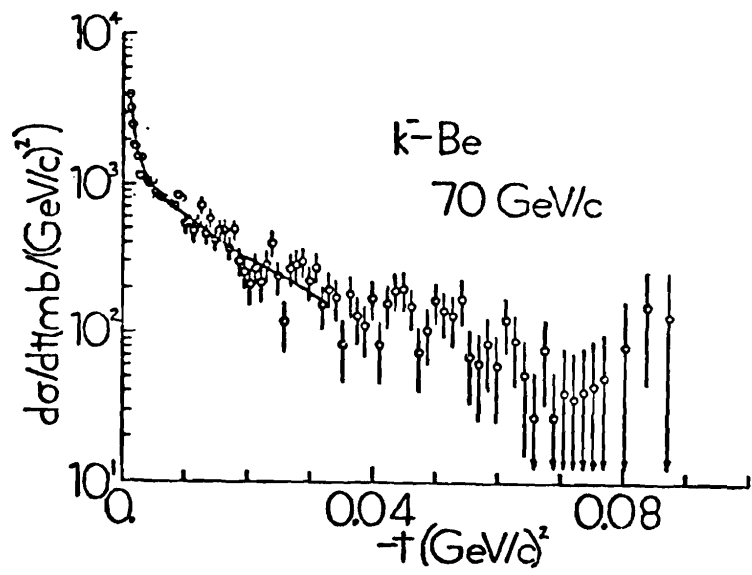
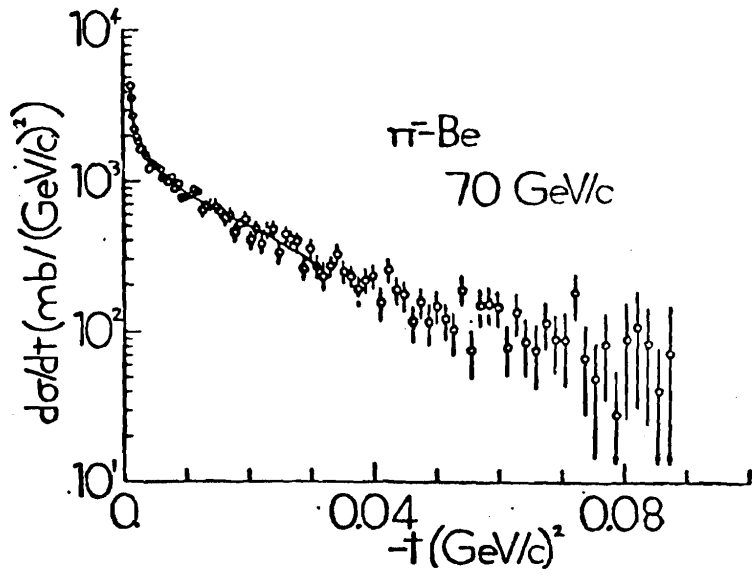


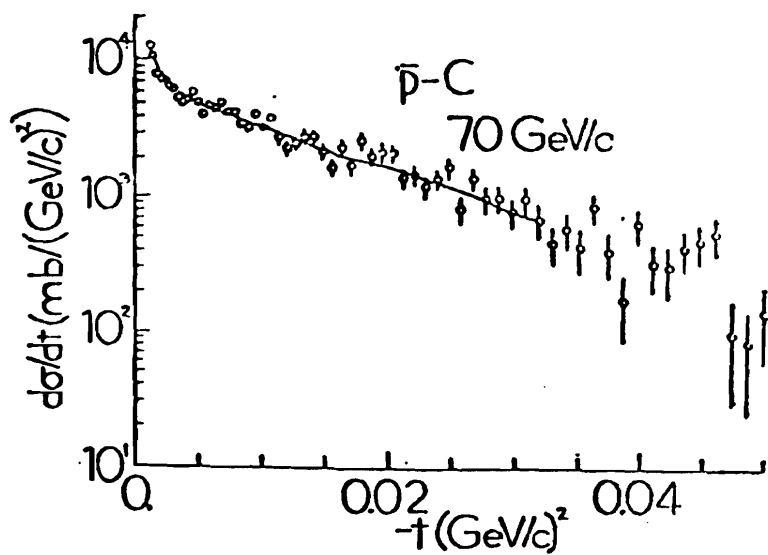
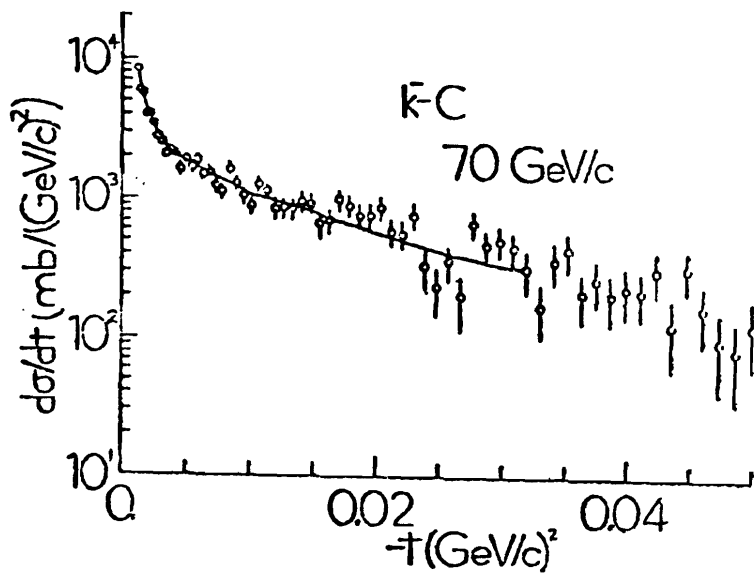
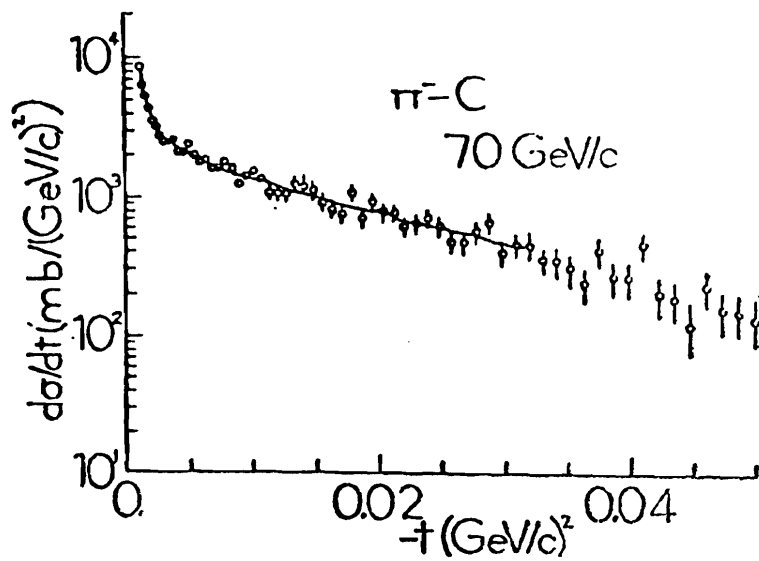


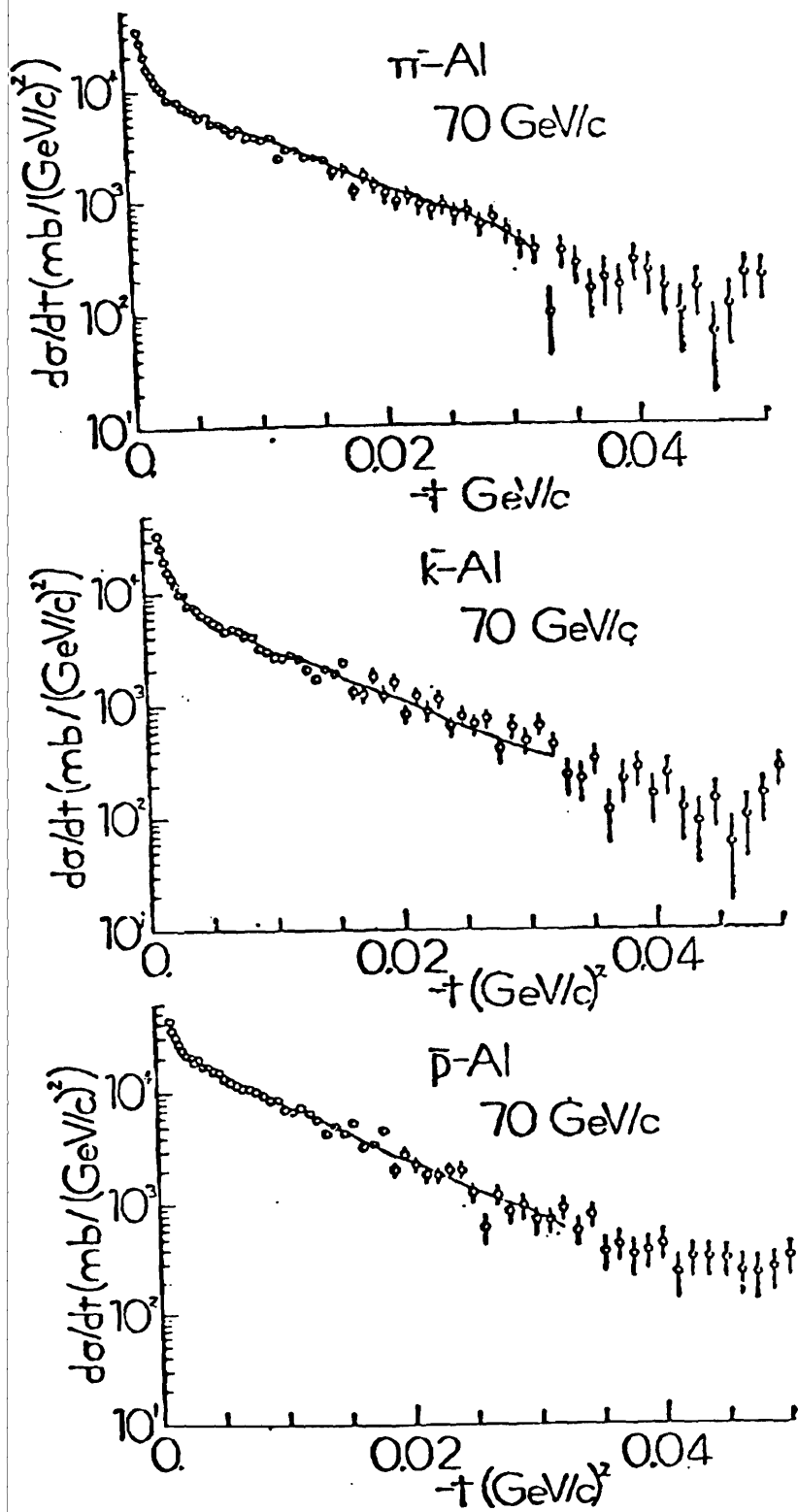


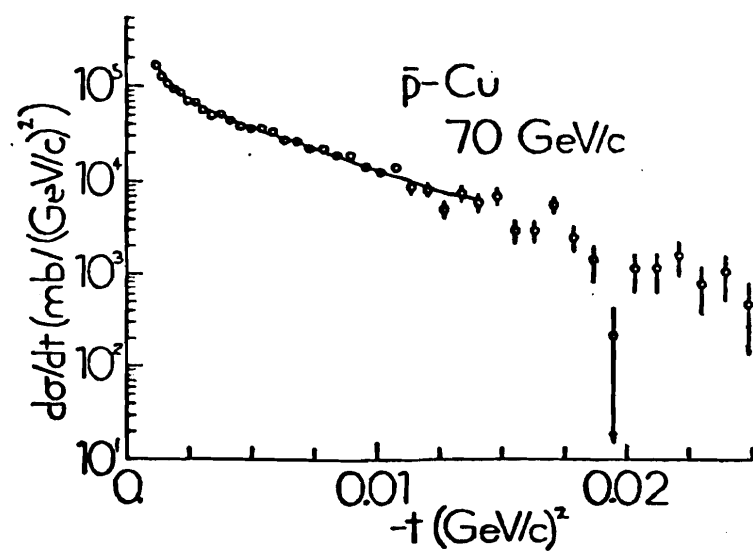
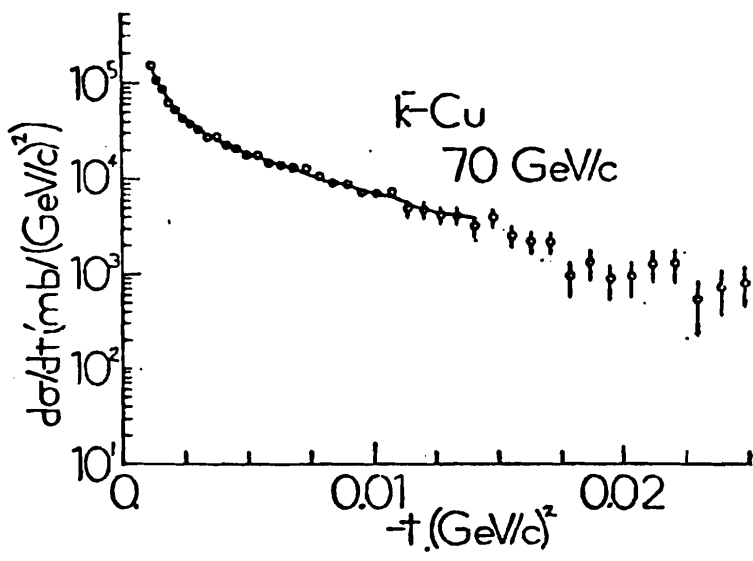
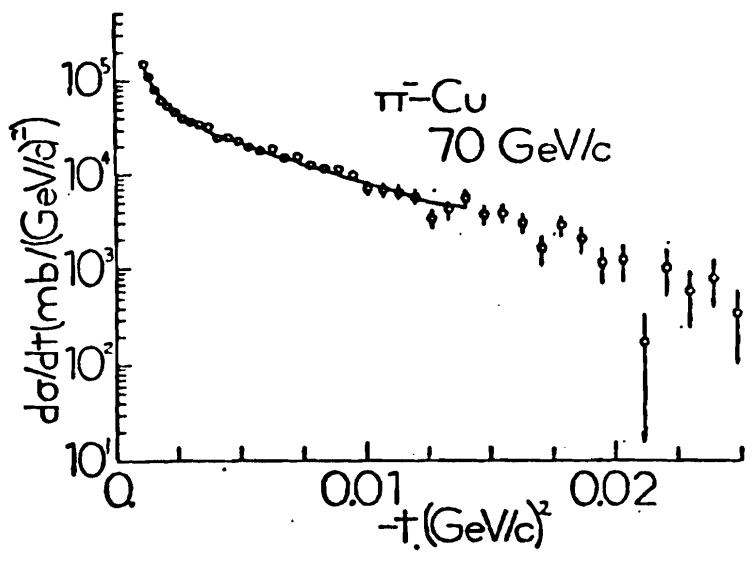


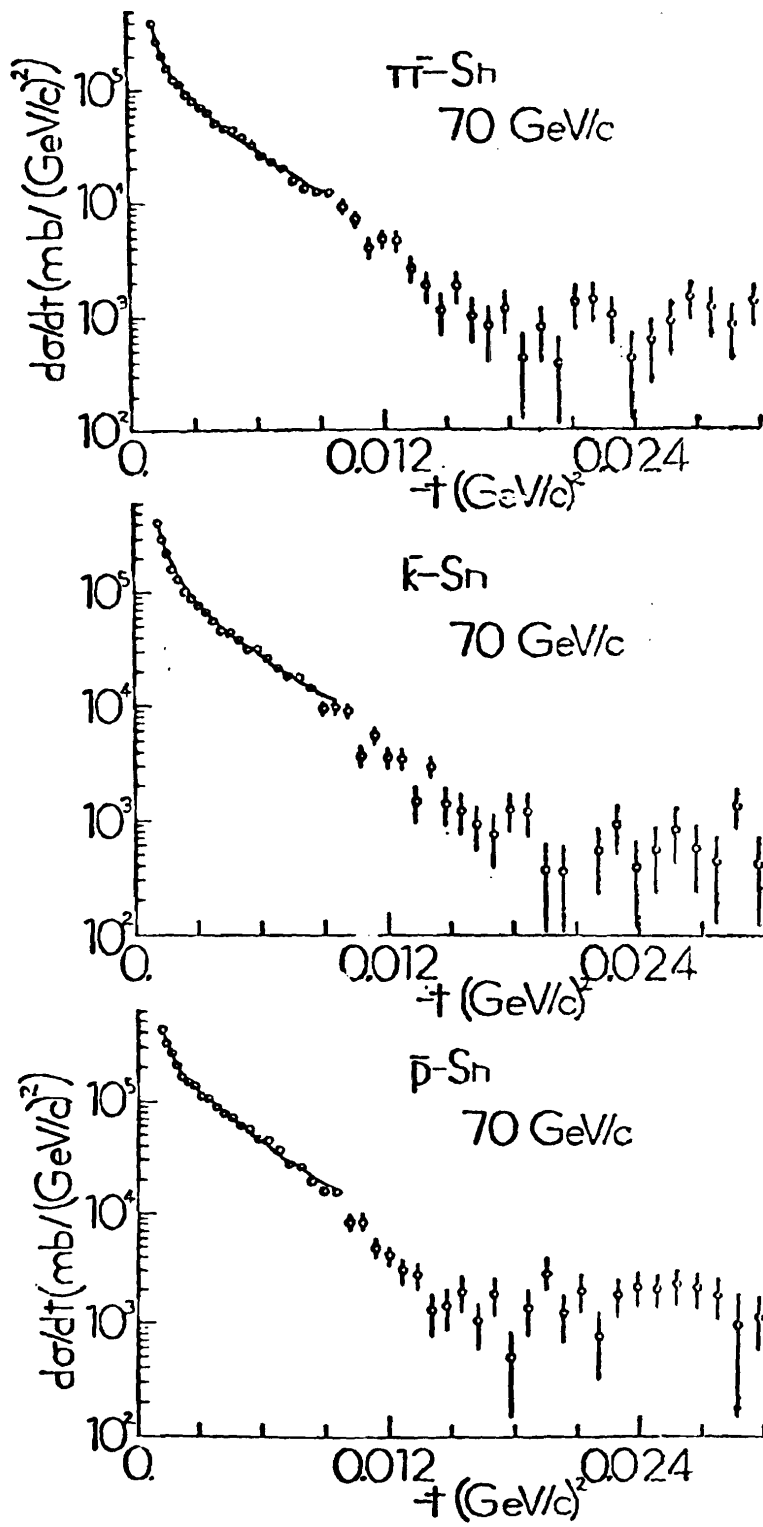


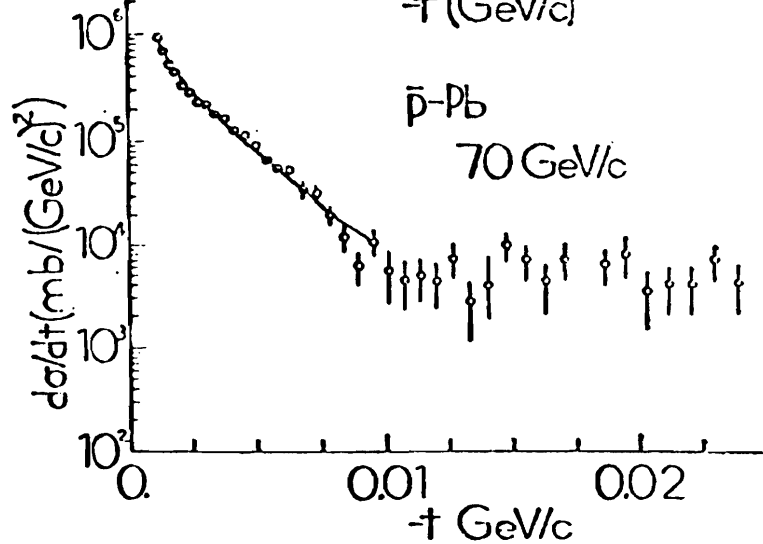
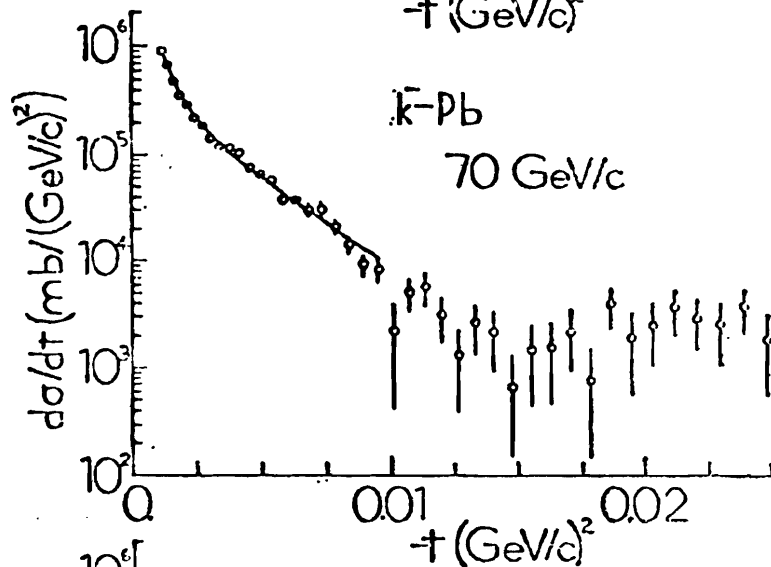
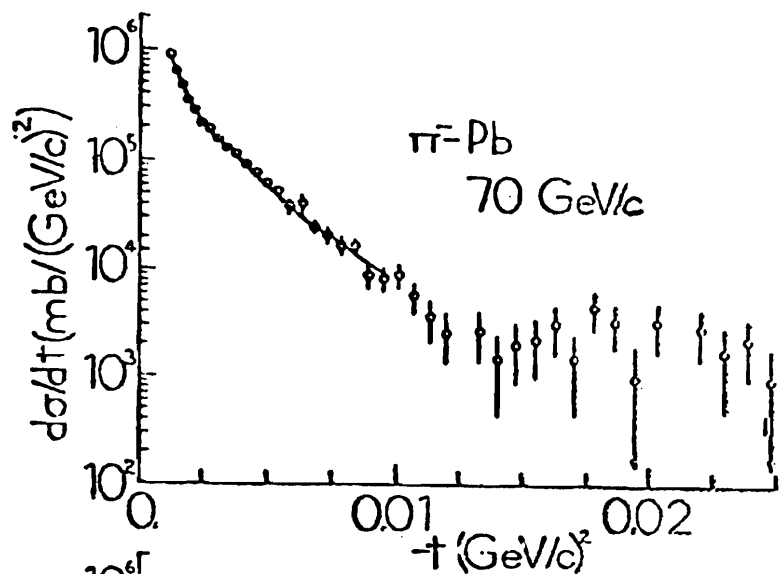


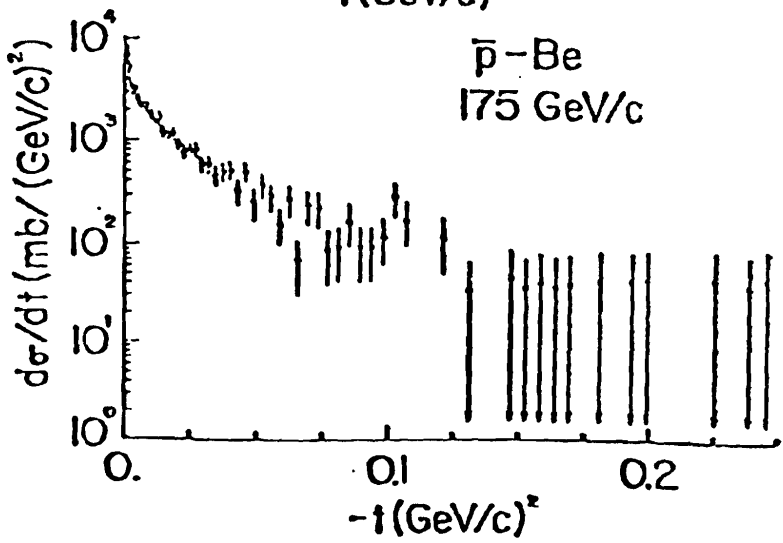
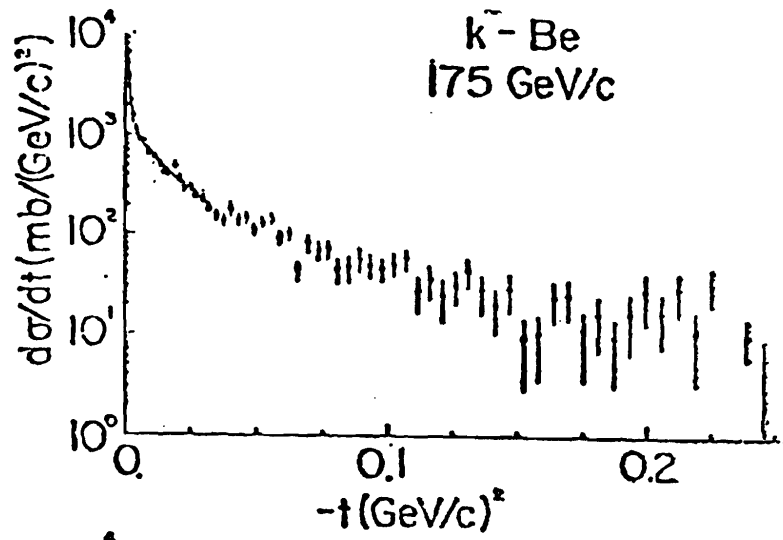
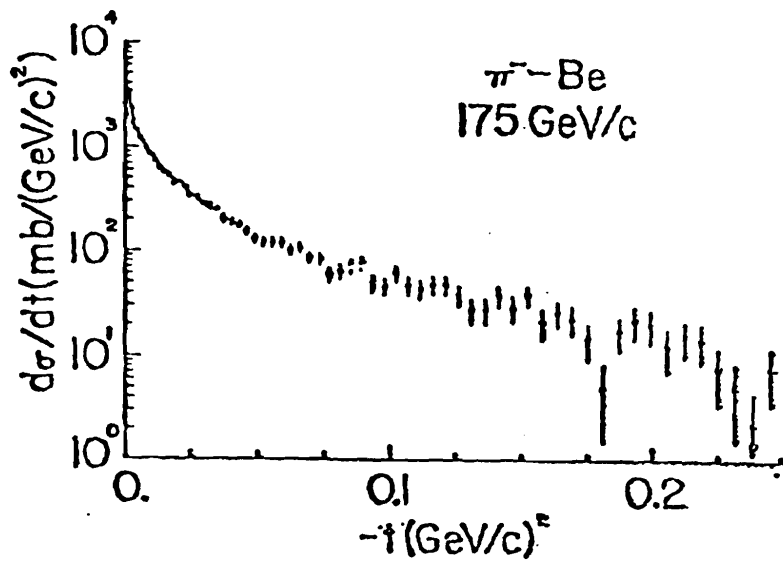


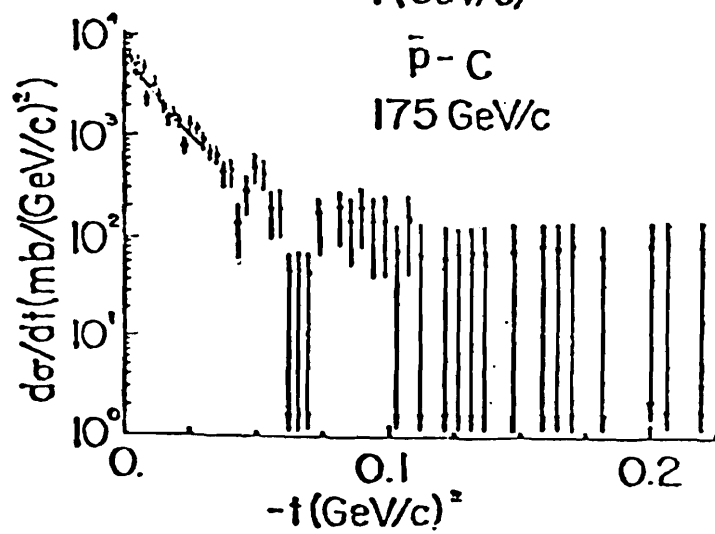
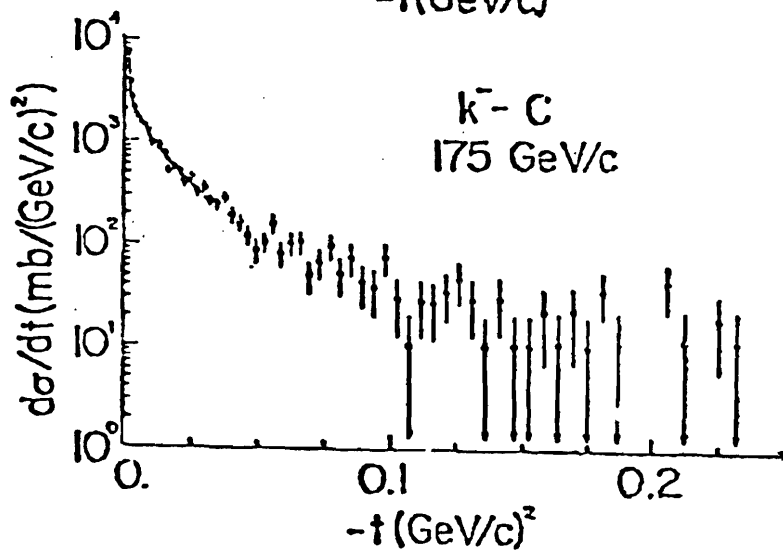
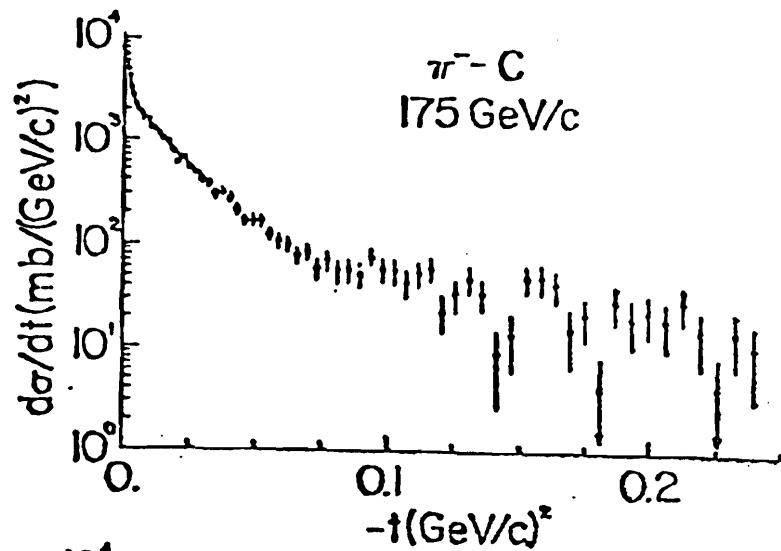


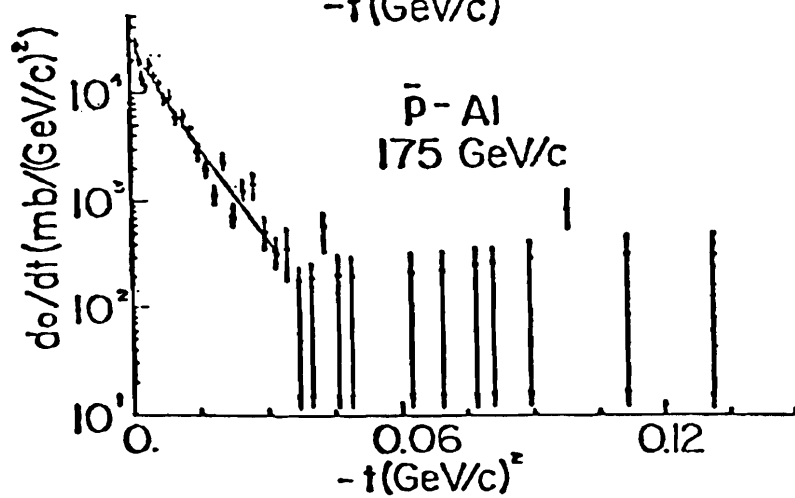
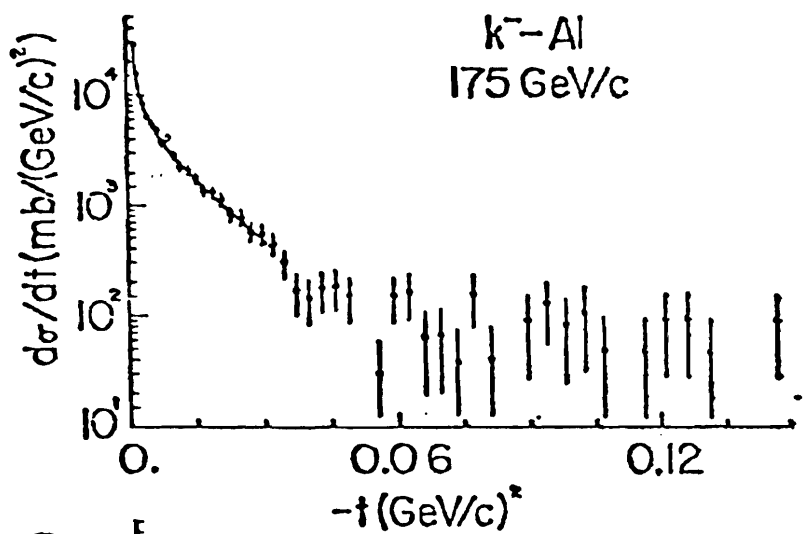
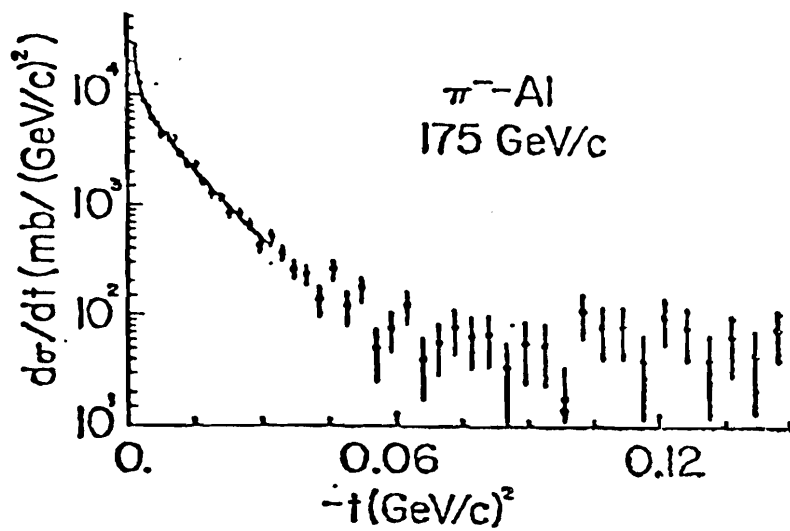


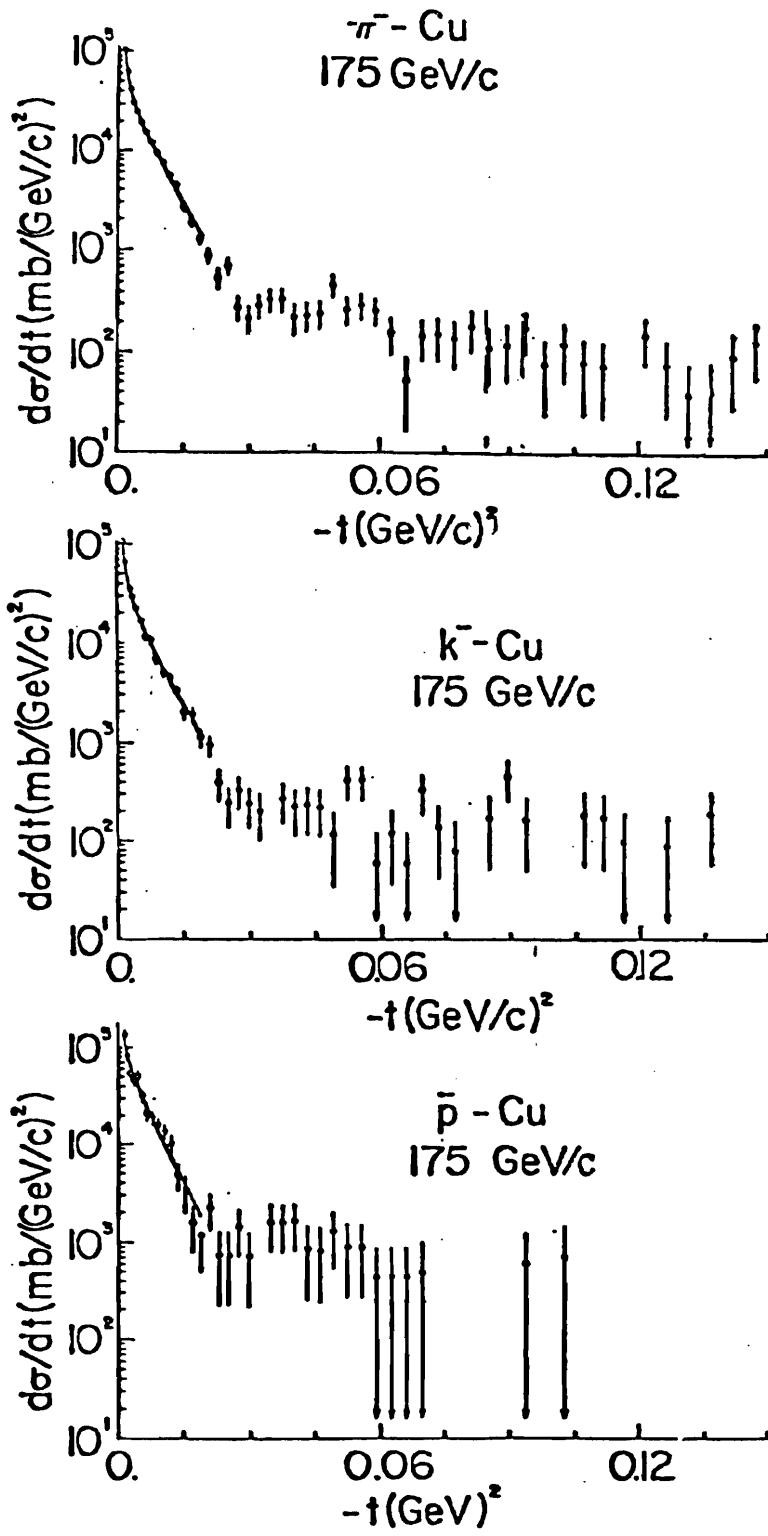


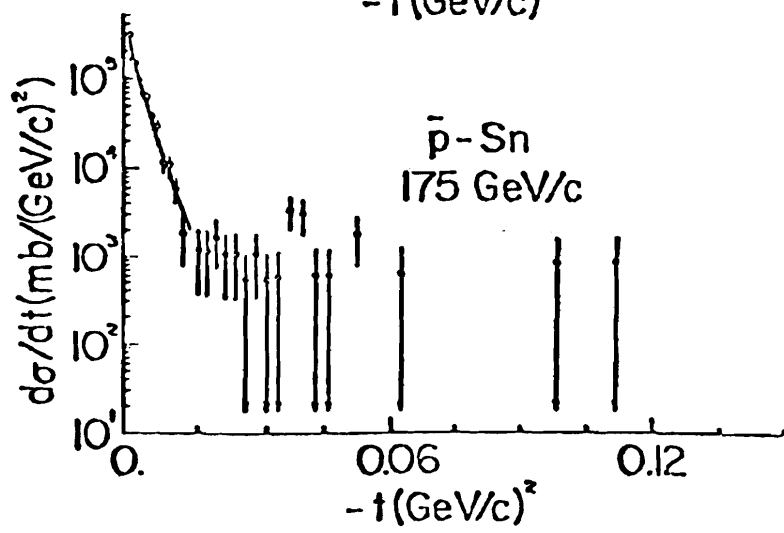
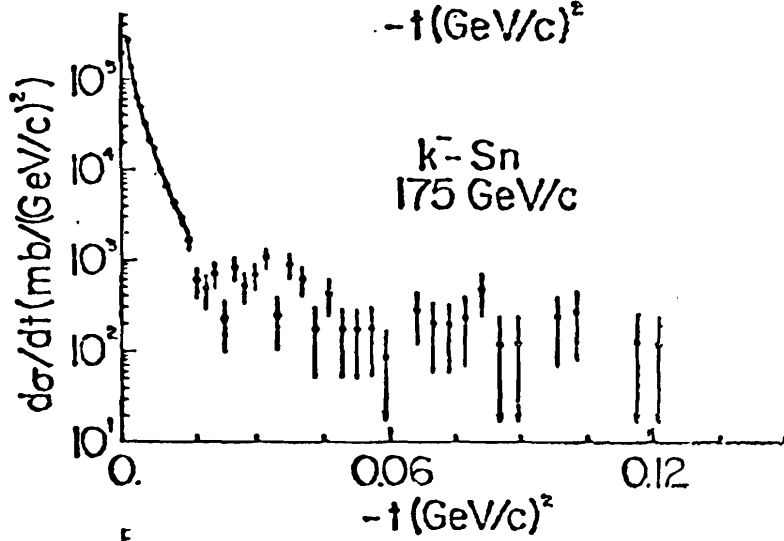
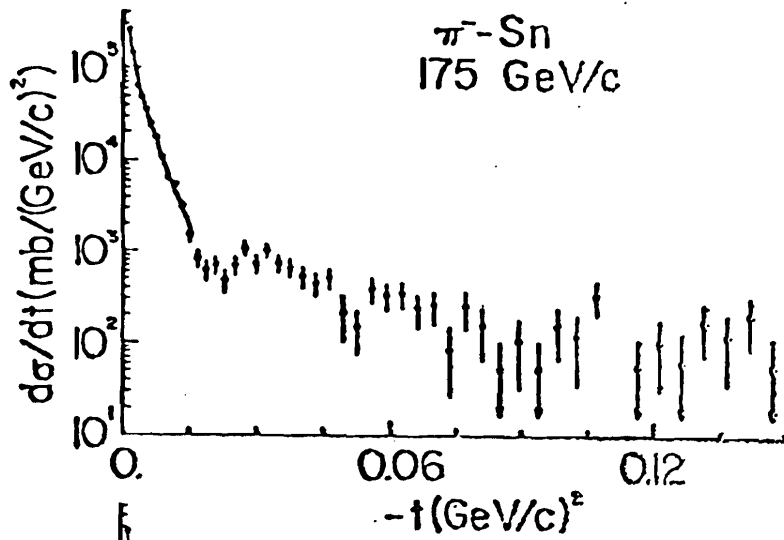


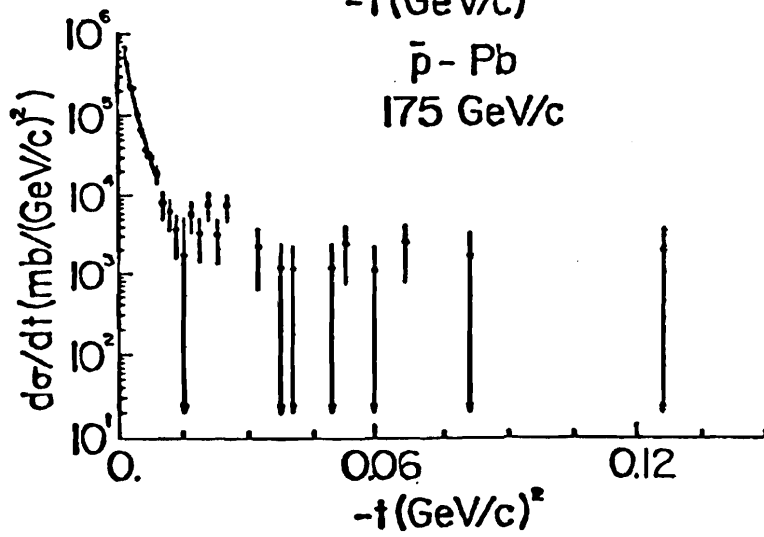
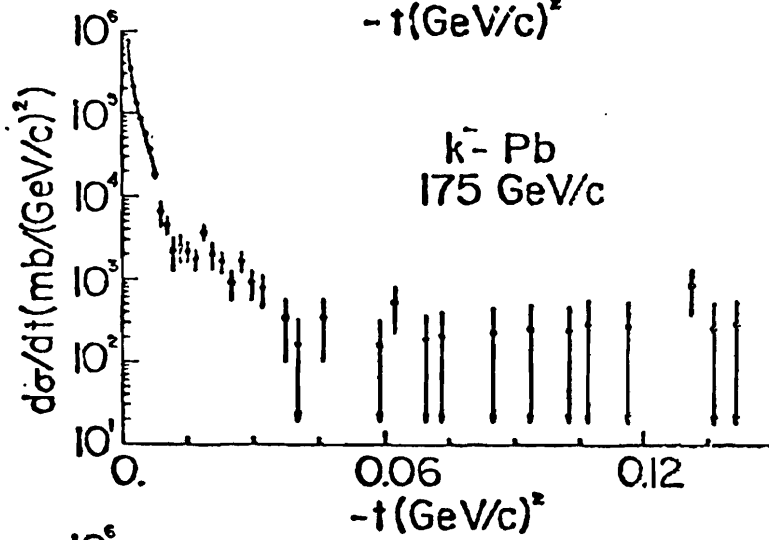
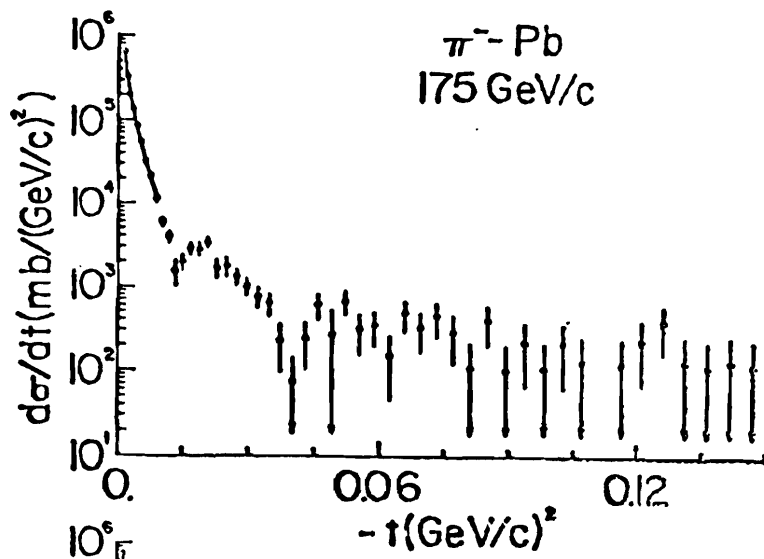










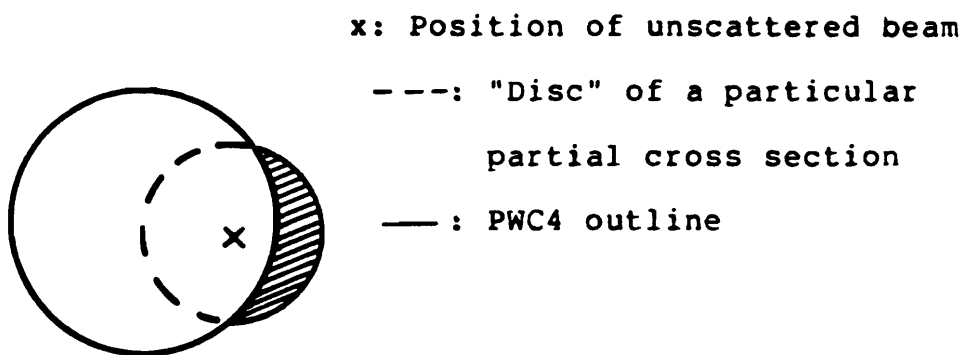


APPENDIX IV

DERIVATION OF SOME RESULTS USED IN THE DIRECT MEASUREMENT OF TOTAL CROSS SECTIONS

A. Derivation of Equation 7.4:

All quantities are as defined in Chapter 7. The situation is schematically sketched in the figure below:



Particles whose trajectories lie in the shaded area are not detected. If a correction for this fact is not made, then the resultant partial cross sections will be greater in magnitude than they actually are.

We first show that there is no need to make an acceptance correction for the target empty data.

Assume the target is such that it has a cross section of zero. Define

$N_k^f(mt)$ = number of particles whose scattering angle is between θ_{k-1} and θ_k in a full (empty) run

$R_k^f(mt) = N_k^f(mt) / I_0^f(mt)$

$I_0^f(mt)$ = number of incident particles in a full (empty) run

Construct the nth partial cross section:

$$\sigma_n = (1/\Gamma x) \ln \left[\frac{\sum_{k=1}^n R_k^{mt}}{\sum_{k=1}^n R_k^f} \right]$$

where

$$\Gamma = N_A \rho x / A$$

N_A = Avogadro's number

x = target length

ρ = target density

A = atomic weight

Notice that $N_k^f(mt)$ has no correction for acceptance losses. Since R_k^f is equal to R_k^{mt} in this hypothetical

case, then

$$\sigma_n = (1/\Gamma x) \ln(1) = 0$$

as expected. Hence there is no need to correct the target empty measurements when they are used in the calculation of the partial cross sections.

Next we look at the realistic case where the cross section due to the target is nonzero.

Let

$N_k^{f(mt)}$ be as above

$N_k^{f,c}$ = corrected number of particles whose scattering angle is between θ_{k-1} and θ_k in a target full (empty) run

$$R_k^{f,c} = N_k^{f,c} / I_0^f$$

The nth partial cross section is given by

$$\sigma_n = (1/\Gamma x) \ln \left[\left(\frac{\sum_{k=1}^n R_k^{mt}}{\sum_{k=1}^n R_k^{f,c}} \right) \right]$$

Notice the target empty measurements need not be corrected for acceptance. We write

$$N_k^f = N_k^{f,i} + N_k^{f,o}$$

where

$N_k^{f,o}$ = number of particles which scattered from material outside of the target in a target full run

$N_k^{f,i}$ = number of particles which scattered from the target in a targetfull run

Then

$$(N_k^f/I_\theta^f) - (N_k^{f,o}/I_\theta^f) = N_k^{f,i}/I_\theta^f$$

But

$$N_k^{f,o}/I_\theta^f = N_k^{mt}/I_\theta^{mt}$$

and thus

$$N_k^{f,i} = I_\theta^f (N_k^f/I_\theta^f - N_k^{mt}/I_\theta^{mt})$$

But

$$N_k^{f,i,c} = N_k^{f,i} / \alpha_k$$

where

α_k = acceptance value for the kth bin

and nence

$$N_k^{f,c} = (I_\theta^f/I_\theta^{mt}) (1-\alpha_k) N_k^{mt} + N_k^f/\alpha_k$$

completing the derivation of Equation (7.4).

B. Derivation of Equation (7.5):

$$\sigma_n = \sigma - \int_{\Omega_n}^0 d\sigma/d\Omega (d\Omega)$$

where

σ_n = nth partial cross section (for scattering angles $> \Omega_n$)

σ = total cross section

$d\sigma/d\Omega$ = differential cross section for all possible processes

Assume $d\sigma/d\Omega$ is dominated by small angle elastic scatters and is of the form

$$N_0 \exp(bt) = N_0 \exp(-b' \theta^2)$$

where

$$b' = bp^2$$

p = incident beam momentum

Thus

$$\sigma_n = \sigma - 2\pi \int [\exp(-b' \theta^2)] d(\cos \theta)$$

Let

$$y = \cos \theta = 1 - \theta^2/2$$

$$dy = -\theta(d\theta)$$

Therefore

$$\sigma_n = \sigma + 2\pi N_0 \int \exp(-b\theta^2) \theta(d\theta)$$

$$\sigma_n = \sigma - A(1 - \exp(-B\theta_n^2))$$

as desired.

C. A Comment Concerning Errors on Partial Cross Sections :

Let N_k^{mt} , $N_k^{f,c}$ be as defined in the first part of the appendix.

Define

$$\sum_{k=1}^n N_k^{mt}(f,c) = T_n^{mt}(f,c)$$

Then

$$\sigma_n = (1/\Gamma_x) \ln[(T_n^{mt}/I_0^{mt}) / (T_n^{f,c}/I_0^f)]$$

Thus $\Delta^2(\sigma_n)$, the error squared of σ_n , is

$$\Delta^2(\sigma_n) = (1/\Gamma_x^2) [(\Delta^2(T_n^{mt})/(I_0^{mt})^2) + (\Delta^2(T_n^{f,c})/(I_0^f)^2)]$$

where

$$\Delta(T_n^{mt}(f,c)) = \text{error on } T_n^{mt}(f,c).$$

But since the situation is described by binomial statistics (either a scatter occurred or it did not)

$$\Delta^2(T_n^{mt}) = I_\theta^{mt} - T_n^{mt}.$$

The formula for $\Delta^2(T_n^{f,c})$ is more complicated due to the presence of the acceptance factors.

We have

$$\begin{aligned} T_n^{f,c} &= \sum_{k=1}^n (I_\theta^f / I_\theta^{mt}) (1 - \alpha_k) N_k^{mt} + \sum_{k=1}^n N_k^f / \alpha_k \\ &= \sum_{k=1}^n w_k N_k^{mt} + \sum_{k=1}^n v_k N_k^f \end{aligned}$$

where

$$\begin{aligned} w_k &= (I_\theta^f / I_\theta^{mt}) (1 - \alpha_k) \\ v_k &= (1 / \alpha_k) \end{aligned}$$

Then

$$\Delta^2(T_n^{f,c}) = \sum_{k=1}^n w_k^2 \Delta^2(N_k^{mt}) + 2 \sum_{i < j} w_i w_j \text{cov}(N_i^{mt}, N_j^{mt})$$

$$+ \sum_{k=1}^n v_k^2 \Delta^2(N_k^f) + 2 \sum_{r < s} v_r v_s \text{cov}(N_r^f, N_s^f)$$

where

$\Delta(z)$ = error on z

$\text{cov}(A,B)$ = covariance between A and B

The quantities $N_k^{f(mt)}$ follow a multinomial distribution. Hence

$$\Delta^2(N_k^{f(mt)}) = I_0^{f(mt)} \left[\frac{N_k^{f(mt)}}{I_0^{f(mt)}} \right] \left[1 - \frac{N_k^{f(mt)}}{I_0^{f(mt)}} \right]$$

$$\text{cov}(N_i^{f(mt)}, N_j^{f(mt)}) = -I_0^{f(mt)} \left[\frac{N_i^{f(mt)}}{I_0^{f(mt)}} \right] \left[\frac{N_j^{f(mt)}}{I_0^{f(mt)}} \right]$$

D. Derivation of Equation (7.7):

First the following lemma is proved.

LEMMA:

Assume there exists two N-dimensional column vectors F and x and $F = Ax$ where A is a $N \times N$ matrix. Assume the $N \times N$ covariance matrix V for the x 's is known. Then Z , the $N \times N$ covariance matrix for the F 's, is

$$Z = AVA^T$$

PROOF:

Let $(F_i F_j)$ be the covariance between F_i and F_j . In reference A4.1 it is shown that

$$\sigma(F_i F_j) = \sum_{m=1}^N \sum_{k=1}^N (\partial F_i / \partial x_k) (\partial F_j / \partial x_m) \sigma(x_m x_k)$$

By definition

$$F_i = \sum_{m=1}^N A_{im} x_m$$

and therefore

$$\partial F_i / \partial x_k = A_{ik}$$

Hence

$$(Z)_{ij} = \sigma(F_i F_j) = \sum_{m=1}^N \sum_{k=1}^N A_{ik} A_{jm} V_{km}$$

$$= \sum_{m=1}^N A_{jm} \sum_{k=1}^N A_{ik} V_{km}$$

$$= \sum_{m=1}^N A_{jm} D_{im} \quad \text{where } D=AV$$

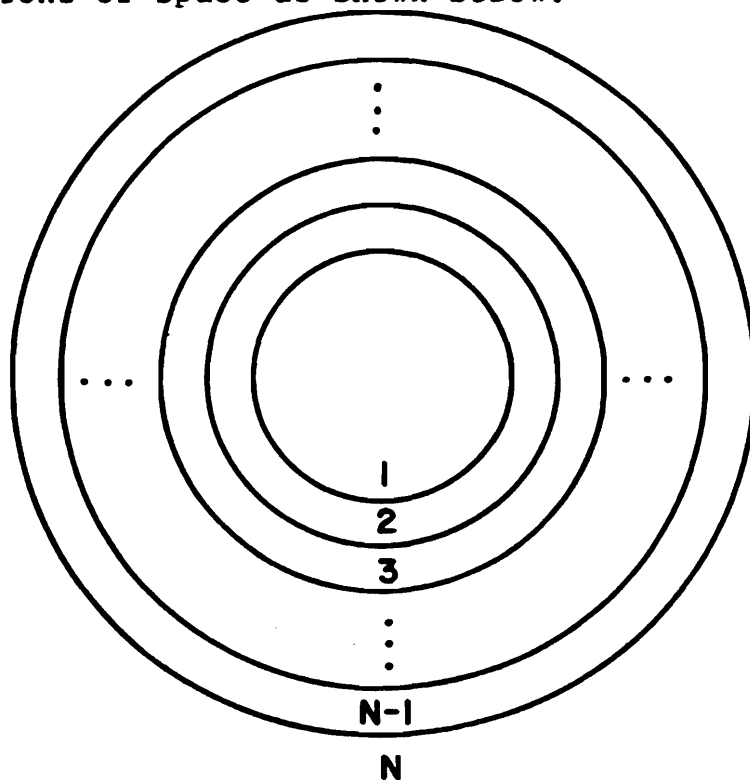
$$= \sum_{m=1}^N D_{im} (A^T)_{mj}$$

Hence

$$Z = AVA^T$$

Q.E.D.

Equation 7.7 is now derived. For each event, the scattered particle's trajectory can lie in one of N regions of space as shown below:



where region 1 represents where unscattered beam particles would go; region N goes to infinity.

The partial cross sections are written as follows:

$$\sigma_1 = \int_{\Omega_1}^{\infty} F(\Omega) d\Omega = \sum_{n=2}^N c_n$$

$$\sigma_2 = \int_{\Omega_2}^{\infty} F(\Omega) d\Omega = \sum_{n=3}^N c_n$$

.

.

.

$$\sigma_{N-1} = \int_{\Omega_N}^{\infty} F(\Omega) d\Omega = c_N$$

where

$$F(\Omega) = d\sigma/d\Omega$$

$$c_i = \int_{\Omega_{i-1}}^{\Omega_i} F(\Omega) d\Omega$$

Thus it is observed

$$\begin{bmatrix} \sigma_1 \\ \sigma_2 \\ \cdot \\ \cdot \\ \sigma_{N-1} \end{bmatrix} = \begin{bmatrix} 1 & 1 & \dots & 1 \\ 0 & 1 & \dots & 1 \\ & & \cdot & \\ & & & \cdot \\ 0 & 0 & 0 & \dots & 1 \end{bmatrix} \begin{bmatrix} c_2 \\ c_3 \\ \cdot \\ \cdot \\ c_N \end{bmatrix}$$

$$\text{or } F = Ax$$

where F and x are $(N-1)$ column vectors and A is a $(N-1) \times (N-1)$ matrix.

Let Z be the $(N-1) \times (N-1)$ covariance matrix for the F 's. Using the above lemma, it is seen that

$$Z = AVA^T$$

where V is the $(N-1) \times (N-1)$ covariance matrix for the c 's. The elements of V are as follows:

$$V_{ii} = \Delta^2(c_i)$$

$$V_{ij} = 0, \quad i \neq j$$

where $\Delta^2(c_i)$ is the standard deviation squared of c_i .

Thus

$$Z = \begin{bmatrix} 1 & 1 & \dots & 1 & 1 \\ 0 & 1 & \dots & 1 & 1 \\ & & \cdot & & \\ 0 & 0 & \dots & 0 & 1 \end{bmatrix} \begin{bmatrix} \Delta^2(c_1) & & & & \\ & \cdot & & & \\ & & \cdot & & \\ & & & \cdot & \\ & & & & \cdot \\ & & & & & \Delta^2(c_N) \end{bmatrix} \begin{bmatrix} 1 & 0 & \dots & 0 & 0 \\ 1 & 1 & \dots & 0 & 0 \\ & & \cdot & & \\ 1 & 1 & \dots & 1 & 1 \end{bmatrix}$$

Equation 7.7 follows from the matrix multiplication and

by noting that

$$\sum_{k=i+1}^N \Delta^2(c_k) = \Delta^2(\sigma_i)$$

where $\Delta^2(\sigma_i)$ is the standard deviation squared of the i th partial cross section.

APPENDIX V

Following Lincoln A. Pajardo^{A5.1}, it is shown that if the differential cross section has the functional form of equations 9.1 and 9.2b (form factor parameterization with an exponential matrix element), then the bound of reference 1.14 (the Roy Bound) cannot be violated. The bound is written in the following form:

$$\theta \geq 3h^2(t_1) - 2|h(t)| - 1$$

where

$$h(t) = [b(t)/b(\theta)] [d\sigma/dt(t)]^{1/2} / [d\sigma/dt(\theta)]^{1/2}$$

$$b(t) = d/dt [\ln(d\sigma/dt)]$$

$$t = 3t_1(1+ct_1)$$

$$c = (8m_{\text{proton}}E)^{-1}$$

$$E = \text{incident beam energy}$$

If $h(t) \geq \theta$ and $h(3t_1(1+ct_1)) \geq h^3(t_1)$, then

$$\theta \geq 3h^2(t_1) - 2h^3(t_1) - 1 \geq 3h^2(t_1) - 2|h(t)| - 1$$

The first expression factors as

$$-[1+2h(t_1)][1-h(t_1)]^2$$

and is always less than zero. Thus the second expression will also be less than zero, and the bound cannot be violated.

If the differential cross section is given by equations 9.1 and 9.2b with the pion radius (r_π), proton radius (r_p), and u greater than or equal to zero, then $h(t)$ is monotonically decreasing with increasing $-t$ and satisfies

$$h(3t_1(1+ct_1)) \geq h(3t_1) \geq h^3(t_1).$$

Thus the Roy Bound cannot be violated if the differential cross section can be parameterized by equations 9.1 and 9.2b.

The above considerations do not apply if the differential cross section has the functional form $\exp(bt+ct^2)$ since this form is not monotonically decreasing. However for this case the bound is violated only for rather extreme values of c . By numerical inspection it was found that at a laboratory energy of 200 GeV, the bound is violated in the region $0.0332 < -t < 0.0334$ $(\text{GeV}/c)^2$ when $b=10$ $(\text{GeV}/c)^{-2}$ and $c=50$ $(\text{GeV}/c)^{-4}$. For $b=10$ $(\text{GeV}/c)^{-2}$ and $c=100$ $(\text{GeV}/c)^{-4}$, the

bound is violated in the region $0.0016 < -t < 0.0175$
 $(\text{GeV}/c)^2$. For $b=10 (\text{GeV}/c)^{-2}$ and $c=200 (\text{GeV})^{-4}$, the
bound is violated in the region of $0.0 < -t < 0.009$
 $(\text{GeV}/c)^2$. For $b=10 (\text{GeV}/c)^{-2}$ there is no violation if
 $c < 48 (\text{GeV}/c)^{-4}$.

APPENDIX VI
CORRECTIONS FOR PLURAL NUCLEAR SCATTERING:
HIGH-t DATA

The following formulae^{6.3} were used to include the effects of plural nuclear scattering on the high-t data. The correction factors for various single scattering terms are presented. The $d\sigma/dt$ used in the fit to the data is given by

$$d\sigma/dt_{\text{fit}} = d\sigma/dt_{\text{single scatter}} [1 + \text{Correction Factor}]$$

SINGLE SCATTERING TERM	CORRECTION FACTOR
$\exp(bt+ct^2)$	$K \exp[.5(-bt-ct^2)]/(-b)$
Eqns. 9.1, 9.2a: $\pi^\pm p$	$K(1-\frac{1}{2}ut)(1+bt)(1+ct)^2/(-u+2b+4c)$
Eqns. 9.1, 9.2a: pp	$K(1-\frac{1}{2}ut)(1+ct)^4/(-u+8c)$
Eqns. 9.1, 9.2b: $\pi^\pm p$	$K e^{-ut/2}(1+bt)(1+ct)^2/(-u+2b+4c)$
Eqns. 9.1, 9.2b: pp	$K e^{-ut/2}(1+ct)^4/(-u+8c)$

where

$$K = N\sigma_{hp}^2/64\pi^2$$

σ_{hp} = hadron-proton total cross section

$$N = N_A \rho x / A$$

N_A = Avogadro's number

ρ = target density

x = target length

A = atomic weight

$$b = r_{\pi}^2 / 6\hbar^2$$

$$c = r_p^2 / 12\hbar^2$$

The correction factor for Eqns. (9.1, 9.2c) is the same as that for Eqns. (9.1, 9.2a).

REFERENCES AND NOTES

- 1.1 R. J. Glauber and G. Matthiae, Nucl. Phys. B21, 135 (1970).
- 1.2 A. S. Goldhaber and C. J. Joachin, Phys. Rev. 171, 1566, (1968).
- 1.3 G. Bellettini et. al., Nucl. Phys. 79, 609 (1966).
- 1.4 H. R. Bleiden et. al., Phys. Rev. D11, 14 (1975).
- 1.5 V. D. Apokin et. al., Serpukhov Preprint Y2/A1-42 (1976).
- 1.6 E. Jenkins et. al., "Proton-Helium Elastic Scattering from 40 to 400 GeV", submitted to the XIX International Conference on High Energy Physics, Tokyo, August 1978; D. Gross et. al., Phys. Rev. Lett. 41, 217 (1978).
- 1.7 G. Giacomelli, Phys. Rep. 23C, 123 (1976); Istituto di Fisica dell'Universita di Bologna Preprint IFUB 77-12 (1977).
- 1.8 D. S. Ayres et. al., Phys. Rev. D15, 3105 (1977).
- 1.9 C. W. Akerlof et. al., Phys. Rev. D14, 2864 (1976).
- 1.10 R. K. Carnegie et. al., Phys. Lett. 59B, 313 (1975).
- 1.11 G. Barbiellini et. al., Phys. Lett. 39B,

- 663 (1972).
- 1.12 J. P. Burq et. al., CERN EP Internal Report 78-7, 12/14178.
 - 1.13 S. M. Roy, Phys. Rep. 5C, 125 (1972).
 - 1.14 S. M. Roy, Phys. Rev. Lett. 43, 19 (1979).
 - 2.1 Also see J. Slaughter et. al., "A High Resolution Spectrometer for a Small Angle Scattering Experiment at Fermilab", to be published.
 - 2.2 J. R. Orr and A. L. Read, Meson Laboratory, Preliminary Design Report, March 1971, Fermilab.
 - 2.3 D. Ayres, "SAS Facility Threshold Cerenkov Counter Operating Instructions", Argonne National Laboratory Report, 1974 (unpublished).
 - 2.4 M. Benot et. al., Nucl. Instrum. Methods 105, 431 (1972).
 - 2.5 R. Anderson et. al., Nucl. Instrum. Methods 135, 267, (1976).
 - 2.6 R. D. Majka, "Sigma Minus - Proton Elastic Scattering at 23 GeV/c", Thesis, Yale University (1974).
 - 2.7 W. Frieze et. al., Nucl. Instrum. Methods 136, 93 (1976).
 - 2.8 S. Dhawan, "A Fast Readout and Geometrical Reconstruction System for Proportional Wire Chambers", unpublished.
 - 2.9 The magnet serial numbers are 2760, upstream,

and 2212, downstream.

- 3.1 S. Dhawan and R. D. Majka, "A Hardware Scatter Detector", IEEE Transactions on Nuclear Science, Vol. NS-22 (1975).
- 3.2 Digital Equipment Corp., Maynard, Massachusetts.
- 6.1 F. James and M. Roos, CERN Computer 7600 Interim Program Library, D506 and D516.
- 6.2 G_p and G_t were taken as follows:
- $$G_p = (1. + (.8)^2 q^2 / 12\hbar^2)^{-2}$$
- $$G_t = \exp(-q^2 R^2 / 6\hbar^2) \text{ where } R \text{ is the}$$
- electromagnetic radius of the target
(see Table 6.4).
- It was found that if a monopole form was used for the pions and kaons, there was negligible effect on the fit results.
- 6.3 L. A. Fajardo, "The Real Part of the Forward Nuclear Amplitude of Hadron - Proton Elastic Scattering Between 70 and 200 GeV/c Incident Momentum", to be submitted as thesis, Yale University; H. A. Bethe, Phy. Rev. 89, 1256 (1953).
- 6.4 The solid lines in figures 6.11 to 6.16 are calculated as follows: the theoretical form of $d\sigma/dt$ is convoluted by the acceptance and resolution of the apparatus. This convoluted form is then divided by the acceptance to arrive

at the fit results as shown in the figures. The fit results still exhibit effects of the apparatus resolution and therefore are not completely smooth.

- 7.1 A. S. Carroll et. al., Phys. Rev. Lett. 33, 932 (1974).
- 8.1 M. Sogard, Phys. Rev. D9, 1486 (1974).
- 9.1 Fermilab SAS, Phys. Rev. Lett. 37, 348 (1976).
- 9.2 F. Jenkins et. al., Fermilab-PUB-78/35-EXP, submitted to Sov. J. Nucl. Phys.
- 9.3 V. Bartenev et. al., Phys. Rev. Lett. 31, 1088, (1973).
- 9.4 R. Schamberger, Jr. et. al., Phys. Rev. D17, 1268 (1978).
- 9.5 G. Hohler et. al., Institut fur Theoretische Kernphysik Preprint, TKP 79-4, June, 1979.
- 9.6 T. T. Chou and C. N. Yang, Phys. Rev. 170, 1591 (1968).
- 9.7 A. Bialas et. al., Acta. Phys. Pol. B8, 855 (1977); N. W. Dean, Phys. Rev. D1, 2703 (1970).
- 9.8 J. J. J. Kokkedee and L. Van Hove, Nuovo Cim. 42, 711 (1966); E. M. Levin and V. M. Shekhter, Leningrad Nuclear Physics Institute Preprint, "Small-Angle Elastic Scattering and Quark Model", 1978; E. M. Levin et. al., Proc. of the IXth Winter LNPI School on Nuclear Physics and

Elementary Particles (Leningrad 1974), Vol. III.

- 9.9 D. A. Andrews et. al., J. Phys. G. 3,
L91 (1977) and references therein.
- 9.10 A. Quenzer et. al., Phys. Lett. 76B, 512
(1978) and references therein.
- 9.11 V. Singh and S. M. Roy, Phys. Rev. Lett. 24,
28 (1970). For more detail, see V. Singh and
S. M. Roy, Phys. Rev. 1D, 2638 (1970).
- 9.12 See also G. Hohler et. al., Institut fur
Theoretische Kernphysik Preprint, TKP 79-8,
July, 1979.
- A4.1 W. T. Eadie et. al., Statistical Methods in
Experimental Physics, North American Elsevier
Publishing Company, Inc., 1971, p. 27.
- A5.1 private communication.

ACKNOWLEDGMENTS

It was told to me when I first started this venture, that success in high energy physics required a true group effort. I can now from personal experience concur with that statement.

I would like to thank my advisor Jack Sandweiss for his advice and encouragement during my years of graduate study. I also wish to thank Jean Slaughter, Lincoln Fajardo, Joseph Lach, Richard Majka, and Laurant Rosselet for their assistance, guidance, and good humor during this experiment. Without them this work would have proceeded a great deal slower, and life would have been a great deal duller.

It is a pleasure to acknowledge the essential contributions of my other collaborators: Charles Ankenbrandt, Muzzafer Atac, Robert Brown, Stanley Ecklund, Peter Gollon, James MacLachlan, Jay Marx, Peter Nemethy, Arthur Roberts, and last but by no means least Gilbert Shen.

Thanks go to Jon Blomquist, Garvie Hale, and Ed Steigmeyer for their invaluable and at times herculean efforts in the set-up of the experiment. I also thank Adrian Disco for the beautiful high resolution PWCs, Satish Dhawan for the design of much of the electronics,

Irving Winters for sundry mechanical designs, and William Frieze for his work on early parts of the experiment. Finally thanks to the Fermilab Computer Operations Group for their helpful and efficient efforts.

I would also like to thank Emily Luisada for her most patient efforts and careful work on the figures in the thesis; in addition, thanks to Frank Hansen and Peter Kobrak for all their help in putting this thesis together. Also thanks must go to Mary Luba and Pat Mascione for their help in typing the thesis.

I would especially like to thank Peter Martin for all his help and patience. Because of his efforts in coordinating resources, I could concentrate on physics and did not need to worry about mundane day to day matters.

Finally I thank my wife Pamela for her part in this work. No matter what happened, I always knew I could count on her; for that I will always be grateful.